

The role of the dendritic cell actin cytoskeleton in the formation and function of the immunological synapse

BY

DESSISLAVA MALINOVA

INSTITUTE OF CHILD HEALTH

UNIVERSITY COLLEGE LONDON

A thesis submitted for the degree of Doctor of Philosophy

2014

Declaration

I, Dessi Malinova, confirm that the work presented in this thesis is my own. Where information has been derived from other sources, I confirm that this has been indicated in the thesis. Analysis of FRAP data shown in Figure 4.9 was done in collaboration with Marco Fritzsche. Lipids use for lipid bilayers experiments in Chapter 4 were prepared by Carla Nowosad. Lentivirus containing shRNA against MKL-1 and WDR1 (Chapter 6) was acquired from Karolin Nowak. Dock8 experiments in Chapter 6 were performed in conjunction with Sarah Ali, a BSc student I supervised.

Abstract

During an immune response, dendritic cells (DCs) capture and process antigen, upregulate co-stimulatory molecules and migrate to lymphoid organs to maximise antigen recognition by rare T cell clones. A crucial step for successful T cell activation is cell-cell interaction at the immunological synapse (IS), the organised contact interface which allows optimal communication. IS formation requires the dynamic remodelling of the actin cytoskeleton to spatially distribute membrane areas with distinct protein compositions. While evidence exists for a role of the T cell cytoskeleton in this process, the driving force behind the specific organisation on the DC side is unknown.

One important actin regulator is Wiskott-Aldrich Syndrome protein (WASp), expressed exclusively in immune cells. Using a murine model, we investigated the role of WASp in DC-mediated actin-dependent synapse formation.

Utilising both confocal and electron microscopy (EM), we observed a disorganised, asymmetric interface between T cells and WASp-deficient DCs. Immunofluorescent staining shows reduced polarisation of certain synapse markers in WAS knock-out conjugates; while high resolution 3D EM reconstructions show severely impaired cell spreading and a reduced contact area. We have used fluorescence recovery after photobleaching (FRAP) to show reduced stability of the actin network in WASp DCs. Our experiments on supported planar bilayers have shown an unexpected interface organisation and highlight a novel role of the DC cytoskeleton in this process.

Crucially, we have demonstrated reduced T cell activating capacity of WASp-deficient DCs, as measured by T cell proliferation, cytokine production and transcription factor expression. The results highlight the critical role of cytoskeletal regulation in DC-mediated IS formation. Further, a second murine immunodeficiency model, Dock8 deficiency, and two novel human primary immunodeficiencies were briefly investigated to examine the role of other actin regulators in normal DC function.

Acknowledgements

Firstly, I'd like to thank my supervisors, Adrian Thrasher and Gerben Bouma, for their advice, support and encouragement. Gerben, your faith in me was endless and much appreciated. MIU has been fun along the way and I'd like to thank all of its members for their technical support and friendship. Several members of the "WASp group" have provided help and advice throughout – thanks to Dale, Marsilio, Austen, Siobhan and Julien.

Huge thanks to Carla for all those lipid preps; and to Hannah and Peter for letting me loose on 3View! Thanks also to Marco for invaluable support during the FRAP analysis. Sue, I don't know where any of us would be without you, thank you for patiently organising us all. Kathy and Mus have been an endless source of wisdom and banter. I'd like to extend a very deep thank you for your friendship. Anna and Ariane - a sincere thank you for your kindness and inspiration. You know my favourite drink, what else is there to say!

Thanks to my Mum, my Dad and my sister for the persistent questioning and gentle encouragement – "Are you nearly there yet?" A word of thanks also goes to my wonderful Ampton Street family – Irene and Jess – who probably know more about immunology than they wanted. Thank you for your chirpy enthusiasm, multiculturalism and spirit of adventure.

Finally, a big thank you goes to Mike, who has had to put up with a variety of questions, dilemmas and crazy ideas. Thank you for your patience and encouragement. I have learnt so much (science)!
Thank you.

Table of contents

Declaration.....	2
Abstract.....	3
Acknowledgements.....	4
Table of contents	5
List of figures and tables	9
Abbreviations.....	13
Chapter 1 – Introduction.....	17
1. <i>Actin</i>	17
Function of actin	17
Structure	18
Arp2/3 nucleates branched actin networks.....	19
Formins nucleate longer unbranched actin filaments	20
Arp2/3, nucleation-promoting factors (NPFs) and Rho GTPases.....	22
Other actin regulators.....	24
2. <i>The Immunological Synapse</i>	27
On the DC side.....	27
Molecular structure and cell morphology	29
Signalling	32
Actin at the synapse.....	37
Cell polarity and MTOC translocation.....	39
The role of integrins.....	41
Function of the synapse	44
Imaging the immune synapse	46
3. <i>The T cell side: TCR signalling, costimulation and cytokines</i>	50
T cell activation	50
T helper cell fate	55

4.	<i>Wiskott-Aldrich Syndrome and WASp</i>	59
	Clinical characteristics and cellular defects	59
	WASp structure and regulation	61
5.	<i>WAS mouse model</i>	66
6.	<i>DOCK8</i>	67
	DOCK8 structure, genetics and protein family	67
	Clinical characteristics and cellular defects	68
	DOCK8 murine model	71
Chapter 2 – Materials and Methods		74
2.1	<i>Materials</i>	74
2.1.1	Media, Buffers and Solutions.....	74
2.1.2	Antibodies and Cell Trackers.....	77
2.1.3	Animals and Cells	80
2.2	Methods.....	82
2.2.1	Cell culture	82
2.2.2	Constructs	83
2.2.3	Lentiviral preparation	86
2.2.4	Western blots and Immunoprecipitation	87
2.2.5	Conjugate formation.....	89
2.2.6	Antigen presentation assays	90
2.2.7	Enzyme-linked immunosorbent assay (ELISA)	90
2.2.8	Q-PCR	91
2.2.9	Microarray analysis	91
2.2.10	Dynabead assays	92
2.2.11	DC adoptive transfer	92
2.2.12	Immunocytochemistry and Immunostaining for FACS	92
2.2.13	Live Imaging and Fluorescence Recovery After Photobleaching (FRAP)	93
2.2.14	Micropits preparation	94
2.2.15	Electron Microscopy	94

2.2.16 Gatan 3view sample processing.....	95
2.2.17 Supported planar lipid bilayers.....	96
2.2.18 Image Processing and Data Analysis.....	96
Chapter 3 – Deregulated actin results in abnormal synapse formation.....	97
3.1 Introduction	97
3.2 Results.....	100
3.2.1 T cell isolation efficiency	100
3.2.2 Bone marrow-derived DCs and comparison of WAS DC markers.....	101
3.2.3 Antigen presentation	104
3.2.4 DC: T cell conjugate formation.....	106
3.2.5 Cell surface markers accumulating at the IS.....	108
3.2.6 High resolution and 3D imaging of conjugates	114
3.3 Discussion.....	119
Chapter 4 – Dynamics of synapse formation	125
4.1 Introduction	125
4.2 Results.....	127
4.2.1 Synapse quantification.....	127
4.2.2 Live imaging	127
4.2.3 Fluorescence Recovery After Photobleaching	130
4.2.4 Bull’s-eye IS pattern	141
4.2.5 Micropits	142
4.2.6 Planar Lipid Bilayers	145
4.3 Discussion.....	167
Chapter 5 – A disorganised immunological synapse is not sufficient for correct T cell activation	173
5.1 Introduction	173
5.2 Results.....	175
5.2.1 CD69 upregulation	175
5.2.2 T cell proliferation.....	177

5.2.3 IL-2 secretion.....	179
5.2.4 QPCR	180
5.2.5 Cytokine ELISA.....	181
5.2.6 In vivo T cell fate induction	183
5.2.7 Microarray analysis	188
5.2.8 DC conditional WAS knockout model	196
5.2.9 Dynabead IP assay.....	199
5.3 Discussion.....	202
Chapter 6 – Abnormal actin regulation in novel primary immunodeficiencies.....	206
6.1 Introduction	206
6.2 Results.....	210
6.2.1 Megakaryoblastic leukaemia (MKL-1).....	210
6.2.2 Actin-interacting protein 1 (AIP1).....	216
6.2.3 Dedicator of cytokinesis (DOCK) 8	222
6.3 Discussion.....	226
Chapter 7 – Discussion.....	231
WASp deficiency results in a more fluid, unstable DC synapse	231
Novel adhesive structures at the IS	234
More to achieve at the IS.....	238
Wiskott-Aldrich syndrome	239
Actin in the immune system	240
References	242
Appendix	290
1. Constructs	290
LNT_mCherry-Actin.....	290
LNT_ICAM-1-EGFP.....	291
2. Anti-MHCII + Anti-ICAM-I (0.25µg/ml) bilayer	293

List of figures and tables

Chapter 1		Page
Figure 1.1	Immunological synapse organisation.	29
Figure 1.2	T cell activation	54
Figure 1.3	WASp domains and autoinhibition	61
Table 1	The major transcription factors determining CD4 T cell fates	56
 Chapter 3		
Figure 3.1	T cell isolation purity	100
Figure 3.2	CD11c expression	101
Figure 3.3	BMDC maturation status	102
Figure 3.4	Total polymerised actin network	103
Figure 3.5	Antigen presentation	105
Figure 3.6	Conjugate formation - FACS	106
Figure 3.7	Conjugate formation - microscopy	107
Figure 3.8	Measuring polarisation of synaptic markers	108
Figure 3.9	Polarisation of synaptic markers	109
Figure 3.10	ICAM-1 polarisation on the DC side	110
Figure 3.11	ICAM-1-GFP polarisation in lentivirus infected DCs	111
Figure 3.12	T cell MTOC polarisation found in dendritic cells	113
Figure 3.13	Electron microscopy synapse imaging	114
Figure 3.14	TEM and 3-view	116
Figure 3.15	DC:T cell contact surface area	117
Figure 3.16	3D reconstructions of EM serial slices	118

Chapter 4

Figure 4.1	Conjugate formation over time	127
Figure 4.2	DC-T cell contacts are shorter or less stable with WAS DCs	128
Figure 4.3	Recovery curve calculations	130
Figure 4.4	Actin-mCherry bleach at 3 different areas	131
Figure 4.5	Actin dynamics in different areas of a cell	132
Figure 4.6	Fluorescence recovery appears much faster in WASp-deficient DCs	134
Figure 4.7	Fluorescence recovery in WAS DCs is augmented at the synapse	135
Figure 4.8	Background-corrected mean fluorescence recovery plotted against time	137
Figure 4.9	Synapse organisation appears to be abnormal in WAS DCs	141
Figure 4.10	Making micropits	142
Figure 4.11	Micropit grid and optimal seeding diameter	144
Figure 4.12	ICAM-1-GFP expressing DCs interacting with bilayers	146
Figure 4.13	Empty bilayer	146
Figure 4.14	Anti-MHCII bilayer	148
Figure 4.15	DC morphology over time	149
Figure 4.16	Actin and MHC surface area and intensity	150
Figure 4.17	Anti-MHCII and anti-ICAM-1 bilayer	153
Figure 4.18	Actin and MHC surface area and intensity	157
Figure 4.19	Podosome quantification on anti-MHCII and anti-ICAM-1 bilayers	160
Figure 4.20	Confirming podosome identity – CD11a	161
Figure 4.21	Confirming podosome identity – capping protein	163
Figure 4.22	Anti-ICAM-1 only bilayers	165
Figure 4.23	Podosome quantification across different bilayer constituents	166
Table 4.1	Exponential fitting parameters	138
Table 4.2	Second-order exponential fit recovery rates	138

Chapter 5

Figure 5.1	No significant defect in CD69 upregulation in WAS DCs	175
Figure 5.2	Proliferation defect at lower levels of induction	177
Figure 5.3	Proliferation defect at lower levels of induction - normalised	178
Figure 5.4	Defective IL-2 production in T cells induced by WAS DCs	179
Figure 5.5	T cell fate master regulators	180
Figure 5.6	T helper cell cytokines	181
Figure 5.7	No significant difference in migration between BL6 and WAS DCs following IV injection	184
Figure 5.8	IFN γ and IL-17 immunostaining	186
Figure 5.9	IL-4 and IL-10 immunostaining	187
Figure 5.10	Electropherograms of RNA samples	189
Figure 5.11	Differentially regulated genes	190
Figure 5.12	Differentially regulated genes – antigen-specific response	191
Figure 5.13	T helper cell differentiation	192
Figure 5.14	T helper cell differentiation - WOVsBO	195
Figure 5.15	Serum autoimmune antibody levels	197
Figure 5.16	Magnetic bead model	199
Figure 5.17	Magnetic bead optimisation for immunoprecipitation	201

Chapter 6

Figure 6.1	Mutation in MKL-1 resulting in loss of protein expression	210
Figure 6.2	DC morphology 5 days post isolation	211
Figure 6.3	Total polymerised actin is reduced in MKL-1 patient cells	213
Figure 6.4	MKL-1 knockdown THP1 cell line	215
Figure 6.5	WDR1 patient lymphocyte actin	217
Figure 6.6	Total polymerised actin in DCs	218
Figure 6.7	Podosome formation	219

Figure 6.8	Podosome volumes	220
Figure 6.9	WDR1 knockdown cell line	221
Figure 6.10	Stable conjugate formation and polarisation of synapse markers	222
Figure 6.11	MTOC polarisation	223
Figure 6.12	Coculture cytokine secretion	225

Abbreviations

ADF/ cofilin	Actin depolymerising factor/ cofilin
AIP	Actin Interacting protein
ANOVA	Analysis of variance
APC	Allophycocyanin (fluorophore)
APC	Antigen presenting cell
Arp2/3	Actin-related protein-2/3
ATP	Adenosine triphosphate
BL6	C57BL/6 wildtype mouse strain
BMDC	Bone marrow derived dendritic cells
BSA	Bovine Serum Albumin
CD	Cluster of differentiation
cDNA	Complimentary DNA (Deoxyribonucleic Acid)
CFA	Complete Freund's Adjuvant
CFSE	Carboxyfluorescein succinimidyl ester
CMFDA	5-Chloromethylfluorescein Diacetate
CMV	cytomegalovirus
CP	Capping protein
DAG	Diacylglycerol
DAPI	4,5-Diamino-2-phenylindole
DC	Dendritic cell
DDAO	dodecyldimethylamine oxide
DIC	differential interference contrast
DMEM	Dulbecco's Modified Eagle Medium
DMSO	Demethyl sulphoxide
DOCK8	Dedicator of cytokinesis 8
DOPC	1,2-dihexanoyl- <i>sn</i> -glycero-3-phosphocholine
DOPE	1,2-Dioleoyl- <i>sn</i> Glycero-3-Phosphoethanolamine-
EDTA	Ethylendiaminetetraacetic acid
ELISA	Enzyme-linked immunosorbent assay
(e)GFP	(enhanced) Green Fluorescent protein
ER	Endoplasmic reticulum
FACS	Fluorescence-activated Cell Sorting
F-actin	Filamentous actin

FCS	Fetal calf serum
FITC	Fluorescein isothiocyanate
FoxP3	Forkhead box P3
FRAP	Fluorescence Recovery After Photobleaching
FS	Forward scatter
FYN	Phenylalanine (F) Tyrosine (Y) Neutral (N); Y293F WASp mutant
GAPDH	Glyceraldehyde 3-phosphate dehydrogenase
GATA3	GATA-binding protein 3
GC	Germinal centre
GDP/GTP	Guanoside diphosphate/triphosphate
GEF	Guanine nucleotide exchange factor
GM-CSF	Granulocyte-macrophage colony-stimulating factor
GTP	Guanosinetriphosphate
HBSS	Hank's Balanced Salt Solution
HLA	Human Leukocyte Antigen
HPV	Human papilloma virus
HSV	Herpes simplex virus
i.v.	Intravenous
ICAM-1	Intercellular adhesion molecule 1
IFN γ	Interferon gamma
IL-	Interleukin-
IPA	Ingenuity Pathway Analysis
IS	Immunological Synapse
ISO	Isotype control
IVC	Individually ventilated cage
KO	Knockout
LB	Luria-Bertani
LFA-1	Lymphocyte function-associated antigen 1
LN	Lymph node
LPS	Lipopolysaccharide
MAL/MKL-1	Megakaryoblastic leukaemia 1
MCV	Molluscum contagiosum virus
MFI	Mean Fluorescence Intensity
MHC	Major Histocompatibility Complex
M-MLV-RT	Moloney Murine Leukemia Virus reverse transcriptase

MOI	Multiplicity of Infection
mRNA	Messenger ribonucleic acid
MTOC	Microtubule organising centre
OVA	Ovalbumin
PBMC	Peripheral blood mononuclear cell
PBS	Phosphate-buffered saline
PCR	Polymerase chain reaction
PDC	Plasmacytoid dendritic cell
PDMS	Polydimethylsiloxane
PE	Phycoerythrin
PEI	Polyethylenimine
PFA	Paraformaldehyde
PID	Primary Immunodeficiency
PIP ₂	Phosphatidylinositol-4,5-bisphosphate
PMA	Phorbol-12-myristate-13-acetate
PSTPIP1	Proline-serine-threonine phosphatase interacting protein
PVDF	Polyvinylidene difluoride
ROI	Region of interest
Rorc	RAR-related Orphan Receptor C
RPMI	Roswell Park Memorial Institute medium
SAP	Shrimp alkaline phosphatase
SCID	Severe combined immunodeficiency
SCR	Scramble
SDS-PAGE	Sodium dodecylsulfate - Polyacrylamide gel electrophoresis
SEM	Scanning electron microscopy
SEM	Standard error of the mean
shRNA	Short hairpin ribonucleic acid
SIM	Structured illumination microscopy
SMAC	Supramolecular activation cluster
SS	Side scatter
STEDM	Stimulated emission depletion microscopy
Tbx21/Tbet	T box transcription factor 21
TCR	T cell receptor
TEM	Transmission electron microscope
TIRF	Total internal reflection fluorescence

TLR	Toll-like receptor
TNF	Tumour necrosis factor
VZV	Varicella-zoster virus
WAS(p)	Wiskott Aldrich syndrome (protein)
WIP	Wasp-interacting protein
XLN	X-linked neutropenia

Chapter 1 – Introduction

1. Actin

Function of actin

The actin cytoskeleton has a large number of diverse roles to support cellular function including structural integrity, movement, and the localisation, clustering and stabilisation of transmembrane proteins; which are crucial in biological processes such as cell division, motility, endocytosis and morphogenesis. These processes are achieved by highly regulated actin network assembly and disassembly (Pollard and Cooper, 2009, Dominguez and Holmes, 2011). This delicately balanced process must depend on tight feedback mechanisms between the cell's requirements, the actin network and its regulators, of which there are over 100. Actin's participation in so many cellular processes is mediated by intimate and extensive interactions with the cell membrane (Doherty and McMahon, 2008). Further, actin can be coupled to transmembrane proteins, such as many immune cell receptors (Barda-Saad et al., 2005), and the extracellular environment, for example through specialised adhesion structures called podosomes (Linder and Aepfelbacher, 2003). Thus dynamic polymerisation and depolymerisation of actin filaments and their anchoring to cellular structures can produce forces required for both whole-cell movements and intracellular transport of proteins, vesicles and organelles. Cells of the immune system are obligatorily highly mobile and thus require actin cytoskeletal regulation for correct spatial and temporal organisation both at cellular level and on a smaller scale, during cell-cell communication. The actin cytoskeleton therefore plays a pivotal role in nearly all stages of immune system function, including haematopoiesis,

migration and cell-cell interaction, which is crucial for initiation of innate and adaptive immune responses.

Structure

Actin is present in two states in almost all eukaryotic cells – free monomers, known as globular or G –actin, which polymerise to form filamentous or F-actin (Reisler, 1993). The monomeric subunit is around 42kDa and is bound to either ADP or ATP (Otterbein et al., 2001, Graceffa and Dominguez, 2003). During filament polymerisation, all actin monomers line up pointing in the same direction to form a filament with structural polarity. The end showing a subunit with an exposed ATP binding site is referred to as the (-) or “pointed” end, while the opposite end is the (+) or “barbed” end. These terms arose from myosin ‘decoration’ experiments investigating actin filament appearance by TEM (Begg et al., 1978). Actin hydrolyses ATP within the filament to produce ADP and a phosphate group (Pi). As the ADP-bound monomers remain bound in the filament for some time, this results in three different species of monomers being present in a filament – ATP-actin, ADP-Pi-actin and ADP-actin (Vavylonis et al., 2005). The proportion of each depends on the filament growth and depolymerisation rates.

Both ends can undergo polymerisation, however, the critical concentration of actin monomers required for -end growth is 8 times larger than that for +end growth. Consequently, most polymerisation occurs at the +/barbed end while depolymerisation occurs at the opposite end (Bindschadler et al., 2004, Vavylonis et al., 2005). Polymerisation can occur at uncapped or severed filament barbed ends, or can be nucleated by several distinct types of proteins (Campellone and Welch, 2010). Although the concentration of actin-GTP in non-muscle cells is high, pure actin monomers do not readily form oligomers and begin elongation (Rosenblatt et al., 1995). The requirement for different nucleators also provides a mechanism for regulation and signal integration. The two main nucleation mechanisms are described below.

Arp2/3 nucleates branched actin networks

The first and best characterised nucleator is the Arp2/3 complex (Welch et al., 1997, Mullins et al., 1998). This seven-subunit complex is able to nucleate branches from existing actin filaments (Volkman et al., 2001, Egile et al., 2005, Pollard, 2007) and in doing so, it generates a branched network, which has been shown to play a crucial role at the leading edge of migrating cells (Pollard and Borisy, 2003). Arp2/3 contains two actin-related proteins (Arp2 and Arp3) and 5 additional subunits (ArpC1-Arp5C); and, like actin, is highly evolutionarily conserved. The complex requires ATP, pre-existing actin filaments and nucleation-promoting factors (NPFs) to initiate new filament growth at an angle of 78° from the mother filament (Mullins et al., 1998, Blanchoin et al., 2000, Achard et al., 2010). Arp2/3 in the cytosol is in an inactive conformation and its binding at a branch junction results in an active conformation, with Arp2 and Arp3 forming the first two subunits of the new daughter actin filament (Rouiller et al., 2008).

The best-characterised NPFs are members of the WASp family, described below. The C-terminal verpulin homology-central-acidic (VCA) domains of these proteins can bind both Arp2/3 and actin monomers and have been described to be both necessary and sufficient for WASp-mediated nucleation (Machesky and Insall, 1998, Miki and Takenawa, 1998, Machesky et al., 1999, Rohatgi et al., 1999). Many studies have investigated the interactions between the VCA and Arp2/3 and it has been suggested that the V region binds to actin monomers, the C region is able to bind to both actin and the Arp2/3 complex, while the A region binds Arp2/3 only (Chereau et al., 2005, Marchand et al., 2001, Kelly et al., 2006, Kreishman-Deitrick et al., 2005). The precise location of binding on individual molecules is still under debate. The conformational change induced in Arp2/3 by NPF binding has been shown in assembled junctions (Volkman et al., 2001, Egile et al., 2005, Rouiller et al., 2008). More recently, Xu *et al.* used electron microscopy to show that the precise conformational change is independent of the nature of the NPF and involves both a slightly twist within Arp2/3 and a further movement of Arp2 within the molecule (Xu et al., 2012). The authors also show that all NPFs observed

partially occluded the actin binding site on Arp2/3, suggesting further structural adjustments must be at play in the context of filament elongation (Xu et al., 2012).

The VCA domain may play a role at several points during nucleation. First, single molecule imaging has confirmed that the VCA domain accelerates the association rate between Arp2/3 and the mother filament (Smith et al., 2013a). Subsequently, there is evidence for a VCA-mediated activation step after filament binding (Marchand et al., 2001, Beltzner and Pollard, 2008, Smith et al., 2013a). Recently, it has been suggested that part of this activation may involve the release of Arp2/3 from VCA, thus coupling filament initiation and release from membrane tether constraints (Smith et al., 2013b). The authors use multi-wavelength single molecule imaging to follow branch formation over time and suggest that upon filament binding, the VCA is released from the Arp2/3 complex prior to filament elongation and that it cannot bind to Arp2/3 complexes in pre-existing branches (Smith et al., 2013b). However, the study used dimerised VCA constructs and it is yet unclear whether similar steps apply to monomers or oligomers of full-length NPFs. Furthermore, the model is incomplete as it does not take into account the conformational changes in Arp2/3, the role of membrane forces in dissociation of the VCA domain or the sequence of events for cytoplasmic, rather than membrane-bound NPFs.

Formins nucleate longer unbranched actin filaments

The formin family provides an example of another type of nucleation. Formins are also highly conserved and contain 2 formin homology domains (FH1 and FH2) (Castrillon and Wasserman, 1994, Wasserman, 1998). FH1 binds profilin, a G-actin binding protein (Imamura et al., 1997, Watanabe et al., 1997); this has been shown to deliver actin monomers to the growing ends of filaments ((Sagot et al., 2002, Romero et al., 2004, Paul and Pollard, 2008); reviewed in (Carrier and Pantaloni, 1997). FH2 domains are sufficient to initiate actin nucleation; they act as homodimers, in an anti-parallel orientation, and abolishing dimerization abolishes actin nucleation (Li and Higgs, 2005, Copeland et al., 2004, Xu et al., 2004). Crystal structures of

mammalian formins show that the dimers form a ring structure (Lu et al., 2007, Shimada et al., 2004).

In contrast to Arp2/3, which effectively caps the pointed filament end, formins act as a processive, leaky cap on the barbed end, where they compete with capping proteins to regulate filament length (Harris et al., 2004, Moseley et al., 2004, Romero et al., 2004, Chesarone et al., 2009, Sagot et al., 2002). It is unclear whether this occurs before or after addition of new actin monomers (Otomo et al., 2005, Paul and Pollard, 2008). There is evidence to suggest that FH2 forms an open or closed ring conformation, which regulates advancement along the filament and actin monomer addition (Otomo et al., 2005).

Among the nucleators, formins have a unique ability to directly regulate both the actin and microtubule cytoskeletons. In vivo, direct interaction with microtubules was first described for the mammalian formin, mDia, in a Rho effector screen; mDia was shown to aid stabilisation and orientation of microtubules (Palazzo et al., 2001). mDia1 and mDia2 have also been shown to interact with microtubules plus end tracking proteins to stabilise microtubules (Wen et al., 2004, Lewkowicz et al., 2008). Further, epifluorescence and TIRF microscopy studies on mDia2 mutants have shown that formins' roles in actin and microtubule regulation can be genetically uncoupled (Bartolini et al., 2008).

Formins play an important role in both nucleation and elongation of actin filaments. They have been shown to drive the formation of several cellular structures, including filopodia (Schirenbeck et al., 2005), lamellipodia (Yang et al., 2007), stress fibres (Tominaga et al., 2000) and phagocytic cup formation (Seth et al., 2006). In terms of cell-cell contact, formins are also required for the assembly of adherens junctions (Kobielak et al., 2004), which contain transmembrane adhesion proteins. Consequently, formins play crucial roles in many cellular processes such as motility, adhesion, morphogenesis and division.

Arp2/3, nucleation-promoting factors (NPFs) and Rho GTPases

Arp2/3 is activated by NPFs to induce polymerisation; and the largest subgroup of NPFs are characterised by a C-terminal VCA domain (also called WCA; WASP homology 2/ connector/ acidic) (Stradal and Scita, 2006, Machesky and Insall, 1998, Miki and Takenawa, 1998). This family of proteins includes WASP, N-WASp (neural-WASp), WAVE1-3, WASH (WASP and SCAR homologue), WHAMM (WASp homologue associated with actin, Golgi membranes and microtubules) and JMY (junction-mediating regulatory protein). Despite the multiple domains present in each of these proteins, they have no intrinsic catalytic activity. Several of these proteins are regulated by autoinhibition in the cytosol (Kim et al., 2000), as described below. One of the mechanisms of releasing this autoinhibition is through the binding of small GTPases, such as Cdc42 and Rac1 (Rohatgi et al., 2000). Binding of Cdc42 and the weaker interaction of Rac1, to WASP was first described in yeast two-hybrid studies and overlay assays. Binding was linked to actin polymerisation and was shown to depend on GTP-bound conformations of the GTPase, although WASp did not activate the GTPase (Aspenstrom et al., 1996, Symons et al., 1996, Kolluri et al., 1996, Abdul-Manan et al., 1999).

The Rho family GTPases are well described regulators of many cellular processes, including cytoskeletal organisation (Nobes and Hall, 1994). They are often described as molecular switches due to their ability to cycle between an active GTP-bound and inactive GDP-bound state (Boguski and McCormick, 1993). The switch is carefully regulated by a large number of activators (GEFs; guanine nucleotide exchange factors) and inactivators (GAPs; GTPase activating proteins) (Etienne-Manneville and Hall, 2002). The three best-characterised members of the Rho GTPase family are Rho (three isoforms- RhoA, RhoB, RhoC), Rac (three isoforms- Rac1, Rac2, Rac3) and Cdc42.

Actin-related structures and cell adhesion

RhoGTPases, through a variety of different effectors, regulate assembly and disassembly of different actin structures, in response to a variety of different external stimuli (Etienne-Manneville and Hall, 2002, Hall, 2005). Rac has been shown to promote the formation of lamellipodia and thus is important for promoting protrusions at the front of a migrating cell (Ridley et al., 1992, Small et al., 2002). Rho has been shown to regulate the formation of stress fibres; it can form contractile actin and myosin filaments and stimulates contractility to allow retraction of the rear of a migrating cell (Ridley and Hall, 1992). It also promotes acto-myosin contraction in smooth muscle cells (Fukata et al., 2001, Sakurada et al., 2001). Cdc42 promotes formation of filopodia (actin-rich, finger-like extensions) (Kozma et al., 1995, Nobes and Hall, 1995) and has been shown to play a role in establishing polarity in yeast, *C. elegans*, *Drosophila*, epithelial cells and neurons (Etienne-Manneville and Hall, 2002).

Rho GTPases are anchored to membranes, where they can initiate actin polymerisation to drive processes such as macropinocytosis, membrane-ruffling and migration (Ridley, 2006). As well as their roles in cell morphology and migration, the Rho GTPases are involved in other processes such as cell-cell interactions, phagocytosis, cell cycle progression, vesicle transport and secretion (reviewed in (Etienne-Manneville and Hall, 2002, Hall, 2005).

Rho GTPases have been described as central regulators of podosome formation (Linder and Kopp, 2005). Podosomes are specialised cell adhesion structures containing an actin core surrounded by a ring of integrins, scaffold and actin-binding proteins (Linder and Kopp, 2005). Podosomes have mainly been described in myeloid cells in contact with the extra-cellular matrix, where they have a role in concentrating proteinases involved in matrix degradation (Linder, 2007). A podosome-based sealing zone is formed by actively bone-resorbing osteoclasts, highlighting the role of podosomes in cell adhesion (Destaing et al., 2003). The adhesion forces created by podosomes turning over behind the leading edge of a migrating cell are important for driving forward propulsion (Calle, 2006a). An example of these is shown in

Movie 4.6. Cdc42 localises to podosomes in macrophages and microinjection of mutated Cdc42 results in impaired podosome formation in macrophages and DCs (Linder et al., 1999, Burns et al., 2001). Conversely, constitutively active Cdc42 expression promotes the formation of podosome-like actin structures in HeLa cells (Dutartre et al., 1996). As described, Cdc42 interacts directly with WASp, to promote Arp2/3 mediated actin polymerisation (Machesky and Insall, 1998, Millard et al., 2004). It has been suggested that this pathway plays a crucial role in podosome dynamics (Linder et al., 1999). WASp-deficient DCs and macrophages show severe defects in podosome formation on glass or fibronectin-coated coverslips (Linder and Kopp, 2005; Humphries et al., 2006). Disruption of Rac1 or RhoA has also been shown to lead to abnormal podosome formation (Burns et al., 2001, West et al., 2000, Ory et al., 2000). However, the precise effect of Rho GTPase disruption in each of these is complicated, suggesting that several Rho GTPases may be involved and the relationship between these is unclear.

Other actin regulators

Nucleation is just one aspect of actin regulation; indeed the actin cytoskeleton is not exclusively made up of actin but also includes many diverse actin-binding proteins resulting in the largest known network of protein-protein interactions (Dominguez, 2004, Pollard et al., 2000).

Profilin, for example, is a G-actin-binding protein, which sequesters actin monomers from the cellular pool (Carlsson et al., 1977). Profilin also has a 10-fold higher affinity for actin-ATP than the ADP-bound actin complex and this has been suggested to aid polymerisation of actin filaments in collaboration with both formin and WASp family members (Ferron et al., 2007, Paul and Pollard, 2008). Together with the diverse effects of the filament-severing protein cofilin (Van Troys et al., 2008), these two proteins can promote actin filament treadmilling.

Gelsolin, and other structurally similar severing proteins (Way and Weeds, 1988), acts to sever existing actin filaments. Its action is dependent on calcium concentration and it may have a role both intra- and extra-cellularly (Sun et al., 1999, Koya et al., 2000).

Actin capping proteins also play an important role in the regulation of actin dynamics. Capping protein (CP) caps actin filament barbed ends, preventing elongation (Caldwell et al., 1989). Using a purified protein system, it has also been shown that CP can increase the frequency of Arp2/3 nucleation, thus affecting actin-mediated motility (Akin and Mullins, 2008). Further, a number of other proteins bind to and regulated CP, suggesting a diverse network able integrate several signals to control actin filament length in a range of processes (Cooper and Sept, 2008).

Myosin motor proteins can organise the cellular actin network and produce forces promoting actin-mediated contraction. These are important both for cell adhesion and migration (Naumanen et al., 2008, Keren et al., 2009). Retrograde flow of actin filaments in migrating cells has been shown to be mainly powered by myosinII and the myosin inhibitor blebbistatin disrupts this flow (Naumanen et al., 2008).

Another group of proteins regulating actin structure are the actin-bundling or crosslinking proteins. These include fascin, villin, filamin and α -actinin; and have been well-described particularly in cell adhesion (stress-fibre formation) or the formation of microvilli and filopodial protrusions (Nakamura et al., 2011, Khurana and George, 2011, Naumanen et al., 2008).

Dorsal and ventral stress fibres attach to cell adhesion structures at one or both ends, they play roles in adhesion, contraction and cell motility and several types may be present in a cell at the same time (Pellegrin and Mellor, 2007, Naumanen et al., 2008). The adhesion structures themselves, such as focal contacts and podosomes, have been described as both adhesion and signal transduction organelles and are rich in integrin molecules (Riveline et al., 2001). Integrins mediate cell-cell and cell-ECM (extracellular matrix) adhesion and can be activated by

a large number of molecules through 'inside-out' and 'outside-in' pathways (Zhang and Wang, 2012). Integrins play crucial roles in survival, migration, adhesion, proliferation and differentiation of immune cells and mutations can cause autoimmunity or immunodeficiency (Zhang and Wang, 2012).

For most cells in the body, organisation in tissues and strict regulation of cell division or migration are crucial for correct function. For immune cells however, functionality is highly dependent on efficient migration, cell division, ability to cross barriers and to form different cell-cell contacts.

2. *The Immunological Synapse*

The immunological synapse (IS) is the name given to the contact interface between cells of the immune system, which acts as a platform for communication between these cells. Although initially described between T cells and antigen presenting cells (APCs; presenting peptide-MHC) (Grakoui et al., 1999), the synapse is now known to form between a number of different cells, including natural killer (NK) cells (Davis et al., 1999) and B cells (Batista et al., 2001). The IS can also form between cells of varying activation status as part of secondary or 'repriming' activation, for example between activated T and B cells (Okada et al., 2005), or between two activated T cells (Sabatos et al., 2008). Although the activated T: B cell synapse has been the prototype for IS formation (Monks et al., 1998, Kupfer et al., 1987, Monks et al., 1997), it is now accepted that dendritic cells (DC), as the main professional antigen presenting cell type, is responsible for most primary activation. Formation of the immune synapse is vital for full immune response priming.

On the DC side

Dendritic cells are professional antigen presenting cells with a widespread distribution in peripheral tissues, as well as both primary and secondary lymphoid organs. Several subtypes, performing different functions, have been described which share generally related morphology. In steady state conditions, four types of DCs have been described in primary and secondary lymphoid organs (spleen and lymph nodes), which include CD4+, CD8+, double negative and plasmacytoid dendritic cells (Wu and Liu, 2007). These cells spend their life restricted to one lymphoid organ; they present foreign and self-antigens in that lymphoid tissue. CD8+ cells are concentrated in T cell areas of the spleen, while CD8- cells are found in the marginal zone though can be induced to migrate to T cell zones using microbial peptides. The plasmacytoid DCs (pDCs) are a relatively round, long-lived cell type, which upon detection

of viral or microbial compounds produce large amounts of type-I interferons (O'Keeffe et al., 2002).

Lymph nodes and peripheral tissues contain two more types of conventional DCs (cDCs) – Langerhans and dermal (CD11b+) DCs. These are migratory subtypes, which act as sentinels in the periphery and present antigens to T cells in the lymph nodes (Shortman and Naik, 2007). During infection or inflammation, further DC subsets develop, including monocyte-derived DCs and TNF-producing and inducible nitric-oxide synthase-producing DCs (Serbina et al., 2003).

Although DCs were originally considered to have a myeloid origin, both common myeloid progenitors (CMPs) and common lymphoid progenitors (CLPs) have shown the potential to differentiate into various DC subsets both in vitro and in vivo (Traver et al., 2000, Manz et al., 2001, Chicha et al., 2004).

In vitro, mouse DC function has been investigated using several culture models for DC development. Splenocytes have been cultured in GM-CSF producing DCs with features reminiscent of inflammatory DCs (Berthier et al., 2000, Shortman and Naik, 2007). Mouse bone marrow (BM) cells have been cultured in GM-CSF or Flt3 ligand to produce conventional migratory DCs, though Flt3L additionally results in differentiation of pDCs (Inaba et al., 1992, Brasel et al., 2000, Gilliet et al., 2002). DCs derived from bone marrow or spleen express comparable levels of MHCII and costimulatory molecules and have been shown to induce similar levels of proliferation and IL-2 secretion by antigen-specific T cells using soluble peptide antigen (Garrigan et al., 1996). Using native protein antigens however, BMDCs maintain their capacity to process antigen longer and were shown to be 50 times better than splenic DCs at stimulating antigen-specific T cells (Garrigan et al., 1996). More recent experiments suggest that BMDCs are able to donate processed antigens to other cells, but unlike splenic primary cells, they are unable to acquire and present antigens from other DCs (Bedford et al., 2008).

As described in this section, it is known that DCs play a role in IS formation and T cell activation, however, the organisation, dynamics and driving forces behind the IS, as well as its importance for the DC have been neglected (Delon and Germain, 2000, Rodriguez-Fernandez et al., 2010).

Molecular structure and cell morphology

The immune synapse was first described in 1998 by Monks *et al.*, as a complex structure formed at the interface between T and B cells, with distinct molecular clusters (Monks et al., 1998). TCR/MHC pairs were shown to concentrate in the central supramolecular activation cluster (cSMAC). These are surrounded by outer rings containing LFA-1/ICAM-1 in the peripheral (p) SMAC, and CD45 in the distal (d) SMAC (Fig1). It has been suggested that this organisation is formed and stabilised by the actin cytoskeleton. The synapse structure was shown to be dynamic, with TCR initially engaged in the outer rings of the interface migrating towards the cSMAC in the centre (Grakoui et al., 1999).

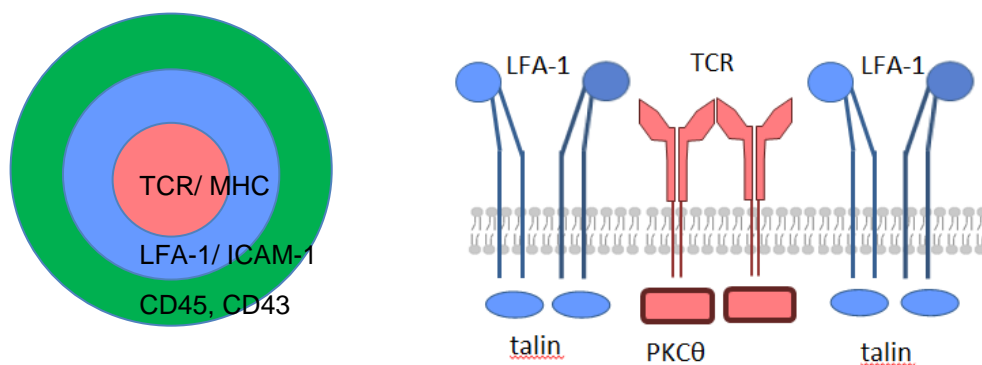


Figure 1.1. **Immunological synapse organisation.**

Monks, C.R., et al., *Three-dimensional segregation of supramolecular activation clusters in T cells*. Nature, 1998. **395**(6697): p. 82-6.

The TCR-peptide-MHC complex is approximately 13nm long so in order to bring the components together and allow antigen-recognition, the opposing membranes of the T cell and DCs must come within this distance, forming a very intimate contact (Garcia et al., 1996, Garboczi et al., 1996, Shaw and Dustin, 1997). The spacing between apposed membrane may be involved in protein sorting and organisation at the interface (Davis et al., 2003, Shaw and Dustin, 1997). Indeed, altering the extracellular length of peptide-MHC complexes has been shown to affect TCR signalling (Choudhuri et al., 2005). A more recent study used a range of fluorescent particles to show that these were excluded according to size from the cSMAC of synapses formed between NK and B cell lines (Alakoskela et al., 2011). However, it is likely that other sorting mechanisms are also at play since exclusion of CD43 from the IS was shown to depend on interactions of its cytoplasmic tail rather than its extracellular size (Delon et al., 2001).

Other molecules also show very specific organisation. The phosphatase CD45 for example, is excluded from the central and peripheral SMAC; it has been suggested that this minimises premature signalling deactivation (Davis and vanderMerwe, 1996, Shaw and Dustin, 1997, Thomas, 1999, Leupin et al., 2000).

As well as signalling and adhesion domains within the synapse, secretory domains in the form of clefts have also been observed in T: DC or cytotoxic T lymphocyte (CTL): target cell contacts (Brossard et al., 2005, Stinchcombe et al., 2001). These may be the target areas for directed secretion and may serve to restrict or concentrate signalling molecules.

In vivo, DCs migrate fast in tissue and upon initial lymph node entry; they then slow down and form networks. T cells move rapidly in a random amoeboid manner, scanning the antigen repertoire present (Miller et al., 2002, Miller et al., 2003, Miller et al., 2004a, Lindquist et al., 2004). Cahalan *et al* showed that as a result of fast T cell locomotion and extensive DC protrusions, each DC contacts up to 5000 T cells per hour, hugely increasing the chance of contacting rare antigen-specific T cell clones (Miller et al., 2004a).

Interactions between helper T cells and antigen-presenting cells may last over 6 hours and require continuous T cell receptor (TCR) engagement (Huppa et al., 2003); although some evidence, especially in vivo, has shown a much more dynamic nature with several short contacts before stable interactions are established (Mempel et al., 2004, Miller et al., 2002). There is evidence to suggest that the length of contact may be influenced by T cell intrinsic factors, such as presence of WASp (Sims et al., 2007), as well as the potency of activation, for example antigen dose (Skokos et al., 2007, Henrickson et al., 2008).

One interesting question is how a highly motile T cell is able to arrest upon encounter of specific antigen-containing MHCII and how it is able to regulate different cytoskeletal systems to switch from a role in migration to one in stable adhesion. Such a stop signal has been proposed to occur early and in vitro studies suggest it may be dependent on intracellular calcium levels (Dustin et al., 1997, Donnadieu et al., 1994, Negulescu et al., 1996). Arrest of cells with high intracellular calcium (above 150 μ M) has also been observed in vivo (Wei et al., 2007b). Complete early T cell arrest is still disputed and some in vivo studies have shown initial slowing of T cells, which is followed by arrest much later, around 24 hours after antigen administration (Mempel et al., 2004, Miller et al., 2002, Miller et al., 2004a). The authors have noted that some events resulting from TCR triggering, for example CD69 upregulation, occur before full T cell arrest. This suggests that even a brief interaction with DCs is sufficient for this early level of activation. No cytokine secretion or CD25 (IL-2 receptor) upregulation was seen (Mempel et al., 2004). T cell arrest has also been suggested to correlate with antigen dose or potency (Henrickson et al., 2008, Skokos et al., 2007, Beemiller et al., 2012) implicating a role for TCR signalling in initiating arrest. Although full T cell arrest may not be required for TCR signalling (Beemiller et al., 2012, Moreau et al., 2012, Friedman et al., 2010), it is often seen during later activation stages (Mempel et al., 2004, Miller et al., 2004b, Hugues et al., 2004, Shakhar et al., 2005).

One model, built on electron microscopy data, proposed that synapse architecture is developed during 4 distinct stages in CD4 cells interacting with cognate-antigen expressing B cells (Ueda et al., 2011). The first stage (around 30 min) involves deep protrusions from the T cells into the interacting APC and the authors suggested that this could increase the surface area scanned by the T cells by around 10-fold. During the second and third stages (1-2hrs), the microtubule cytoskeleton is reorganised and the T cell MTOC repositioned beneath the contact zone. After around 4 hours, a flattening of the cell-cell interface and repositioning of the Golgi complex towards the IS, correlated with cytokine secretion, are characteristic of the fourth stage (Ueda et al., 2011). Although it is unclear whether this mechanism of organisation is employed by other cell types in other contexts, this study does highlight the importance of dynamic synapse organisation and how dynamics could play an important role in regulating cell-cell communication.

One in vitro study showed that after initial contact of T cells with DC, mature DCs were able to extend membrane protrusions and migrate their cell body towards the interacting T cell in a Rho GTPase-dependent manner; which immature DCs were unable to do (Benvenuti et al., 2004a). The authors suggest this may be a specialised feature of the mature DC cytoskeleton in order to stabilise the DC: T cell contact.

It is clear that formation of the IS between T cells and dendritic cells, requires the dynamic organisation of actin, described in the previous section, to spatially distribute activation clusters (Monks et al., 1998) with distinct protein compositions.

Signalling

Upon TCR engagement, the activation of tyrosine kinases and calcium mobilisation precede IS formation. Recognition of peptide-MHC promotes conformational changes within the TCR and TCR-bound CD3. Lck and Fyn (Src family kinases) phosphorylate tyrosine residues in the immunoreceptor tyrosine-based activation motifs (ITAMs) in the cytoplasmic CD3 δ , ϵ , γ and ζ

chains, initiating downstream TCR signalling (Abram and Lowell, 2007). ZAP-70, another tyrosine kinase is recruited to the phosphorylated TCR (Chan et al., 1992) (see Figure 1.2, p48). ZAP-70 is also phosphorylated by Lck, and in turn phosphorylates LAT (linker for activation of T cells), allowing recruitment of PLC γ and SLP76. The former generates IP $_3$ to induce calcium mobilisation; and DAG for membrane recruitment of downstream proteins including PKC θ (protein kinase C θ) and activators of the mitogen-activated protein kinase (MAPK) pathway (Huse, 2009). The latter, interacts with the kinase Itk, the guanosine nucleotide exchange factor (GEF) Vav-1 and the non-catalytic adaptor protein Nck (Koretzky et al., 2006). Nck interacts with several Arp2/3-regulating factors such as WASp and WIP to trigger actin polymerisation, perhaps initiating the retrograde flow discussed above. Vav-1 can activate Cdc42 to regulate WASp directed actin polymerisation (Reicher and Barda-Saad, 2010). Negative regulation is also present in these early signalling events. One example is the tyrosine phosphatase CD45, which can activate but also inhibit Lck by removing activating phosphotyrosine residues (Thomas and Brown, 1999).

Several lines of evidence have led to the understanding that the majority of TCR signalling actually occurs in TCR microclusters, long before they reach the cSMAC. TCR signalling is initiated before formation of the cSMAC (Krummel et al., 2000, Lee et al., 2002) and the cSMAC itself has relatively low levels of activated Lck and ZAP-70 (downstream of TCR activation). By contrast, putative markers of TCR signalling, Lck and PKC θ , colocalise with the pSMAC (Lee et al., 2002). Using total internal reflection fluorescence microscopy, Campi *et al* demonstrated TCR microclusters generated after cSMAC formation arise in the periphery and contain around 10-17 TCRs (Campi et al., 2005). Further studies showed continuous formation of microclusters and the recruitment of SLP-76 and phosphorylated Lck and ZAP-70 (Yokosuka et al., 2005). Association with these molecules is lost towards the cSMAC, where TCR signalling appears to be terminated (Varma et al., 2006). Further, treating T cells with the Src tyrosine kinase inhibitor PP2, resulted in inhibition of Lck and Fyn – tyrosine kinases important for TCR

activation. This blocked ZAP70 recruitment to the IS but not microcluster formation, suggesting that microclusters are the sites of TCR signalling (Campi et al., 2005).

With such experimental approaches however, it can be difficult to dissect the precise roles different synapse areas and the protein composition in these. Computational models can be useful to delineate the roles of separate processes by changing individual factors. Lee *et al* included the basic principles of TCR signalling; such as TCR phosphorylation, ZAP70 recruitment and phosphorylation, adaptor recruitment, basic feedback loops and receptor translocation; in a mathematical model of synapse interface organisation (Lee et al., 2003b). They were able to show that the cSMAC enhances TCR triggering by concentrating antigen, TCR and downstream signalling molecules but this increased receptor activation in turn leads to more complete phosphorylation and receptor degradation. The overall effect is to downregulate TCR signalling in the cSMAC over time, thus its initial role in receptor activation might have been overlooked by experimental analysis alone. Thus the cSMAC controls the balance between strong TCR signalling, sufficient for full T cell activation, and signal limitation, to protect T cells from overstimulation and apoptosis.

The authors use a model of poor cSMAC formation to experimentally confirm computational findings. CD2AP, which interacts with the cytoplasmic domain of the adhesion protein CD2, is required for correct molecular patterning at the synapse and formation of a cSMAC (Dustin et al., 1998). CD2AP^{-/-} T cells do not form clearly defined c- and pSMAC in cell-cell conjugates but show homogeneous distribution of TCR and integrins. These cells showed increased proliferation and IL-2 secretion; and due to such prolonged overstimulation, they also exhibited enhanced apoptosis compared to controls (Lee et al., 2003b).

This model has further implications for TCR signalling cascades following high vs low affinity agonists. High affinity antigens may be able to induce signalling without cSMAC formation. The time necessary for receptor-ligand binding is short enough compared to the rate of dissociation that signalling complexes do not need to concentrate in the cSMAC.

Indeed, both mathematical models and experiments analysing T cells on lipid bilayers, suggest that clustering of fully activated and phosphorylated TCRs in the cSMAC favours their internalisation and degradation. Strong cSMAC signalling can be seen only upon blocking receptor degradation (Lee et al., 2003b). Mossman *et al* showed further support for this level of signalling regulation by using patterned substrates to reduce lateral protein mobility (Mossman et al., 2005). They showed that mechanically trapping TCR microclusters in the periphery of the synapse resulted in prolonged signalling in these clusters.

TCR downregulation has been shown to involve internalisation of receptors and targeting to lysosomes (Valitutti et al., 1997). The concentration of multivesicular bodies in the cSMAC suggests that this is the site of receptor internalisation (Varma et al., 2006). Further, ubiquitin and the TSG101 protein, part of the ESCRT-I complex which sorts ubiquitinated substrates for degradation, are required for the formation of a cSMAC in T:B cell conjugates (Vardhana et al., 2010). Studies of weakly binding MHC agonists provide support for the cSMAC receptor degradation paradigm. Transgenic T cells expressing reduced affinity TCRs are able to reduce cSMAC accumulation of TCRs and thus diminish receptor downregulation (Cemerski et al., 2007). TSG101 is not recruited to the cSMAC of these synapses and does not alter the size or signalling capacity of TCR microclusters, suggesting it plays no role in early TCR signalling (Vardhana et al., 2010).

The above studies suggest the cSMAC has an important role in detecting antigen strength/potency as it can amplify signals from weak ligands while limiting those from strong ones.

A recent study investigated how many of these synaptic components are recruited and involved in signalling at the immune synapse over time (Philipsen et al., 2013). The authors use antigen-specific B:T cell conjugates and show several distinct stages of synapse evolution and maturation. After initial T cell re-orientation, the cSMAC (containing CD3 ϵ) began to appear after 10minutes of contact. Around 30-60minutes, co-stimulatory proteins such as CD86 and CXCR4 were recruited, suggesting structural reinforcement; while CD45R was excluded from

the synapse area. The authors have shown a gradual increase in pZAP70, pLAT and pSLP76, suggesting elevated signalling, which peaked between 60-120minutes. While these results are consistent with previous studies showing prolonged contacts and increased binding forces between T cell and APC (Hosseini et al., 2009), the authors imply that signalling gradually shifts from the pSMAC (peak at 60min) to the cSMAC (higher at 120min), which has not been described previously.

There is also controversy surrounding the steady state stoichiometry of surface TCR-CD3 complexes. One study has shown a mixture of single molecules and complexes of between 2-20 TCR subunits (Schamel et al., 2005). The authors suggest that the coexistence of these species aids sensitivity and allows for distinction between high and low antigen concentrations. More recently, it has been suggested that TCR and LAT are located in separate 'protein islands' on the surface of resting cells. Upon TCR engagement, these domains concatenate forming signalling microclusters (Lillemeier et al., 2010). Although this is a useful model combining levels of temporal and spatial regulation, the precise mechanism is likely to be more complicated. Vesicles carrying signalling molecules have been described as key players in correct spatiotemporal synaptic organisation (Soares et al., 2013). It has been suggested that two populations of pLAT clusters coexist at the synapse interface: one is pre-existing round clusters, similar to resting cells, the other have an elongated shape which is the result of Rab27a-Rab37-Ti-VAMP- targeted vesicle fusion. Soares *et al* suggests it is the latter form of clusters which preferentially recruit pSLP76 and thus transduce TCR signalling. Exact LAT signalling localisation remains an area of active research. Some have suggested that the majority of signalling occurs as a result of phosphorylating plasma membrane LAT (with a small contribution from the vesicular pool) – (Houtman et al., 2006, Balagopalan et al., 2013). Others however, have shown evidence for SNARE-mediated LAT vesicles which dock at the synapse and it is this recruited population of LAT, rather than pre-existing surface LAT clusters, that is responsible for downstream signalling (Purbhoo et al., 2010, Williamson et al., 2011, Larghi et al., 2013). The precise organisation of TCR and downstream signalling molecules requires

further analysis or confirmation; in particular, the use of new super-resolution microscopy techniques may provide more insights.

Actin at the synapse

The vast majority of studies point to a centripetal actin flow as the major driving force behind the specific organisation of the synapse (Barda-Saad et al., 2005, Billadeau et al., 2007, Kaizuka et al., 2007, Hartman et al., 2009, Yu et al., 2010). When T cells were treated with actin-depolymerising drugs, TCRs failed to polarise and did not show free lateral diffusion (Krummel et al., 2000). TCR stimulation has been shown to induce dramatic cytoskeletal changes which mould the interface between the T cell and APC (Gomez and Billadeau, 2008). Actin polymerisation drives radially symmetric spreading to increase contact surface area with the APC. F-actin is then shaped into a peripheral ring, which has been suggested to regulate trafficking and clustering of synaptic components (Bunnell et al., 2001, Varma et al., 2006, Nguyen et al., 2008, Sims et al., 2007, Babich et al., 2012).

Kaizuka *et al* showed robust, symmetric polymerisation-driven retrograde flow coupled to the flow of TCR and ICAM-1 microdomains (Kaizuka et al., 2007). In these experiments, the movement of TCR microclusters was reported to be at 40% of the speed of actin flow. Some elegant experiments using molecular mazes have provided further evidence for centripetal actin flow beneath the membrane, which translocates TCR microclusters towards the cSMAC (DeMond et al., 2008). The authors suggest that the size of the microcluster or its activation state may either initiate inward actin flow or induce coupling of the clusters to the actin network. DeMond *et al* were able to suggest an explanation for the uncoupling of translocation speeds seen previously, namely many weak, transient interactions between actin and individual receptors within a cluster, which maintain cluster attachment over time. Further, Ilani *et al* showed that TCR microcluster movement as well as signalling from these

clusters are dependent on myosin IIA (Ilani et al., 2009). This study however did not determine the site of action of myosinII or the precise organisation of F-actin in the IS. More recently, actin dynamics have been shown to affect the kinetics of interactions between TCR and MHC (Huppa et al., 2010, Huang et al., 2010), highlighting the importance of the actin network in TCR signalling. Conversely, laterally restricted TCR microclusters can slow down local actin cytoskeleton dynamics in a direction-dependent manner (Yu et al., 2010, Smoligovets et al., 2012).

Centripetal movement of actin is well-characterised – the actin network undergoes continuous polymerisation towards the leading edge (the distal SMAC, responsible for cell spreading over the APC), establishing a flow of existing actin filaments in the opposite direction. Retrograde flow is dependent on continued actin depolymerisation (Vallotton et al., 2004) and depolymerisation in the central region of the contact has been observed in T cell dynamically interacting with lipid bilayers (Beemiller et al., 2012). This organisation could be expected to depend on actin depolymerising proteins and regulators. Indeed disrupting cofilin function has been shown to interfere with IS formation and results in functional abnormalities in proliferation and cytokine secretion (Eibert et al., 2004). Beemiller *et al* suggest that while polymerisation is still the driving force behind actin flow (Varma et al., 2006, Kaizuka et al., 2007), generating a lower viscosity region in the centre allows continuous movement of actin, which compresses the TCR microclusters into the central low actin region (Beemiller et al., 2012).

Although confocal imaging suggests clearance of actin from the cSMAC (Orange et al., 2003), it is unlikely that this is complete. Higher resolution structured illumination microscopy (SIM) or stimulated emission-depletion microscopy (STEDM) show residual actin across the centre of NK cell synapses (Brown et al., 2011, Rak et al., 2011). Rak *et al* in particular show granules surrounded by an actin network, which provides support for a role of actin and myosinII in exocytosis (Masedunskas et al., 2011, Nightingale et al., 2011). Further high-resolution studies

are required to understand the organisation of actin in the cSMAC and these would have to consider actin as a 3D structure, including networks running both parallel and perpendicular to the IS interface and their respective roles in IS formation.

It has been proposed that the immunological synapse represents a symmetric version of the organisation present in a migrating cell, where the cSMAC corresponds to the uropod, the pSMAC corresponds to the lamellum and the dSMAC to the lamellipodium (Dustin, 2007). If this is the case, one can conclude that the myosinII-regulated contraction of transverse actin bundles seen in migration (Gardel et al., 2010), may co-operate with polymerisation-driven forces during the formation, organisation and long-term stabilisation of the synapse. Evidence for this was provided in a study by Yi and colleagues, who use fluorescently tagged actin and myosin to reveal a concentric ring of actomyosin arc contraction in the lamellum/pSMAC, surrounded by actin retrograde flow in the lamellipodium/dSMAC (Yi et al., 2012). Using different inhibitors the group was able to show that both actin-dependent forces are required for TCR clustering into the cSMAC. There is also evidence for a role of myosinIIA in calcium signalling and correct Zap-70 localisation (Yu et al., 2012).

Cell polarity and MTOC translocation

Lymphocyte polarisation plays a role in regulating their function. TCR signalling results in the mobilisation of the microtubule organising centre (MTOC) towards the IS (Gomez and Billadeau, 2008). Further, during the formation of natural killer (NK) cell synapses, the NK cell adheres to its target and polarises its actin cytoskeleton. The MTOC then translocates towards the target cell, reminiscent of T cell synapses. In T cells interacting with immobilised, photoactivatable peptide-MHC, MTOC repositioning has been shown to occur within 2 minutes of activation (Huse et al., 2007, Quann et al., 2009). TCR stimulation and the early TCR signalling molecules, including Lck, ZAP70, LAT and SLP-76, have been shown to be important (Sedwick et al., 1999, Kuhne et al., 2003, Lowin-Kropf et al., 1998); indeed T cells contacting

several APCs are able to polarise towards that presenting most peptide-MHC (Depoil et al., 2005, Huse et al., 2007), presumably by detecting level of TCR stimulation.

MTOC polarisation, which also results in the migration of Golgi and endoplasmic reticulum (ER), has been proposed to allow recruitment of lytic granules and degranulation in CTL and NK cells specifically towards the target cell (Orange, 2008). Requirement for directional secretion has also been described in CD4 cells, which appear to utilise two distinct secretory pathways – a multidirectional chemokine pathway and a polarised cytokine secretion pathway which is crucially dependent on WASp function (Huse et al., 2006, Morales-Tirado et al., 2004). Another role of T cell MTOC polarisation may be the orientation of the T cell for asymmetric cell division, which may be involved in developing memory T cells (Chang et al., 2007).

Microtubules are bipolar, similar to actin filaments, and their positive ends radiate outwards with negative ends capped at the MTOC. MTOC reorientation appears to depend on pulling forces created by minus-end directed microtubule motors (Huse, 2009). Dynein is one such microtubule motor; its localisation to the IS is still not completely understood though some evidence suggests it may interact with ADAP, which is recruited to the LAT-Slp76 complex (Combs et al., 2006). Accumulation of diacylglycerol (DAG) and a cascade of PKC isozymes at the synapse have also been linked with recruitment of dynein and MTOC polarisation (Quann et al., 2009, Quann et al., 2011). Ezrin, a protein acting as a bridge between the cytoskeleton and the plasma membrane has been suggested to regulate Discs-large homologue 1 (Dlg1) localisation (Lasserre et al., 2010). Depletion of Dlg1 itself reduced MTOC polarisation to the IS, which may implicate the Dlg1-containing Scrib complex, and its mutually inhibitory interactions with the Par (partitioning defective) complex, in immune cell polarisation and synapse formation (Nelson, 2003, Huse, 2011). Indeed, there is some evidence for a role of these polarity complexes in T cell polarity upon IS formation although this mechanism seems to develop later and may be involved in long-term maintenance rather than initiation of polarization (Ludford-Menting et al., 2005, Bertrand et al., 2010). In NK cells, VAV1 has been

identified as a regulator of both actin and microtubule dynamics required for cytotoxicity at the IS (Graham et al., 2006). In CD8 T cells, Cdc42 has been shown to play a role in MTOC reorganisation (Stowers et al., 1995). Further, the Cdc42-interacting protein 4 (CIP4) interacts with WASp, Cdc42 and tubulin and is required for full MTOC migration in NK cells (Banerjee et al., 2007).

Although the precise molecular mechanism needs clarification, coupling to a functional actin cytoskeleton appears to be essential (Orange et al., 2002, Graham et al., 2006). F-actin clearance from the central synapse area (cSMAC) appears to be required for migration of the MTOC towards the IS and to allow lytic granules to reach the plasma membrane (Stinchcombe et al., 2006, Huse, 2012, Orange et al., 2003, Andzelm et al., 2007), though some residual actin appears to play a part in completing exocytosis (Brown et al., 2011, Rak et al., 2011). Coordination between the actin and microtubule cytoskeleton is also apparent in studies of casein-kinase I- δ (CKI δ) and IQGAP1, which interact with both actin- and microtubule-binding proteins, and when depleted in Jurkat cells or NK cell lines respectively, result in diminished MTOC polarisation (Zyss et al., 2011, Stinchcombe et al., 2006).

A recent study challenged the motor-driven cortical sliding mechanism for MTOC relocation (Yi et al., 2013). Their optical trap experiments showed two distinct stages in the process – MTOC translocation and docking. Their imaging suggested that MTOC polarisation is the result of dynein-driven microtubule end-on capture-shrinkage directly to a point in the centre of the synapse (Yi et al., 2013). It would be interesting to see if evidence for this mechanism develops further.

The role of integrins

The integrin LFA-1 (CD11a/CD18) has been shown to play a crucial role in the organisation of the NK cell IS (Liu et al., 2009). Binding of LFA-1 to its ligand induces actin reorganisation and NK cell polarisation (Mace et al., 2009). Activation of LFA-1 separates the two cytoplasmic tails

of this integrin, allowing talin to bind to the β -chain (CD18) and stabilise the open, active conformation. Talin subsequently activates actin polymerisation by two separate pathways. It can recruit the actin nucleator Arp2/3 through association with vinculin. Talin can also recruit PIPKI γ (phosphatidylinositol 4-phosphate 5-kinase type I) to the activated LFA-1. The product of PIPKI γ , PIP2 (phosphatidylinositol-4,5-bisphosphate) in turn recruits WASp (Mace et al., 2010).

The first LFA-1 ligand identified was ICAM-1 (Dustin et al., 1986, Rothlein et al., 1986). LFA-1 can be fully activated by cluster organisation through lateral mobility or increased force due to binding to ICAM-1 (Zhu et al., 2008, Dustin, 2009b). LFA-1 can also be activated through inside-out signalling, the precise details of which are still elusive. TCR activation recruits Vav, which can itself recruit talin to directly interact with cytoplasmic integrin tails as discussed above (Gomez and Billadeau, 2008). The accumulation of DAG, following TCR signalling, also results in the recruitment of the Rap-1 GEF C3G (Krawczyk et al., 2002, Nolz et al., 2008). Rap-1 is thought to activate RIAM (Rap-GTP interacting adaptor molecule), which in turn allows recruitment of vinculin and talin (Nolz et al., 2007). Talin is required for LFA-1 mediated cell adhesion (Smith et al., 2005, Mace et al., 2009). Several studies have demonstrated the importance of LFA-1 in combination with an activated receptor for the symmetric organisation of the IS (Somersalo et al., 2004, Anikeeva et al., 2005, Markiewicz et al., 2005).

Although clearly crucial for T cell: APC adhesion, there is also evidence for a role of LFA-1 in signal transduction (Abraham et al., 1999, Perez et al., 2003). An early report by van Seventer *et al* showed that engagement of LFA-1 by plate-bound ICAM-1 enhanced T cell activation following TCR/CD3 cross-linking (Vanseventer et al., 1990). LFA-1 engagement was also able to enhance total T cell activation induced by PMA and ionomycin, suggesting that the adhesive role of LFA-1 in this process was irrelevant. Abraham *et al* expressed a covalently coupled class II-peptide complex in order to increase the density of surface MHC/OVA compared to cells pulsed with exogenous peptide. They were able to show that increasing the density of

effective antigens by more than 10000 times, compared to the minimum required for naive T cell activation, does not induce T cell proliferation in the absence of ICAM-1 engagement (Abraham et al., 1999). Thus LFA-1 engagement affects both the quantity and quality of TCR signalling. The idea that integrins transduce signals is not novel (reviewed in (Dedhar and Hannigan, 1996, Parsons, 1996).

In support of this idea, it has been shown that LFA-1 engagement results in activation of PKC δ , which phosphorylates the β 2 chain of the integrin, promoting the release of JAB-1 (Perez et al., 2003). JAB-1 (Jun-activating binding protein 1) has been shown to modulate the activity of the transcription regulating complex AP-1 (Bianchi et al., 2000). Perez *et al* demonstrated increased translocation of phosphorylated c-Jun to the nucleus in T cells with CD3, CD28 and LFA-1 stimulation compared to CD3/CD28 alone. Further, the authors identified cytohesin-1 as the mediator of Erk1/2 phosphorylation following LFA-1 activation. Erk1/2 activity leads to c-Fos expression, which together with c-Jun forms AP-1, an early response transcription factor. Their results showed that these pathways promoted T cell activation (CD69, CD25 and IL-2 expression) and proliferation. A combination of antagonists against both JAB-1 and cytohesin-1 resulted in higher inhibition of IL-2 production than either antagonist alone. The authors also suggest that LFA-1 engagement polarises T cells towards a Th1 effector cell fate (discussed in chapter 5).

Altogether these results suggest that LFA-1 activation can transduce signals independent of the TCR signalling pathway and thus fine tune T cell signalling. One unanswered question is whether different LFA-1 ligands result in distinct downstream signalling. In the above study, Perez *et al* use soluble ICAM-2 to activate LFA-1 and downstream JAB-1 and cytohesin-1. In their hands, soluble ICAM-1 did not induce phosphorylation of Erk1/2. They suggest that this may reflect a distinction in signal transduction, though it is unclear whether they tested the effect of different ICAMs on the JAB-1-c-Jun pathway.

Cytohesin-1, through its GEF activity, has been shown to play a role in chemokine-induced leukocyte arrest and trans-endothelial migration (Weber et al., 2001). If different LFA-1 ligands do result in distinct downstream signalling, it is easy to see how ICAM-2 and -3 may be more important in the process of extravasation, while ICAM-1 regulates LFA-1 signalling during other processes, such as immune synapse formation. Another possibility may be a difference between soluble, cell surface and immobilised LFA-1 ligands. For example, plate-bound ICAM-1 has been shown to induce F-actin reorganisation downstream of LFA-1 (Porter et al., 2002).

LFA-1 has an important function in vivo as blocking its adhesion (independent of ligand) using LFA-1 antagonists has been shown to inhibit delayed-type hypersensitivity (Winqvist et al., 2001) and suppress inflammation in a peritonitis model (Weitz-Schmidt et al., 2001).

Like TCR microclusters, LFA-1 in the pSMAC is also highly dynamic (Sims et al., 2007, Kaizuka et al., 2007). This suggests that the IS represents a structure balancing many dynamic processes to produce a stable interaction, rather than employing more long-term adhesive forces. This may help to explain the similarities in the actin networks and regulators between the synapse and the motile T cell scanning structure dubbed the kinapse (Dustin, 2009b) (discussed in previous sections).

Function of the synapse

The role of the immune synapse is also still not fully understood. Many studies suggest it directs polarised release of cytokines in CD4 cells (Kupfer et al., 1991, Poo et al., 1988) or limits the area for secretion of perforin and granzymes by cytolytic cells to prevent bystander effects (Stinchcombe et al., 2001, Liu et al., 2009, Stinchcombe et al., 2011). While cytolytic molecules must be contained towards specific target cell, many chemokines for example need to be dispersed into the cellular environment. Huse *et al* have proposed that CD4 cells have directionally distinct pathways for exocytosis of different secreted factors (Huse et al., 2006). The authors show that Th1 cells secrete IL-2 and IFN γ directionally towards the synapse, while

TNF secretion is scattered and multidirectional. The two secretion pathways appeared to utilise distinct secretion proteins. This polarised secretion was also shown to be dependent on intact microtubule function. Further, the authors investigated cytokine secretion in Th2 and found IL-10 to be synaptically directed, while IL-4 localised to dispersed compartments throughout the cell (Huse et al., 2006). It is unclear whether similar bimodal secretion occurs in other T cell types or other immune cell lineages.

The precise organisation of secretory modules is also controversial. Stinchcombe et al have suggested a split central region architecture, where secretion occurs alongside the cSMAC (Stinchcombe et al., 2001). More recent evidence in T cells suggests that secretion can occur in various parts of the synapse (Beal et al., 2009). Further, the cytolytic synapse formed by NK cells appears to be able to form several actin-poor secretory domains at multiple sites (Rak et al., 2011, Brown et al., 2011).

Others have shown a very extensive, bidirectional communication involving gap junctions at the IS (Mendoza-Naranjo et al., 2011); and even trogocytosis – the intercellular exchange of membrane patches with different compositions (Ahmed et al., 2008). Crucially, cell polarisation and MTOC translocation described above can be expected to play a role in establishing a cell division plane parallel to the synapse interface in T cells, to allow asymmetric division seen upon specific antigen recognition (Chang et al., 2007, Oliaro et al., 2010).

Synapses between different cells are likely to have different functions and although many of the molecular complexes may be similar, there is no reason to believe that formation and organisation will involve the same processes and final outcomes. Whatever the organisation or role of the IS between T cells and DCs, there is general agreement that it leads to optimal T cell activation through both receptor signalling and degradation (Lee et al., 2003b). Further, the role of the T cell actin cytoskeleton in this process is widely accepted (Gomez and Billadeau, 2008, Dustin, 2009a). Most of our knowledge of synapses described so far comes from the more intensively studied T cell: B cell and T cell: lipid bilayer immune synapses. Although there

is evidence that the DC: T cell synapse forms a similar structure (Lee et al., 2002, Benvenuti et al., 2004b, Bouma et al., 2011) this has been controversial. Other groups, using fluorescence and electron microscopy, have suggested that DCs preferentially form a multifocal synapse (Brossard et al., 2005, Tseng et al., 2008).

As discussed, T cells are able to endocytose and degrade spent TCRs at the cSMAC. It is unclear whether similar event downregulation occurs on the DC side of the synapse. One group has suggested that peptide-MHC complexes are internalised and rapidly recycled back to the surface in a pathway distinct from newly synthesised MHCII molecules (Walseng et al., 2008). It is still unknown whether this recycling to the surface is targeted to cell: cell contacts in mature, polarised DCs.

Imaging the immune synapse

Large scale in vivo imaging is useful in determining the cell: cell interactions at play in relevant immunological environments during a whole-organism immune response. Lindquist et al for example, combine fluorescent marker expressing transgenic mice and two-photon microscopy to visualise lymph node DC networks and compare mature and immature cells (Lindquist et al., 2004). Multi-photon studies have revealed that T cells can migrate up to ten times faster than other cell types and arrest upon antigen encounter to allow activation (Stoll et al., 2002, Bousso et al., 2002, Miller et al., 2002, Mempel et al., 2004).

On a smaller scale, imaging the IS interface requires increased speed and resolution, in a set imaging plane. Several techniques have been developed to allow imaging in the interface plane and avoid reconstruction from multiple optical sections. Oddos et al used optical tweezers and confocal microscopy to show CD3 clustered in the centre of a T cell: B cell interface, with microclusters being formed in the periphery and some fluorescence loss in the very centre

which could correspond to internalisation (Oddos et al., 2008). The intricate cell capture and alignment however, result in very low throughput in this type of imaging.

Another system designed to induce IS formation in the horizontal imaging plane was developed by Biggs et al (Biggs et al., 2011). The group created PDMS micropits designed to capture single T cell: APC conjugates. The substrates allow analysis of multiple conjugates in a single imaging field thus significantly increasing throughput. Although this method proved useful for detailed analysis of an artificial APC system, it may be more difficult to maintain the interface plane when imaging cells of different sizes and shapes.

Supported planar bilayers have become an extremely useful method of imaging and modelling the IS interface. Supported bilayers are commonly formed from phospholipid liposomes, which fuse together on clean glass coverslips. Signalling or adhesion related proteins can be anchored to the upper leaflet of the bilayer and remain laterally mobile (Groves and Dustin, 2003). Although a more artificial technique for T cell activation, presenting MHC-peptide complexes and costimulatory molecules in this way can fully recapitulate the SMAC pattern on the T cell surface, described initially by Kupfer and colleagues. The use of total internal reflection fluorescence (TIRF) microscopy to image supported planar bilayers has improved resolution and increased the signal-to-noise ratio observed. In TIRF, the laser beam is directed at the glass surface at an angle greater than the critical angle, resulting in total reflection. The sample is illuminated by an evanescent wave produced, which penetrates no more than 200nm into the cell (Groves and Dustin, 2003). The technique allowed several groups to follow the translocation of TCR microclusters from the periphery to the cSMAC over time and led to the discovery that signalling-competent microclusters are formed continuously in the periphery (Varma et al., 2006, Yokosuka et al., 2005). Patterned substrates have also been used to analyse the importance of microcluster translocation (Groves and Dustin, 2003, Yu et al., 2010).

Single molecule fluorescence resonance energy transfer (FRET) combined with lipid bilayers has shown that F-actin networks beneath the synapse can regulate the TCR: MHC interaction by affecting the off-rate (Huppa et al., 2010).

Single-molecule localisation microscopy, such as photoactivated localisation microscopy (PALM) or stochastic optical reconstruction microscopy (STORM), can provide information about the nanoscale organisation of molecules at the synapse. It involves cycles of photoactivation, detection and bleaching of a fraction of molecules to build up an image of the population of fluorophores. This overcomes the diffraction limit of most light microscopy and allows resolution of around 20nm. This type of microscopy has been used by two groups to resolve how TCR and LAT come together during the initial stages of signalling. Mark Davis and colleagues combined PALM with membrane sheet electron microscopy to suggest that TCR and LAT are segregated in 'protein islands' at steady state, which concatenate but do not mix during signalling (Lillemeier et al., 2010). Dan Davies and Katharina Gaus used optical tweezers, confocal microscopy and PALM, combined with a novel method for data analysis to differentiate between LAT in the plasma membrane or that located in sub-synaptic vesicles (Purbhoo et al., 2010, Williamson et al., 2011). They argue that this vesicle-associated LAT population is recruited and phosphorylated upon TCR activation, without vesicle fusion with the plasma membrane. The differences in findings between these studies may reflect difference in cell types, time points or T cell activation methods used.

A recent study used STORM microscopy to examine the role of ITAM phosphorylation and suggested that this step was essential for induction of proliferation but dispensable for IL-2 production in T cells (Guy et al., 2013). This is an elegant example of how super-resolution microscopy can be used to address functional questions. Furthermore, the study also suggested a link between surface TCR-Notch1 clusters and the actin cytoskeleton through interaction with Vav1. Further analysis of this pathways would be invaluable for understanding the role of F-actin in IS formation.

In NK cells, structural illumination microscopy (SIM) and stimulated emission depletion (STED) microscopy have been used to study the actin cytoskeleton and have provided evidence for remodelling of the actin meshwork upon activation to create holes for the release of lytic granules (Brown et al., 2011, Rak et al., 2011).

Micromanipulation experiments have also shed light on interactions during T cell activation by analysing the affinity, kinetic rates and duration of TCR: MHC-peptide bonds between a T cell and a biomembrane force probe (BFP; bead attached to red blood cell). Initially it was shown that the strength, of an agonist bond correlated with a faster on-rate, unlike many other systems directed by off-rates (Huang et al., 2010). More recently, the same group used BFPs to show that force applied to the TCR:MHC complexes has differential effects on agonist and antagonist interactions. For agonists, force prolongs the lifetime of a single bond, described as a catch bond. For antagonists, force shortens the bond lifetime, resulting in a slip bond. The magnitude, duration and timing of the force applied, were all shown to affect T cell activation, highlighting a mechanosensory role for the TCR (Liu et al., 2014).

Recent advances in microscopy have greatly improved our understanding of T cell activation, however, further developments in high-speed imaging and 3D super-resolution, as well as analytical methods are required for a complete picture of how the signalling, adhesion and cytoskeletal systems combine and are controlled over time to contribute to the induction of tolerance or immunity. In particular, imaging events on the DC side would provide useful clues about how this contributes to IS organisation. Further adaptation of the supported planar bilayer system for DCs could be useful. In addition, super-resolution imaging techniques applied to cell: cell conjugates will be required to confirm findings in artificial bilayer systems.

3. *The T cell side: TCR signalling, costimulation and cytokines*

T cell activation

DCs are the most efficient antigen presenting cells (Mellman and Steinman, 2001). Antigen taken up by DCs is processed and presented by MHC class II to CD4+ T cells. Recognition of the antigen, along with expression and activation of costimulatory molecules results in activation of antigen-specific CD4+ T cells, leading to lymphoproliferation, cytokine secretion and upregulation of other activation markers (Caruso et al., 1997).

T cell activation is commonly described as a three-signal process. Signal 1 involves TCR recognition of a cognate peptide-MHC complex. As described in the previous section, this results in phosphorylation of CD3 chains initiating a cascade which results in calcium mobilisation, activation of GEFs and eventually gene transcription (Haskins et al., 1984, Cantrell, 1996, Smith-Garvin et al., 2009).

The second signal is provided by surface costimulatory molecules (Jenkins et al., 1990, Schwartz, 1992, Jenkins and Johnson, 1993). Interestingly, studies have suggested that the initial response of the immune system is similar for the first 3-4 days regardless of whether the eventual outcome is tolerance or immunity (Kearney et al., 1994). Such a late decision has been proposed to suggest that costimulatory signals must play an important role in polarisation of the immune response, rather than simply TCR antigen recognition (Gerard et al., 2013). This is supported by studies suggesting that TCRs can respond to multiple antigens, thus correct downstream activation may be dependent on other qualitative levels of stimulation (Colf et al., 2007, Felix et al., 2007).

Costimulatory ligands CD80 and CD86, expressed primarily on APCs, interact with CD28 or CTLA-4 on T lymphocytes and play a role in regulating T cell responses (Linsley et al., 1991). CD80 and CD86 are type I transmembrane proteins, members of the immunoglobulin superfamily, with short cytoplasmic domains and extracellular domain similar to Ig variable

and constant region (Peach et al., 1995). The cytoplasmic domains have been implicated in T cell activation, thus highlighting the role of the dendritic cell cytoskeletal network in signal transduction (Tseng et al., 2005). Further, MHCII signalling has also been shown to induce surface B7 (CD80) upregulation (Nabavi et al., 1992) to provide increased costimulation for T cells.

While CD28 appears to be expressed on a large number of T cells (Gross et al., 1992), CTLA-4 expression is restricted to activated T cells (Freeman et al., 1992, Linsley et al., 1992). CD28 provides a positive costimulatory signal by enhancing production of IL-2, reducing the threshold of TCR triggering for activation and promoting organisation of the IS (Viola et al., 1999, Wulfig et al., 2002). Transduction of B cell lines with B7 has been shown to provide sufficient costimulatory signal to induce T cell proliferation (Azuma et al., 1992, Norton et al., 1992). CD28 engagement was shown to be required for full activation of PKC θ , which in turn activates AP-1 and NF- κ B transcription factors (Sun et al., 2000, Coudronniere et al., 2000, Huang et al., 2002). Upon ligand binding, tyrosines in the cytoplasmic tail of CD28 are phosphorylated by Src-family kinases and in turn recruit proteins such as PI3K, Grb2, Vav1 and ITK (Huse, 2009). Most of these downstream effectors are also recruited upon TCR activation, suggesting that CD28 enhances TCR signalling through similar pathways (Acuto and Michel, 2003).

CTLA-4 on the other hand plays an important inhibitory role by blocking IL-2 gene transcription (partly by inhibiting the nuclear translocation of NF-AT (nuclear factor of activated T cells)) and inhibiting T cell proliferation (Krummel and Allison, 1996, Brunner et al., 1999). Further, CTLA-4-deficient mice show polyclonal T cell expansion resulting in lymphoproliferative disease with the majority of peripheral T cells exhibiting an activated phenotype (Waterhouse et al., 1995, Tivol et al., 1995). CTLA-4 deficiency also appears to result in preferential CD4 T cell expansion as depletion of CD8 cells in these mice has no effect on lymphoproliferation, while CD4 depletion prevents lymphoproliferative disease (Chambers et al., 1997). CTLA-4 ligation also

results in tyrosine phosphorylation (Miyatake et al., 1998) which may recruit phosphatases to dephosphorylate local TCR signalling effectors (Huse, 2009). CTLA-4 also has a 10-fold higher affinity and 100-fold higher avidity than CD28 for binding to CD80 and CD86 (vanderMerwe et al., 1997, Metzler et al., 1997) which may allow it to compete CD28 off these ligands.

More recently it was shown that CD80 localises to the IS in rings around central TCR clusters, where it is required for the synaptic accumulation of CD28, CTLA-4 and PKC θ in activated T cells. Deletion of the CD80 cytoplasmic domain abrogated synaptic organisation and led to reduced T cell proliferative response (Tseng et al., 2005). As the segregation of CD28 and TCR depends on the cytoplasmic tail of CD80, removal of this resulted in colocalisation of CD28 and TCR, correlating with reduced T cell activation. This provides strong evidence for the idea that segregation of some synaptic components is crucial for correct function.

TCR activation alone, in the absence of costimulatory signals, was shown to induce a type of anergy or antigen tolerance in T cells, which could be rescued by addition of IL-2 or CD28 stimulation (Jenkins et al., 1991, Schwartz et al., 1989, Finck et al., 1994). Though this is harder to show *in vivo*/ *in primary cells* (Chen et al., 1994, Shahinian et al., 1993). Furthermore, these interactions can affect signalling qualitatively, for example, CD80 and CD86 do not induce identical downstream signalling responses (Freeman et al., 1995, Bluestone, 1995).

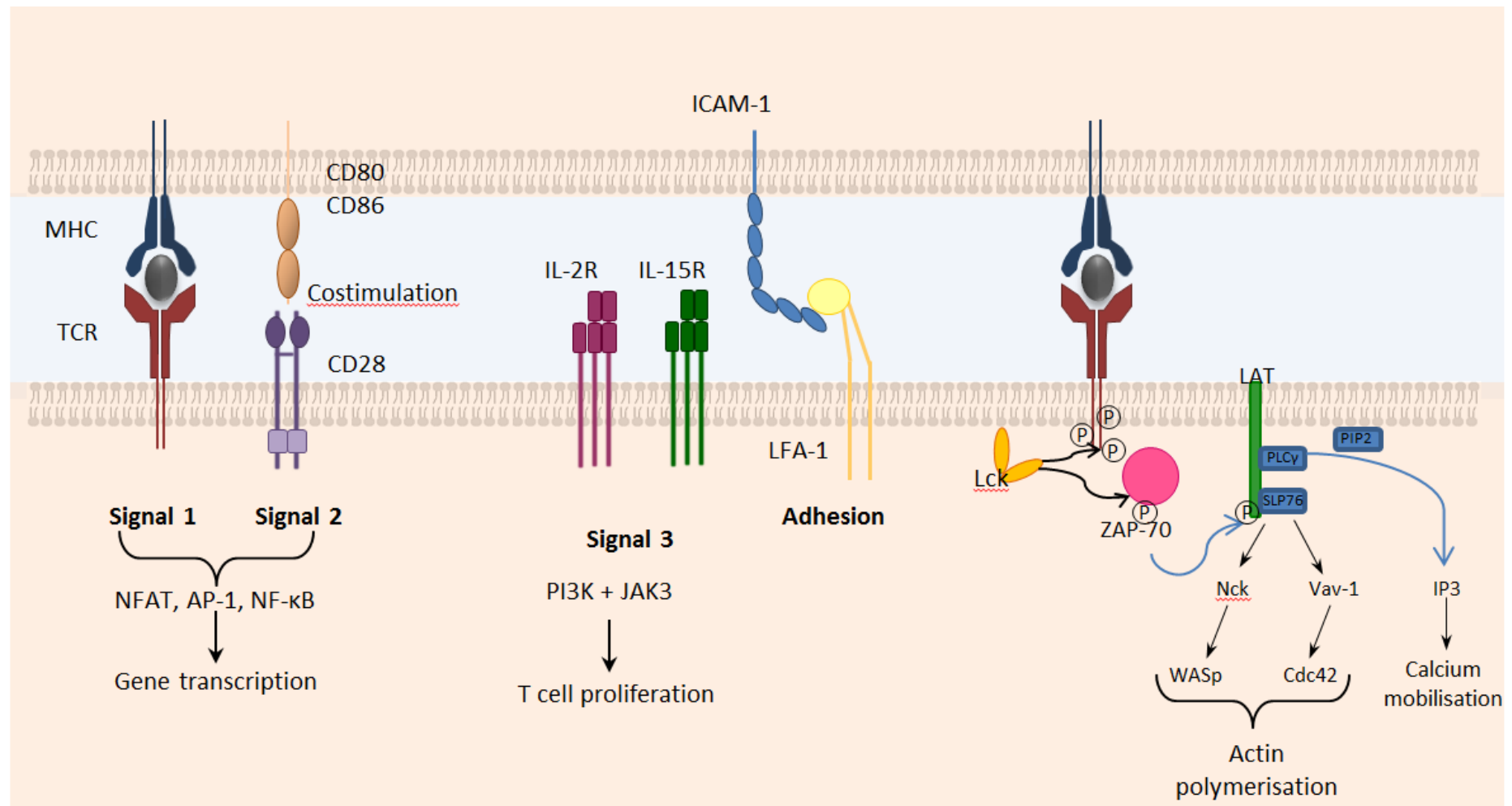
Signal 3 during T cell activation is provided by inflammatory cytokines and has also been described as the 'danger signal' provided to T cells in response to pathogens (Curtsinger et al., 1999). Early studies suggested that adjuvants, such as CFA or LPS, when administered with antigen, result in greater clonal expansion and no induction of tolerance, most likely by inducing strong inflammatory cytokine responses (Pape et al., 1997). In the absence of signal three, T cells have been shown to become tolerant rather than activated (Curtsinger et al., 2003). Cytokines can act directly on CD4 cells through T cell surface receptors (Dinarello, 1988, Weaver et al., 1988) or indirectly, by inducing increased costimulatory molecule expression on APCs (Liu and Janeway, 1991, McLellan et al., 1996, Yang and Wilson, 1996). Different types of

T cells require different cytokine stimulation, for example CD4 T cells have been shown to respond to IL-1, while CD8 require IL-12 for complete activation (Curtsinger et al., 1999). In order to respond correctly to a particular antigen, the immune system must also assimilate information about the nature of the antigen. Signal three can convey this information and, for example, polarise T helper cells towards the required subset (Scott, 1993). Each T cell subtype is then characterised by its cytokine secretion profile, which correlates with its function (Kapsenberg, 2003).

Figure 1.2 summarises the three-signal model described above and the events that lead to actin mobilisation downstream of TCR activation.

The three-signal model may be more complex than expected as some evidence suggests DC-mediated Th1 polarisation requires IFN γ production by a third cell, such as a previously activated T cell, thus supporting a three-cell T cell activation model (Abdi et al., 2006, Corthay, 2006). In this model NK cells, $\gamma\delta$ T cells, mast cells, basophils and eosinophils could all contribute to Th cell polarisation (Corthay, 2006).

Figure 1.2. **T cell activation.** The figure illustrates cell-cell contact between a T cell and an APC; and the three signals described to be involved in T cell activation – TCR triggering, costimulation and cytokine responses. ICAM-1 and LFA-1 represent a crucial adhesion mechanism for stable interaction. A brief summary of signalling downstream of the TCR is presented on the RHS.



T helper cell fate

Activation of T helper cells directs them towards one of several differentiation pathways. At least 4 major types of T-helper cell have been identified – Th1, Th2, Th17 and Treg. Th1 cells produce predominantly IFN γ and play a role in responses to intracellular infections, culminating in activation of cytotoxic T lymphocytes. IL-12 is produced by DCs and polarises T cell to a Th1 response (Abdi, 2002). Th2 cells are critical for fighting extracellular parasites and produce a variety of interleukins including IL-4, leading to B cell differentiation into plasma cells (Mosmann and Coffman, 1989). Th17 cells, through production of IL-17a, IL-17f and IL-22, are involved in immune responses against extracellular bacteria and fungi (Miossec et al., 2009). Tregs are important for regulating lymphocyte activation and function, and are thus crucial for maintaining immune tolerance (Vignali et al., 2008).

Differentiation into each T-helper cell subset is controlled through the activity of master regulators (transcription factors) and is determined by the nature of the antigen, its affinity to the TCR and the cytokine milieu at the time of T cell activation. Cytokine receptors are non-covalently bound to tyrosine kinases of the Janus kinase family. Ligation, dimerisation or clustering of the receptors brings the JAKs in close proximity and allows cross-phosphorylation. This leads to both recruitment and phosphorylation of signal transducers and activators of transcription (STATs). Phosphorylation results in a conformational change in the STAT protein leading to homo- or hetero-dimerisation. This allows dissociation from the receptor, nuclear translocation and regulation of transcription (Heim, 1999). Different STATs interact with different cytokine receptors and result in distinct transcription profiles. As reviewed by Zhu and Paul (Zhu and Paul, 2010), the relative amounts of cytokines and transcription factors determine the diversity and stability of the T helper cell subsets induced. The master regulators for the major subsets are described in Table 1.

Master regulator	CD4 lineage	General pathway
T-bet (<i>TBX21</i>)	Th1	STAT1 activated by IFN γ induces further T-bet expression (Lighvani et al., 2001)
GATA3 (<i>GATA3</i>)	Th2	STAT6 activated by IL-4 upregulates GATA3 expression (Kaplan et al., 1996), though GATA3 is involved in several step of CD4 development (Ho et al., 2009)
ROR γ T (<i>RORC</i>)	Th17	IL-6, IL-21 and IL-23 are critical for STAT3 activation and induction of ROR γ T, critical for IL-17 production (Veldhoen et al., 2006, Korn et al., 2007)
FoxP3 (<i>FOXP3</i>)	Treg	TGF β , through Smad3, and STAT5 are critical for FoxP3 induction (Davidson et al., 2007)

Table1. **The major transcription factors determining CD4 T cell fates.** Gene names are given in brackets.

As well as cytokine signalling, it has been proposed that co-stimulators and antigen dose may influence the final Th effector response (reviewed in (Murphy and Reiner, 2002)). Details of how each factor regulates the transcription pathways are unknown. It was shown that activation of the Th2 response through GATA3 requires CD28 co-stimulation (Rodriguez-Palmero et al., 1999). Although the study does not consider the physiological relevance of this alongside the STAT6 pathway, the idea of additional Th response polarising mechanisms during cell-cell contact is gaining support. LFA-1 signalling was shown to have the opposite effect and was proposed to skew the CD4 response towards a Th1 type (Salomon and Bluestone, 1998, Smits et al., 2002).

Another theory (Amsen et al., 2004) suggests that APCs express different Notch ligands to induce either Th1 or Th2 differentiation. A Th2 response is induced by Jagged-mediated Notch activation, which leads to conversion of RBPJk from a transcriptional repressor to an activator, which in turn binds to a conserved region in the *IL4* promoter allowing IL-4 (and thus GATA3) expression by bypassing STAT6. Conversely, the Delta ligand (the other family of Notch ligands) induced a Th1 response though the mechanism behind this is not understood.

There is also evidence pointing towards a role for the immune synapse in Th fate commitment (Maldonado et al., 2004). Maldonado *et al* show co-polarisation of IFNGR (IFN γ receptor) with TCR to the IS, leading to a Th1 response. IL-4 blocked the observed co-polarisation through STAT6 activation. The strength of the synapse may be an important regulating factor. Several groups have shown that varying the strength of the contact, either through antigen dose or antigen affinity for TCR, can alter T helper differentiation (Hosken et al., 1995, Constant et al., 1995, Tao et al., 1997b). Tao *et al* for example, suggest that the importance of CD28 ligation in inducing IL-4-producing Th2 cells is dependent on the strength of primary signal stimulation (restricted to cases where T cells receive a low dose of TCR priming).

More recently, Purvis *et al* showed that low-strength T cell activation through the TCR/CD3 complex (using a lower CD3/CD28 bead: T cell ratio, in the presence of Th17 cytokines in culture) promotes an increased Th17 response, only in the presence of anti-CD28. Nuclear translocation of NFATc1 occurred following either high or low TCR signal strength activation, however binding of NFATc1 to the proximal region of the IL-17 promoter was only detected following low signal strength activation (Purvis et al., 2010).

By contrast, Bouguermouh *et al* (Bouguermouh et al., 2009) showed that anti-CD28 stimulation suppressed differentiation of anti-CD3-activated CD4⁺ T cells into IL-17-producing cells through an IL-2 and IFN γ -dependent mechanism. This group used a soluble anti-CD28 mAb instead of bead-mediated activation. It is unclear whether the variation in these results is due to different types of antibodies or TH17-polarising cytokine cocktails/milieu used. If indeed CD28 costimulation has an inhibitory role in Th17 differentiation, synaptic disorganisation leading to reduced CD28 stimulation could result in increased Th17 differentiation and therefore Th17-associated inflammatory responses.

It is easy to envisage how disrupted expression of cell surface molecules or synaptic organisation of DCs may have an effect on tuning the Th fate induced. Organisation of

integrins, cytokine receptors and co-stimulatory molecules may be crucial and an abnormal actin cytoskeleton can cause defects in this process.

While there has been a lot of research on the T cell side of the conjugate, little is known about how the DC cytoskeleton affects synapse formation, though there is evidence for its involvement (Al-Alwan et al., 2001, Benvenuti et al., 2004a, Bouma et al., 2011).

4. *Wiskott-Aldrich Syndrome and WASp*

Clinical characteristics and cellular defects

Much of our understanding of the involvement of the actin cytoskeleton in immune cells comes from studying patients with actin-related immunodeficiencies. Wiskott-Aldrich syndrome (WAS) in particular has provided an insight into the importance of actin regulation for lymphocyte function (Nguyen et al., 2007). While fewer studies have focussed on the APC, it is likely that similar mechanisms may be involved. In this thesis, deficiency of the actin-regulating Wiskott-Aldrich Syndrome protein was chosen as a model system to study the involvement of the DC actin cytoskeleton.

Wiskott-Aldrich Syndrome is a rare but severe X-linked immunodeficiency affecting 2-4 live births per million. It is characterised by eczema, microthrombocytopenia, autoimmunity and an increased risk of lymphoid malignancies (Thrasher, 2002, Ochs and Thrasher, 2006). The disease results from the loss of WASp expression/activity (Derry et al., 1994) and over 300 unique mutations have been recorded with further mutations being identified regularly (Massaad et al., 2013, Safaei et al., 2012). Deletions and early terminations, which abolish WASp expression, result in severe disease. Missense mutations, which may reduce protein expression or function, cause milder forms of disease such as X-linked thrombocytopenia (Zhu et al., 1995, Albert et al., 2010). WASp activating mutations have also been described; these result in X-linked neutropenia (Devriendt et al., 2001, Ancliff et al., 2006). The increase in cellular actin caused by active mutants can cause cytogenetic abnormalities and defects in mitosis and cytokinesis (Moulding et al., 2007).

Unlike N-WASp, another member of the WAS family of proteins, WASp expression is restricted to the immune system, where its mutation results in a range of actin-related abnormalities in many basic immune cell functions. These include myeloid cell defects, such as reduced migration, chemotactic responses and phagocytosis in macrophages and DCs; and lymphocyte

defects such as reduced cell surface protrusions, poor T cell proliferation and TCR capping, reduced marginal zone B cells and abnormal humoral responses (Notarangelo et al., 2005, Blundell et al., 2010, Thrasher and Burns, 2010).

This broad range of defects results in a complex immunodeficiency due to cell-intrinsic and migration defects, as well as defects in cell-cell communication. One complex effect of this is autoimmunity and autoantibody production, which has been described both in patients (Schurman and Candotti, 2003) and murine models (Nikolov et al., 2010). Many factors have been described to contribute to this including increased apoptosis, reduced IL-2 secretion, chronic stimulation, impaired NK cell cytotoxicity and impaired phagocytosis (Schurman and Candotti, 2003, Blundell et al., 2010). Severe invasive infections, atopic eczema, colitis and hyper IgE found in WAS patients and murine models strongly indicate impaired Th1 and augmented Th2 responses (Imai et al., 2004).

As well as its role in actin regulation, WASp may be involved in transcriptional regulation (Huang et al., 2005, Taylor et al., 2010). Independently of its actin polymerisation activity, WASp was shown to control the nuclear translocation of the transcription factors NFAT2 and NFκB (RelA) in NK cells (Huang et al., 2005). The same group showed WASp interaction with the proximal promoter locus of the *Tbx21* gene and suggested that the reduced Tbet mRNA and protein levels in WASp deficient cells partly explain the Th1/Th2 imbalance in WAS (Taylor et al., 2010). Recently, Looi *et al* used CHIP and microarray assays to show interaction of WASp with RNA polymerase II and differential transcription profiles in myeloid cells expressing constitutively active WASp (Looi et al., 2014). The role of actin and its regulators in the nucleus is still not fully understood.

WASp structure and regulation

WASp is a modular protein, containing an N-terminal EVH1 (also called WH1) domain, a GTPase binding domain (GBD), a polyproline domain, and a C-terminal VCA (verpolin/cofilin/acidic) domain involved in autoinhibition (Kim et al., 2000). The presence of multiple domains and lack of enzymatic activity suggest that WASp can act as a scaffold to recruit a range of other adaptors, kinases and actin-binding proteins (Figure 1.3). This would suggest that WASp is an important platform with a role in signal integration from many molecular pathways to Arp2/3. Intramolecular interaction between the GBD and VCA domains results in a closed conformation, allosterically blocking VCA interaction with Arp2/3. WASp activators disrupt GBD-VCA interactions, relieving autoinhibition and allowing WASp to bind and activate Arp2/3 (Kim et al., 2000).

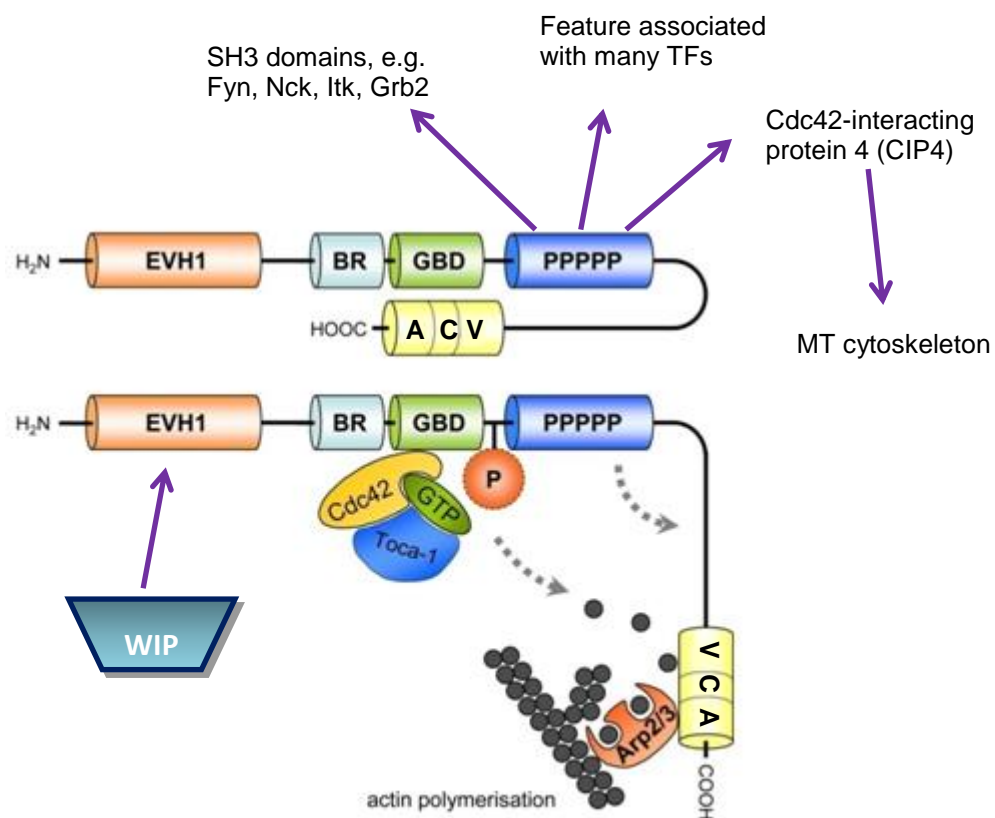


Figure 1.3. **WASp domains and autoinhibition.** Adapted from Bouma *et al* (Bouma et al., 2009)

In an active conformation, WASp binds Arp2/3 via its VCA domain (Figure 1.3). This complex initiates the formation of a new filament, branching from an existing one at a 70° angle (Mullins et al., 1998). The VCA domain also binds actin monomers, thus providing a concentrated local pool.

Tyrosine phosphorylation at Y291 in human WASp (Y293 in murine WASp) has been proposed to play a critical role in WASp activation (Cory et al., 2002, Blundell et al., 2009). Numerous groups have shown that phosphorylation occurs both in vitro and in vivo and the residue is a target for several kinases, including Btk and Fyn, and the phosphatase PTP-PEST (Torres and Rosen, 2003). WASp has been shown to interact with the SH3 domains of Scr family kinases, in particular Fyn, in human and mouse hematopoietic cells (Banin et al., 1996, Sakuma et al., 2012). Further evidence suggests specific phosphorylation and dephosphorylation by Fyn and PTP-PEST (interacting with WASp via PSTPIP1) respectively, are required for synapse formation and T cell activation (Badour et al., 2004). Phosphorylation may activate WASp through disruption of the autoinhibited conformation or stabilisation of the 'open' molecule. Tyrosine phosphorylation of WASp may also target the protein for proteasome-mediated degradation (Blundell et al., 2009), resulting in a self-limiting response.

Binding of the lipid PIP₂ or (the GTPase) Cdc42-GTP to WASp is also thought to destabilise the inactive conformation and allow binding of the Arp2/3 complex to the VCA domain. Higgs and Pollard show that WASp alone or in combination with Cdc42-GTP, is unable to stimulate actin nucleation by Arp2/3. (Higgs and Pollard, 2000) Their evidence suggests that addition of phosphatidylinositol 4,5 bisphosphate (PIP₂) activates actin nucleation, which is then further increased by Cdc42. Purified N-WASp has also been shown to be activated by Cdc42 and PIP₂ (Rohatgi et al., 2000).

During IS formation, it was shown that T cell CD28 engagement induced F-actin filopodia, which required Cdc42 activity (activated through Vav phosphorylation but independent of ZAP-70) (Salazar-Fontana et al., 2003). Both Cdc42 and WASp are recruited to the IS in an antigen-

dependent manner, following Zap-70 signalling (Cannon et al., 2001). Interestingly, Cannon *et al* show WASp recruitment to the IS is independent of Cdc42 but does require the WASp proline-rich region, which is necessary and sufficient for correct WASp targeting and may interact with SH3 domain containing proteins, such as Nck (Riverolezcano et al., 1995, Cannon et al., 2001). Nck has been shown to bind both SLP-76 and Vav-1 directly, which may provide a link between localisation and activation of WASp (Barda-Saad et al., 2010, Pauker et al., 2012). Grb2, another SH3 domain containing protein was also shown to interact with the polyproline domain of WASp family proteins, with a preference for their active confirmation (Carlier et al., 2000). Binding was shown to be simultaneous with Cdc42 and the two proteins enhanced actin polymerisation by N-WASp synergistically (Carlier et al., 2000).

Another player in the regulation of WASp is the WASp-interacting protein (WIP). Around 80% of WAS patients present mutations in the WIP binding site (Volkman et al., 2002). Possibly the best accepted theory is that WIP acts as a chaperone to prevent WASp degradation by the proteasome (de la Fuente et al., 2007). WIP was found to regulate both WASp localisation, in this case to DC podosomes, and calpain-mediated degradation (Chou et al., 2006). Indeed, both WIP and WASp tyrosine phosphorylation have been shown to regulate the stability and localisation of WASp to podosomes and consequently are critical for the maintenance of podosome turnover required for migration (Chou et al., 2006, Macpherson et al., 2012).

Others have suggested that WASp exists as a complex with WIP in resting T cells, which acts to block activation by Cdc42. Upon TCR activation, WIP and WASp form a larger complex with ZAP-70 and the adaptor CrkL; the whole complex is recruited to lipid rafts at the IS, where WIP can be phosphorylated by PKC θ to release WASp from inhibition, while WASp is now in close proximity to Cdc42-GTP for activation (Sasahara et al., 2002). It is still unclear at what point WIP dissociates from WASp. This provides a very different model from the one discussed above suggesting recruitment by Nck; several different mechanisms for recruitment may be important for signal integration and transduction to the cytoskeleton. A more recent study,

investigating vaccinia virus actin-mediated motility, built on previous results showing interaction between WIP and Nck (Anton et al., 1998), showed that WIP contains two Nck-binding sites and its interaction with N-WASp is essential for N-WASp recruitment to virus particles (Donnelly et al., 2013).

One of the earliest direct observations of WASp kinetics came from Blanchoin *et al*, who used light microscopy to show relative rigid braches as a result of nucleation by Arp2/3, activated by WASp (Blanchoin et al., 2000). More recently however, the model has been challenged with the suggestion that WASp proteins may work as dimers to interact with both Arp 2 and Arp3 subunits and bring 2 actin monomers into the complex (Padrick et al., 2011, Padrick et al., 2008). While this is still controversial, it may prove to be a useful model of how WASp proteins integrate a large number of signals and what directs the orientation of the actin daughter filament.

A recent paper has suggested a new model of temporal regulation of actin polymerisation by WASp (Smith et al., 2013b). The authors suggest that WASp dissociates form the nucleation complex prior to filament elongation and propose this as a mechanism of releasing the growing actin filament network from the membrane-bound nucleation promoting factor (Smith et al., 2013b).

WASp at the immunological synapse

Wasp has a key role in transducing signals from cell surface receptors to the actin cytoskeleton. The cell-intrinsic role for WASp in immunological synapse formation has been well described. NK cells from WAS patients have decreased cytotoxicity due to impaired conjugate formation (Orange et al., 2002). Further, WAS NK cells show normal accumulation of Arp2/3, vinculin and talin downstream of LFA-1 but are unable to increase actin polymerisation and polarise the actin network towards the IS (Mace et al., 2010). In T cells, WASp has been proposed to play a role in lipid raft regulation (Dupre et al., 2002) or actin mediated synapse organisation downstream of CD2 (Badour et al., 2003). Several others have shown WASp to be a critical factor in T cell IS formation (Sims et al., 2007, Calvez et al., 2011). Sims *et al* showed that WASp and PKC θ have opposing effects at the IS; WASp promotes the symmetric formation of the IS, while PKC θ is involved in symmetry breaking and induces a migratory phase in T cells (Sims et al., 2007).

A role for WASp in IS formation on the dendritic cells side is also emerging and has been shown to be important for activation of CD4 and CD8 T cells (Bouma et al., 2011, Pulecio et al., 2008).

5. WAS mouse model

WASp-deficient murine model will be used to isolate bone marrow and produce bone marrow-derived dendritic cells (BMDCs). Snapper *et al* disrupted the murine WASP gene in a TC-1 ES cell line with a targeted insertion of a neomycin-resistance gene in the reverse orientation into exon 7 (Snapper et al., 1998). The WASp-null ES clones were used to generate chimeric mice, which are bred to generate WASp^{-/-} animals. The mice exhibit normal lymphoid development but reduced numbers of peripheral lymphocytes and platelets and abnormal T cell capping and proliferation responses (Snapper et al., 1998). Although originally based on the Sv/129 background, these were crossed to the C57BL/6 (BL6) background, which were used in the following experiments. A second murine model, with a neomycin insertion in exon 4, also shows defects in lymphocyte development (Zhang et al., 1999).

WASp is expressed exclusively in haematopoietic cells and appears to be more important for peripheral homeostasis than development and thymic production (Meyer-Bahlburg et al., 2008, Bouma et al., 2009). WAS affects cells of both the innate and adaptive immune systems. It affects cells in a variety of ways, for example, macrophages show impaired phagocytosis, megakaryocytes produce fewer and smaller platelets, Tregs fail to proliferate and show reduced suppressive activity (Thrasher and Burns, 2010, Humblet-Baron et al., 2007). Osteoclasts and DCs from the Snapper mouse model exhibit defective chemotaxis (Burns et al., 2001), homing (de Noronha et al., 2005) and formation of podosomes (Burns et al., 2001, Calle et al., 2004). WASp deficiency in DCs results in impaired T cell priming, not only as a result of inefficient migration, but also due to the formation of a spatially and functionally abnormal synapse (Bouma et al., 2007, Pulecio et al., 2008). These results suggest that WASp plays a critical role in DC-mediated IS formation. As discussed above, DCs are involved not only in activation of CD4 cells but also in their commitment to a particular T helper subset. An imbalance in the induced lineages may explain some of the characteristic symptoms of WAS, such as eczema and autoimmune reactions.

6. DOCK8

Similar to WAS, human mutations of other actin regulators have been described, which in many cases lead to severe immunodeficiencies, highlighting the crucial role of actin in the immune system. One recently-described example is the DOCK8 deficiency. The last chapter of this thesis describes work performed to characterise this and two novel actin-related immunodeficiencies.

DOCK8 structure, genetics and protein family

Dedicator of cytokinesis 8 (DOCK8) is part of the Dock180-related family of atypical GEFs. As described above, GEFs activate Rho GTPases by facilitating the switch from a GDP- to GTP-bound state; Rho GTPases in turn, integrate extracellular signals and transduce these to effector molecules (e.g. Cdc42 activation of WASp) to produce an appropriate cytoskeletal response (Miyamoto and Yamauchi, 2010). The original GEFs were described as a group of structurally related proteins containing a pleckstrin homology (PH) domain and a dbl homology (DH) domain with GEF activity. In contrast, the DOCK proteins have a distinct structure, lacking DH domains but containing two dock homology regions, DHR1 and DHR2 (also known as CDM-zizimin homology (CZH1 and CZH2) domains). In most DOCK proteins, the DHR1 binds phosphatidylinositol triphosphate (PIP3), thus localising the protein to the plasma membrane; while the DHR2 interacts with Rho GTPases and contains the catalytic site for GEF activity (Cote and Vuori, 2007, Meller et al., 2005). The additional domains present on some family members have been used to segregate the Dock180-related group into several subfamilies (Meller et al., 2005). DOCK8 belongs to the DOCK-C subfamily which is characterised by the absence of domains other than DHR1 and DHR2. Similar to other actin regulators, the DOCK180-related proteins are involved in a large number of diverse cellular processes including migration, phagocytosis, cytotoxic responses and polarisation. More specifically for immune cells, dysregulation in such actin processes can result in abnormalities in adhesion, activation of integrins, podosome formation and immunological synapse organisation.

DOCK8 was isolated in a yeast two-hybrid screen for proteins interacting with Cdc42 (Ruusala and Aspenstrom, 2004); this has recently been confirmed by pull down experiments and has been shown to be dependent on the DHR2 domain (Harada et al., 2012).

DOCK8 is a 1701 amino acid protein shown to localise to cell edges during lamellipodia formation (Ruusala and Aspenstrom, 2004). The 47 exon *DOCK8* gene, spanning 190kb, was mapped to chromosome 9p24 (Griggs et al., 2008). *DOCK8* mRNA is present throughout most tissues, with strong protein expression in haematopoietic cells and peripheral blood mononuclear cells (PBMCs).

In a large scale study using genome-wide single nucleotide polymorphism (SNP) analysis and homozygosity mapping, Engelhardt *et al* showed that the majority of mutations identified (63%) were large deletions; the rest included small indels or point mutations resulting in in-frame or out-of-frame nonsense mutations. These can result in a loss of DOCK8 expression due to nonsense-mediated mRNA decay (Engelhardt et al., 2009).

Clinical characteristics and cellular defects

In 2009, DOCK8 was independently described as the cause of severe immune deficiency in both humans and mice (Randall et al., 2009, Zhang et al., 2009, Engelhardt et al., 2009). Clinical characteristics include severe food and environmental allergies, middle ear infections, pneumonia or bronchitis and cutaneous viral infections, with the most common culprits being human papilloma virus (HPV), molluscum contagiosum virus (MCV), herpes simplex virus (HSV) and varicella-zoster virus (VZV) (Zhang et al., 2009, Chu et al., 2012). Systemic viral infections are rarely detected, suggesting antiviral immunity is defective locally within the skin (Engelhardt et al., 2009); though non-immune cells present in skin layers do not express DOCK8 protein (Su et al., 2011). Increased susceptibility to viral infections is seen in other PIDs such as WAS and “leaky” SCID (Modiano et al., 1995, Saijo et al., 1998, Artac et al., 2010). As in WAS this could be the result of a combination of factors including defective skin barrier,

reduced numbers of T cell, impaired T cell proliferation and antiviral cytokine production, and abnormal migration into infected tissues (Zhang et al., 2010). Pneumonia, caused by a wide spectrum of gram-positive and gram-negative bacteria and fungi, gastrointestinal tract infections, eczema, eosinophilia and IgE dysregulation have also been attributed to DOCK8 deficiencies (Zhang et al., 2009, Engelhardt et al., 2009).

On a cellular level, defects have been described in T cell homeostasis with reduced T cell numbers and impaired in vitro proliferation of CD8 (Zhang et al., 2009, Engelhardt et al., 2009) or both CD4 and CD8 populations (Engelhardt et al., 2009), similar to that seen in WAS. Dasouki *et al* used a T cell receptor excision circle (TREC) assay to show that the number of TRECs was very low or undetectable in 3 patients, suggesting impaired T cell production or efflux from the thymus (Dasouki et al., 2011). This defective thymopoiesis or efflux might help to account for the reduced numbers of T cells in patients. It may also result in a restricted T cell repertoire, contributing to the pathology.

An imbalance of Th1/ Th2 CD4 subtypes has been suggested as several DOCK8 patients present with elevated levels of IL-6 and IL-10 (Dasouki et al., 2011). An increased Th2 response would increase isotype-switching in B cells and result in IgE overproduction. Increased serum IgE is also seen in Wiskott Aldrich syndrome, in which abnormal T cell function is a central player in disease pathology, further suggesting that variability in IgE levels may be the result of T cell dysregulation.

Th17 cell differentiation and survival has also been shown to be impaired, as measured by production of IL-17 or expression of the Th17 master regulator ROR γ t (Milner et al., 2010, Al Khatib et al., 2009). IL-17 and proinflammatory cytokines in turn have a role in inducing production of antimicrobial peptides by keratinocytes and bronchial epithelial cells (Minegishi et al., 2009); thus the reduced numbers of Th17 cells may explain the susceptibility to fungal infections in DOCK8 patients.

As in WAS deficiency, production of anti-viral cytokines IFN- γ and TNF- α by CD8 T cells is also decreased in DOCK8, although perforin content and cytotoxic granule release appear normal (Zhang et al., 2009). There is evidence for an essential role of DOCK8 in CD8 T cell survival and memory maintenance, whether due to loss of memory T cells or the development of an “exhausted” phenotype in circulating T cells (Lambe et al., 2011, Randall et al., 2011). It is still unclear to what extent defective TCR signalling, cytokine production and homeostatic proliferation of peripheral cells contribute to the overall T cell defects. The defective functioning of CD8 T cells, which normally assist in tumour surveillance, may contribute to the higher rate of malignancies in DOCK8 patients. Around 20% of patients develop at least one type of cancer and the most common malignancies are squamous cell carcinoma and lymphoma (Su et al., 2011).

Similar to WAS, DOCK8 deficient mice exhibit a lack of marginal zone B cells (Randall et al., 2009). Further, B cells show impaired immunological synapses due to a failure to concentrate the integrin ICAM-1 in the pSMAC; however, intracellular calcium flux and ERK phosphorylation were normal (Randall et al., 2009).

Dendritic cell (DC) function is also affected in the absence of DOCK8. DOCK8 DCs were unable to induce T cell activation and proliferation, which was not a result of defective antigen uptake or presentation (Harada et al., 2012). Adoptive transfer experiments showed that migration of DOCK8 null DCs to draining lymph nodes was less than 25% of control levels and velocity of migration within dermal tissues was severely reduced. Further, DOCK8 DCs were unable to polarise and extend protrusions when migrating through 3D collagen gels. Two-photon microscopy provided evidence for defective intra-nodal DC migration as DCs failed to migrate into lymph node parenchyma for T cell priming (Harada et al., 2012).

So far, there is one study of DOCK8-deficient natural killer (NK) cells, whose absolute numbers in patients appear normal. Unlike WAS NK cells, and total actin content of DOCK8 NK cells was indistinguishable from controls, however, patient cells were unable to polarise F-actin towards

the lytic synapse. Clustering of CD18 and polarisation of perforin and the microtubule organising centre (MTOC) were also impaired (Mizesko et al., 2013). Cytolytic activity of WAS deficient NK cells can be restored by IL-2 as the cytokine can bypass WASp to use the homologous effector WAVE2 (Orange et al., 2011). This was not the case for DOCK8 NK cells; IL-2 stimulation had no effect on NK cell functions in the absence of this upstream activator (Mizesko et al., 2013).

Many of the symptoms described, such as rash, elevated IgE and susceptibility to autoimmunity, are very similar to those described in WAS (Thrasher and Burns, 2010). As an effector of the Rho GTPase Cdc42, WASp presumably acts downstream of DOCK8 and the similar clinical manifestations may reflect the overlapping signalling pathways. While WASp function may also be diminished in DOCK8 patients, this cannot explain the complete phenotype of DOCK8 patients. Unlike WAS, DOCK8 expression is not restricted to the haematopoietic system, it would be interesting to see whether reconstitution of the immune system would correct disease pathology. Similar to WAS, the disease pathology is likely to be the result of a combination of cellular defects including the inability of B cells to generate high-affinity antibodies and sustain GCs; the absence of T cell memory; defects in DC migration and capacity to prime T cells; as well as reduced NK cell cytotoxicity.

DOCK8 murine model

Around the same time as the characterisation of the human disease, Randall *et al* identified two independent mutations (*primurus(pri)* and *captain morgan(cpm)*) in DOCK8 through an ethylnitrosurea (ENU) mutagenesis screen for mutations affecting antibody response maturation (Randall et al., 2009). DOCK8 mutation was shown to impair B cell immunological synapses and affect B cell ability to mature and contribute to the germinal centre subset. Diminished survival and selection of DOCK8 B cells resulted in severely reduced numbers of high affinity IgG⁺ B cells (Randall et al., 2009). Integrin interaction has been shown to play a role in lowering the threshold for B cell activation and allowing affinity maturation in germinal

centres, which is necessary for adaptive immunity (Carrasco et al., 2004, Cantor et al., 2009). ICAM-1 expression on follicular dendritic cells (FDCs) has been suggested to inhibit apoptosis of GC B cells so the failure of DOCK8 B cells or APCs to organise an immunological synapse may result in the loss of a survival signal in the form of integrin costimulus (Randall et al., 2009).

The *pri* knockout model has also highlighted cell-intrinsic defects in DOCK8 CD8 cells after thymic development (Randall et al., 2011). CD8 cells had a shorter lifespan, produced a poor memory response and were unable to polarise LFA-1 towards the IS upon contact with DCs.

In mice, *Dock8* mutations replicate many of the cellular defects described in patients yet mice show no obvious clinical phenotype, similar to WAS knockout animals (Snapper et al., 1998, Zhang et al., 1999). This could be the result of maintenance in a pathogen-free environment.

AIMS

This project aims to gain more insight into the role of dendritic cells in IS formation. Increased understanding of DC biology may contribute to the development of instruments for modulating immune responses and may help to advance treatment of WAS. The role of the DC in IS formation is under-represented and requires further investigation.

It is hypothesised that impaired actin polymerisation in WASp DCs results in malformed IS, which is not sufficient to sustain intercellular signalling required for full T cell activation.

Using a WASp-deficient murine model the project aims to investigate how defective cytoskeletal regulation in DCs affects:

- The formation and organisation of the IS
- The actin dynamics and structural stability of the IS over time
- The functional consequences of IS formation between T cells and WASp-deficient DCs

Further, the project aims to compare IS formation in WAS DCs with the more recently described DOCK8-deficient DCs, allowing a direct comparison of the function of each of these components of an actin-regulating pathway.

Finally, basic immune cell functions will be investigated in two novel actin-related primary immunodeficiencies.

Chapter 2 – Materials and Methods

2.1 Materials

2.1.1 Media, Buffers and Solutions

All media used were supplied by Gibco unless otherwise stated.

Aprotinin	Sigma Aldrich (A1153)
AquaPoly Mount	Polysciences, Inc.
Avidin/ Biotin block	Invitrogen (004303)
DNA (plasmid) isolation	QIAprep Spin Miniprep Kit (Qiagen)
DNA loading buffer	0.25% bromophenol blue, 0.25% xylene cyanol, 30% glycerol, in dH ₂ O.
ELISA block buffer	1% BSA in PBS + 0.05% NaN ₃
ELISA Reagent diluents	0.1% BSA, 0.05% Tween 20 in PBS, pH7.4
ELISA stop solution	2N H ₂ SO ₄
ELISA wash buffer	0.05% Tween 20 in PBS
Eα-GFP	From Paul Garside, University of Glasgow
Ficoll-Paque	GE Healthcare (17-1440-03)
Fixatives	4% PFA (confocal microscopy) 4% PFA + 0.025% glutaraldehyde (immunogold) 1% PFA + 3% glutaraldehyde (routine TEM and 3View)
Freezing media	10% DMSO, 40% FCS, in DMEM or RPMI
GM-CSF (human)	Peptotech (300-03)
GM-CSF (murine)	Invitrogen, PMC2015
Hybridoma media	RPMI + 6%FCS + PenStrep + β-mercaptoethanol
Isolation Kits	CD4+ T cell isolation kit II, mouse – Miltenyi 130-095-248 CD14 Microbeads, human – Miltenyi 130-050-201

IL-4 (human)	Peprotech (200-04)
LPS	Sigma, L2654
Luria-Bertani (LB) Broth/Agar	Sigma Aldrich
Lysis buffer	1% IGEPAL or NP40, 130mM NaCl, 20mM Tris-HCl pH7.4, 1mM EDTA, 10mM NaF, 1% aprotinin, 10µM pepstatin, 10µg/ml leupeptin, 50µM calpastatin and 1mM PMSF.
MACS buffer (for magnetic cell separation)	0.5% BSA, 2mM EDTA, in PBS
Mouse IL-2 DuoSet ELISA	R&D SystemsDY402
Mouse IFN γ DuoSet ELISA	DY485
Mouse IL-17 DuoSet ELISA	DY421
Mouse IL-4 ELISA Ready-SET-Go	eBioscience
Mouse IL-10 ELISA Ready-SET-Go	
Normal mouse serum block	DakoCytomation, X0910 (dilute to 2% in PBS)
NuPAGE Tris-Acetate Mini Gels	Invitrogen
OVA ₃₂₃₋₃₃₉	Anaspec (27024)
Ovalbumin	Fluka, BioChemika, 05440
PageRuler Prestained protein ladder	Thermo Scientific (26616)
PenStrep	Added to culture media to final concentration of 100U of penicillin and 100µg of streptomycin per ml.
Phosphate buffered saline	1x cell culture grade PBS (Gibco); 10x stock (Fisher Bioreagents)
Pierce Crosslink Immunoprecipitation Kit	Thermo Scientific (26147)
Pierce ECL Western Blotting Substrate	Thermo Scientific
Platinum qPCR SuperMix-UDG with ROX	Invitrogen, 11743-500
Pluronic solution	SigmaAldrich F-68 10% (P5556)
Protein A+G Agarose	Source Bioscience (PRAG25-AS-2)
Reducing buffer	NuPAGE Sample Reducing buffer NP0009
Restriction enzymes and digest buffers; T4 DNA Ligase; Polymerase; Shrimp Alkaline Phosphatase; Klenow	Commercially available enzymes from Promega, Fermentas and NEB.
Reverse transcription reagents	Invitrogen: DNaseI (18068-015);

	<p>Random primers (48190-011);</p> <p>10mM dNTP Mix (18427-013);</p> <p>RnaseOut ribonuclease inhibitor (10777-019);</p> <p>M-MLV reverse transcriptase (28025-013)</p>
RNA isolation	Rneasy Mini Kit (Qiagen)
RT-PCR primer/probe mix	TaqMan Gene Expression Assays, Applied Biosystems
Running buffers	<p>NuPAGE MOPS SDS 20x, NP0001-02</p> <p>NuPAGE MES SDS 20x, NP0002</p>
TE	0.05% Trypsin-EDTA, Gibco
TMB	Tetramethyl Benzidine chromogen solution; eBioscience (00-4201-56)
Transfer buffer	NuPAGE 20x, NP0006-1
Western and IP blocking buffer	5% skimmed milk in PBS + 0.1% Tween
Western and IP Loading buffer	<p>Laemmli buffer: 125mM Tris HCl, 4% SDS, 20% glycerol, 10% 2-mercaptoethanol, 0.004% bromophenol blue.</p> <p>NuPAGE: Sample buffer (Invitrogen NP0007) + Reducing Agent (Invitrogen NP0004).</p>
Western stripping buffer	Re-blot Plus Strong, Millipore

2.1.2 Antibodies and Cell Trackers

Primary Antibody + Host species	Clone	Manufacturer
α -tubulin mouse	B-5-1-2	SigmaAldrich
α -tubulin rat	YL1/2	Santa Cruz
Capping protein (CapZ) rabbit		Millipore (AB6016)
CD11a-biotin (LFA-1) rat	I21/7	Leinco Technologies
CD11c-eFluor450 armenian hamster	N418	eBioscience
CD3-PE-Cy5 rat	17A2	BD Pharmingen
CD3e-PE armenian hamster	145-2C11	BD Pharmingen
CD4-APC rat	GK1.5	eBioscience
CD4-FITC rat	L3T4	eBioscience
CD45 rat	I3/2.3	Santa Cruz
CD54 rat	YN1/1.7.4	BioLegend
CD54-biotin rat	YN1/1.7.4	BioLegend
CD62L-APC rat	MEL-14	eBioscience
CD69-PE Armenian hamster	H1.2F3	BioLegend
Ea52-68 peptide on I-Ab - biotin	eBioY-Ae	eBioscience
γ -tubulin mouse	GTU-88	Sigma Aldrich
GAPDH	6C5	Santa Cruz
I-Ab- biotin mouse	KH74	BD Pharmingen
Integrin- β 2 mouse		Santa Cruz sc-8420
MKL1 rabbit		Sigma HPA030782
MKL1 N-terminus rabbit		Sigma SAB4502519
MRTF-A goat		Santa Cruz sc21558
N-WASp goat		Santa Cruz sc-10122
Nck mouse	108/NCK	BD Biosciences
Nck-1 mouse	NC-20 (same as 20B-1H9)	GeneTex (GTX23215)
Nck rabbit	Y531	Abcam
TCR a/b Armenian hamster	H57-597	Caltag Laboratories

Vinculin mouse		Sigma V4505
Vinculin rabbit		Abcam ab73412
WASp rabbit		Cell Signalling Technology
WASp mouse	B-9	Santa Cruz
WDR1 goat		Santa Cruz sc-160907
WIP goat		Santa Cruz sc-16882
Secondary Antibody		Manufacturer
Anti-mouse IgG-Gold 10nm		Sigma Aldrich (G7652)
Anti-rabbit IgG-Gold 10nm		Sigma Aldrich (G7402)
Anti-mouse HRP		DAKO
Anti-rabbit HRP		DAKO
Anti-goat HRP		Santa Cruz sc-2768
Anti-hamster Dylight549		Serotec
Anti-mouse AlexaFluor488		Molecular Probes
Anti-rabbit AlexaFluor405		Molecular Probes
Anti-mouse AlexaFluor633		Molecular Probes
Anti-rabbit AlexaFluor633		Molecular Probes
Anti-rat Dylight405		Serotec
Anti-rat AlexaFuor564		Molecular Probes
Anti-rat Cy5		Jacksons ImmunoResearch
Anti-mouse Cy5		Jacksons ImmunoResearch
Anti-rat FITC		Jacksons ImmunoResearch
Isotype Controls		
Armenian hamster IgG-PE		
Armenian Hamster IgG–Pe-Cy5		
Mouse IgG1-PE		
Mouse IgG2b – biotin		

Rat IgG1-PE		
Rat IgG2b-FITC		
Rat IgG2b – PE		
Dyes, Stains and Trackers		Manufacturer
Amersham Cy5 Maleimide Mono-Reactive Dye		GE Healthcare
Cell Trace CFSE Cell Proliferation Kit		Life Technologies, Molecular Probes (C34554)
CellTracker Green CMFDA (5-Chloromethylfluorescein Diacetate)		Life Technologies, Molecular Probes (C7025)
CellTrace™ Far Red DDAO-SE		Life Technologies, Molecular Probes (C34553)
DAPI (4',6-diamidino-2-phenylindole)		
Phalloidin AlexaFluor 633		Invitrogen, A22284
Other		
High Precision Microscope Cover Glasses (<i>Deckgläser 24x24m</i>)		Marienfeld Laboratory Glassware (01 070 52)
FluoroDish (live imaging dishes) Dish 35mm; Glass 23mm; thickness 0.17mm; Poly-D-Lysine coated		World Precision Instruments FD35PDL
Glass slides – Superfrost		Thermo Scientific
MicroAmp Optical 96-well Reaction Plate (QPCR)		Applied Biosystems N8010560
ELISA plates		Nunc Maxisorb

2.1.3 Animals and Cells

- B017.10 Kindly provided by Dr.med. Stefan Porubsky, Heidelberg University, Germany.
- 293T Human Embryonic Kidney cell line, purchased from European Collection of Cell Cultures (ECCC).
- THP1 Human monocytic cell line, a gift from J Metelo, MIU.

C57BL/6 wildtype mice purchased from Charles River.

WAS and FYN: WAS knockout and Y293F phosphorylation-null knock-in mice were bred in house. The WAS KO was created by targeted insertion of neomycin resistance gene (neo) into exon 7 of the WASP gene, resulting in complete loss of RNA or protein expression (Snapper et al., 1998). The FYN strain contains a Tyr293Phe mutation in exon 9 of the WAS gene.

OT-II transgenic mice (expressing OVA peptide-specific transgenic TCR) were bred in house.

Dock8 strain was bred in house as homozygotes. These express a Ser1827Pro mutation in exon 43 of the Dock8 gene. This was originally described by Randall *et al* and named *primurus* (Randall et al., 2009).

All animals were housed in Individually Ventilated Cages (IVCs) and experiments were performed in accordance with Home Office legislation.

Bone marrow dendritic cell (BMDC) cultures – BMDCs were generated by culturing bone marrow cells of BL6 or WAS mice in the presence of GM-CSF (20 ng/ml) for 7 days. Bone marrow was obtained by flushing the femur of mice, using a 25g needle, on day 0. The single cell suspension was then cultured at 4×10^6 cells per 10cm culture dish in 10ml of complete RPMI, supplemented with 20ng/ml recombinant murine GM-CSF. Fresh media supplemented with 20ng/ml GM-CSF was added on days 2 and 5. On day 7, cells were harvested using cell scrappers, washed in fresh media and pulsed with 100ng/ml LPS only (control – mature cells) or with LPS in combination with 100µg/ml ovalbumin or the OVA₃₂₃₋₃₃₉ peptide (OVA-presenting; for antigen-specific T cells). BMDCs were harvested for experimental use on day 8.

Isolation of CD4+ cells from OT-II mice

CD4+ T cells were isolated from spleens and lymph nodes (inguinal, mesenteric and brachial) by negative selection using a Miltenyi Biotec CD4+ T cell Isolation Kit (130-095-248) as per manufacturer's instructions. Briefly, a single-cell suspension was obtained by passing spleen and lymph nodes through a 40µm filter. Spleen suspensions were incubated in 10ml 1xRBC Lysis buffer for 5 minutes to lyse erythrocytes; this was quenched by adding 30ml PBS. Cells were counted, centrifuged at 300g for 10min and resuspended in 40µl/ 10⁷ cells of MACS buffer. CD4+ Biotin Antibody Cocktail (containing CD8a, CD11b, CD11c, CD19, CD45R, CD49b, CD105, MHC and Ter-119 antibodies) was added to the cell suspension at 10µl/10⁷ cells. This was incubated at 4°C for 10min then diluted by adding 30µl/10⁷ cells MACS buffer. Anti-Biotin Microbeads were added at 20µl/10⁷ cells and incubated at 4°C for 15min. Cells were washed by adding 2ml/10⁷ cells of MACS buffer and centrifuged at 300g for 10min. Pellets were resuspended in 500µl for up to 10⁸ cells and magnetic separation was performed on LS columns on a MACS MultiStand magnet. Column flow-through was collected, containing enriched, untouched CD4+ T cells. T cells were activated using Mouse T-Activator CD3/CD28 Dynabeads (Invitrogen, 114.52D), or Concanavalin A (Sigma Aldrich, C5275) as positive controls for T cell activation and proliferation.

Human peripheral blood dendritic cell cultures

10-20ml of patient or control blood was diluted 1:1 with RPMI, layered onto an equal volume of Ficoll-Paque and centrifuged at 2300rpm (1000g) for 20minutes, without brake. Peripheral blood mononuclear cells (PBMC) were collected from the Ficoll/serum interface and washed twice in RPMI. CD14-positive cells were then magnetically labelled and positively selected on LS columns (Miltenyi Biotec). The column flow-through, representing the unlabelled lymphocyte fraction, was collected for further experiments. CD14 positive cells were eluted from the column as per manufacturer's instructions and washed in RPMI. These were seeded on day 0 at 1x10⁶ cells/well in 6-well plates in complete growth media (RPMI +10% FCS +

Pen/Strep) supplemented with 100ng/ml rhGMCSF and 25ng/ml rhIL-4. Fresh cytokines were added on day 3; cells were harvested for use on day 6 or 7.

2.2 Methods

2.2.1 Cell culture

Adherent cell lines:

293T cells were cultured in Dulbecco's MEM-Glutamax, supplemented with 10% heat inactivated fetal calf serum (FCS) and 1% Penicillin/Streptomycin (Pen/Strep). Cell monolayers were grown in 75cm² or 175cm² culture flasks at 37°C, 5% CO₂. When confluent (90-95%) cells were washed in PBS to remove serum, and incubated in trypsin-EDTA for 5-10 minutes to detach the monolayer. Cells were split 1:10 using complete DMEM.

Non-adherent cell lines:

B017.10 were maintained in suspension in RPMI-GlutaMAX supplemented with 6% FCS, 1% Pen/Strep and 50µM beta-Mercaptoethanol. Cells were grown in upright 75cm² flasks at 37°C, 5% CO₂. Cells were passaged every 2-4 days.

THP1 cells were cultured in suspension in RPMI-Glutamax supplemented with 10% FCS and Pen/Strep. Cells were maintained at 0.5-1x10⁶ cells/ml. To split, cells were collected and centrifuged at 200g for 5 min, resuspended in fresh media and replated at 1:10. To differentiate into dendritic cells, THP1 cells were cultured in the presence of 10ng/ml rhIL-4 (recombinant human interleukin-4) and 10ng/ml rhGMCSF (granulocyte-macrophage colony stimulating factor) for 6 days. 4x10⁶ cells/well were plated in 12-well plates in 1.5ml of complete media with cytokines. Cells were split on days 2 and 5 with addition of fresh cytokines. On day 6 or 7, both adherent and suspension cells were harvested for use.

2.2.2 Constructs

Maps were created and cloning strategies designed in VectorNTI. The following techniques were used in the creation of several vectors. Plasmid maps are included in the Appendix 1.

LNT_LifeAct-mCherry

LNT_Nck-ECFP

LNT_Nck-Cerulean

The following plasmids were acquired for further cloning or lentiviral preparation.

Gift from M Blundell: pHR_SEW

pHRsincpptSEWW^{WT}

pHRsincpptSEWW^E (Y291E)

pHRsincpptSEWW^F (Y293F)

Gift from G Bouma: LNT_SFFV_ICAM-1-GFP

Gift from D Moulding: LNT_mCherry-Actin

Bought from Clontech: pmCherry-N1

pEGFP-C2

pECFP-C1

Gift from S Shetty: pNLS_Cerulean

Cloning strategies

Polymerase chain reaction: 1unit of Pfu polymerase was used for 200ng DNA in a 25ul reaction. The thermal cycler was set up as follows:

2min at 95°C

35 cycles of: 30s at 95°C

30s at gradient*

2min15s at 72°C

10min at 72°C

Hold at 4°C

Restriction endonucleases:

Reactions were made up as per manufacturer's instructions using Promega, NEB or Fermentas restriction enzymes. 1-4 μ of DNA were digested for 1-2 hours in the optimal buffer and temperature recommended by the manufacturer.

Blunting digested ends:

If required, Klenow DNA polymerase I was used to fill in 5' or digest 3' overhangs. The reaction is performed at room temperature for 15 minutes with the addition of Klenow and 2mM dNTPs.

DNA dephosphorylation:

Shrimp alkaline phosphatase (SAP) was used to remove phosphate groups after digestion and prevent vector re-ligation. DNA was incubated with 1 μ l of enzyme at 37°C for 1hr, followed by heat inactivation at 65°C for 15 minutes.

Ligation:

After manipulation, DNA was run on a 1% agarose gel to resolve digested fragments. Bands were excised and purified from the agarose using a Qiagen gel extraction kit. Compatible digested and purified fragments were mixed with T4 DNA ligase and incubated at 14°C overnight. Vector and insert fragments were mixed in proportions calculated by the following equation, using 100ng of vector and a 3: 1 insert: vector ratio:

$$ng\ vector \times \frac{kb\ insert}{kb\ vector} \times ratio = ng\ insert$$

$$100ng \times \frac{kb\ insert}{kb\ vector} \times 3 = ng\ insert$$

Preparation of chemically competent bacteria

500ml LB was inoculated with DH5 α E. Coli and incubated at 37°C with agitation until the culture reached an optimal density of 0.4 at 600nm (1cm pathlength). The culture was spun down at 5000rpm (2000g) for 10 minutes at 4°C. The pellet was gently resuspended in 125ml

ice cold 100mM MgCl₂ and centrifuged at 4000rpm (1200g) for 10 minutes. The pellet was resuspended in 250ml of ice cold 100mM CaCl₂ and incubated on ice for a minimum of 20 minutes. The bacteria were spun down again and resuspended in 10ml of ice-cold, sterile 85mM CaCl₂ containing 15% glycerol w/v. 100µl aliquots were snap frozen in liquid nitrogen and stored at -80°C.

Transformation of competent bacteria

Competent E. Coli DH5α were mixed with 500ng of plasmid DNA and incubated on ice for 30 minutes. A heat shock at 42°C for 45seconds was applied, followed by a further 2 minutes on ice. 200µl of sterile LB broth was added and the bacteria were allowed to recover in a 37°C shaking incubator for 1 hour. Cultures were then plated on an agar plate with the appropriate antibiotic selection and incubated overnight at 37°C to allow growth of colonies derived from single bacteria. Colonies were then selected for inoculation of 5ml LB cultures.

Isolation/ purification of plasmid DNA

5ml cultures were pelleted and plasmid DNA was isolated using QIAprep Spin Miniprep Kit according to manufacturer's instructions. DNA was eluted in 30-50µl distilled water. The DNA was digested and resolved on a 1% agarose gel to confirm the presence of the correct plasmid construct.

Large scale plasmid production

500ml of LB with the appropriate antibiotic was inoculated with 500µl bacteria and incubated overnight at 37°C. The bacteria were pelleted by centrifugation at 5000g for 15 minutes and plasmid DNA was extracted using QIAprep Spin Maxiprep Kit according to manufacturer's instructions.

2.2.3 Lentiviral preparation

Transforming the packaging cell line

The transfection mixture comprises 40µg vector construct (pHR_LNT), 10µg pMD.G2 (vector containing envelope genes) and 30µg pCMV-dR8.74 (vector containing gag/pol packaging genes) added to 5ml Optimem media per flask. This was filtered (0.22µm) filter and added to 5ml Optimem with 1µl 10mM polyethylenimine. The transfection mixture was incubated at room temperature for 20minutes. 10ml were added to each 175cm² flask of 293T cells, seeded at 1.5×10^6 cells/flask 24hours previously. After 4 hours, the transfection mixture was removed and replaced with fresh complete DMEM.

Virus harvesting and concentration

After 48hours the culture medium was collected, filtered through a 0.22µm filter and ultracentrifuged at 23 000rpm (50000g), for 2hours to pellet the virus particles. These were resuspended in 150µl PBS and incubated on ice for 1 hour to allow virus resuspension. Virus aliquots were stored at -80°C.

Titration of virus suspension

293T cells were seeded at 50 000 cells per well in a 5-fold serial dilution of virus from 1/100 to 1/10⁶. After 72 hours, the cells were harvested and analysed by flow cytometry to determine the percentage of positive cells. The virus titre was calculated by multiplying the number of cells seeded by the dilution and the percentage positive cells.

Infection of primary DCs

BMDCs were cultured in GMCSF as previously described. On day 5, before feeding, cells were harvested, counted and replated at 5×10^5 cells per well (12-well plate) in 500µl of conditioned media. Cells were allowed to settle for 30min at 37°C before addition of virus at an MOI = 5 (multiplicity of infection). This was incubated for a further 30min, followed by addition of 1.5ml of fresh complete media supplemented with 20ng/ml GMCSF. Cells were harvested on day 8 for further experiments.

Infection of THP1 cell line

Stable cell lines of control (SCR shRNA) or knockdown (e.g. MKL-1, WDR1) THP1 cells were created by infecting THP1s with a lentivirus expressing the appropriate shRNA construct using a protocol identical to that for primary DCs. 24 hours after infection, THP1 cells were spun down and resuspended in complete RPMI media supplemented with 0.6µg/ml puromycin (selection for resistance gene encoded in construct).

2.2.4 Western blots and Immunoprecipitation

Cell pellets were resuspended in ice-cold lysis buffer (50µl per 1×10^6 cells) and lysed on ice for 10 minutes. Lysates were centrifuged to pellet cell debris; supernatants were transferred to a new eppendorf tube and mixed with an equal volume of 2x loading buffer and heated at 70°C for 10 minutes. Cell lysates were separated on 12-14% NuPAGE Bis-Tris gels loaded with 30µl sample per well. Fermentas PageRuler Prestained Protein Ladder was included as size marker and gels were run at 160V for 1-1¼ hours.

Blots were transferred onto Millipore Immobilon P membrane (activated in methanol for 5 minutes) at 18V for 45 minutes.

Membranes were blocked using 5% skimmed milk in PBS-tween (0.1%) and antibodies were used at 1/1000 in 5% milk with 0.1% Tween 20. Secondary antibodies (anti-mouse and anti-rabbit HRP conjugated) were also used at 1/1000 dilution.

Peroxidase activity was detected using SuperSignal West Femto Chemiluminescent Substrate (Thermo Scientific).

To analyse protein interactions, cells were lysed and one of three methods for immunoprecipitation was followed.

- A. Cell lysates were pre-cleared using normal mouse IgG1 and A/G PLUS-Agarose beads for 1 hour at room temperature to remove non-specifically bound proteins. Cleared lysates were incubated with anti-Nck (BD) or anti-WASp (SantaCruz) antibodies overnight, then pulled down with Protein A/G PLUS-Agarose beads. Immunoprecipitates were collected by centrifugation, washed in PBS, resuspended in reducing buffer and boiled. Immunoblots with anti-WASp and anti-Nck were carried out on the polyvinilidene difluoride (PVDF) membranes.
- B. Antibodies for IP (e.g. anti-Nck, BDBioSciences) were crosslinked to agarose beads using the Pierce Crosslink Immunoprecipitation Kit, according to manufacturer's instructions. Lysates were then added to columns containing the labelled beads and incubated at 4°C on a rotator overnight. The bead suspension was washed and immunocomplexes eluted and analysed for protein content on Immobilon membranes as above.
- C. Primary antibody (WASp, B9) was conjugated to Protein G Dynabeads as per manufacturer's guidelines. Samples were incubated with the Dynabeads on a rotator for 2 hours at room temperature. Dynabead-Ab-Ag complexes were washed in PBS three times and transferred to a new tube. Denaturing elution was performed in NuPAGE Sample Buffer+ Reducing Agent, for 10minutes at 70°C.

2.2.5 Conjugate formation

Conjugate adhesion by FACS: 1×10^6 DCs (LPS only or LPS/OVA pulsed) were resuspended in 2ml complete RPMI and CMFDA dye (Molecular Probes, Invitrogen) was added to a final concentration of 0.2 μ M. 1×10^6 CD4⁺ T cells per sample were resuspended to 1×10^6 /ml in complete RPMI and labelled in 1 μ g/ml DDAO. Both cell types were stained for 30min at 37°C, then washed and resuspended in complete RPMI for 30min at 37°C. DC T cells were mixed 1:1 in round-bottom polystyrene tubes in a total volume of 250 μ l; and centrifugated at 400rpm (30g) for 5min to encourage conjugate formation. Suspensions were incubated at 37°C for 1 hour and conjugate adhesion was analysed by flow cytometry. CMFDA was detected in the FITC channel; DDAO in APC channel.

Slides for confocal microscopy: Ovalbumin-pulsed or LPS control only DCs were harvested on day 8 and mixed with CD4⁺ OT-II cells at a ratio of 1:5 (typically 80 000DCs and 400 000T cells) in a small volume (typically 200 μ l) and spun gently (400rpm (30g) for 5 min) to enhance contacts between cells. The suspension was incubated at 37°C for 10-100min (see individual experiments) to allow conjugate formation. The loose pellets were resuspended gently and pipetted onto poly-L-Lysine-coated glass slides. Incubation at room temperature for 2-5minutes allowed cells to settle onto the coated slides, which were then washed and the cells fixed in 4% PFA at room temperature for 20 minutes.

Pellets for electron microscopy: DCs and OT-II cells were mixed at cell ratios of 1:3 (typically 1×10^6 DCs+ 3×10^6 T cells). These were centrifuged and incubated as above. Fixation was performed in suspension by adding an equal volume of 4%PFA supplemented with 0.05% gluteraldehyde. Suspensions were centrifuged and the fixative removed. Cell pellets were resuspended in 50 μ l of PBS, followed by addition of 50 μ l of 2% low-gelling temperature agar (above 37°C).

2.2.6 Antigen presentation assays

E α -GFP: Immature BL6 and WAS BMDCs were pulsed with varying concentrations (0.01 – 100 μ g/ml) of E α -GFP protein (a gift from P Garside, University of Glasgow) in combination with LPS (as above), on day 7. E α presentation was detected 24hours later by flow cytometry using an antibody specific for the E α peptide in context of MHC class II peptide (Yae; see antibody list).

T cell proliferation: Isolated CD4+ T cells were stained in a final working concentration of 10 μ M CFSE diluted in serum-free media for 10 minutes at 37°C. Staining was quenched by adding 5 volume of ice-cold complete RPMI and incubating on ice for 5 minutes. Cells were pelleted and washed by resuspending in fresh media twice. CFSE-stained T cells were cocultured with BL6 or WAS DCs (pulsed with LPS with or without OVA) at ratios of 1:1 and 1:5. Three days later, cells were harvested and immunostained for CD4. CFSE staining was analysed by flow cytometry, gating on CD4-positive cells only.

IL-2 production: Unlabelled CD4+ T cells were cocultured with DCs for 48hours, as above, at DC: T cell ratios of 1:1 and 1:5. Plates were centrifuged, supernatants collected and IL-2 content determined by ELISA as per manufacturer's instructions. (R&D systems: Mouse IL-2 DuoSet DY402)

2.2.7 Enzyme-linked immunosorbent assay (ELISA)

Cytokine secretion was measured from 24 and 48hr DC: T cell coculture supernatant using R&D systems Duo Set ELISA kits, as per manufacturer's instructions. Briefly, high protein-binding capacity 96-well plates (Nunc MaxiSorb) were coated with capture antibody against the selected cytokine at 4°C overnight. These were washed and blocked (see ELISA solutions in table) and supernatants were added at pre-determined dilutions. Plates were incubated for 2hours at room temperature, washed and biotinylated detection antibody was added and incubated for a further 2 hours. Unbound antibody was washed off and streptavidin-bound horseradish peroxidase (HRP) added for 30min. 1x TMB solution was added as a substrate for

HRP and incubated at room temperature for 15-30minutes. Sulphuric acid stop solution (2N H₂SO₄) was added and absorbance at 450nm was measured on an Optima FLUOStar plate reader.

2.2.8 Q-PCR

DC: T cell suspensions, cocultured at 1:5 ratio for 48hrs in a 96-well plates, were pelleted and lysed. Total mRNA was isolated using the RNeasy Mini Kit (QIAGEN, 74104). DNA contamination was removed by a 15-minute incubation at room temperature with DNaseI. RNA strands are split by addition of random primers and incubation at 65°C for 5 minutes. Reverse transcription was carried out at 37°C for 2 hours using MMLV-RT, followed by heat inactivation at 70°C for 15 minutes. 1µl of this reaction volume containing cDNA was used for a 25µl RTQ-PCR reaction, using TaqMan primer/probe mix and Platinum qPCR SuperMix-UDG with ROX. Samples were set up in triplicates for each experiment. Δ CT values were calculated against murine GAPDH controls. Briefly, CT values were averaged for all replicates. Δ CT values were calculated (CT(gene of interest) -CT(GAPDH)). $\Delta\Delta$ CT values were calculated by dividing the Δ CT value of each experimental sample by the BL6 LPS control value for the respective gene. Fold change from BL6 LPS was calculated as $2^{(-\Delta\Delta CT)}$. Results were averaged across 5 repeat experiments.

2.2.9 Microarray analysis

T cells were isolated from DC:T cell cocultures 48hours after culture. RNA was extracted and DNA contamination removed as above. RNA quality and concentration were determined on 2100 Bioanalyser. An Affimetrix GeneChip Mouse Genome 2.0 Array was used to analyse over 39000 transcripts. An average for each condition was calculated and fold change (FC) analysis performed in the GeneSpring software. Data was consequently imported into Ingenuity Systems IPA8, which was used to create Figures 5.13 and 5.14.

2.2.10 Dynabead assays

Matured DCs were incubated on ice in a 1:1 mix of anti-MHC (I-Ab)-biotin and anti-ICAM-1-biotin antibodies for 40 minutes. Antibodies were used at a dilution of 1/100 in PBS, and 50 μ l per 10⁶ cells. After 40 minutes, cells were washed in PBS and resuspended in Dynabeads M-270 Streptavidin, at a cell: bead ratio of 1:3. The suspension was incubated at 37°C for 30-40 minutes and cell-bead complexes were separated using a Dynabead magnet.

These were used for immunofluorescent staining and confocal analysis or lysed for immunoprecipitation as described above.

2.2.11 DC adoptive transfer

DCs were pulsed with LPS only and LPS/OVA overnight, then labelled with CFSE as described in section 2.2.6 above. 4x10⁶ labelled cells were injected into the tail vein of OT-II mice. Three mice were used per condition in each experiment. Two days post injection, spleens and lymph nodes were collected and CD4⁺ cells were isolated using a Miltenyi Biotec kit. 5x10⁵ CD4⁺ cells per well were added to 96-well plates in 200 μ l in media supplemented with PMA (10ng/ml), ionomycin (1.5 μ M) and brefeldin A (1 μ g/ml) for 5 hours. CD4⁺ cells were then washed and stained for FACS analysis as described below.

2.2.12 Immunocytochemistry and Immunostaining for FACS

Coverslips (*Deckgläser 24x24mm*): Cells were allowed to adhere onto poly-L-lysine coated slides or coverlips and fixed in 4% paraformaldehyde (PFA) for 30 minutes. Cell membranes were then permeabilised in 0.1% triton for 5 minutes. To block Fc receptors, cells were incubated in PBS with 5% serum from the secondary antibody host (mouse, goat, rat or rabbit) for 20 minutes. If necessary, endogenous biotin was blocked using an Avidin/Biotin block kit (Invitrogen) as per instructions.

After washing off blocking agents, the primary antibody was added at 1/50-1/100 dilution for 1 hour at room temperature. This was washed off with 3x 5 minute washes in PBS and secondary antibody was added at a dilution of 1/100-1/200. Other staining agents, such as DAPI (DNA) and fluorescently-tagged phalloidin (F-actin), were also added at this stage. After 45minutes, the washing was repeated and coverslips were mounted using AquaPolymount.

For analysis of podosomes, coverslips were coated with fibronectin (10µg/ml) for 1hour at 37°C or overnight at 4°C. Coverslips were washed in PBS and primary DCs or THP1 cells were seeded for up to 2hours at 37°C. Once adhered, cells were fixed and stained following the protocol above.

FACS: Cells were washed in complete media and stained for surface markers (e.g. CD3, CD4, CD11a/c, CD69) using fluorophore-conjugated antibodies at 1/100 dilution in PBS-BSA (1%) for 45minutes. Cells were washed in PBS twice and fixed in 4%PFA for 15minutes, followed by any permeabilisation or intracellular stain required (e.g. cytokine stain in T cells from DC adoptive transfer). Conjugated antibodies were also used for intracellular stains, diluted to 1/50 in PBS-BSA (1%) for 1 hour.

2.2.13 Live Imaging and Fluorescence Recovery After Photobleaching (FRAP)

Conjugates were formed between T cells and lentivirus-infected DCs as described above. These were allowed to settle in a glass-bottom dish for 20minutes at 37°C. All imaging was performed using the Zeiss LSM710 system with a 63x oil objective. Fluorophores were excited using 488nm and 561nm lasers for EGFP and mCherry constructs respectively.

For FRAP, conjugate suspensions were also seeded in glass imaging dishes. Successful conjugates were chosen for FRAP on the basis of sufficient fluorescent construct expression. For the basic analysis, images were acquired every 100ms, at a digital zoom x8 and a 63xmagnification objective. 1.5x3µm rectangle region of interest (ROI), in the synapse, cortex

or cytoplasm of the DC, was bleached. Pre-bleach images were acquired for 2s, followed by bleaching of the ROI with 5 iterations of 100% laser power with 488 and 561nm lasers. Fluorescence recovery was measured for 30s after the bleach. Recovery curves were normalised and averaged. Halftimes were calculated according to the time taken for fluorescence to reach half of the final intensity.

To separate the actin networks involved, only imaging parameters were changed. Images were acquired every second with a digital zoom of 27x (5x5 μ m area). Pre-bleach images were acquired for 5s, followed by bleaching of a 1x1 μ m circular ROI. Fluorescence recovery was measured for 2minutes after the bleach.

2.2.14 Micropits preparation

Coverslips containing the micropits (kind gift from M Biggs, Columbia University) were affixed to 6-well plates, in which the bottom of the dishes was cut out, using an even layer of vacuum grease to prevent leakage. The wells were filled with 3ml serum-free media and placed inside a DNA SpeedVac. Air pressure was slowly decreased to around 20-25 Torr to extract air from the micropits. From this point on the pits remained completely submerged in liquid to prevent contact with the atmosphere which would reintroduce air, preventing cell seeding. The coverslips were incubated in 10% pluronic acid solution for 30minutes at 37°C to prevent protein adsorption. The micropits were washed in PBS to remove residual pluronic acid; and buffer exchanged with serum-free media. For cell seeding and imaging conditions see results section 4.2.5.

2.2.15 Electron Microscopy

Conjugates were fixed in 1% PFA + 3% glutaraldehyde or Karnowski fixative for 20min at room temperature. Samples were pelleted and resuspended in low gelling temperature agar (TypeVII, 2-Hydroxyethylagarose; Sigma, A4018). The agar was allowed to set at room

temperature. The agar blocks were post fixed in osmium tetroxide, followed by dehydration in increasing percentages of ethanol (70-100%). Conjugates were embedded in epoxy resin, which was polymerised at 60°C. Samples were sectioned with an ultramicrotome using a diamond knife and sections were loaded onto 300mesh grids. Uranil acetate was used as a positive stain to provide contrast.

2.2.16 Gatan 3view sample processing

DC: T cell conjugates were fixed in 2% PFA+2% gluteraldehyde for 1hour at room temperature. These were set as above into 2% low gelling temperature agar. The resulting gel was cut into small pieces (<2x2mm) using a razor blade. The samples were washed 5 times for 3 minutes each in cold 0.15M cacodylate buffer containing 2mM calcium chloride. (Each wash referred to below comprises 5 x 3min washes.) These were then incubated for 1hour on ice in 0.3M cacodylate buffer with 4mM calcium chloride combined with an equal volume of 2% aqueous osmium tetroxide (EMS) and 3% potassium ferrocyanide. After the heavy metal incubation, samples were washed in dH₂O and placed in filtered thiocarbohydrazide solution for 20min. Sample were washed and placed in 2% osmium tetroxide in dH₂O for 30min for a second osmium stain. After washing, samples were incubated in 1% uranyl acetate at 4°C overnight. On the following day, Walton's en bloc lead aspartate staining was performed for 30min, as previously described (Walton, 1979). Finally, samples were washed and dehydrated sequentially in ice-cold solutions of 30%, 50%, 70%, 90%, 100% and 100%(anhydrous) ethanol. Samples were placed in a viscous embedding agent (Fluka Durcupan) on a rotor overnight. Finally, these were embedded in a fresh, thin layer of resin, which was polymerised in a 60°C oven for 48hours.

For imaging, resin block were cut to the size of each sample, mounted onto cryo pins using cyanoacrylate glue and trimmed further to created clean edges. Samples were coated in gold

palladium for 5min under argon. Cutting and imaging are performed under variable pressure, at a magnification of 50,000x and a Z step of 100nm.

2.2.17 Supported planar lipid bilayers

Glass coverslips were cleaned in Pirahna solution (3:1 mixture of sulphuric acid and 30% hydrogen peroxide). These were dried under Argon flow and glued to chamber slides (Sigma, C7182). When set, lipids (a gift from C Nowosad, Tolar lab, NIMR) were added in 250µl to each chamber. 1,2-Dioleoyl-*sn*Glycero-3-Phosphoethanolamine-N-(cap Biotinyl) (DOPE-cap-biotin) was mixed at a molar ratio of 1:100 with 1,2-dihexanoyl-*sn*-glycero-3-phosphocholine (DOPC; both from Avanti Polar Lipids) in chloroform, and used to produce planar lipid bilayers as described previously (Tolar et al., 2009). Following washing, 5µg/ml of streptavidin in PBS was added for 15mins. Following washing, chambers were incubated with 0.5µg/ml biotinylated antigen (anti-MHCII-Cy5 and/or anti-ICAM-1 antibodies) in PBS for 30min. Chambers were washed in HBSS, to allow complete buffer exchange; and pre-incubated at 37°C prior to addition of cells.

2.2.18 Image Processing and Data Analysis

Post-acquisition image processing and intensity quantification were performed using ImageJ (NIH, USA). FACS data was analysed using FlowJo. Gatan data was processed using DigitalMicrograph and Amira. GraphPad Prism 5 and Microsoft Excel 2010 were used for graphical representation and statistical analysis. Unless otherwise stated, a paired or unpaired t-test was used as appropriate, to determine significance between two separate groups. CT values from QPCR results were analysed using 7000 System SDS Software by Applied Biosystems. Origin Lab was used for FRAP analysis as described in recent publications (Fritzsche et al., 2013). GeneSpring and Ingenuity Pathway Analysis were used for analysis of microarray data in Chapter 5.

Chapter 3 – Deregulated actin results in abnormal synapse formation

3.1 Introduction

Although the T cell actin cytoskeleton has been shown to be important for the formation of the immunological synapse ((DeMond et al., 2008, Ilani et al., 2009, Yu et al., 2010, Krummel et al., 2000)), the role of the dendritic cell actin network has not been studied in such detail. To elucidate its role in immunological synapse formation, the murine model of Wiskott Aldrich syndrome was used as a model for cytoskeletal dysfunction. Several characteristics of successful synapse formation were compared between WAS and control DC: T cell conjugates *in vitro*.

The T cell integrin, LFA-1 (also known as CD11a/CD18 and $\alpha_L\beta_2$), is involved in the adhesion between DCs and T cell, initially establishing the interaction through weak binding and later to stabilise this during formation of a mature synapse (reviewed in (Dustin, 2009a, Hogg et al., 2011, Kinashi, 2005). T cell LFA-1 has been shown to polarise towards the DC upon stable immunological synapse formation (Lub et al., 1997, Wulfing and Davis, 1998).

Integrins are important for leukocyte trafficking and function in the immune system. In addition to their crucial role in cell-cell adhesion, data is emerging to support the idea that integrins can also act as bidirectional transmembrane receptors and transduce biological signals. As previously discussed, it is difficult to elucidate the exact pathways in T cells, in particular for outside-in signalling, due to the blurred distinction between direct LFA-1-mediated signalling and the effects of prolonged or augmented signalling from other

receptors. Despite this, evidence increasingly points to a role of LFA-1 in signal transduction (Abraham et al., 1999, Weber et al., 2001, Perez et al., 2003). Furthermore, it has been shown that LFA-1 binding to its ligand ICAM-1 results in the accumulation of the adaptor protein talin, which in turn recruits vinculin and Arp2/3. Through its association with type I phosphatidylinositol 4-phosphate 5-kinase (PIP5K), talin recruitment results in elevated levels of PIP₂ at the site of LFA-1 ligation, leading to recruitment of WASp and subsequently increased actin polymerisation (Mace et al., 2010). Although these experiments were conducted in NK cells, they provide a clear mechanism which links integrin activation and cytoskeletal rearrangement.

In this chapter, several methods were used to study DC: T cell adhesion and the characteristics of successful synapse formation. As well as LFA-1, these studies also focused on its dendritic cell ligand, ICAM-1. ICAM-1/LFA-1 interactions have been shown to occur in the pSMAC (Monks et al., 1998).

Another parameter reflecting correct DC: T cell interaction is T cell MTOC polarisation and docking. This was first documented over 30 years ago (Geiger et al., 1982), though the signalling pathways regulating MTOC docking are still unclear. It has been suggested that MTOC polarisation is driven by localised accumulation of diacylglycerol (DAG) at the IS and DAG-dependent activation of PKC (Quann et al., 2009). MTOC docking has also been linked to Lck signalling (Tsun et al., 2011), L-plastin phosphorylation (De Clercq et al., 2013b) and cdc42 (Pulecio et al., 2010).

Serial block face electron scanning microscopy was used to further probe the general structure of a synapse. This technique, originally developed in the field of neuroscience for imaging of whole tissue sections, involves sample sectioning with an ultra-microtome, followed by imaging of each consecutive block face by collecting the backscattered electron image (¹ see

¹ http://www.gatan.com/knowhow/knowhow_15/3view.htm

footnote for reference). The technique was optimised for samples of DC: T cell conjugates in suspension.

This chapter aims to establish the validity of WAS DCs as a model for actin-deficiency in synapse formation; to consolidate the previously suggested role for the DC actin cytoskeleton at the IS; and to examine the morphological differences in synapse formed between CD4+ T cells and control or WASp-deficient DCs.

3.2 Results

3.2.1 T cell isolation efficiency

To create an antigen-specific system, T cells were isolated from OT-II mice, expressing a transgenic TCR which recognises ovalbumin (OVA) in the context of MHC class II. CD4⁺ T cells were isolated using a Miltenyi Biotec negative selection kit and purity was checked by flow cytometry using an anti-mouse CD3-FITC conjugated antibody. Over 95% efficiency was achieved. The untouched, enriched CD4⁺ T cells were used for experiments.

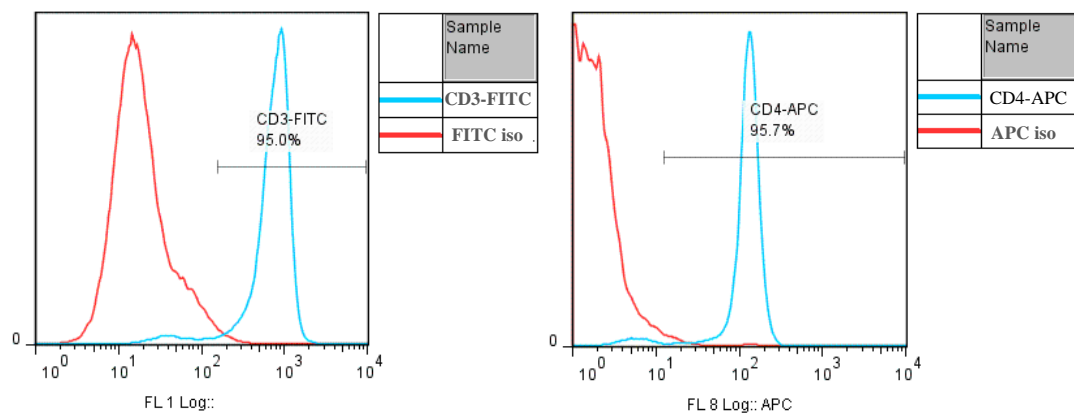


Figure 3.1. **T cell isolation purity.** Red histograms represent isotype control stain. Blue histograms represent anti-CD3 or anti-CD4 labelled cells.

3.2.2 Bone marrow-derived DCs and comparison of WAS DC markers

BMDCs of control (BL6), WASp deficient (WAS) and WASp phospho-null mutant (FYN) mice were cultured for 7 days in the presence of GM-CSF and matured overnight with the addition of LPS. Figure 3.2 shows surface expression of CD11c, in immature and LPS-matured DCs, which is upregulated during myeloid differentiation (Corbi and Lopez-Rodriguez, 1997).

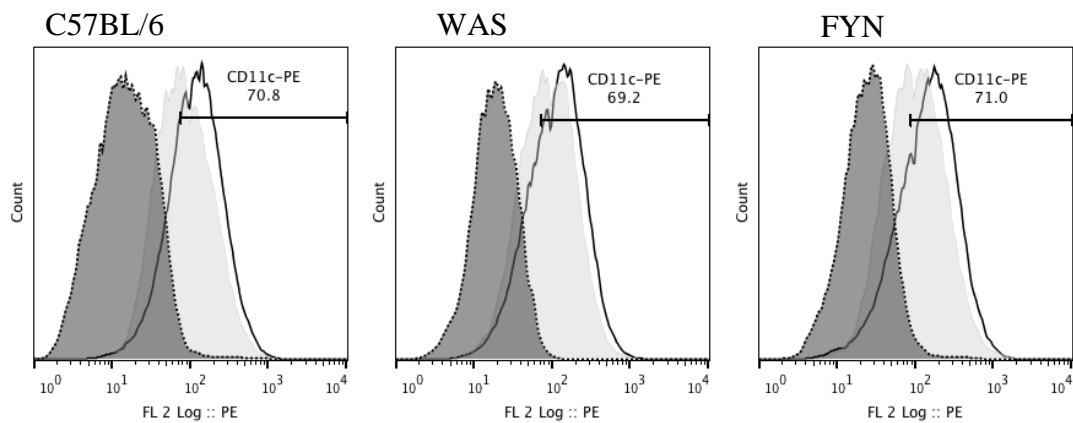


Figure 3.2 **CD11c expression.** Grey-filled histograms represent immature DCs; black lines represent LPS-matured cells; black dashed, filled histograms represent isotype controls. Bars quantify percentage of cells stained positive above isotype control for each DC type.

Expression of MHCII, CD80 and CD86 was checked to ensure DCs were of comparable maturation status. Figure 3.3 shows upregulation of all three markers upon maturation of DCs. Further, surface expression levels are similar in cells from all three strains, suggesting a similar level of maturation.

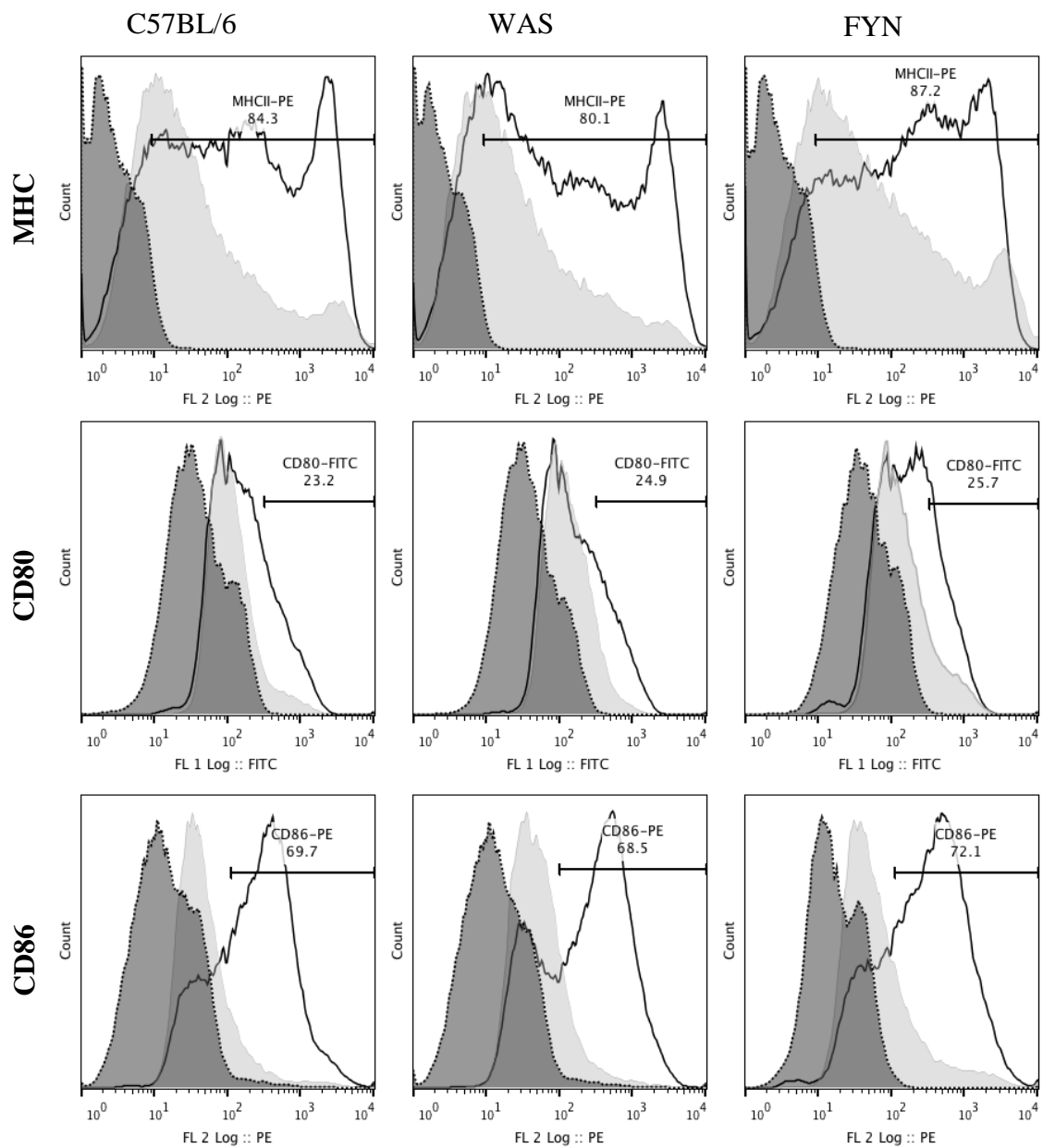


Figure 3.3. **BMDC maturation status.** DCs were stained on ice with fluorophore-conjugated antibodies and analysed by flow cytometry. Grey-filled histograms represent immature DCs; black lines represent LPS-matured cells; black dashed, filled histograms represent isotype controls. Bars quantify percentage of cells stained positive above isotype control.

Phalloidin-647

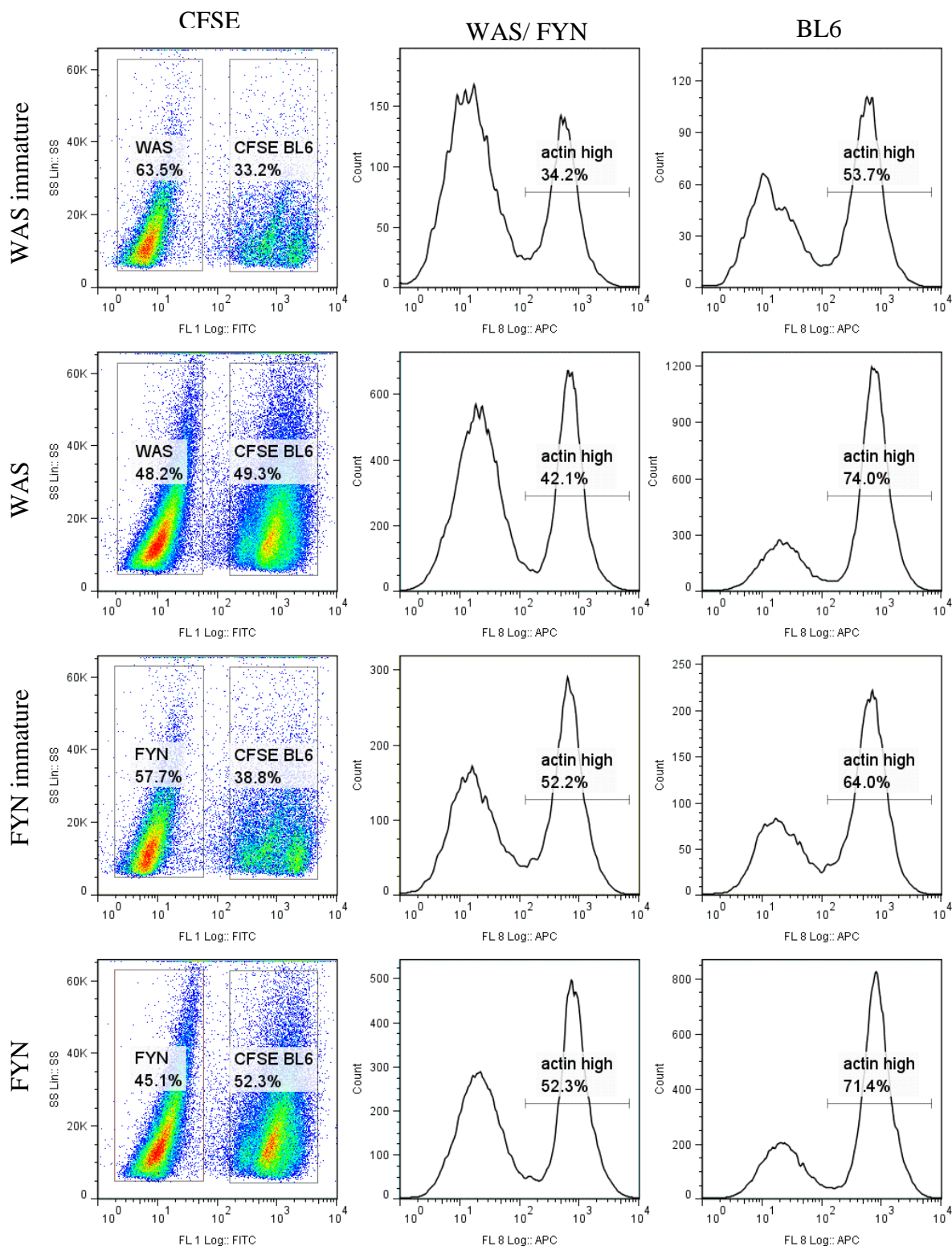


Figure 3.4. **Total polymerised actin network.** The CFSE-stained C57BL/6 and unstained WAS or FYN populations are gated separately in the FITC dotplots (left column). Polymerised actin in these is then compared – in the middle column histograms represent WAS or FYN; right column represent C57BL/6. Bars (“actin high” gate) quantify the percentage of each population which shows a strong phalloidin stain.

Loss of expression or function of WAS is predicted to affect actin polymerisation as a result of reduced Arp2/3-mediated nucleation. The total polymerised actin network was measured by staining with phalloidin. As this stain is very sensitive to any variation in staining protocol, including cell number and permeabilisation, staining was performed in mixed population samples. CFSE-labelled control DCs were mixed with unlabelled WAS or FYN DCs. These were then permeabilised and stained together. Fig3.4 shows C57BL/6 DC populations contain a larger proportion of cells with highly polymerised actin (larger percentages of 'actin high' cells in the BL6 histograms). Similar results were obtained when either WAS or FYN DCs were CFSE-labelled and mixed with unlabelled C57BL/6 DCs, confirming that the difference in actin is not a result of the additional stain in control cells. The experiment confirms that WAS and FYN DCs are impaired in actin polymerisation and thus show a decreased total F-actin network.

3.2.3 Antigen presentation

Presentation of particulate antigen has previously been shown to be defective in WASp-deficient DCs (Westerberg et al., 2003). To confirm that differences in synapse formation were not a result of poor antigen presentation, an E α -GFP antigen presentation assay was performed. BMDCs were matured with LPS and cultured in varying concentrations of E α -GFP (0.1-100 μ g/ml). The DCs normally take up this antigen, process it by cleaving off the GFP tag and present the E α peptide on MHC II molecules at their surface. E α in the context of MHCII is then recognised by the Yae antibody (Rudensky et al., 1991, Ghimire et al., 2012). No significant difference in surface E α presentation was seen between control and WAS DCs at any of the concentrations tested (Figure 3.5). This confirms previous reports that soluble antigen, unlike particulate antigen (Westerberg et al., 2003), is taken up, processed and presented normally in WAS DCs.

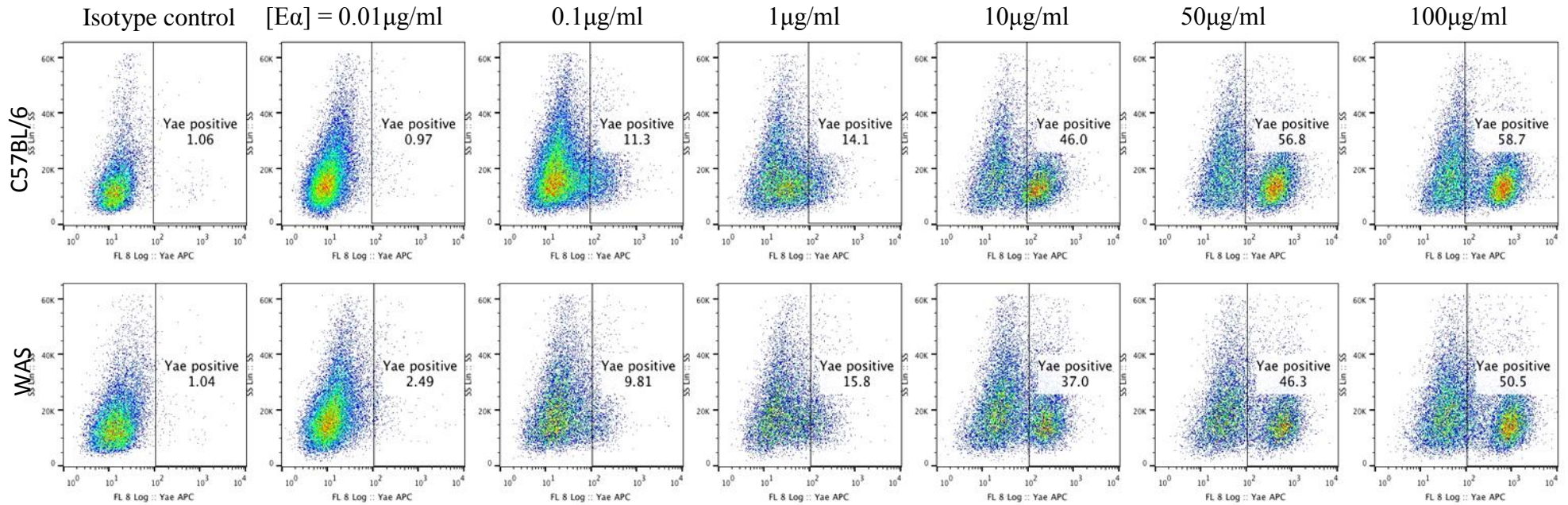
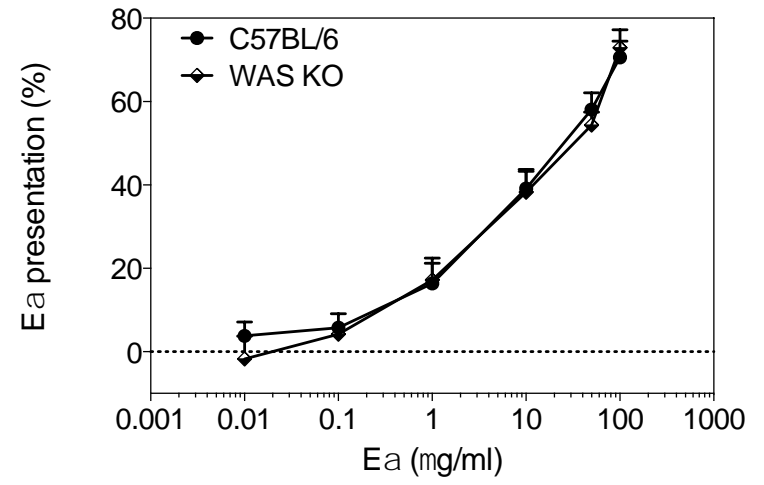


Figure 3.5 **Antigen presentation.** Proportion of Yae positive cells (expressing Eα peptide on MHC class II). DCs were cultured overnight with LPS and a range of Eα peptide concentrations. Cells were then stained for surface Eα using the Yae antibody. Positive cells are characterised as those showing fluorescence higher than the isotype control for each cell type. FACS plots show one representative experiment. Means values from 4 separate experiments are plotted in the graph on the right.



3.2.4 DC: T cell conjugate formation

To investigate the ability of WAS DCs, compared to BL6, to form stable conjugates CMFDA-stained DCs and DDAO-stained T cells were cocultured for 1 hour and conjugate adhesion was analysed by FACS. Stable conjugates were detected as double positive events. Figure 3.6 shows representative dotplots indicating the percentage of double positive conjugates. The proportion of successful conjugates was very low, suggesting that many of the synapses may be disrupted as a result of the sample preparation technique.

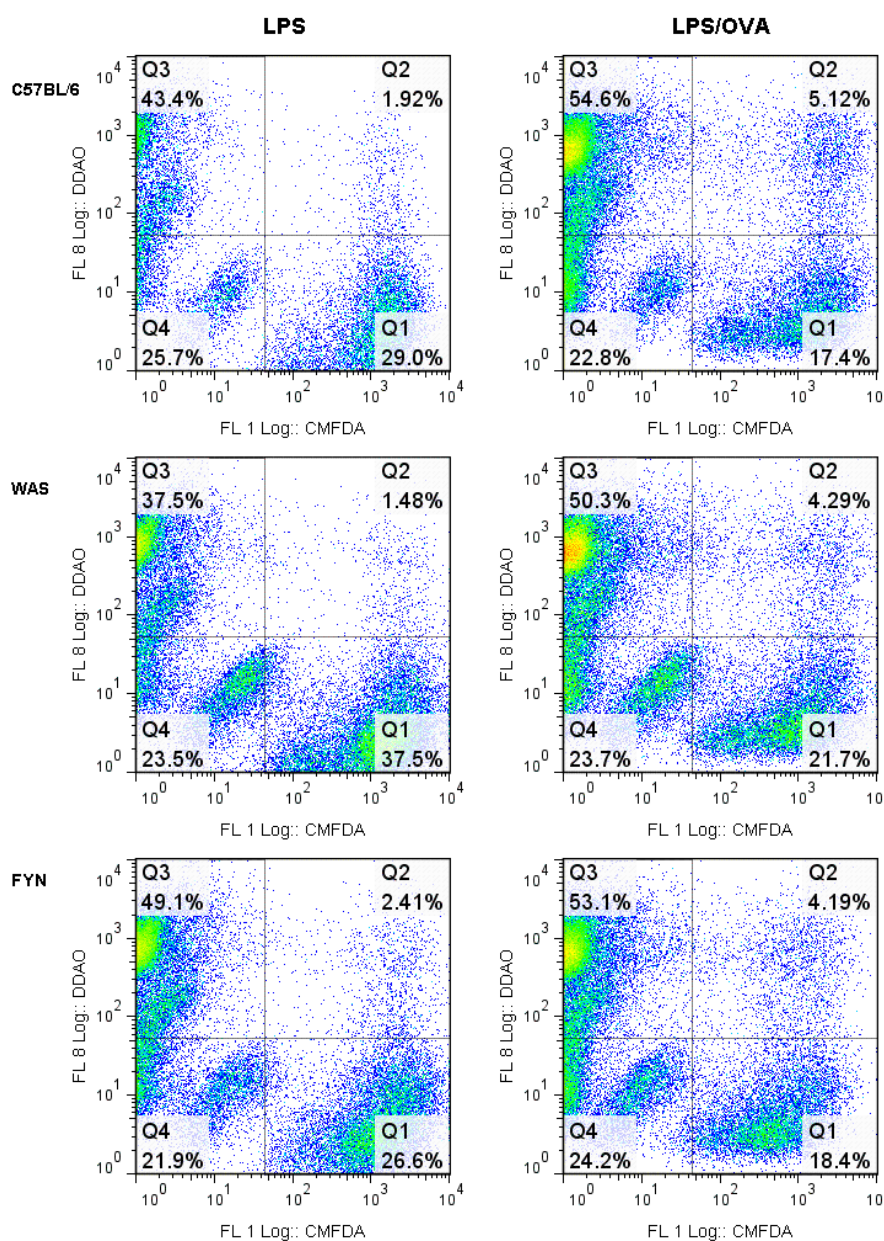


Figure 3.6. **Conjugate formation - FACS.** CMFDA-DCs and DDAO-T cell were cocultured for 1 hour at 37°C. Conjugates were gently resuspended and analysed by flow cytometry. Double positive events (in Q2) represent DC: T cell conjugates.

Therefore, conjugate formation was also studied by immunofluorescence to quantify the number of synapses formed more accurately. DC and T cells were cocultured at a 1:3 ratio for 45 minutes and seeded on poly-L-lysine slides at room temperature for a further 10 min. Cells were fixed and stained for specific surface markers. Successful conjugates were characterised as those showing an extensive, intimate contact between the DC and T cell, as shown in Fig 3.7 (white arrows). The graph in Figure 3.7 shows the percentage of DCs which had engaged T cells, out of the total DC population.

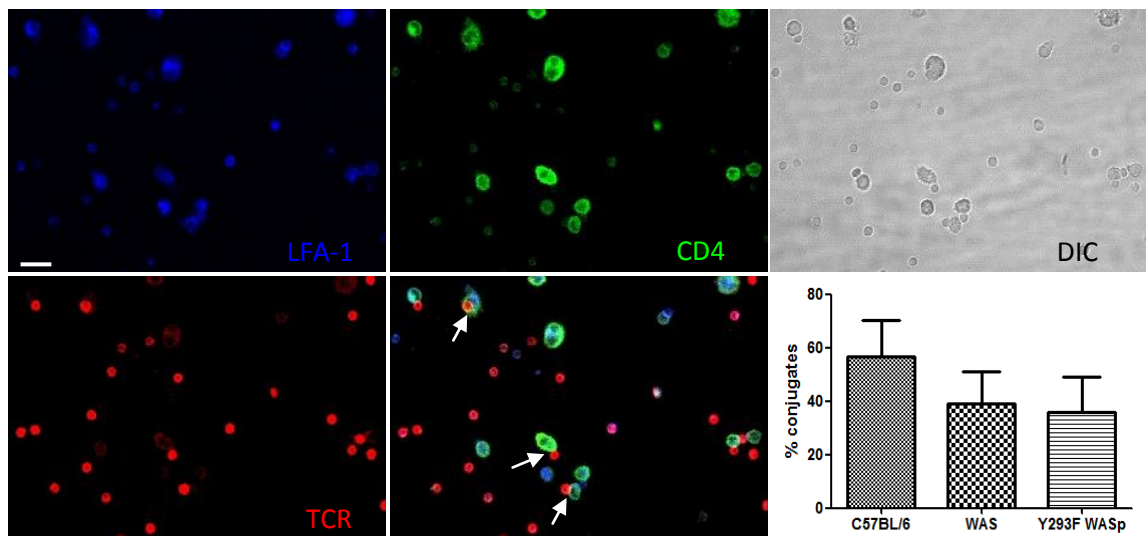


Figure 3.7. **Conjugate formation - microscopy.** DC: T cell cocultures, seeded on poly-L-lysine slides, were stained for LFA-1, CD45 and TCR. DCs forming conjugates (white arrows) were quantified as a percentage of total DC number.

The proportion of synapses is reduced in samples with WAS-deficient DCs or DCs expressing inactive WAS protein (FYN) compared to control.

3.2.5 Cell surface markers accumulating at the IS

There is evidence for polarisation of several cell surface markers towards the contact interface, as discussed in the introduction. Immunofluorescent stains were performed to investigate whether these polarise correctly in WAS DCs. To allow quantification of T cell markers, such as TCR and LFA-1, the T cell cortex was split into two areas of similar size – the side contacting the DC and the opposite side. Fluorescence in each cortical half was measured and the synapse side was divided by the opposite side to obtain a polarisation ratio (Fig 3.8).

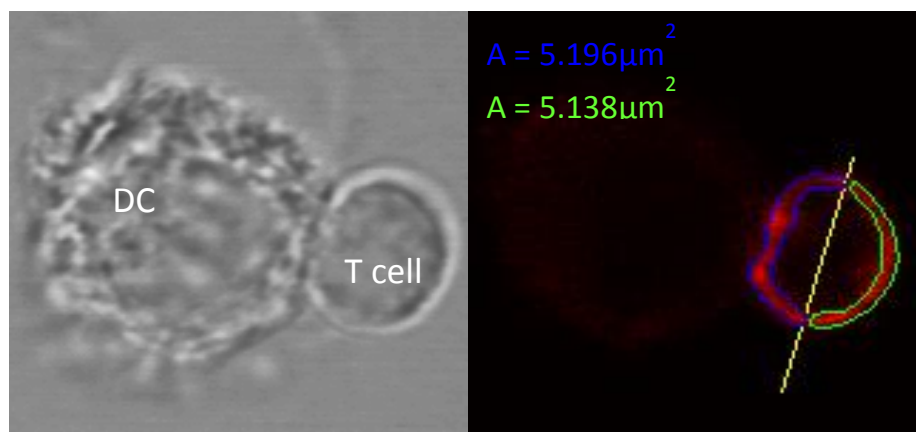


Figure 3.8. **Measuring polarisation of synaptic markers.** Yellow line represents division of T cell parallel to the plane of the cell-cell interface. Blue area ($5.196\mu\text{m}^2$) represents T cell half facing the contact, green area represents opposite side.

This analysis was performed for cell surface molecules that are known to accumulate in different regions of the IS. CD45 was analysed as a marker for dSMAC, LFA-1 is present in the pSMAC, and the TCR gathers in the cSMAC. Polarisation of these markers is quantified in the scatter plots in Figure 3.9.

There is evidence for TCR polarisation in productive synaptic contacts (Alarcon et al., 2011, Biggs et al., 2011, Hashimoto-Tane et al., 2011). TCR polarisation shown in Fig 3.9 appears very modest; and no significant difference in TCR polarisation was detected between T cells contacting BL6, WAS or FYN DCs using an unpaired t test. However, a one-sample t-test against a hypothetical value of 1.0 reveals a significant difference between this and the calculated polarisation ratios for BL6 and FYN DCs conjugates (BL6 $p=0.0023$; FYN $p=0.0288$). This was not

the case for WAS ($p=0.0637$), suggesting that the polarisation ratio of TCR molecules in T cells interacting with WAS DCs was not significantly different from 1.0.

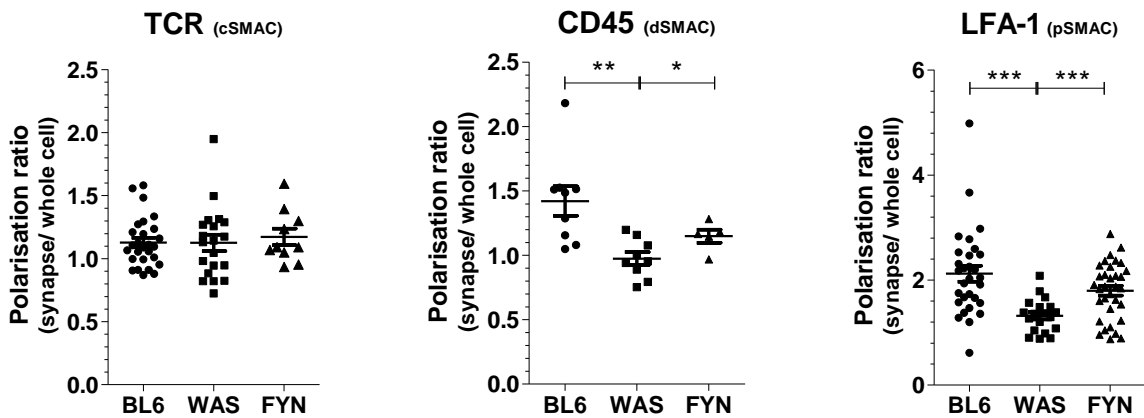


Figure 3.9. **Polarisation of synaptic markers.** DC: T cell conjugates were fixed and immunostained for TCR, CD45 and LFA-1. Polarisation of these markers towards the synapse was analysed as described in Figure 3.8. Significance levels:

* $p = 0.05-0.01$; ** $p = 0.01-0.001$; *** $p < 0.001$

CD45 is a distal SMAC marker apparently excluded from the central region of the IS (Graf et al., 2007). CD45 shows slight polarisation towards the synapse in T cells contacting BL6 DCs, which is partially or severely reduced in FYN and WAS respectively.

LFA-1, the integrin implicated in synaptic organisation, localise to the pSMAC (Graf et al., 2007, Cambi et al., 2006, Jo et al., 2010). LFA-1 was also found to polarise towards the IS in T cells contacting control but not WAS or FYN DCs.

As WASp absence was restricted to DCs, any difference in the polarisation of T cell markers must be induced by the DC. As LFA-1 showed the largest polarisation defect, polarisation of its ligand on the DC surface, ICAM-1, was investigated by immunofluorescence. ICAM-1 has previously been shown to direct specific synaptic organisation in cytotoxic immune synapses (Liu et al., 2009). Total surface ICAM-1 levels were similar between mature, OVA-pulsed BL6, WAS or FYN DCs. (Fig 3.10a). However, while BL6 DCs polarise ICAM-1 towards the T cell

synapse; the polarisation ratio was significantly reduced in WAS DC conjugates. FYN DCs showed intermediate polarisation ratios.

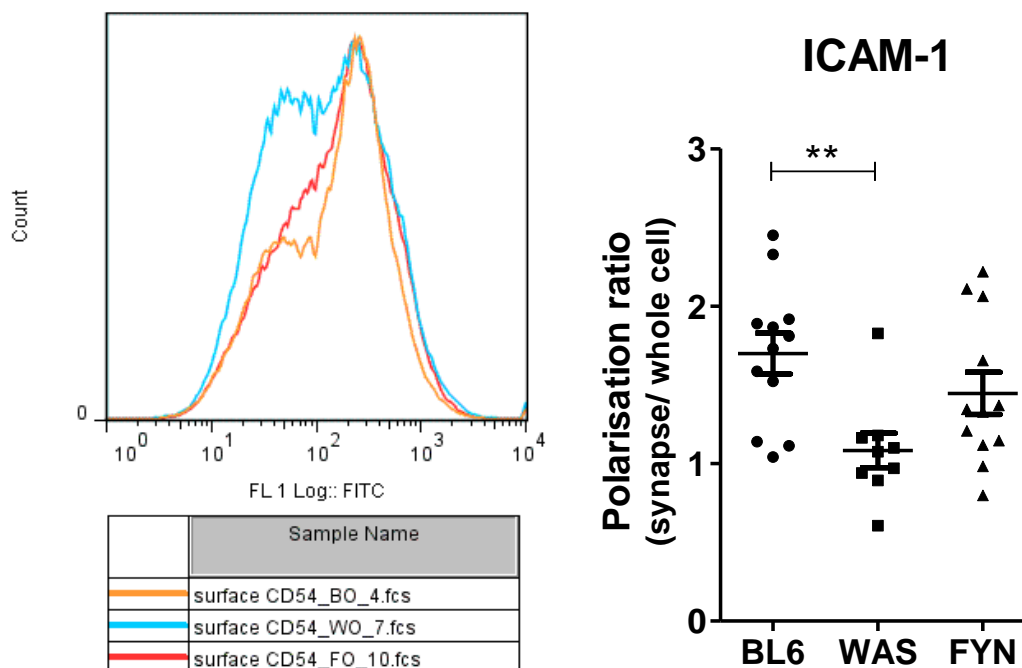


Figure 3.10. **ICAM-1 polarisation on the DC side.** Histogram shows similar levels of surface ICAM-1 in mature OVA-pulsed BL6 (BO), WAS (WO) and FYN (FO) DCs. DC: T cell conjugates were immunostained for ICAM-1. Polarisation was measured as described in Figure 3.8, by splitting the DC, rather than the T cell, into 2 roughly equal-sized opposing sides. A minimum of 10 conjugates were analysed for each strain in 3 separate experiments. Significance level: ** $p = 0.0026$.

To confirm these findings, primary DCs were infected with a lentivirus containing an ICAM-1-GFP construct (Bouma et al., 2011). DC: T cell cocultures were formed as above and incubated for 30, 45 or 60 minutes to form conjugates; then seeded and fixed as above. In control DCs, ICAM-1-GFP was strongly polarised towards the T cell. WAS DCs showed a significant reduction in ICAM-1 polarisation at all time-points tested (Fig3.11). The number of cells showing polarised ICAM-1 with a polarisation ratio >1.25 , quantified in Figure 3.11b, was significantly reduced in WAS DC cocultures. FYN DCs were not significantly different from control BL6.

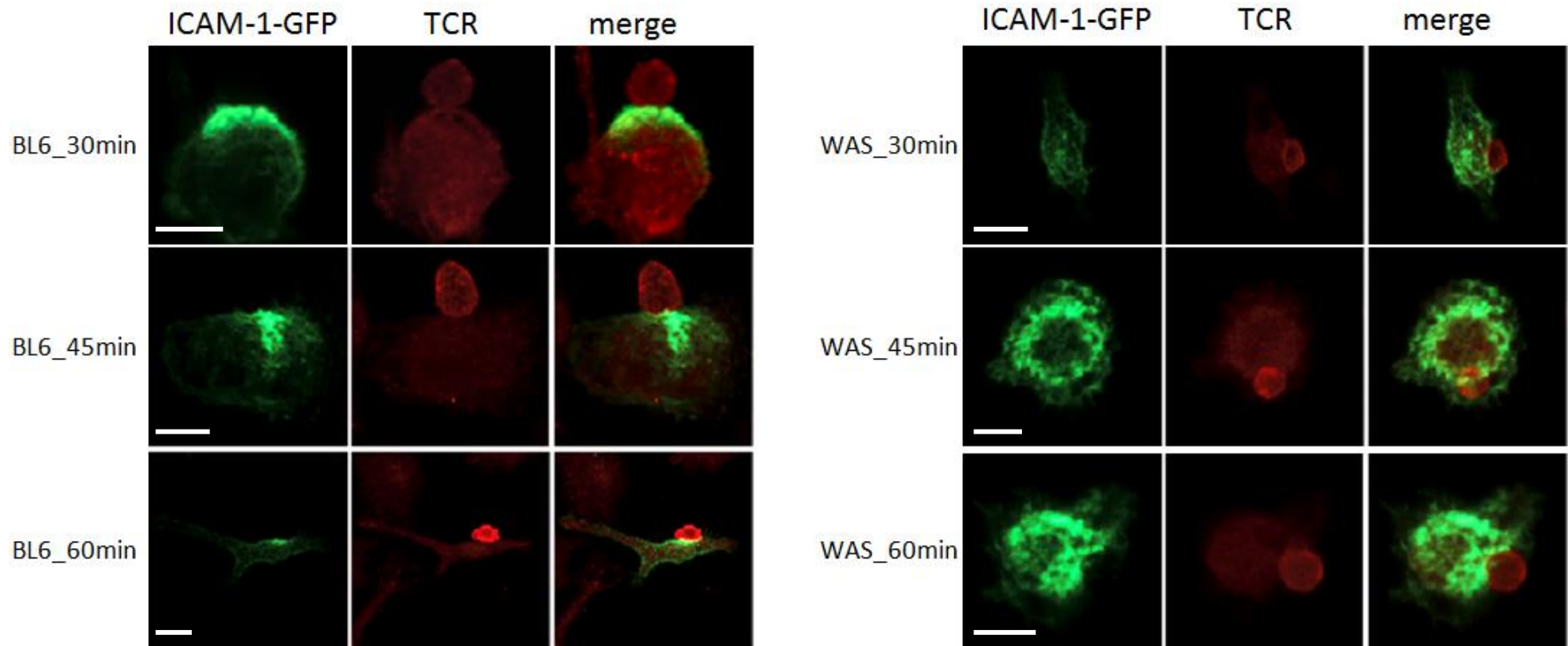
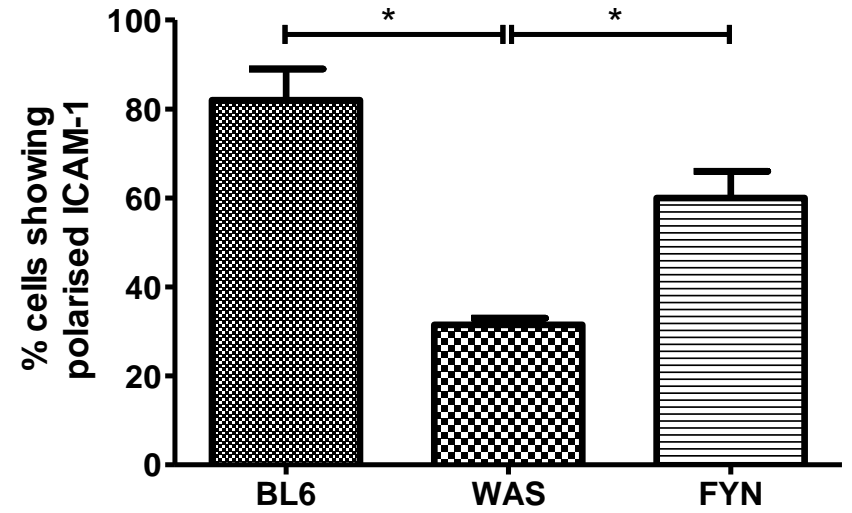
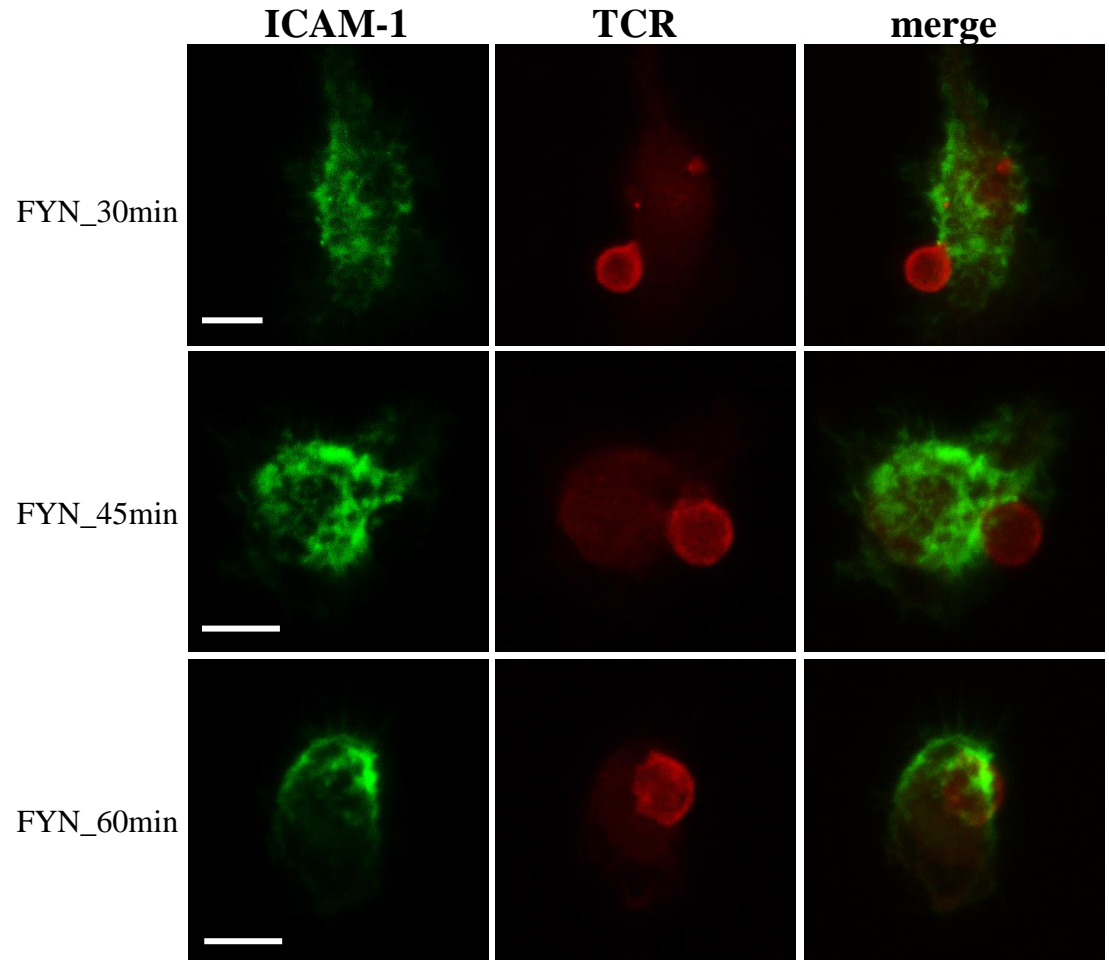


Figure 3.11. **ICAM-1-GFP polarisation in lentivirus infected DCs.** Conjugates were seeded on poly-L-lysine slides and fixed at different timepoints. Scale bars = 10 μ m. Cells with polarisation ratio >1.25 were quantified. Cell percentages were converted into arcsin values to account for the variation limits of percentages. T tests were then performed to compare the different cocultures. BL6 vs WAS $p=0.028$; BL6 vs FYN $p=0.075$; WAS vs FYN $p=0.044$.



Polarisation of the T cell MTOC towards the DC: T cell interface has been reported to occur as part of IS formation (Pulecio et al., 2010) and suggests a role for the microtubule cytoskeleton. Immunofluorescent staining for γ -tubulin, a nucleating component of the MTOC, shows polarisation in T cells synapsed with normal DCs. This appears defective in T cells synapsed with WAS DCs (Fig 3.12), as the MTOC appeared to be located randomly in each T cell. FYN DCs induce an intermediate phenotype, significantly different from both BL6 and WAS. No polarisation of the DC MTOC was observed in either strain.

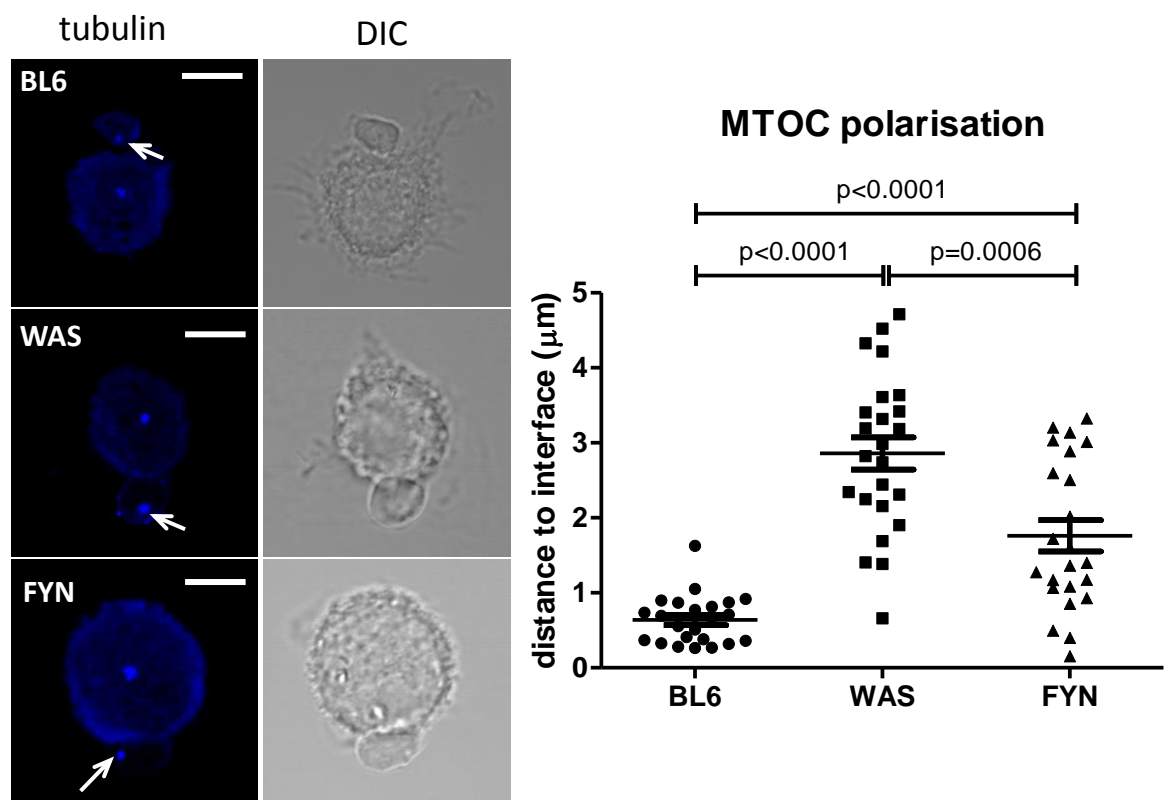


Figure 3.12 **T cell MTOC polarisation found in dendritic cells.** DCs were cocultured with T cells for 1 hour, placed on poly-L-lysine coated microscope slides and stained for γ -tubulin. The distance between the T cell MTOC and the DC was measured in ImageJ by drawing the shortest possible straight line between the MTOC and the DC surface. Representative BL6 and WAS conjugates are shown above. White arrows highlight the position of the T cell MTOC. Scale bar = 10 μ m. A minimum of 20 cells were analysed in 3 separate experiments and an unpaired t test was used to compare populations.

3.2.6 High resolution and 3D imaging of conjugates

To increase imaging resolution, several electron microscopy (EM) techniques were utilised, the importance of which has been recognised by a number of groups (Williams et al., 2007, Ueda et al., 2011).

First, similar to immunofluorescence MTOC stains, EM studies confirmed that no DC MTOC polarisation was seen towards the synapse; the DC MTOC was often observed in detail in the centre of most DCs (Fig3.13).

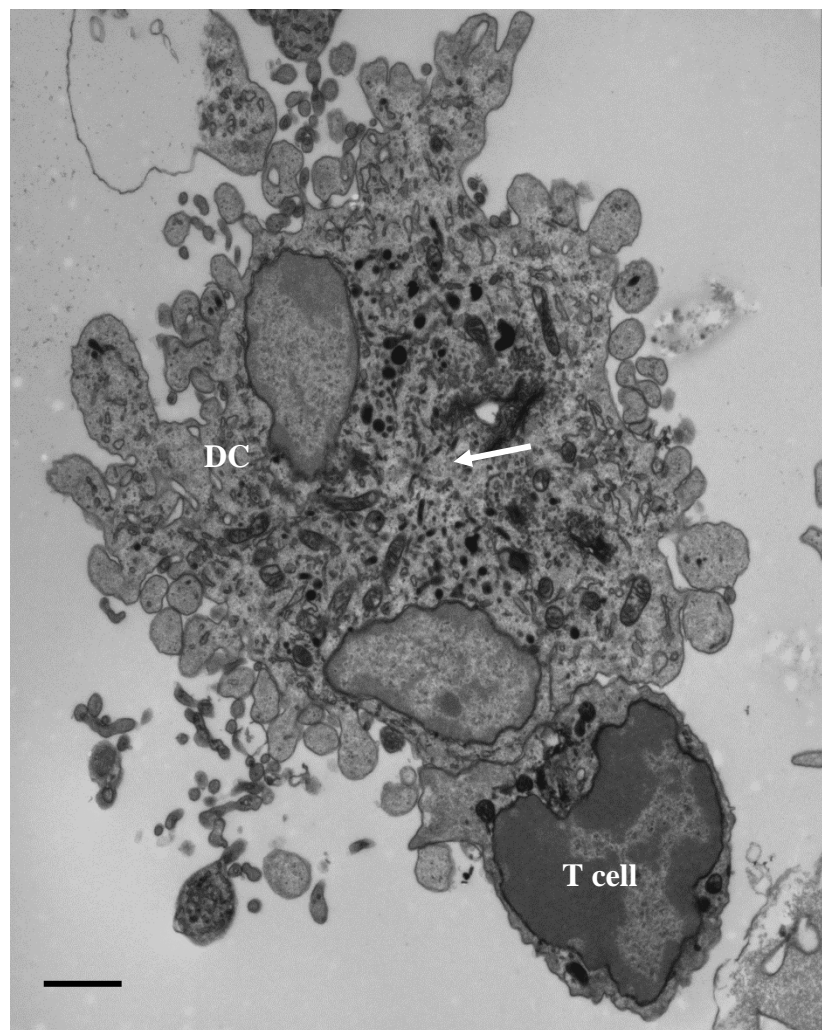


Figure 3.13 **Electron microscopy synapse imaging.** Arrow denotes position of MTOC. Scale bar = 2 μ m.

EM images of control DC conjugates often showed very intimate contacts between the T cell and DC. One method to analyse this further was electron tomography, a technique which

involves tilting the electron beam at incremental angles through the centre of the sample, on a transmission electron microscope (TEM). Although this technique proved useful for visualising some level of 3D detail, it was not sufficient to build up a complete 3D image of conjugates and allow quantification of membrane contacts.

Serial block face scanning electron microscopy allows us to produce 3D reconstructions of EM data. Using the Gatan-3view technology (Denk and Horstmann, 2004), samples are sectioned with an ultra-microtome and each consecutive block surface is imaged. Figure 3.14 shows representative slices through conjugates of T cells with BL6, WAS or FYN DCs on the left; and illustrates the analysis performed to calculate the conjugate contact area (right). The individual slices show the very close apposition of the T cell and DC membranes across the whole synapse site in BL6 conjugates (top). FYN DCs appear to induce similar contacts (bottom). WAS DCs however, appear to interact in a much less intimate way, through a smaller contact interface (middle panel).

The process illustrated on the right, involves creating a stack of the individual slices and drawing each cell outline on each slice. Several tools in the Amira software allow detection of pixels belonging to each cell, making the process more objective and reliable. Amira uses the selection on each slice to reconstruct a 3D model (Isosurface reconstruction) of the DC: T cell conjugate.

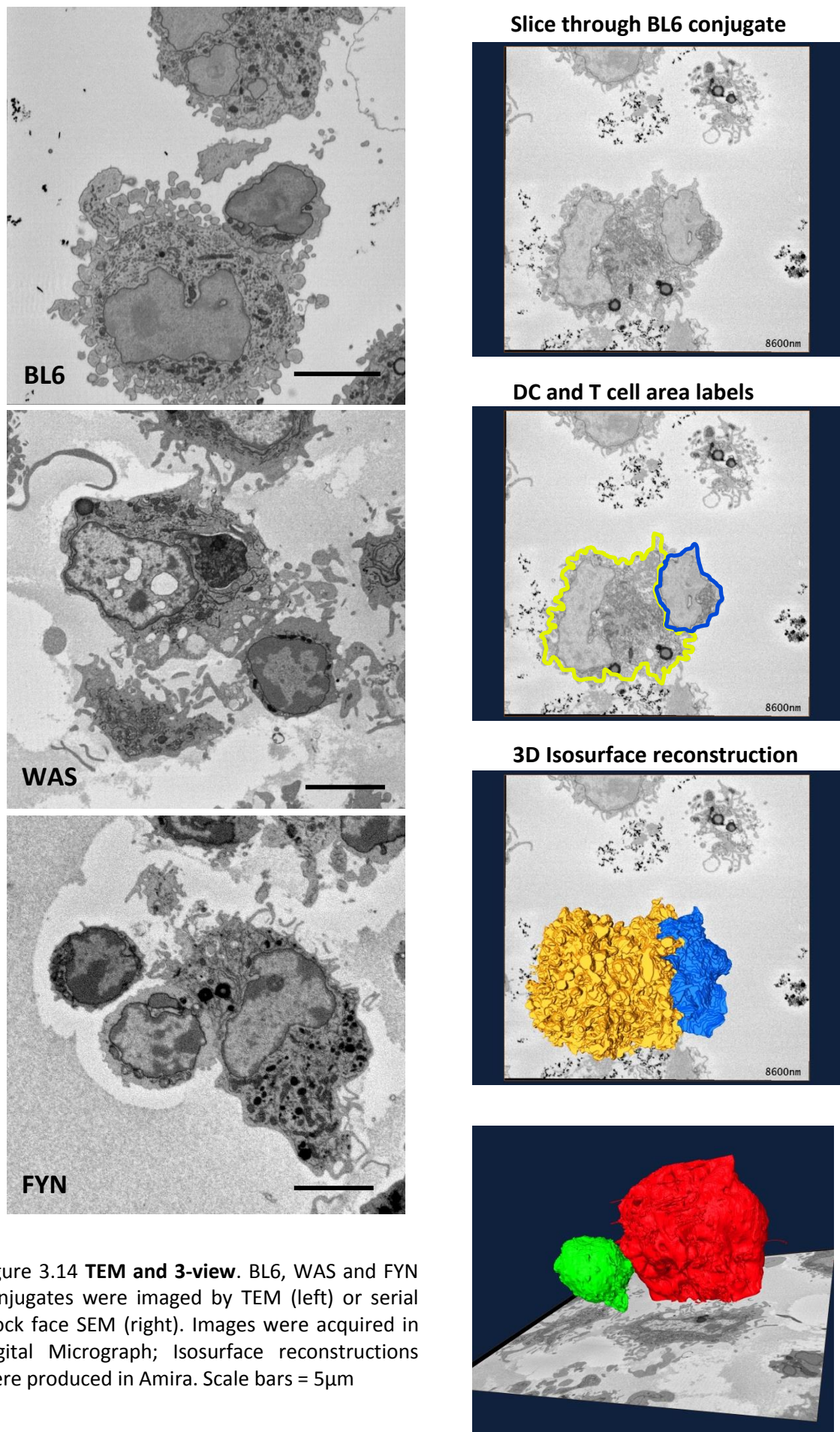


Figure 3.14 **TEM and 3-view**. BL6, WAS and FYN conjugates were imaged by TEM (left) or serial block face SEM (right). Images were acquired in Digital Micrograph; Isosurface reconstructions were produced in Amira. Scale bars = 5 μ m

By outlining the perimeter of each cell on each slice imaged, a detailed 3D isosurface was created, allowing the measurement of contact area between the two cells and comparison between the mouse strains.

During conjugate formation, BL6 DCs induce T cell spreading, thus increasing the contact surface area. They also seem to undergo cytoskeletal rearrangement to allow the T cell to settle in a 'pocket' on the DC surface (Fig 3.16 top). Minimal T cell spreading was seen when T cells formed conjugates with WAS DCs, while FYN DCs induced an intermediate state. The difference can be seen clearly in Movies 3.1-3.3. The contact area for each conjugate was quantified as a percentage of the total T cell surface area and this is shown in Figure 3.15. As OT-II T cell for all conjugates were identical, the differences in T cell spreading observed must be a result of the differential expression or function of WASp in the DCs. This highlights the crucial role of the dendritic cell actin cytoskeleton in correct synapse formation.

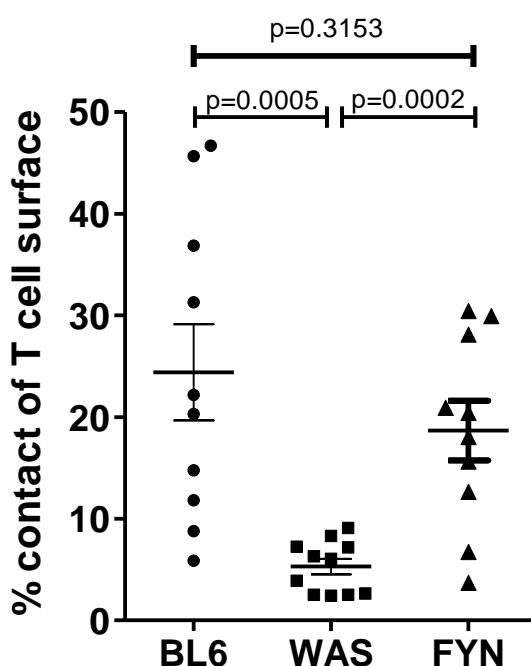


Figure 3.15 DC: T cell contact surface area. After isosurface reconstruction, contact area was measured using the 'Measure patches' function in the Amira software. Contact area was normalised relative to T cell size so is presented as a percentage of total T cell surface area. A minimum of 10 conjugates of each DC type was analysed. An unpaired t test was used to test significance between DC types.

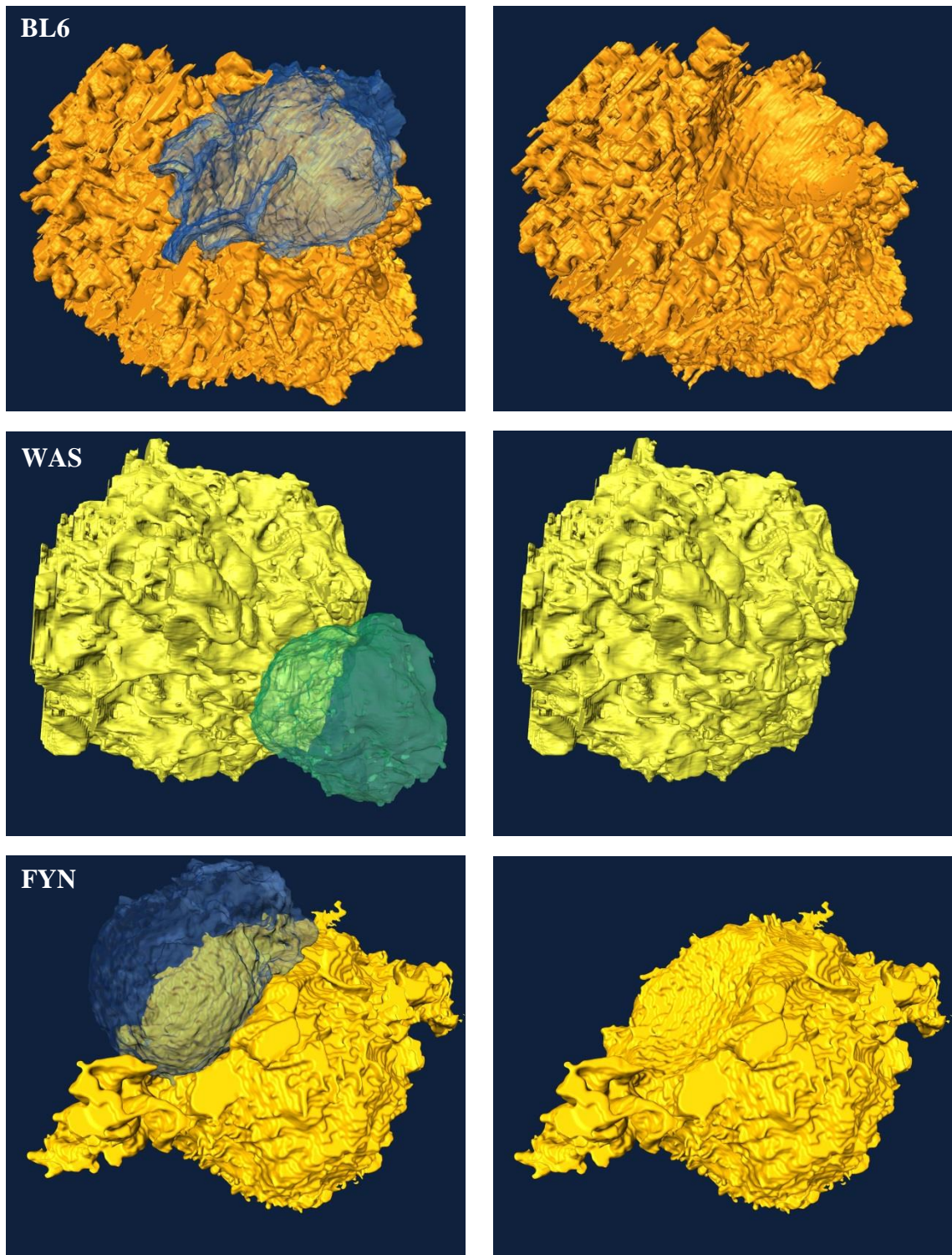


Figure 3.16 **3D reconstructions of EM serial slices.** In BL6 conjugates, the T cell (blue) appears to spread out and to lie in a 'pocket' on the DC (orange). Representative WAS and FYN conjugates are shown. Transparent T cells shown in the top panel are removed to visualise the surface contact site on the DC (bottom panel). Images were acquired in Digital Micrograph; Isosurface reconstructions were produced in Amira.

3.3 Discussion

Firstly, it is important to highlight that the antigen-specific T cells used for conjugate formation expressed WASp normally and were of the same origin throughout all experiments. Consequently, the differences in their responses reflect a DC-intrinsic dysfunction, resulting from WASp deficiency, which abrogates the DCs ability to induce normal synapse formation.

Upon stimulation with LPS, WAS DCs show a similar maturation status, as measured by surface expression of MHCII, CD80 and CD86; and similar levels of surface CD11c expression (Fig 3.2 and 3.3). This suggests that any synapse differences are not due to abnormal dendritic cell phenotype or poor maturation. Further, antigen uptake, processing and presentation of soluble antigen were found to be normal in WAS DCs, as previously described (Westerberg et al., 2003).

WAS DCs contain less total polymerised actin (Fig 3.4). Actin plays a crucial role in cell integrity, transmembrane protein clustering, membrane organisation and mechanosensing. Thus, reduced actin polymerisation, or a reduced total F-actin network, may mean the cell is less responsive to external physical cues, less able to form precise structures; and less able to transport, concentrate or stabilise many transmembrane proteins.

This appears to be the case for ICAM-1, the LFA-1 ligand with a previously described role in synapse organisation (Graf et al., 2007, Liu et al., 2009, Jo et al., 2010). Although the surface levels of ICAM-1 were similar between BL6 and WAS DCs, ICAM-1 polarisation towards the IS was defective in WAS DC contacts (Fig 3.10). It has been proposed that an active actin-cytoskeleton dependent mechanism is responsible for membrane ICAM-1 translocation towards the synapse and reduced ICAM-1 polarisation in WAS DCs is compatible with this mechanism (Jo et al., 2010). Jo *et al* however, also suggest uptake and recycling of ICAM-1, which is directed to the IS through adhesion to LFA-1 (Jo et al., 2010). Experiments presented here cannot exclude the possibility that a feedback mechanism from the T cell LFA-1 exists to

reinforce ICAM-1 clustering on the DC surface. However, the fact that LFA-1 polarisation towards the interface was abnormal in T cells contacting WAS DCs (Fig 3.9), suggests that DC-mediated ICAM-1 polarisation provides the driving force for this process.

A similar idea has been described for the localisation of CD80 and its T cell ligands CD28 and CTLA (Tseng et al., 2005). The cytoplasmic domain of CD80 was shown to be critical not only for its own organisation at the synapse, but also for that of its ligands CD28 and CTLA and the downstream kinase PKC θ .

A defect in integrin polarisation towards the synapse, and therefore reduced integrin density, would result in reduced adhesion, which could explain the reduced number of stable conjugates of WAS DCs seen in Fig 3.7. This supports previous studies showing that blocking LFA-1 function abolishes interaction forces in T cell: APC conjugates, as measured by atomic force microscopy (AFM) (Hosseini et al., 2009). Reduced integrin binding at the synapse could also account for the reduced contact interface seen in EM and 3View experiments (Fig3.14 and 3.15), by essentially minimising or eliminating the pSMAC in WAS DC conjugates. It would be interesting to directly observe LFA-1 or ICAM-1 localisation at high resolution by performing immunogold labelling for EM. AFM comparing BL6 and WAS DC conjugates would also provide supporting data.

In addition to defective integrin polarisation, CD45 translocation was also observed to be impaired. A defect in CD45 polarisation towards the synapse could have an effect on downstream signalling. CD45 is a protein tyrosine phosphatase, which is essential for TCR-mediated T cell activation (Altin and Sloan, 1997). In T cells, CD45 regulates Src family kinases such as Lck and Fyn (Chan et al., 1994). For example, it is known to dephosphorylate the negative regulatory tyrosine residue Y505 on Lck (Wang and Johnson, 2005, Duplay et al., 1996, Seavitt et al., 1999). It may also have other targets at the IS, including TCR and ZAP-70 (Furukawa et al., 1994, Mustelin et al., 1995). CD45 organisation or concentration at the synapse may be crucial for maintaining the correct pTyr signature for the correct association of

synapse components and activation or inhibition of signalling pathways. It is easy to see how in T cells contacting WAS DCs, defective CD45 polarisation towards the synapse may result in altered signalling. Further experiments are required to investigate whether this is directly due to the instability of the actin network or indirectly due to integrin adhesion defects, as has been proposed for CD45 exclusion from the cSMAC (Graf et al., 2007).

MTOC polarisation may also be linked to integrin adhesion. Early studies into MTOC polarisation suggested the process was dependent on TCR signalling. Sedwick *et al* showed that when a T cell simultaneously contacted cells expressing either peptide-MHC complexes or ICAM-1, the T cell MTOC polarised mainly towards the cell expressing MHC (Sedwick et al., 1999). In addition, there is evidence for the requirement of several downstream signalling proteins, including tyrosine kinases (Lck and Zap70) and scaffolding proteins (Slp76 and LAT) (Lowin-Kropf et al., 1998, Kuhne et al., 2003). Although initially it was thought that LFA-1 did not play a role, more recently evidence has shown that it is required for complete, robust MTOC polarisation (Yi et al., 2013). Yi *et al* also show that the driving force behind MTOC repositioning can cause deep membrane invagination at the contact surface of “frustrated” conjugates thus implicating a strong force anchored at the IS. If LFA-1 does play a role in MTOC migration, it is easy to see how this would be perturbed in T cells contacting WAS DCs, where LFA-1 polarisation is abrogated.

Recently, LFA-1 localisation and activation have been linked to L-plastin phosphorylation (Wang et al., 2010, Wabnitz et al., 2010). L-plastin is an actin-crosslinking protein that allows formation of tight actin bundles (Morley, 2012). Blocking L-plastin function results in abnormal IS formation, cytokine secretion and MTOC docking (De Clercq et al., 2013b). If LFA-1 plays a role in T cell MTOC polarisation, other mechanisms affecting LFA-1 organisation can be predicted to have effects similar to L-plastin. This supports results presented in this chapter showing that lack of WASp in DCs results in poor LFA-1 polarisation on the surface of T cells, which in turn affects T cell MTOC relocation. However, the results cannot rule out an LFA-1-

independent mechanism which may be defective during induction by WAS DCs. Further investigation into signal transduction between actin or LFA-1 and the microtubule cytoskeleton is required.

The exact mechanism of MTOC polarisation is still controversial. Until recently, it was thought that a complex containing the microtubule motor dynein and the adaptor protein ADAP was responsible for pulling the MTOC towards the synapse in a sliding motion (Combs et al., 2006, Billadeau et al., 2007). However, as mentioned earlier, a recent model suggests end-on microtubule capture and depolymerisation provides the main driving force behind microtubule organisation (Yi et al., 2013). The link between the microtubule and actin cytoskeleton in either model is not completely understood and research into this could provide important clues regarding loss of MTOC polarisation both in T cells intrinsically lacking WASp and wildtype T cells contacting WAS DCs. Further, although the exact role of MTOC polarisation in CD4 cells is unclear, if this is similar to its role in polarised secretion in CD8 and NK cells (reviewed in (Billadeau et al., 2007)), perturbed cytokine secretion in CD4 T cells could affect T cell activation, or the cytokine milieu produced. However, there is evidence to suggest that polarised cytokine release in CD4 cells requires actin polymerisation downstream of Cdc42 but not MTOC polarisation (Chemin et al., 2012).

Contrary to previous observations by Pulecio *et al*, no polarisation of the DC MTOC was seen in BL6 or WAS DCs by confocal or electron microscopy (Pulecio et al., 2010). However, another recent publication also highlighted the importance of intact DC function for IS formation but found no DC MTOC polarisation towards the synapse (Bouma et al., 2011).

The FYN DCs showed an interesting phenotype throughout all of these experiments. Expression of the phospho-null Y293F WASp results in recovery of ICAM-1 polarisation in DCs, and consequently LFA-1 polarisation on the T cell (Fig 3.9, 3.10, 3.11). This suggests that phosphorylation of WASp is not essential for either of these – ICAM-1 localisation, or its ligation to LFA-1. This may point to a different regulator of WASp at the synapse (such as

Cdc42 binding, WIP or dimerisation). Alternatively, it may suggest that WASp activation and its role in actin polymerisation are not crucial for ICAM-1 localisation, for example WASp may be involved in stabilising the actin network at the IS, rather than active polymerisation.

Further, contact area, as measured in 3D conjugate reconstructions, is increased to normal levels in FYN, compared to WAS DC conjugates. FYN DCs are able to induce T cell spreading over their surface and form the 'pocket' described for BL6 DCs (Fig 3.16). This provides support for the adhesion hypothesis described above, suggesting that LFA-1 polarisation and interaction with ICAM-1 are important for pSMAC organisation and stable, intimate synapse formation.

Polarisation of the T cell MTOC however in FYN, although improved compared to WAS, is still significantly different from the close apposition seen in the BL6 IS (Fig 3.12). As previously discussed, this may be due to an LFA-1 –independent mechanism involved in MTOC relocation, which is deficient in WAS and perhaps dependent on WASp phosphorylation.

Several questions remain unanswered. It would be interesting to compare the mechanisms and regulators behind 'pocket' formation in DCs and phagocytic cup formation, which has been shown to be abnormal in WAS (Leverrier et al., 2001, Lorenzi et al., 2000, Tsuboi and Meerloo, 2007). Interestingly, formation of the phagocytic cup has been compared to IS formation, in particular downstream of Dectin-1 receptor ligation to particulate β -glucans (for example, yeast) (Goodridge et al., 2011). Dectin-1 is able to differentiate between soluble and particulate β -glucans; and downstream of the latter, it is able to induce cytoskeletal remodelling, phagocytosis and exclusion of the phosphatases CD45 and CD148, as has been described in T cell synapses (Cordoba et al., 2013). Questions remain about whether all of these structures involve some initial mechanosensing to determine the function and organisation of the final structure; or whether the phagocytic cup is a kind of evolutionary precursor for the mechanisms developed in the formation of the IS. In terms of the role of WASp however, Tsuboi and Meerloo, suggest the phosphorylation of WASp is important for

phagocytic cup formation in macrophages (Tsuboi and Meerloo, 2007), which does not seem to be the case for 'pocket' formation in FYN DCs seen in Fig 3.16.

Further, it would be interesting to study whether WAS deficiency in DCs affects T cell calcium influx, DAG and PKC signalling, as well as the localisation of PAR3-PAR6-aPKC complex, which have all been implicated in MTOC polarisation (Quann et al., 2011, Quann et al., 2009, Dustin et al., 2010, Merino et al., 2012, Huse, 2012).

In summary, results presented in this chapter showed significant differences between WAS and BL6 DCs in a number of physical IS characteristics, including integrin polarisation and induction of T cell MTOC relocation. Consequently, there may be significant differences in cell: cell adhesion, synapse organisation over time and T cell activation, which may contribute to the immunological defects seen in WAS patients.

Chapter 4 – Dynamics of synapse formation

4.1 Introduction

The immune synapse has been described to last for several hours (Huppa et al., 2003) with constant contact between the two cells. The physiological relevance of this remains elusive. It has been suggested that the long-lived cSMAC provides increased local concentration of TCR and pMHC, which may slow down disengagement or allow re-engagement (Lin et al., 2005). The precise mechanism behind this lasting contact is unclear though there is strong evidence for the involvement of actin and integrins (Sims and Dustin, 2002). Despite this stability, the synapse is a highly dynamic structure.

First, at a macrostructural level, the morphology of the synapse undergoes several changes through distinct stages (Ueda et al., 2011). It has been suggested that there are at least 4 distinct stages in CD4+ T cell synapse formation, starting with T cell pseudopodia penetrating deeply into the APC, followed by centriole positioning close to the contact site and enlargement of the Golgi complex with membrane activity becoming polarised towards the APC (Ueda et al., 2011). Furthermore, observations of T cell activation in lymph nodes suggests T cells make multiple contacts with APCs and are thus able to break and reassemble the IS structure several times (Mempel et al., 2004, Miller et al., 2002).

As well as whole cell movements and adhesion, the dynamic nature of the synapse is also crucial for movements on a much smaller scale – the movement of transmembrane proteins,

such as TCR/pMHC, costimulatory molecules and integrins, in the plane of the cell-cell interface; as well as the endocytosis of proteins from the synapse, by either cell, as part of the recycling process (Lee et al., 2003a, Grakoui et al., 1999).

The main determinants of cortical actin's structural integrity and mechanics are the length distribution of actin filaments, the cross-link nature and the density of the actin network (Gardel et al., 2004, Kasza et al., 2010, Bai et al., 2011). In steady state, actin assembly, disassembly and cross-linking are balanced so that the thickness, structure, composition and mechanical properties of the cortex remain constant. During processes such as cell migration or cell-cell interaction, these parameters of the actin network must be changed to build a cortical actin network more suited to the precise function/process. This is achieved by actin regulatory proteins, which control the delicate balance between a dynamic and stable network.

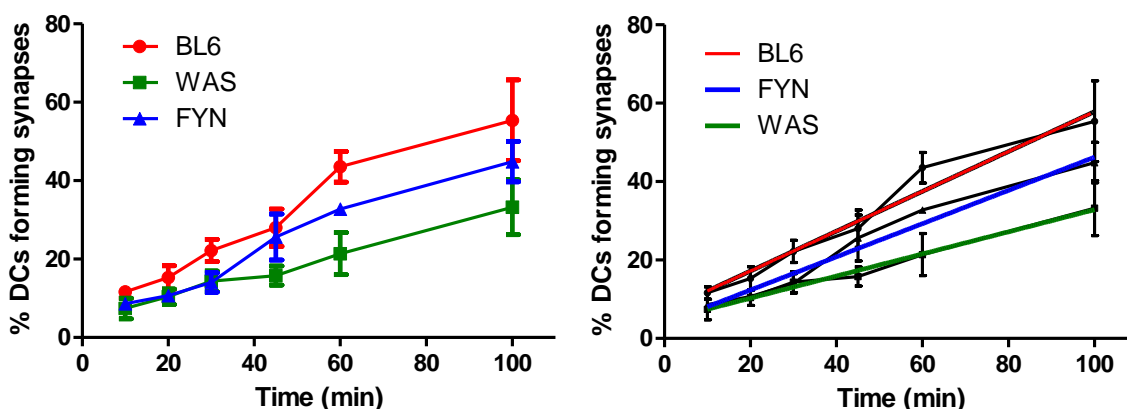
As actin has been shown to play a key role in synapse organisation (Chapter 3 and (Bunnell et al., 2001, Campi et al., 2005, Mayya and Dustin, 2010, Monica Gordon-Alonso, 2010)), it is predicted that actin's ability to form stable yet dynamic networks underlies the long-lasting and flexible synaptic structure. Disturbing the function of actin regulators in DCs, such as WASp, would be expected to result in abnormal cellular actin dynamics and the formation of less stable and poorly organised IS.

This chapter aims to investigate any differences in duration of stable contacts between control and WAS DC synapses using live imaging; examine the dynamic organisation of synapses in the plane of the cell-cell interface; investigate the stability of the actin network at the IS; and determine the degree to which different actin properties are affected resulting in poor synapse formation by WAS DCs.

4.2 Results

4.2.1 Synapse quantification

In Chapter 3, conjugate numbers were quantified after a set incubation time of 45 minutes. To follow the number of conjugates formed over time, a similar experiment was conducted as a time course of 10-100 minutes. Figure 4.1 shows that WAS DCs formed fewer conjugates, compared to BL6; and this was consistent at every time point. Linear regression analysis shows the change over time (slope) between BL6 and WAS is significantly different. FYN DCs showed a smaller reduction in the number of conjugates formed. At initial time points they appear similar to WAS, while later efficiency of conjugate formation increases. Consequently, linear regression shows the slope of the FYN data is similar to BL6, while the total number of conjugates (the elevation) is reduced.



Comparison	Slope	Elevation/ Intercept
BL6/WAS	$p=0.0001$	*
BL6/FYN	$p=0.2545$	$p=0.0033$
WAS/FYN	$p=0.0109$	*

Figure 4.1 **Conjugate formation over time.** DC: T cocultures were seeded on poly-L-lysine slides at given intervals after coculture (10, 20, 30, 45, 60 and 100minutes). Conjugate numbers were quantified as in Figure 3.7 (left). A linear regression fit was performed on the resulting data; fitted lines are shown in the graph on the right. Statistics are summarised in the table.

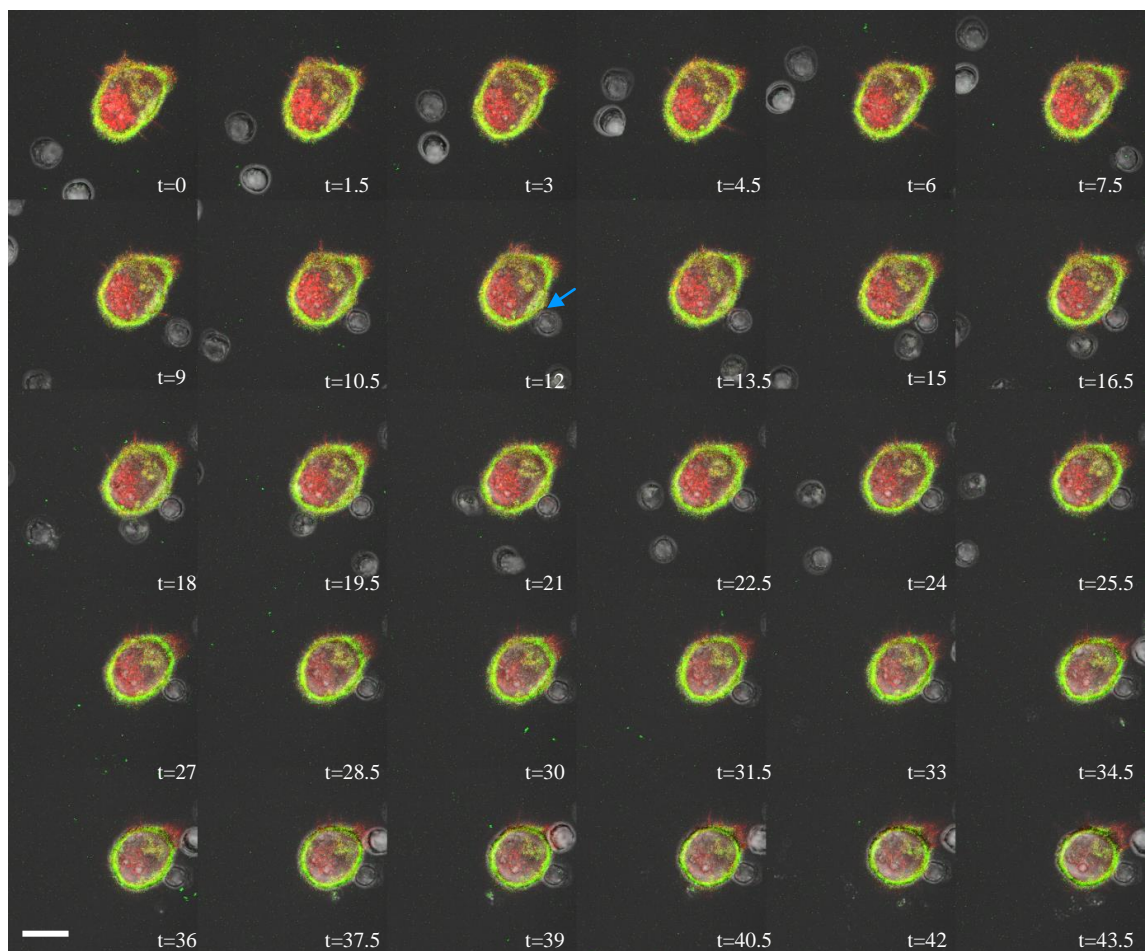
*Due to difference in slopes, it is not possible to test whether the intercepts differ significantly.

4.2.2 Live imaging

To assess the stability of the DC: T cell conjugates formed, synapse formation was followed in real time. Mature, OVA-pulsed DCs expressing LifeAct-mCherry (Riedl et al., 2008) and ICAM-1-GFP were transferred to glass-bottomed imaging dishes on day 7 of the BMDC differentiation culture. OT-II CD4⁺ cells were added just prior to imaging to focus on the initial contacts. The montages below represent live imaging in Movies 4.1 and 4.2.

BL6 DCs formed stable, long-lasting contacts, which on average last over 30 minutes and results in a slight rounding of the DC. In contrast, WAS DCs rarely formed such stable contacts with T cells. In Figure 4.2, two T cells come into view, make brief contacts with the WAS DC and appear to 'bounce off' it several times before migrating away (blue arrows in WAS montage).

C57BL/6



WAS



Figure 4.2 **DC-T cell contacts are shorter or less stable with WAS DCs.** The montages above are taken from live-imaging data over 45minutes. Images are taken at intervals of around 1.5minutes, starting 5 minutes after addition of T cells. Each image represents a maximum projection of 3 slices of the z-stack (10 slices total). LifeAct (actin) is shown in red and ICAM-1 in green. Time is given in minutes. Blue arrows highlight contacts, as described in the text. Scale bars = 10 μ m.

The blue arrow in the BL6 montage highlights the start of a stable contact and the DC and T cell remain in a conjugate for the rest of the imaging period. The arrows in the WAS montage show brief contacts in between which the T cell appears to roll along the DC surface but not form a stable synapse. A longer live imaging period would be beneficial for both the BL6 and WAS samples. This type of imaging however does not allow enough resolution to study the subtle molecular changes at the synapse.

4.2.3 Fluorescence Recovery After Photobleaching

In addition to live imaging, an analysis of the stability of the actin cytoskeleton at the synapse site would be beneficial. To investigate molecular changes at the synapse, FRAP was used to study actin dynamics. BL6 and WAS BMDCs were transduced on day 3 with a vector expressing Actin-mCherry to allow fluorescent imaging of actin.

An area of the Actin-mCherry expressing DC was selectively photobleached using 5 iterations of 100% laser power with 488 and 561nm lasers. Fluorescence intensity was measured for between 15 and 30s after the bleach. After bleaching, recovery of fluorescence occurs as a result of repopulation of the area by non-bleached molecules. Binding of actin to other proteins or immobile structures in the cell, including incorporation in stable low-turnover filaments, results in slower recovery of fluorescence.

The graph in Figure 4.3 shows a typical normalised recovery curve and highlights the different parameters that can be derived from the data. The two most important parameters taken into account for basic analysis are the half-time, which is the time taken for fluorescence to recover to half of the final intensity; and the immobile fraction, which reflects the difference between pre-bleach and final intensities giving us a measure of the proportion of actin that cannot be replaced.

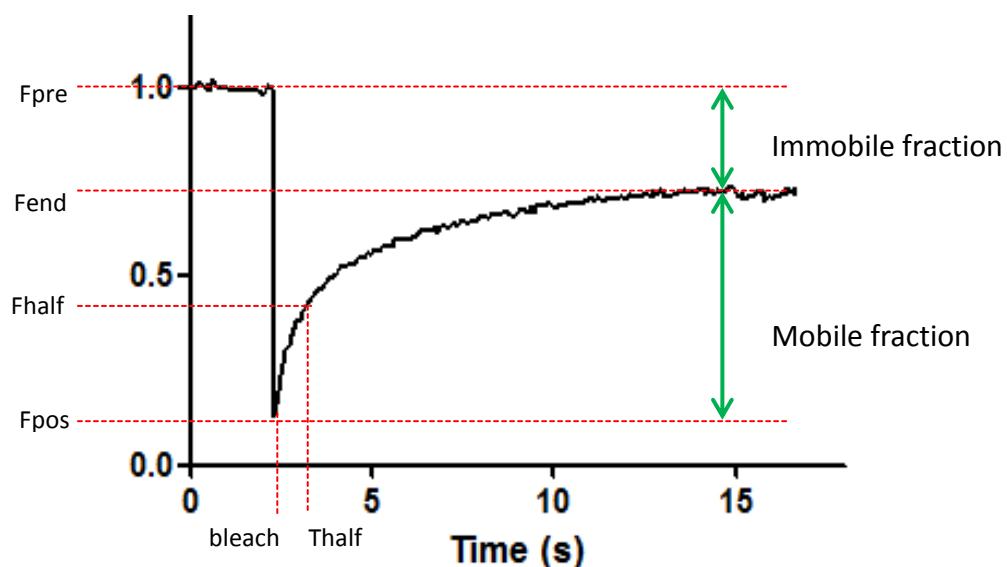


Figure 4.3 Recovery curve calculations.

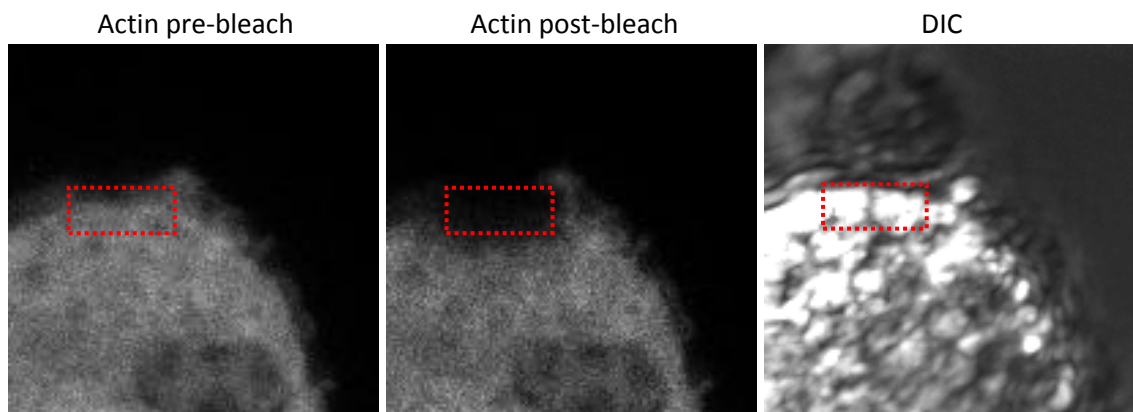
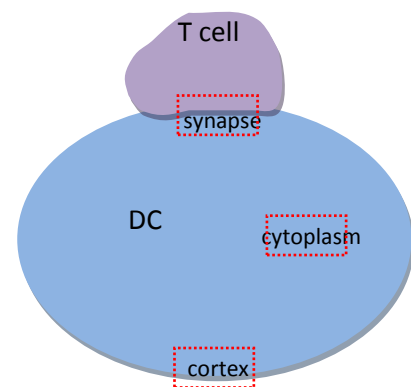


Figure 4.4 **Actin-mCherry bleach at 3 different areas.** Red dashed outline indicates region of interest (ROI) bleached. DIC image shows that this is a synapse ROI at the DC: T cell interface.



Each of three areas was bleached independently – synapse, cortex or cytoplasm. Post-bleach intensity dropped to around 20-30% of pre-bleach value. The images above are single slices through a conjugate, representing an example of a synapse ROI bleach.

As expected, recovery of cytoplasmic actin is much faster and more complete, compared to the cortex or synapse areas (Fig4.5). The lower proportion of polymerised actin in the cytoplasm, compared to cortex and synapse, allows faster diffusion of actin monomers back into the bleached area. Turnover of actin polymers itself, although more rare in the cytoplasm compared to the cortex, may be much faster due to a higher concentration of free actin monomers and a lower concentration of actin bundling and cross-linking proteins.

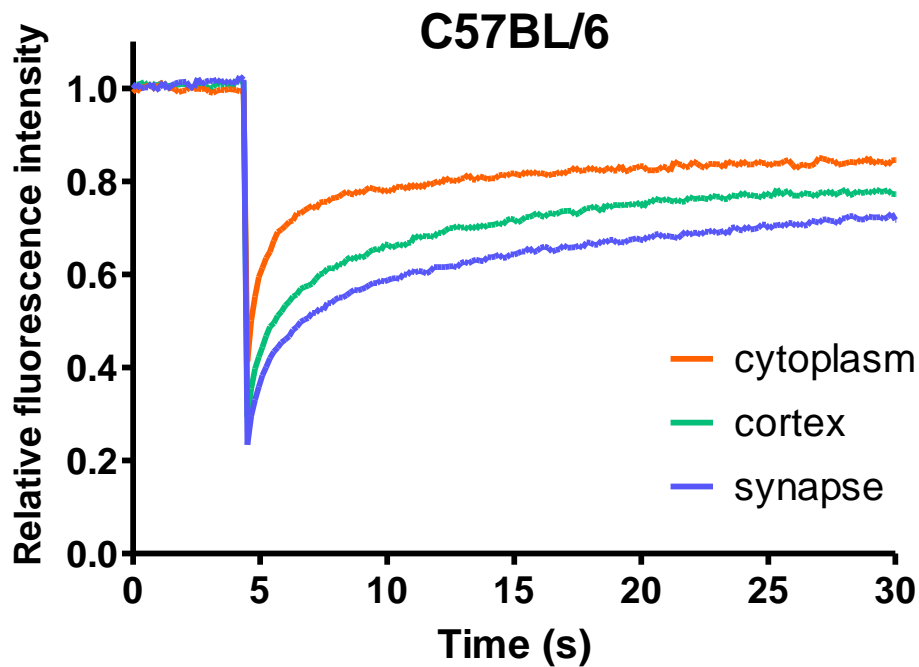


Figure 4.5 **Actin dynamics in different areas of a cell.** Recovery of actin-mCherry fluorescence is plotted against time for each different ROI. Fluorescence is normalised against pre-bleach value and an average of 15 curves is plotted.

Further, WASp-deficient DCs consistently show faster recovery than control BL6, consistent with the idea that the WASp DC cytoplasm may be less dense due to a lower proportion of polymerised actin. (Figure 4.6)

Since actin-mCherry is overexpressed from the same promoter in BL6, WAS and FYN DCs, unless WAS-deficiency has an effect on actin post-translational regulation, we can assume there is a similar level of total actin in both cells. Consequently, the fact that WASp-deficient cells contain less polymerised actin (Fig 3.4), suggests there may be a higher proportion of actin monomers. An increased concentration of actin monomers would allow faster diffusion and polymerisation. This faster treadmilling is reflected in the shorter half-time of fluorescence recovery and, indirectly, the lower immobile fraction in WASp-deficient DCs (less polymerised actin at a given time).

Decreased recovery half-life suggests increased turnover of actin filaments and therefore reduced overall polymerisation. The lower immobile fraction in the WAS DCs shows that more of the actin can be replaced post-bleach, perhaps suggesting a reduced stability of the actin network in the WAS DC compared to control.

The differences between the control and WASp-deficient DCs appear exaggerated at the synapse. This confirms the difference in protein composition between the synapse and the rest of the cell cortex, highlights the involvement of actin in this structure and implicates an additional regulatory mechanism at the synapse. The longer half-time and higher immobile fraction, suggest greater stability of the actin cytoskeleton at the synapse of normal DCs. (Figure 4.7)

Interestingly, actin-mCherry in FYN DCs recovers normally in the cortex and cytoplasm, resulting in recovery curves similar to BL6. This would suggest that the presence of WASp alone, even as a phosphorylation-dead mutant, is sufficient for normal actin dynamics in the cortex. One possible explanation is that in the cortex and cytoplasm, WASp is activated mainly through mechanisms other than phosphorylation. Alternatively, in these areas WASp may have a role independent of its Arp2/3 binding function, for example by acting as a scaffold for other proteins. At the synapse however, FYN DCs show actin recovery similar to WAS-deficient DCs. This suggests that at the synapse, phosphorylation of WASp is crucial for its role in regulating actin dynamics.

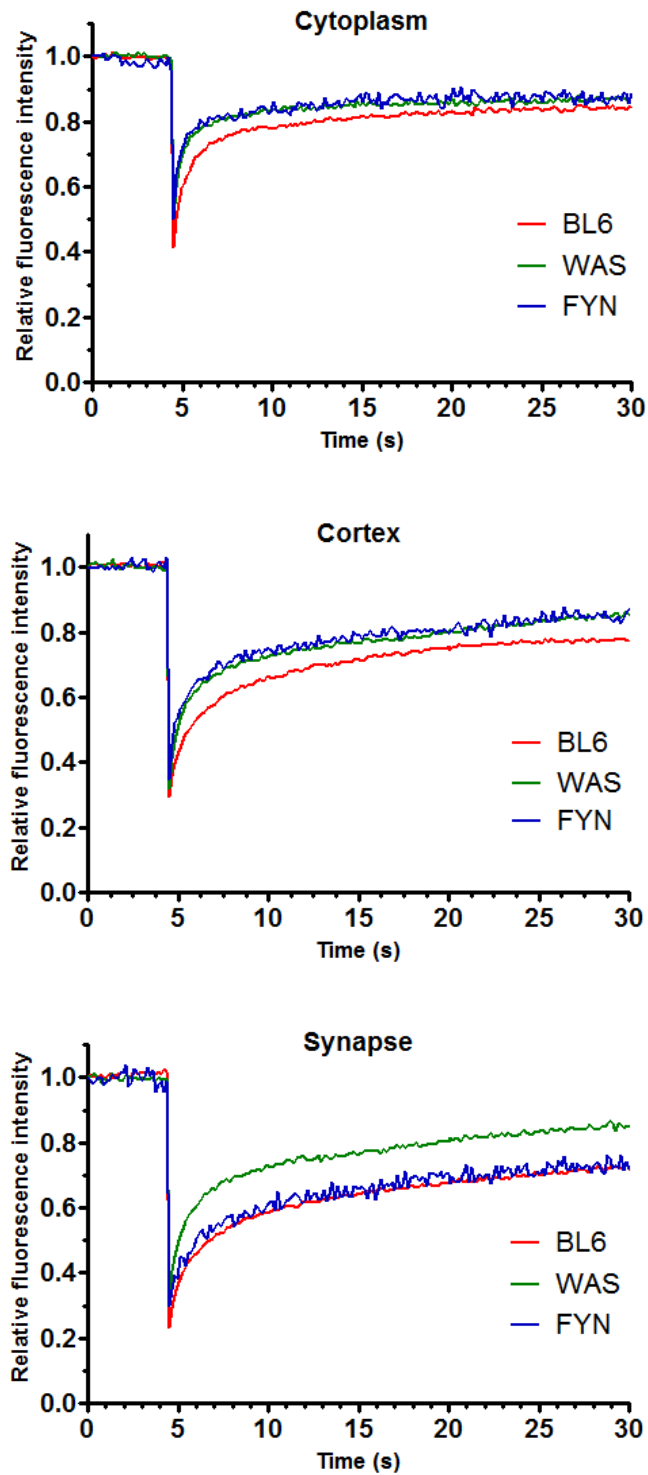


Figure 4.6 **Fluorescence recovery appears much faster in WASp-deficient DCs.**

Normal or WAS DCs expressing Actin-mCherry were incubated with T cells for 40 minutes. The cell suspension was then added to a glass-bottomed 35mm imaging dish and allowed to settle for 20 minutes. Conjugated DCs were chosen on the basis of sufficient Actin-mCherry expression and no drift within the field of view. Three areas were bleached for comparison. The curves shown here are averages of normalised, background-corrected data for at least 15 cells.

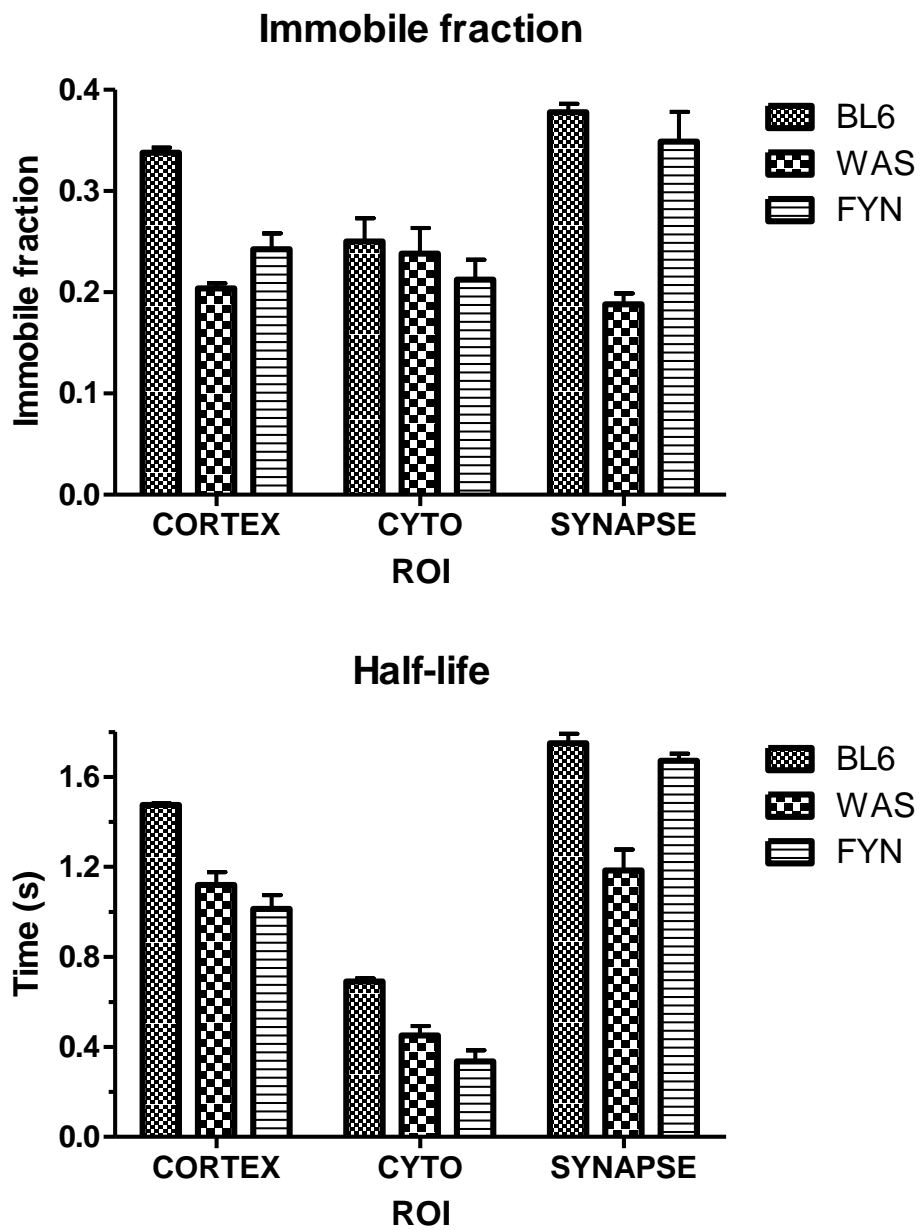


Figure 4.7 Fluorescence recovery in WAS DCs is augmented at the synapse.

Comparison with other areas bleached in the conjugated cells (cortex or cytoplasm) shows a bigger difference in half-time and immobile fraction of actin between control and WAS at the synapse.

↑ polymerisation = ↓ turnover = ↑ half life

Although this basic analysis was useful in highlighting some of the differences between control and WAS DC synapses, several parameters were altered to improve the FRAP set up and allow for more sophisticated calculations. First, the area of the bleached region was reduced to a circle of $1\mu\text{m}$ diameter ($2\times 5\mu\text{m}$ rectangle previously) to allow fast, symmetric diffusion of actin monomers into the bleached area from all directions. Given the fast rate of diffusive recovery, $D \approx 20\mu\text{m}^2/\text{s}$ (Fritzsche et al., 2013), and the small size of the bleached region, this also minimises the diffusion component of the FRAP recovery curve. Further, the total area imaged was reduced to $5\times 5\mu\text{m}$ in order to increase imaging speed. Once the validity of these parameters was confirmed, the temporal resolution of imaging was reduced to 1 frame per second. This allows enough resolution to detect actin recovery through polymerisation but minimises the photo-damage caused during imaging. At higher frame rates, many actin monomers are bleached and the detected recovery is much lower than actual filament recovery.

A recent paper described reactive recovery (that resulting from association/dissociation rather than diffusion of proteins) in terms of first-order reaction kinetics.

$F(t) \approx [1 - \exp(-t\omega_d)]F_0$, where F_0 represents pre-bleach fluorescence and ω_d is the rate of turnover, which is linked to half-life calculated from FRAP experiments ($t_{1/2} = \ln 2 / \omega_d$). This exponential function would describe the simplest recovery, resulting from one type of reaction. It is likely that several molecular reactions contribute to cortical actin turnover and it has been suggested that fluorescent recovery can be represented as the sum of several exponential functions (where each one represents a different molecular turnover process) (Fritzsche et al., 2013). Thus, by separating the components of the recovery curve, the rates and proportions of the separate actin networks contributing to recovery can be calculated.

As before, OVA-pulsed Actin-mCherry-expressing DCs from either BL6, WAS or FYN mice were used to form conjugates with OT-II T cells. FRAP was performed using the parameters

described above. The recovery curves of actin at the cortex or synapse of BL6, WAS and FYN DCs are shown in Figure 4.8.

The fitting parameters, R^2 and χ^2 for first-, second- and third-order exponentials are shown in Table 4.1. Second-order exponential fit described the curves best, suggesting that two different actin networks contribute to actin recovery. Rates of recovery and proportions of each actin network are shown in Table 4.2.

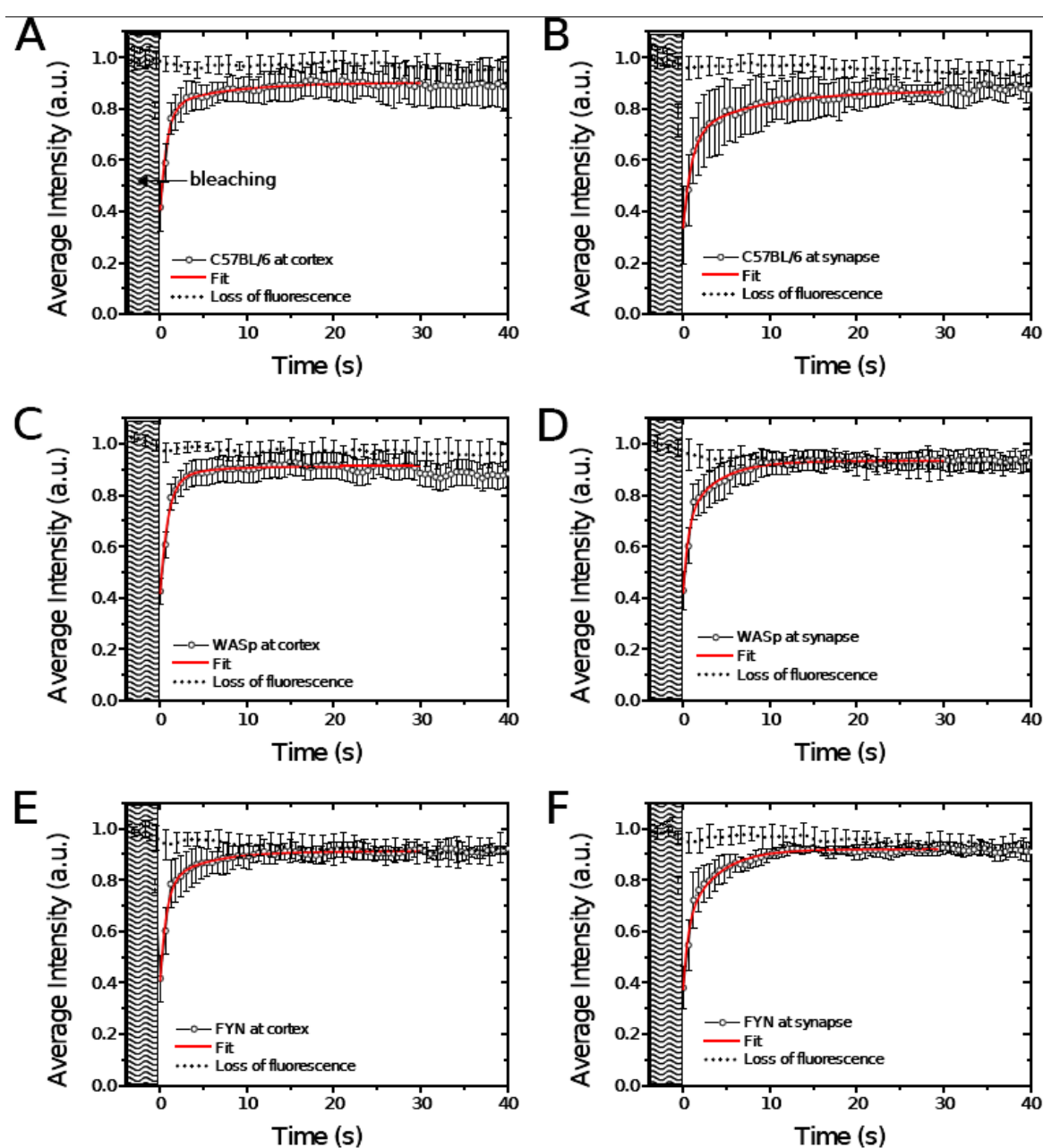


Figure 4.8 **Background-corrected mean fluorescence recovery plotted against time.** Error bars represent SEM. Red solid line represents second order exponential fit. Dotted line shows fluorescence loss due to imaging. Mean values from 10 curves are presented.

Multi exponent fit	R^2_{1st}	χ^2_{1st}	R^2_{2nd}	χ^2_{2nd}	R^2_{3rd}	χ^2_{3rd}	N	
Cortex	C57BL/6	0.9	0.09	0.97	0.03	0.97	0.03	10
	WAS	0.9	0.09	0.97	0.03	0.97	0.03	11
	FYN	0.89	0.111	0.95	0.05	0.95	0.05	10
Synapse	C57BL/6	0.89	0.06	0.96	0.02	0.96	0.02	10
	WAS	0.94	0.1	0.97	0.04	0.97	0.04	8
	FYN	0.89	0.2	0.92	0.14	0.92	0.14	13

Table 4.1 Exponential fitting parameters.

Multi exponent fit	$\omega_{d,1}$ (s^{-1})	p-value	f1	$\omega_{d,2}$ (s^{-1})	p-value	f2	N	
Cortex	C57BL/6	1.28 ± 0.1	-	0.78 ± 0.08	0.14 ± 0.04	-	0.22 ± 0.02	10
	WAS	1.28 ± 0.1	0.99	0.78 ± 0.08	0.14 ± 0.04	0.99	0.22 ± 0.02	11
	FYN	1.42 ± 0.1	<0.01	0.82 ± 0.08	0.24 ± 0.04	<0.01	0.18 ± 0.04	10
Synapse	C57BL/6	1.02 ± 0.14	<0.01	0.81 ± 0.08	0.13 ± 0.04	0.99	0.19 ± 0.05	10
	WAS	1.68 ± 0.3	<0.01	0.81 ± 0.06	0.27 ± 0.04	<0.01	0.19 ± 0.02	8
	FYN	1.84 ± 0.1	<0.01	0.81 ± 0.1	0.28 ± 0.04	<0.01	0.19 ± 0.08	13

Table 4.2 Second-order exponential fit recovery rates.

The analysis revealed the presence of two distinct actin subpopulations in DCs, as previously described in cell lines (Fritzsche et al., 2013). The rate of the first network ($\omega_{d,1}$) describes a fast-recovery network which comprises short branched filaments with a fast turnover rate. The slower network, described by $\omega_{d,2}$, comprises longer actin filaments, nucleation and stabilisation of which may be mediated by formins (Fritzsche et al., 2013, Kovar et al., 2006).

The proportion of each subpopulation is represented by F1 and F2. In BL6 DCs, around 78% (f1 column) of actin recovery occurred through the fast, Arp2/3-dependent network. In the steady-state cortex, rate of this recovery was $1.28 \pm 0.1s^{-1}$. In the synapse, the proportion of this fast, branched network was increased, however its rate of recovery decreased to $1.02 \pm 0.1s^{-1}$, which is significantly different to the cortex. This shows there is some level of stabilisation (decreased recovery rate) of the actin network during synapse formation, and may also suggest a more densely branched network (increased proportion of short branched filaments).

The longer formin-mediated filaments contribute to around 22% (f2 column) of actin recovery at the cortex, at a rate of $0.14 \pm 0.04\text{s}^{-1}$. In the synapse, the rate of recovery of this network does not change, though the overall proportion of it is slightly decreased. This is most likely to be a result of increased short branched actin, rather than a decrease in the absolute amount of long filaments.

According to this analysis, the WAS DC cortex is similar to BL6, suggesting that WAS function is not required for maintenance of cortical actin in steady state. This conflicts with data presented in Fig 4.7, highlighting the difference in sensitivity between the two techniques. At the synapse, lack of WASp results in increased recovery rates of both networks compared to BL6 DCs, similar to previous basic analysis (Fig4.6, 4.7). The increased recovery of the fast network may result from an inability to stabilise actin and provide a platform for the IS. Loss of stability suggests more diffusion and random motion of both G-actin and different filament subpopulations, resulting in more fluidity beneath the membrane. Furthermore, the recovery rate at the WAS synapse is increased even compared to the WAS cortex. This could be the result of increased local actin monomer concentration or short-filament polymerisation through other pathways, as a result of the external signals provided at the synapse to increase actin polymerisation.

It is interesting that the rate of the second, slow-recovery network is also increased in the WAS synapse. If the actin network does become polarised towards the synapse through mechanisms independent of WASp, but then cannot be organised and stabilised due to the lack of WASp, this could provide more building blocks (in the form of short actin filaments), which could be annealed to form longer formin-dependent filaments. It has been shown for example that this is the case at the leading edge of some migrating cells (Mejillano et al., 2004) – short branches can anneal end to end to form long filaments. Alternatively, if short-filament polymerisation or stabilisation is reduced, while the rate of filament severing is unaffected,

this would also result in an increase in the fast, branched network, which would then be translated into an increase in the long-filament network.

Unexpectedly, actin in FYN DCs recovers faster after bleaching in the steady state cortex. Although the results from WAS DCs suggest WASp is not required for cortical actin maintenance, its presence in a non-functional state may result in a dominant negative effect. Phosphorylation-dead WASp may still interact with several proteins, such as the SH3-domain containing Nck and Ikk. As this inactive WASp cannot then interact with Arp2/3 and polymerise actin, it may effectively render other proteins inactive by sequestering them away from potential compensatory pathways (which, as discussed, may be acting in the WAS DC cortex). Similarly at the synapse, both the fast and slow network recovery rates are increased, suggesting that the actin network is even less stable than in WAS DC synapses.

4.2.4 Bull's-eye IS pattern

The stability and organisation of the actin network is likely to affect clustering and localisation of transmembrane proteins within the synapse as observed in Chapter 3. A bull's-eye pattern interface has been described in T cells (Monks et al., 1998). Although one could expect the interacting APC to mirror this organisation, it is still unclear whether DCs form a similarly organised interface. The bull's-eye pattern described contains areas with distinct protein compositions: cSMAC (TCR-red), pSMAC (LFA-1-blue) and dSMAC (CD45-green). Figure 4.9 shows that WAS DC conjugates form irregular and asymmetric interfaces compared to BL6 control. Though the synapse exhibits a concentrated TCR area, it does not form the typical bull's-eye pattern, highlighting that WASp is an important regulator during this process.

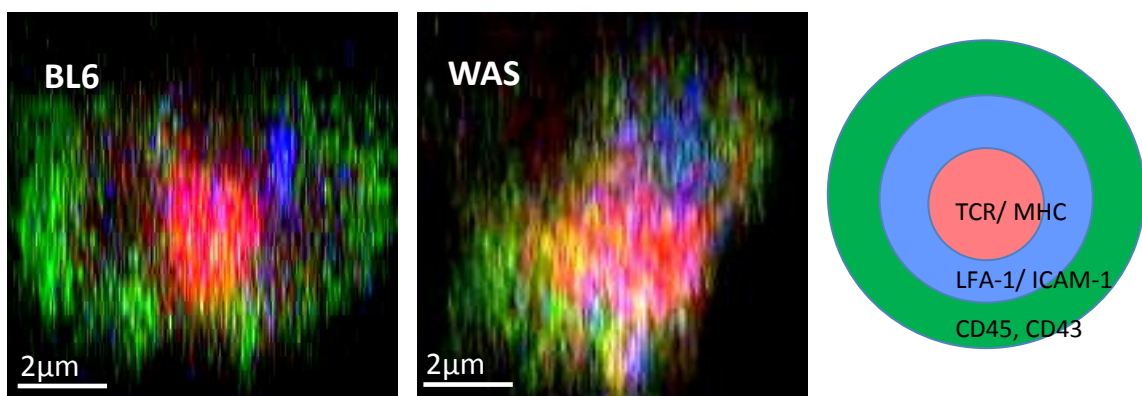


Figure 4.9 **Synapse organisation appears to be abnormal in WAS DCs.** 3D reconstructions of stacks of serial fluorescent images allow us to view the synapse across the Z plane and thus to image the interface between the two cells. Representative reconstructions for BL6 and WAS DCs are shown.

4.2.5 Micropits

Given that the maximum Z-plane resolution with the confocal system is around $0.5\mu\text{m}$, which is 2-3 times worse than resolution in the xy dimension, imaging the synapse in the plane of the interface would improve the level of detail acquired. One attempt to achieve this was using novel micropit technology.

Micropits have been developed using a silicon master mould to transfer arrays of pits ($40\mu\text{m}$ deep with a diameter between $15\text{-}23\mu\text{m}$) onto a PDMS-coated coverslip. DCs and T cells are sequentially loaded into these pits to form conjugates with an IS interface in the imaging plane. This would allow faster imaging and greater resolution, with the possibility of following synapse-formation in live cells.

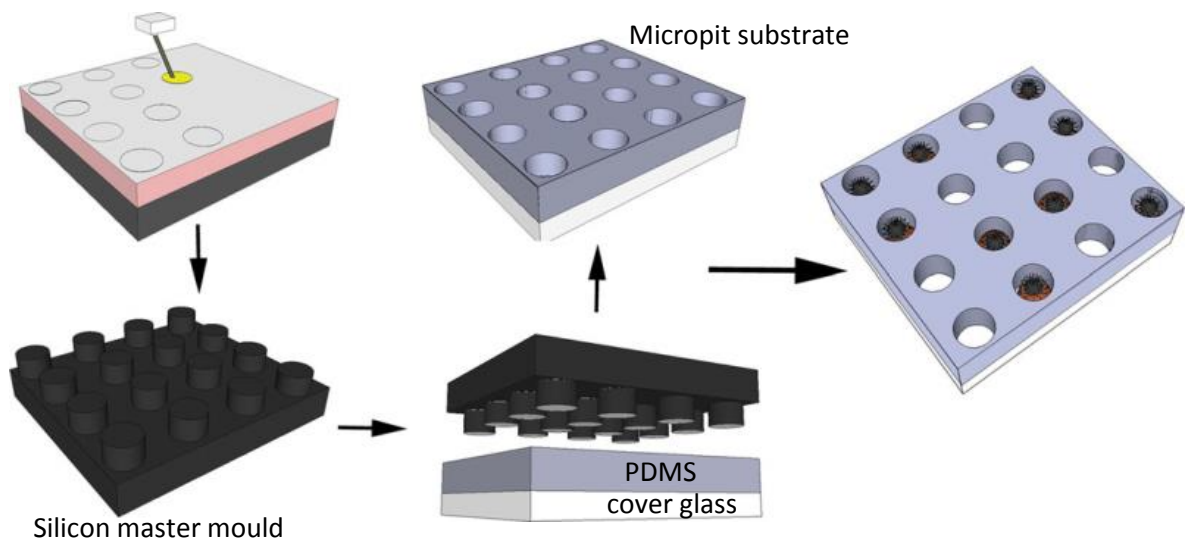


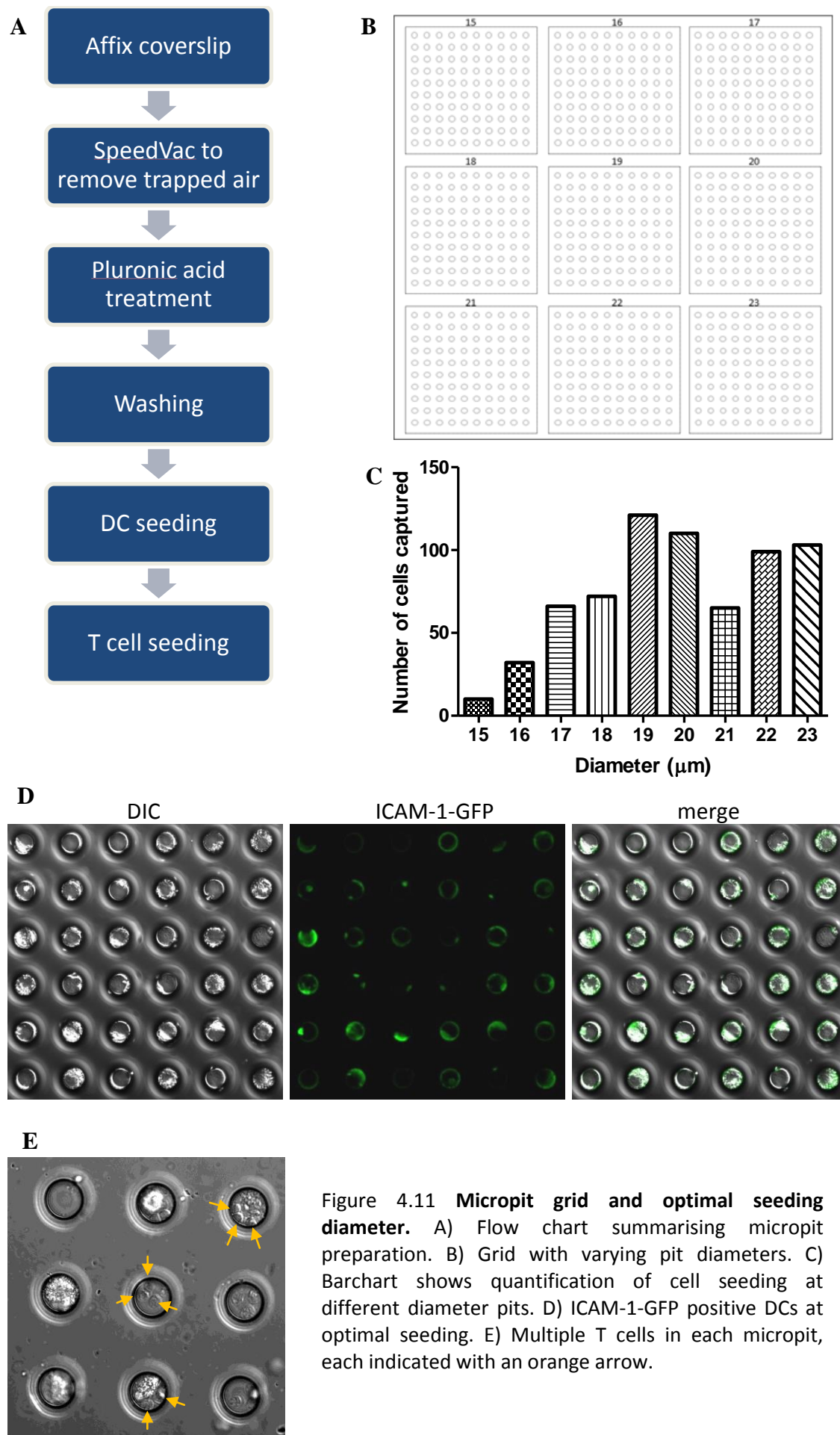
Figure 4.10 **Making micropits.** This illustrates the process of producing the master mould (by photolithography and reactive ion etching) and using this to create the pits in the PDMS substrate. Adapted from Biggs *et al* (Biggs *et al.*, 2011).

The micropits (a gift from M Biggs) were previously optimised for cell lines of different, less variable sizes compared to the primary DCs used in these experiments. In order to achieve the high-throughput imaging expected by this method, seeding and imaging conditions had to be optimised. Micropit preparation is described in Materials and Methods section 2.2.12 and

briefly summarised in Figure 4.11a. The DCs used expressed ICAM-1-GFP introduced by infection with a lentiviral construct. Micropits were imaged using a scanning laser confocal microscope, combining fluorescence and DIC (differential interference contrast) modalities. To optimise cell seeding, parameters such as incubation time, cell number, volume and micropit diameter were adjusted. A volume of 500µl was found to be sufficient to completely cover the micropits and 5×10^5 DCs was enough for seeding without an excess of uncaptured cells. The best DC seeding was seen after incubation at 37°C for 1 hour.

To investigate the optimal micropit diameter, pits ranging from 15-23µm across were designed and cell seeding in each was quantified (Figure 4.11 b and c). The largest number of DCs were captured in 19 or 20µm micropits. DC seeding was also high in 22 or 23µm pits, however, these allowed entry of multiple cells and cell movement within the pit, and were thus not optimal for imaging. 19-20µm diameter pits were chosen for further experiments.

Although less prevalent at smaller diameters, on many occasions multiple T cells enter one pit, as seen in Figure 4.11 e. Many of these do not form stable contacts with the DCs, however, they are not washed off during the cell seeding stages, perhaps due to the depth of the micropits. These do not allow accurate imaging of cell-cell interfaces so other imaging techniques were sought to investigate interface organisation.



4.2.6 Planar Lipid Bilayers

Glass-supported planar lipid bilayers allow imaging of synapse formation with high spatial and temporal resolution (Groves and Dustin, 2003). The aim of these bilayer experiments was to investigate the differences in IS organisation over time between BL6 and WAS DCs in the plane of the interface. Unless otherwise indicated, all bilayer images represent single section in the z-plane capturing the contact interface.

Most studies into synapse formation have investigated the interaction of T cells with an MHC-peptide-loaded bilayer. A previous student in the lab, in collaboration with a group in New York (M Dustin, New York University), used a novel lipid bilayer system to observe DCs in an investigation of gamma-chain function (C Beilin, in process of submission). Experiments presented here use a different set up and a pilot experiment was designed to validate the system for analysis of DC interactions. Bilayers were loaded with biotinylated anti-MHC and anti-ICAM-1 antibodies. These are linked to the biotinylated bilayer using a streptavidin bridge. The antibodies spread evenly and are laterally mobile (tested by FRAP) allowing the formation of an immune synapse. The biotinylated anti-MHCII antibody was labelled with Cy5 (Amersham Cy5 Maleimide Mono-Reactive Dye) and separated by gel permeation chromatography on a Sephadex G25 column. The anti-ICAM-1 antibody was not conjugated to a fluorescent dye; instead DCs were infected with a lentiviral vector containing an ICAM-1-GFP construct.

Figure 4.12 shows BL6 and WAS DCs interacting with a planar lipid bilayer containing anti-MHCII and anti-ICAM-1. BL6 DCs formed a condensed MHCII cluster in the centre of the synapse area, surrounded by a ring of ICAM-1, reminiscent of cSMAC and pSMAC in the previously discussed bulls-eye organisation. WAS DCs showed a more diffuse MHCII pattern and disorganised, asymmetrical ICAM-1.

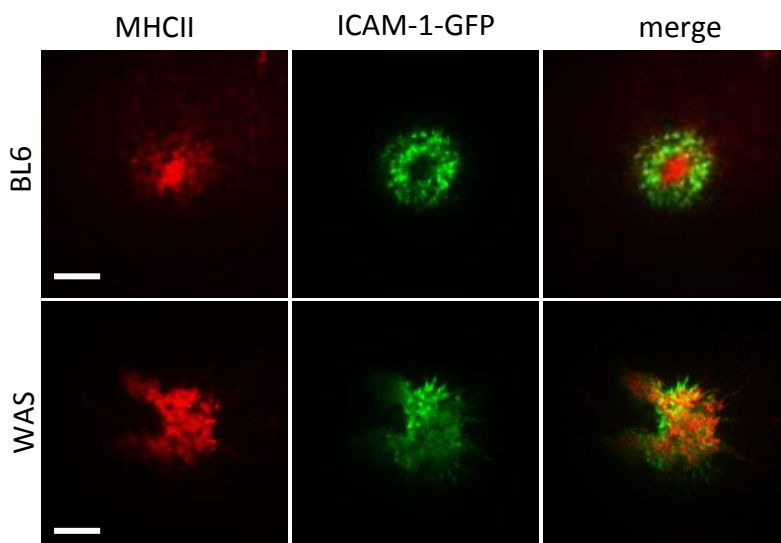


Figure 4.12
ICAM-1-GFP expressing DCs interacting with bilayers. Anti-MHCII-Cy5 is in red, ICAM-1-GFP in green. The antibodies were added to final concentration of 0.5 $\mu\text{g}/\text{ml}$. Chambers were fixed 30mins after addition of DCs. Scale bars = 5 μm .

DCs added to chambers containing empty streptavidin-only lipid bilayers did not form stable interactions with the bilayer. Very few cells were present in chambers after fixation and washing, for both BL6 and WAS DCs. Further, those that were present remained rounded and did not form the surface MHCII patterns seen previously (Fig 4.13). The biotinylated anti-MHCII antibody stains the lipid surface uniformly. This suggests the ‘synapse’ organisation seen in Figure 4.14 is not an artefact of DCs interacting with the lipid bilayer or streptavidin molecules but is result of MHCII and ICAM-1-specific ligation.

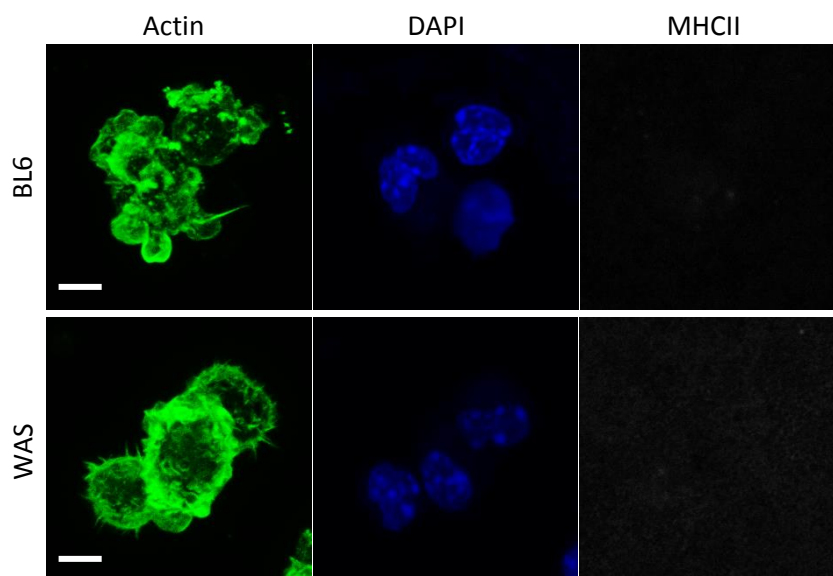


Figure 4.13 **Empty bilayer.** Chambers were fixed 30mins after addition of DCs. Cells were permeabilised and stained with DAPI, phalloidin-488 and anti-MHCII-Cy5. Scale bars = 10 μm .

To dissect the roles of different synapse components during IS formation, and investigate the contribution of each to the defect seen in WAS synapses, anti-MHC and anti-ICAM-1 were added to lipid bilayer chambers separately.

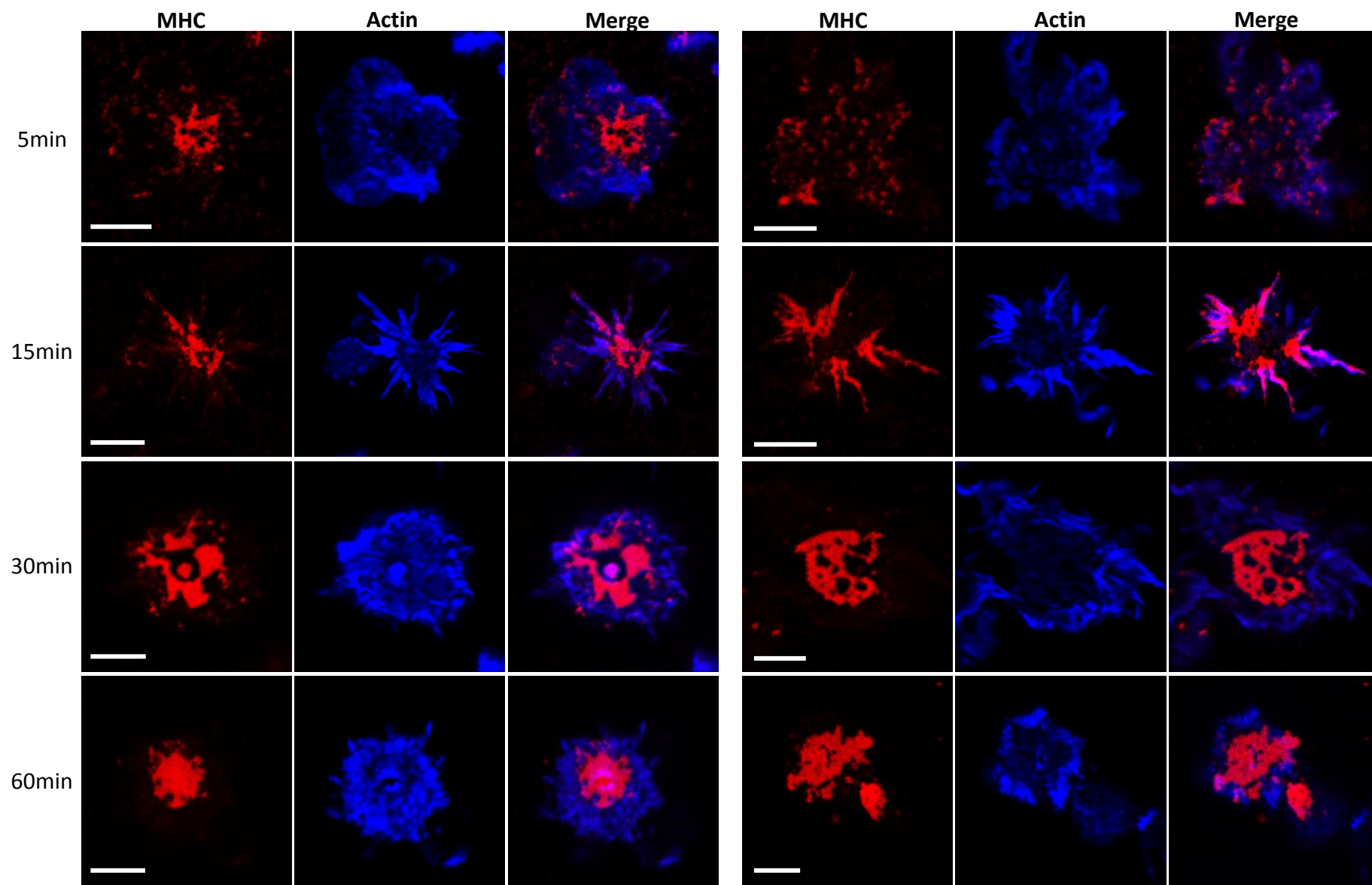
Anti-MHCII only

On bilayers containing anti-MHCII only, BL6 control DCs appeared to form a progressively more organised cSMAC over time. Cells fixed 5 minutes after addition to chambers showed many peripheral microclusters of MHCII; whereas those fixed at 30 or 60min formed a much larger, rounder, more intense, central MHCII cluster. WAS DCs appeared to organise this structure much more slowly and the resulting cSMAC was often asymmetrical and less complete (Figure 4.14).

Interestingly, there were also differences in cell morphology, as illustrated by phalloidin-stained outlines (Figure 4.15). Although both BL6 and WAS DCs spread on the bilayer at 5min, by 15min around 60% of BL6 DCs formed radial spiked protrusions. Significantly fewer WAS DCs formed similar structures (around 25%). Some WAS DCs presented a partial phenotype, where half of the cell formed protrusions ('half spikes').

At 30 and 60 minutes, around half of BL6 DCs formed a distinct actin-rich structure in the centre of the synapse. This was on average 1.5-3 μ m in diameter. Only around 25% of WAS DCs formed these actin dots. The role of these previously undescribed structures is unclear. It is unknown whether they occur in T cell: DC synapses or are artefacts resulting from DCs interacting with a non-deformable substrate.

Figure 4.14 (next page) **Anti-MHCII bilayer**. Cy5-labelled anti-MHCII antibody was added to the chambers at 0.5 μ g/ml. After washing, BL6 or WAS DCs were added to the chambers and these were fixed at set timepoints (5, 15, 30, 60min). Cells were stained with Phalloidin-488 and imaged. BL6 DCs are shown on the left; WAS on the right. Scale bars = 5 μ m.



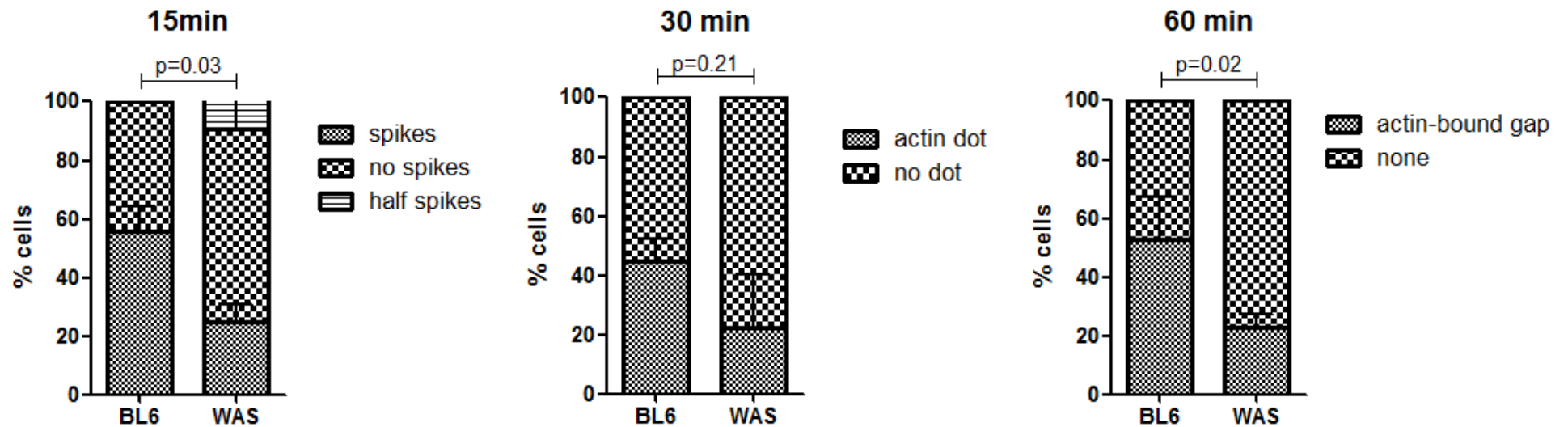


Figure 4.15 **DC morphology over time.** At each time point over 200 cells from 2 separate experiments from each strain were counted and analysed. At 15minutes, these were classed as cells forming spikes or no spikes. At 30 and 60minutes, cells were scored as containing an actin-rich 'dot' or not. Significance values are based on a two-way ANOVA analysis with paired BL6 and WAS observations across experiments.

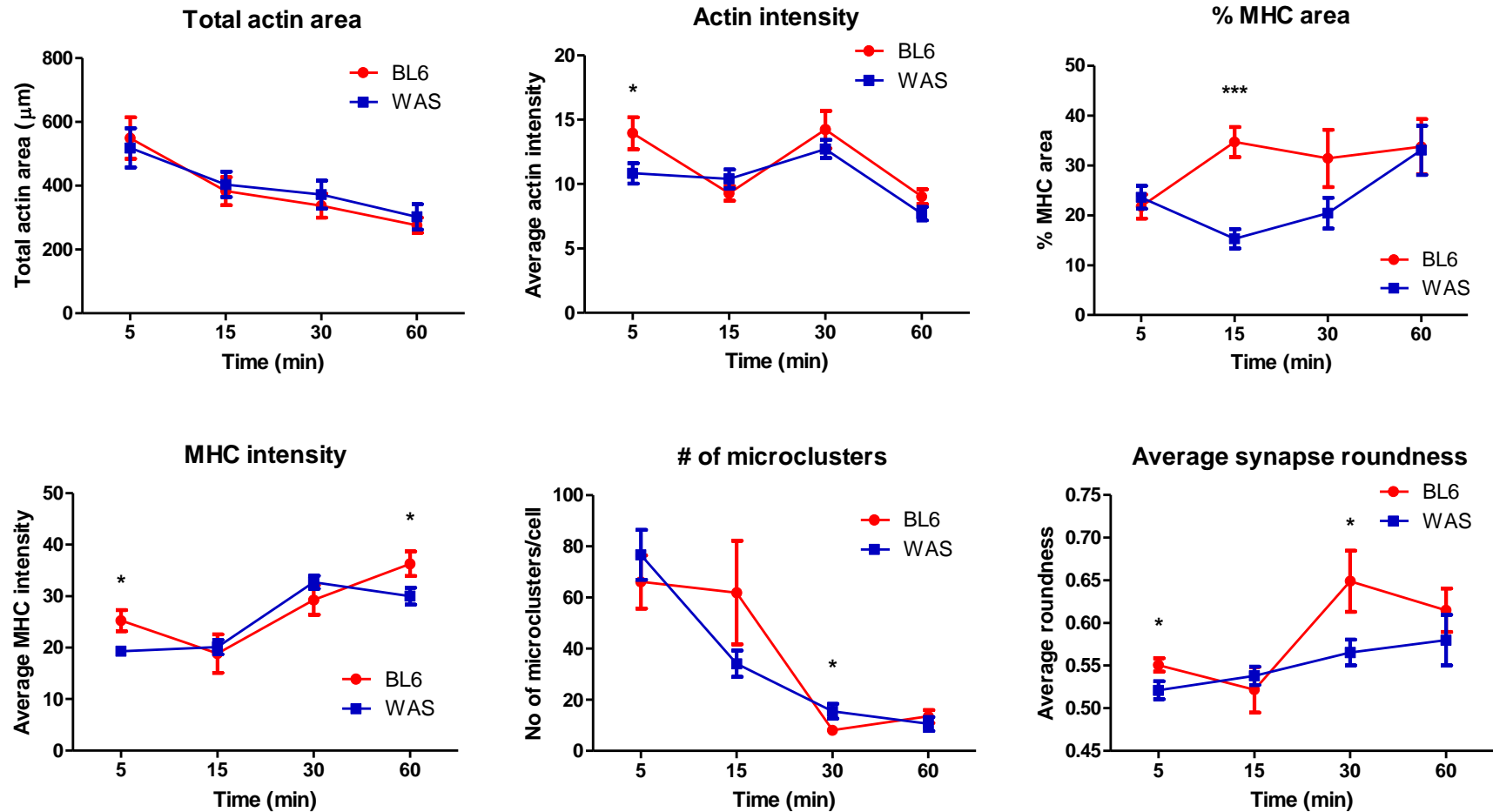


Figure 4.16 **Actin and MHC surface area and intensity.** Images of single DCs on an anti-MHCII bilayer (see Figures 4.15 and 4.16) were analysed. Parameters were measured in Fiji for 15-20 cells of each strain at each timepoint. Significance was calculated using a paired t-test at each timepoint. * $p=0.01-0.05$; ** $p=0.001-0.01$; *** $p<0.001$.

Other parameters were measured to further characterise differences between BL6 and WAS synapse organisation with time (Figure 4.16). Cell spreading was analysed by measuring total actin area in contact with the bilayer. The average actin intensity over that area was also measured. Similarly, the area of MHC was analysed by selecting all pixels above a threshold and measuring the total size and average intensity within this selection. MHCII area is presented as a percentage of the total cell area. The number of microclusters per cell and the circularity of the synapse are also plotted against time.

Cell spreading and contact area appear to be similar between BL6 and WAS DCs at all timepoints tested. Average actin intensity also shows little difference, perhaps reflecting the fact that this method of phalloidin staining and imaging is not sensitive or reliable enough for direct comparison of separate samples with small differences.

Total MHC area as a percentage of the contact area was significantly larger in BL6 DCs compared to WAS at 15minutes. This may reflect the greater number of microclusters formed in BL6 cells or a larger cSMAC formation. Initially, both types of cells form similar numbers of MHCII clusters (around 70 per cell). In BL6 DCs, the number of these microclusters appears to be maintained at 15minutes. This may reflect maintenance of pre-formed clusters for longer or continued microcluster formation over a larger time frame compared to WAS DCs. By 30 and 60 minutes, the number of MHCII clusters is considerably reduced in both BL6 and WAS DCs. MHC intensity on the other hand increases with time, implicating continued recruitment and concentration of MHCII to the contact interface. Synapse roundness was the final parameter quantified using the Fiji Measure feature. The significantly higher roundness in BL6 synapses at 5 and 30minutes reflects more symmetrical contact interfaces. By 60 minutes, WAS DCs appear to reach a similar level of circularity. The spikes formed by BL6 cells at 15minutes are evident in both the actin and MHCII stains and manifest in a drop in synapse roundness at 15 minutes.

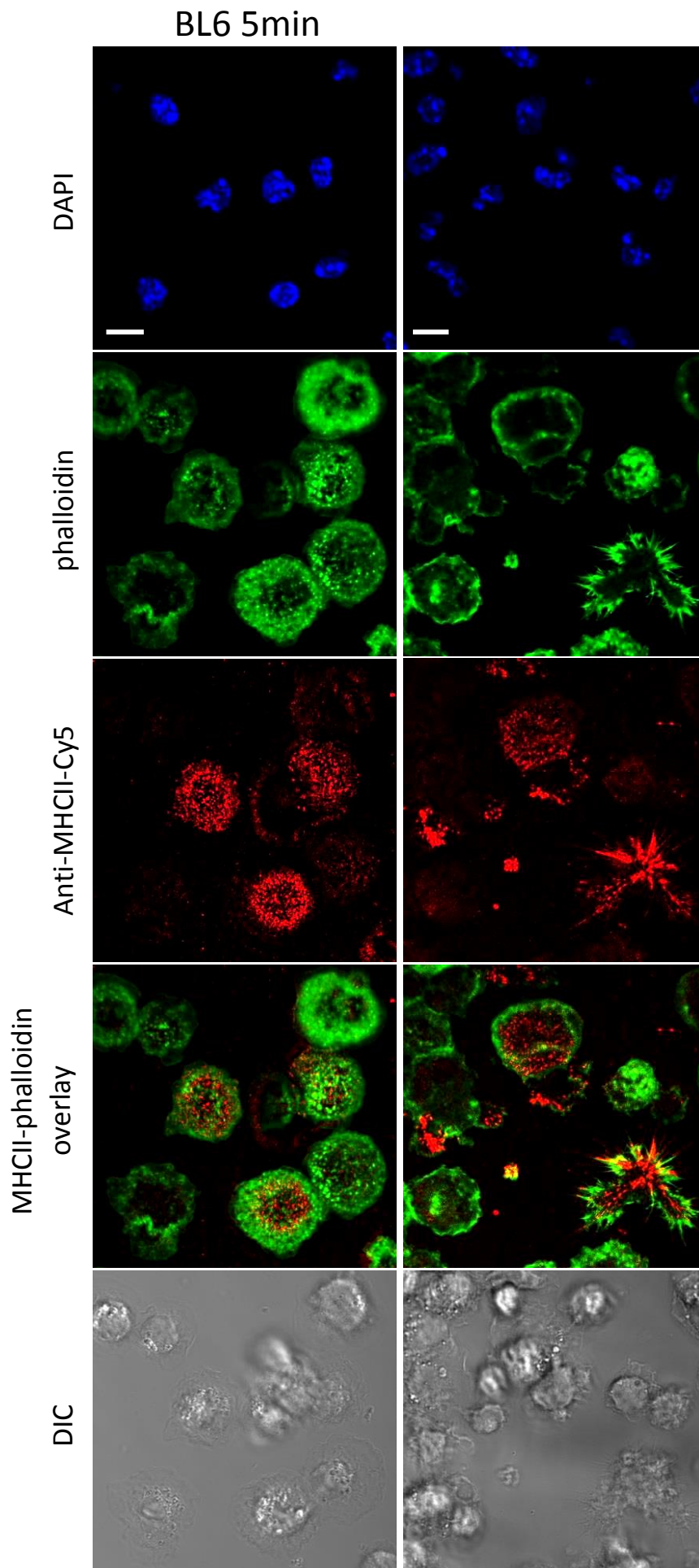
Anti-MHCII and anti-ICAM-1

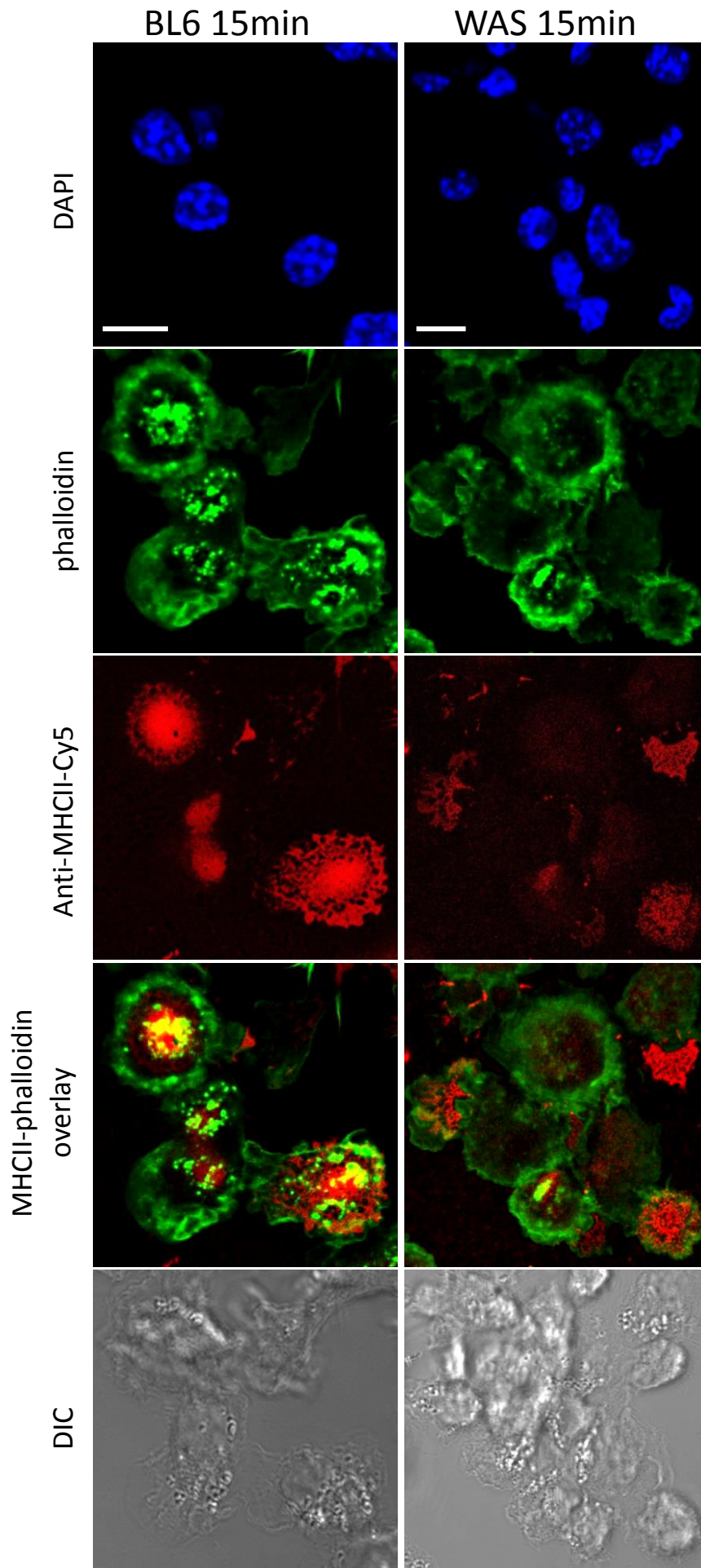
To reconstitute cell-cell synapse formation more fully, anti-ICAM-1 was added to the bilayer. Mathematical models predict that addition of ICAM-1 to lipid bilayers should allow a cSMAC to form more readily in T cells on planar bilayers compared to contacting APCs (Lee et al., 2003a, Qi et al., 2001). These suggest that the higher ligand mobility in bilayers compared to APCs and the fact that only one of the interacting membranes is deformable, both result in easier reorganisation of membrane proteins. Several lines of evidence point to a role for ICAM-1 in organising the synapse interface, by concentrating TCR, antigen and downstream kinases in the cSMAC. Enhanced receptor activation in the cSMAC results in increased receptor degradation, thus resulting in an intense yet self-limiting activation response. To test the role of ICAM-1 on the dendritic cell during synapse formation, biotinylated anti-ICAM-1 was added to the bilayer and cell interactions were assessed as before.

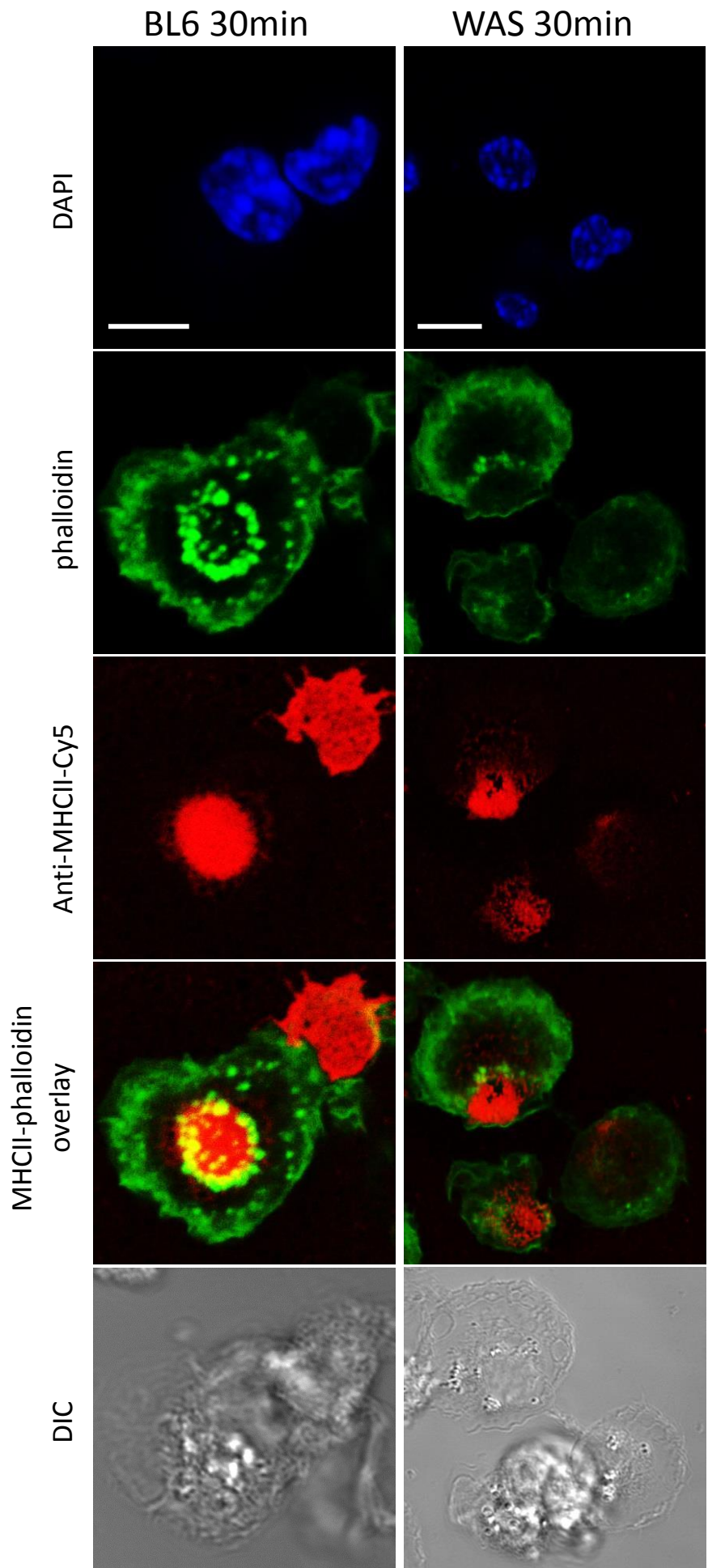
In agreement with the above studies, control DCs formed a compact MHCII cSMAC faster when interacting with bilayers containing both anti-ICAM-1 and anti-MHCII compared anti-MHCII alone (compare Figures 4.17 and 4.14).

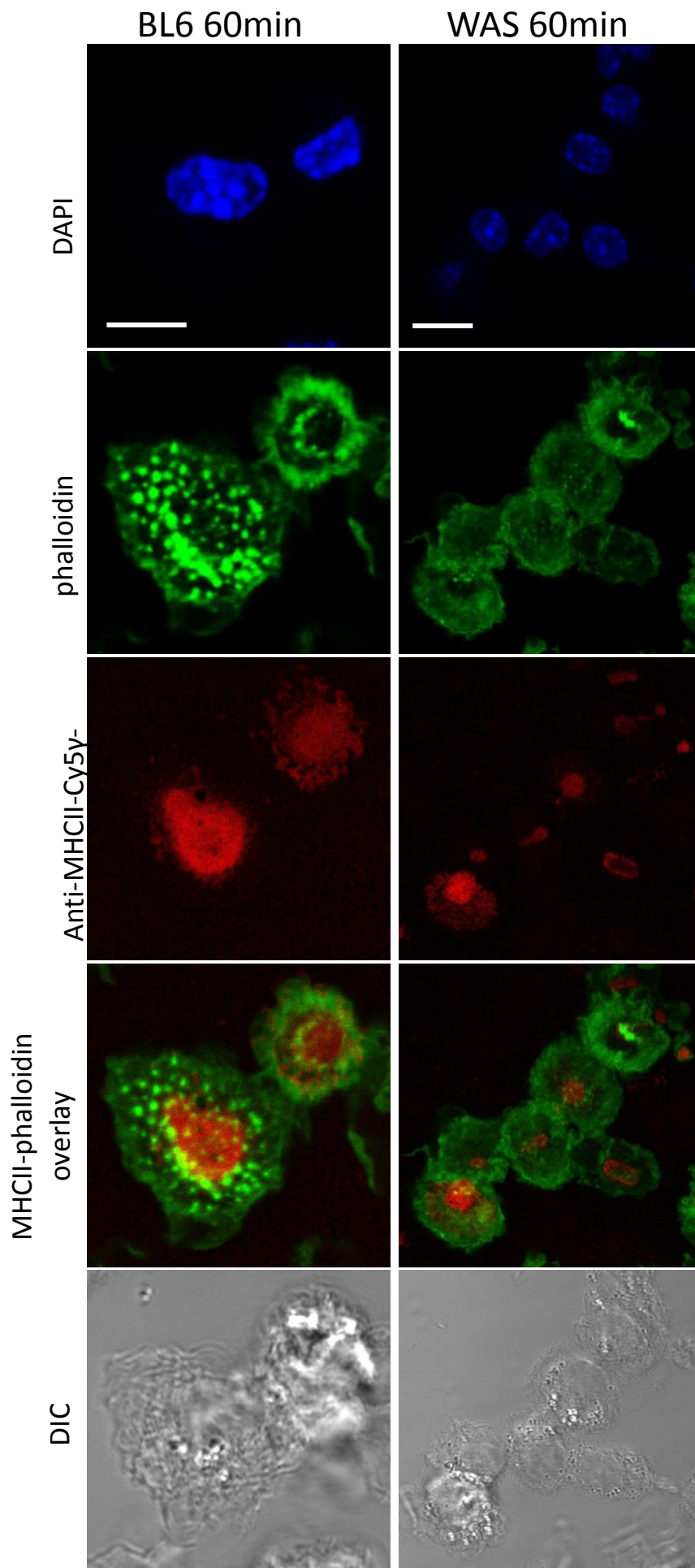
BL6 DCs were able to mobilise MHC molecule and form a concentrated central area faster than WAS DCs. This can be seen in Movies 4.3 (BL6) and 4.4 (WAS).

Figure 4.17 (next 4 pages) **Anti-MHCII and anti-ICAM-1 bilayer.** Anti-ICAM-1 and Cy5-labelled anti-MHCII antibodies were added to the chambers to a final concentration of 0.125µg/ml and 0.5µg/ml respectively. After washing, BL6 or WAS DCs were added to the chambers and these were fixed at set timepoints (5, 15, 30, 60min). Cells were stained with Phalloidin-488 and DAPI and visualised by confocal microscopy. BL6 DCs are shown on the left; WAS in the right panel for each time point. Scale bars = 5µm









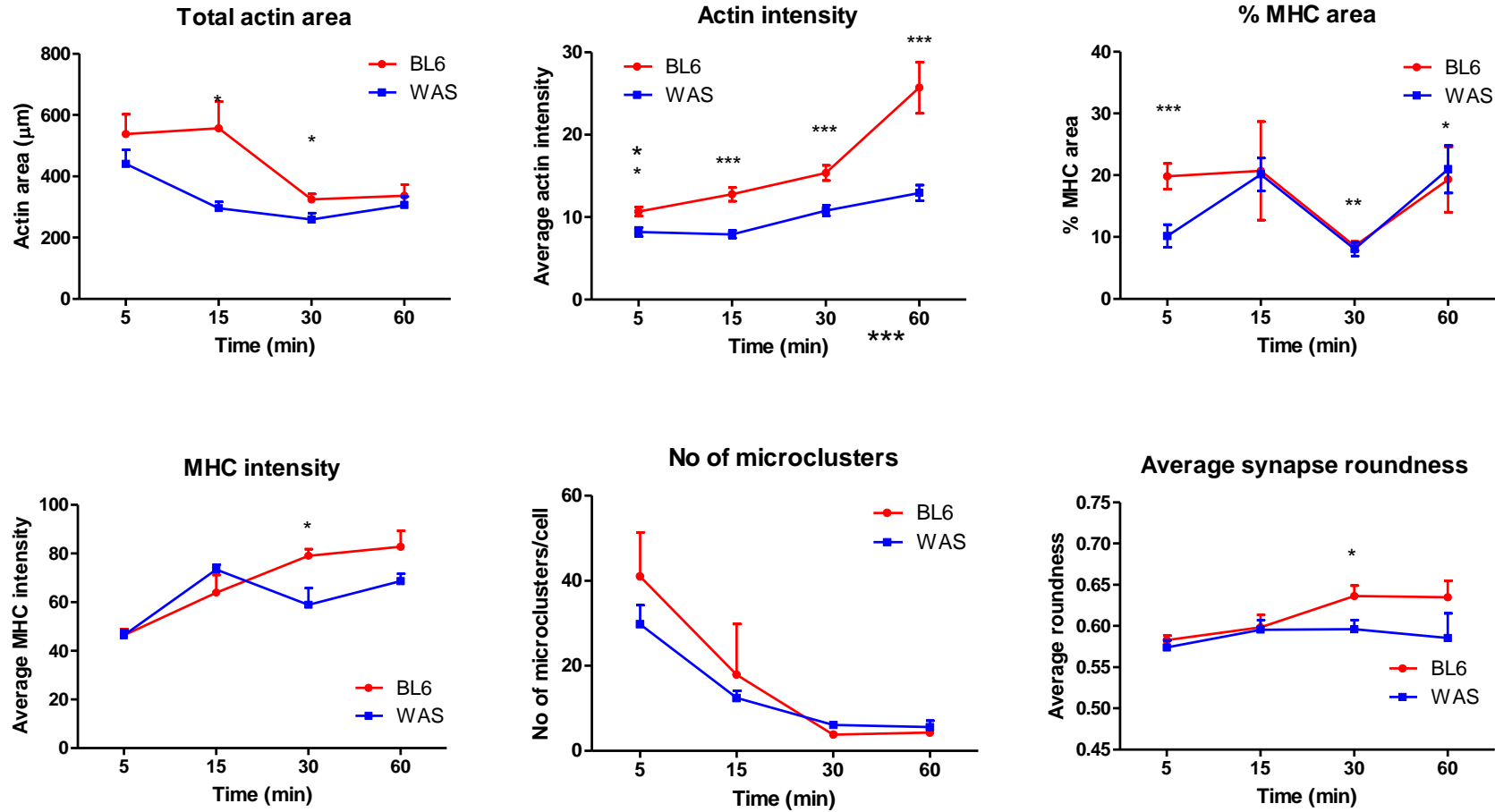


Figure 4.18 **Actin and MHC surface area and intensity.** Images of DCs on an anti-MHCII and anti-ICAM-1 bilayer (see Figures 4.18) were analysed. Parameters were measured in Fiji for 15-20 cells of each strain at each timepoint. Significance was calculated using a paired t-test at each timepoint. *p=0.01-0.05; **p=0.001-0.01; ***p<0.001.

Compared to the anti-MHCII only bilayer, the total actin area (total contact area) for BL6 cells this time is increased, suggesting that the interaction of ICAM-1 with the bilayer allows cells to spread and thus increase contact surface area. In this case, WAS DCs show a significantly reduced contact area at 15 and 30 minutes. Interestingly, there were also very few cells of either BL6 or WAS displaying the spike protrusions seen on the MHC only bilayer.

The actin intensity of BL6 cells was significantly higher both compared to WAS DCs (Fig4.18) and compared to BL6 DCs on MHC only bilayers (Fig4.16). This may reflect more stable contacts as a result of ICAM-1 activation and increased actin polarisation. The appearance of podosome-like protrusions in BL6 cells may provide support for this, as discussed later.

MHC area as a percentage of the total contact appears lower on bilayers containing both anti-MHC and anti-ICAM compared to MHC only. This is in agreement with the increase in total contact area due to more widespread adhesion mediated by anti-ICAM-1. There is an interesting drop in % MHC area at 30minutes, which appears to reflect a contraction or compaction of the cSMAC, rather than increased cell spreading. MHC intensity, as before, increases over time in the BL6 DCs. This appears reduced in WAS DCs, perhaps as a result of poorer recruitment and concentration of MHCII molecules.

The number of microclusters formed is lower in BL6 cells on bilayers containing anti-ICAM-1 in addition to anti-MHC, compared to anti-MHC only. This highlights the fact that these bilayers promote faster, more complete formation of the cSMAC. Interestingly, the number of microclusters is also reduced in WAS, suggesting that ICAM-1 ligation can increase cSMAC formation in WAS cells, albeit not to the same level as BL6, despite reduced actin polymerisation.

Average synapse roundness, in agreement with other parameters above, also increases earlier compared to MHC only bilayers. The round central area of MHC is formed earlier and as

mentioned, there is little evidence of spikey cells at 15minutes upon ICAM-1 ligation. WAS DCs do not form the same circular, symmetric synapses at 30 and 60 minutes.

As mentioned previously, control DCs formed striking rings of actin point protrusions, similar to the adhesive structures called podosomes. This has not been described previously in a synapse setting. Several concentrations of anti-ICAM-1 were tested in an attempt to determine whether the number and size of these structures was dose-dependent. The images in Figure 4.17 represent bilayers with 0.125 μ g/ml anti-ICAM-1 and 0.5 μ g/ml anti-MHCII. While MHC ligation was kept constant, two other anti-ICAM-1 concentrations were tested - 0.25 μ g/ml and 0.5 μ g/ml. Images from other concentrations are included in Appendix 2. Podosome-like protrusions were formed in a similar percentage of cells at all three concentrations of anti-ICAM-1 tested (Figure 4.19). A significantly lower number of WAS DCs formed podosome-like structures. Those which did were not as prominent and did not organise in a ring pattern (Figure 4.17). A reduced ability to form podosomes has been well described in WASp-deficient cells (Monypenny et al., 2011, Calle et al., 2004, Olivier et al., 2006, Linder et al., 1999).

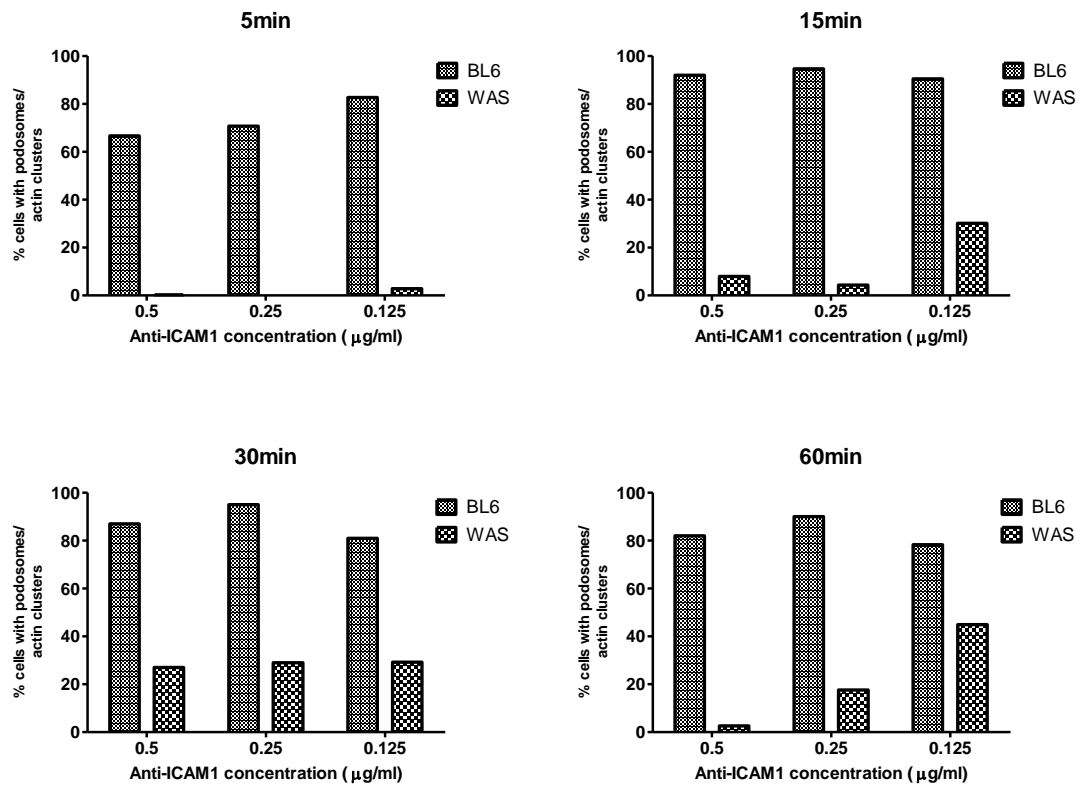


Figure 4.19 **Podosome quantification on anti-MHCII and anti-ICAM-1 bilayers.** Around 100 cells were counted for each concentration at each time point and the number of cells containing actin protrusions was noted. Results represent a single experiment.

Further analysis was required to confirm the identity of these actin-rich protrusions. The diameter of these structures in BL6 cells was measured and found to be within the range quoted for podosome sizes in literature, 0.5-1 μ m (Linder and Aepfelbacher, 2003, Linder and Kopp, 2005).

Podosomes are characteristically described as adhesion sites containing an actin-rich core surrounded by a ring of scaffold or actin-binding proteins, such as talin, vinculin and paxillin, as well as integrins. Beta-1 integrins have been shown to localise to the core, while β 2 and β 3 integrins mainly localise to the outside ring (reviewed in (Linder and Kopp, 2005)). CD11a (also known as ITGAL or integrin alpha L) is major partner of the β 2 chain and the heterodimer these form is more commonly known is LFA-1.

Figure 4.20 shows a stain for CD11a in BL6 and WAS DCs. In BL6 DCs this appears to form rings around individual actin protrusions in a manner reminiscent of true podosomes. Relation to LFA-1 would have to be confirmed with a CD18 or β 2 immunofluorescent stain. Representative images have been chosen from a 15minute time point, however, rings of CD11a were present in BL6 cells at all time intervals.

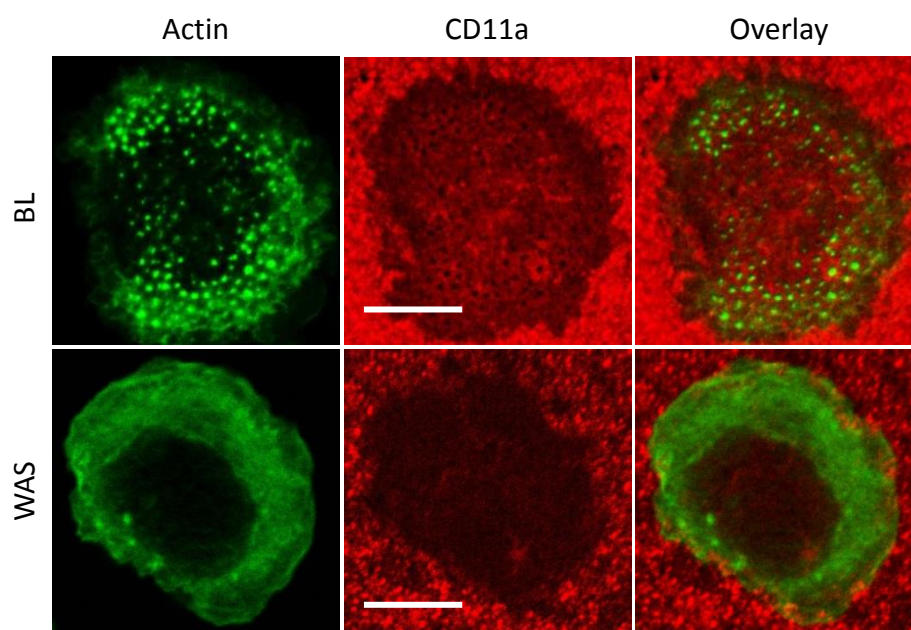


Figure 4.20 **Confirming podosome identity – CD11a.** Bilayer chambers containing both anti-MHCII and anti-ICAM1 were fixed and permeabilised 15 minutes after cell seeding. A rat anti-CD11a antibody was used to detect murine CD11a; this was followed by an anti-rat-564 secondary antibody. Scale Bar = 5 μ m.

A further stain for the alpha unit of human F-actin capping protein (CapZ) was included. Heterodimers of α and β subunits cap barbed ends of actin filaments to prevent polymerisation and depolymerisation. The role of capping proteins in podosome formation or stability is unclear. Figure 4.21 shows fixed and permeabilised DCs on bilayers containing both anti-MHC and anti-ICAM-1. The cells are stained with phalloidin, revealing the characteristic ring of podosomes. At all time points, $62.7 \pm 4.76\%$ (SEM; a total of 80 cells across all times were analysed) of cells showed colocalisation of capping protein with actin in the podosomes. Further, the images show that podosomes are initially situated within “clouds” of actin, as previously described in osteoclasts (Destaing et al., 2003). These must contain some F-actin components as they are detected by phalloidin.

Finally, to investigate turnover of podosomes at the synapse, live imaging on lipid bilayers using TIRF microscopy was utilised. BL6 DCs were infected with a lentivirus containing a LifeAct-mCherry construct in order to follow filamentous actin dynamics in real time. Two days post infection, cells were matured and added to bilayers containing both anti-MHC and anti-ICAM-1. Imaging was initiated 5min after addition of cells and images were taken at 5 second intervals in both Cy5 (MHCII) and Cy3 (LifeAct-mCherry) channels for a total of 20minutes. Movie 4.5 shows MHCII gathering in the Cy5 channel. Unfortunately, actin labelling was diffuse which made it difficult to focus in the correct z-plane in TIRF mode for the duration of the imaging. Faint dots of actin can be seen from around 120seconds on. These appear to move and undergo constant fusion and fission suggesting that turnover of F-actin itself is faster than that of the podosomes. Although improved imaging is required for complete analysis, these podosomes appear dynamic, with a half-life of individual structures not significantly different from published data: a minimum of 2minutes in osteoclasts (Destaing et al., 2003), 1minute in macrophages (Evans et al., 2003), and between 30seconds and 10minutes in DCs (Calle et al., 2004). Podosome clusters however, appears stable for up to 60 minutes.

Movie 4.6 shows a migrating DC slowing down upon interaction with a T cell, leading to a final arrest. Although in this case the DC is interacting with a glass substrate rather than supported

planar bilayers, it is included as a comparison of migration-related podosomes and the ring structure seen in synaptic podosomes.

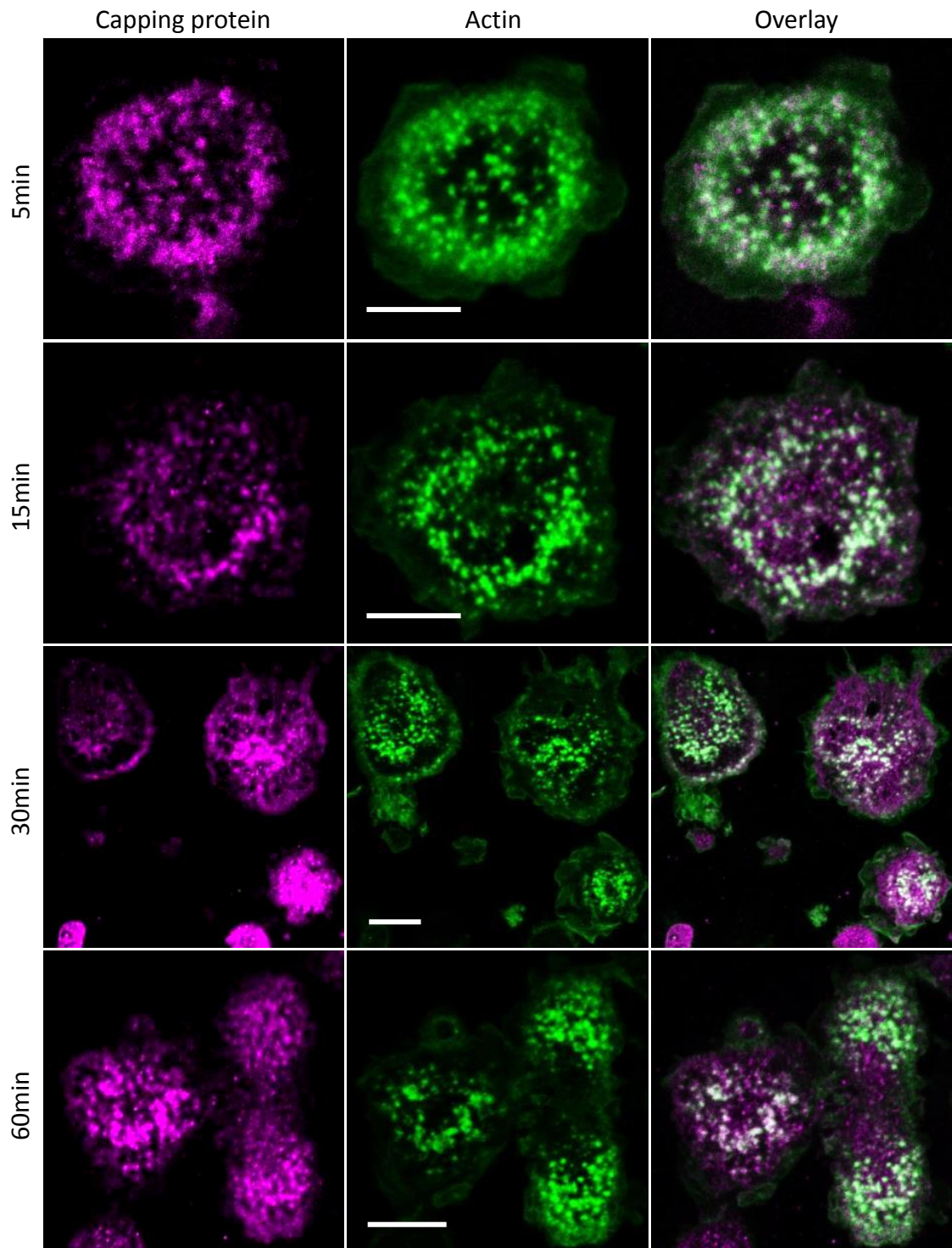


Figure 4.21 **Confirming podosome identity – capping protein.** Fixed and permeabilised cells were stained with phalloidin-488 (green) and a rabbit polyclonal antibody against capping protein, followed by a secondary anti-rabbit-633 antibody (purple). Areas of colocalisation appear white in the overlaid images. Scale bar = 5 μ m.

Anti -ICAM-1 only

To test whether activation of ICAM-1 alone could induce podosome formation in DCs, biotinylated anti-ICAM-1 was added to lipid bilayers alone. Figure 4.22 shows representative images from these bilayers. DAPI was used to aid identification of individual cells; while phalloidin-488 was used to visualise polymerised actin. Similar to empty bilayers (Figure 4.13), cells which were stained with anti-MHCII after fixation on the bilayer (i.e. did not interact with anti-MHC during the experiment) do not form the characteristic MHCII microclusters and cSMACs. BL6 DCs formed podosomes in around 80-85% of cells, whereas WAS cell were unable to form similar structures. This suggests that activation of ICAM-1 alone is sufficient to induce podosome formation in mature DCs interacting with a lipid bilayer.

Initially this appeared to be a synapse-independent process, which simply requires integrin adhesion. However, it was noted that BL6 cells interacting with anti-ICAM-1 only did not form rings of podosomes around the central MHC cluster as seen before. Instead podosomes appeared more disorganised and asymmetric and were often found in small clumps (Figure 4.22).

Although the function or mechanism behind podosome ring formation in DCs is unknown, rings were so prominent in cells interacting with anti-MHC anti-ICAM-1 bilayers that they appeared specifically localised to surround the central MHCII concentrated area.

The number of BL6 cells displaying rings of podosomes was quantified as a percentage of the total number of cells containing podosome structures. This is shown in Figure 4.23. The percentage of cells forming podosome rings was significantly reduced when cells interact with either anti-MHCII or anti-ICAM-1 compared to interaction with both. This suggests that downstream signalling from both MHCII and ICAM-1 is required for the organisation of podosomes at the synapse interface of DCs.

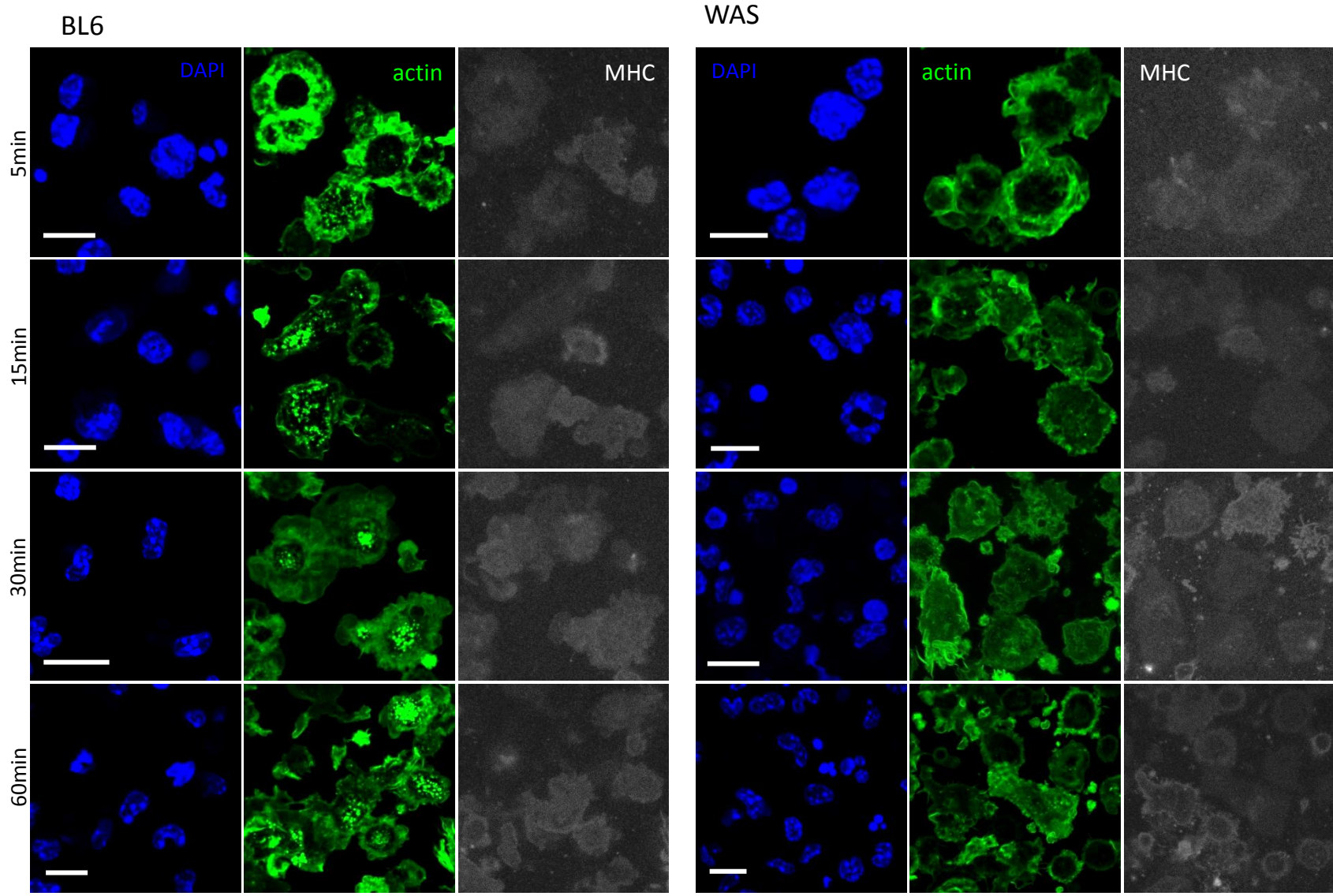


Figure 4.22
Anti-ICAM-1 only bilayers.
Cells were fixed and permeabilised at specified intervals; and stained with DAPI, phalloidin-488 and anti-MHCII-Cy5. Scale bar = 10µm.

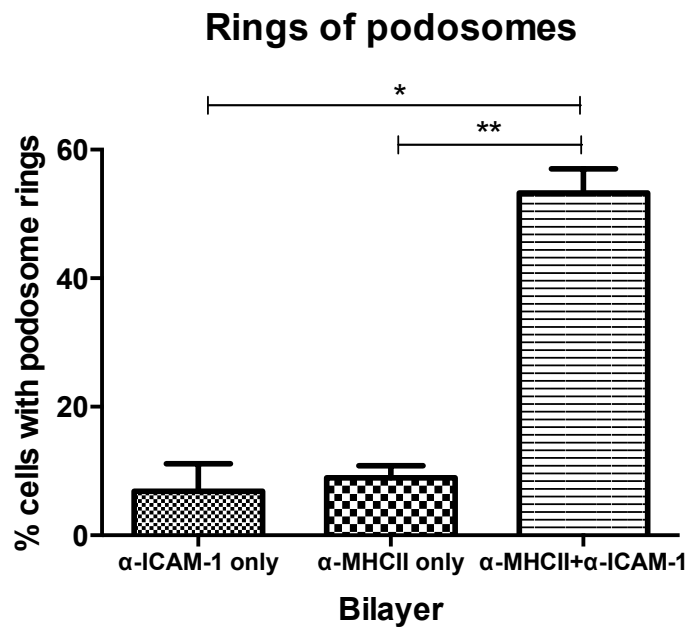


Figure 4.23 **Podosome quantification across different bilayer constituents.** Over 150 podosome-containing cells from two separate chambers were counted and scored for the presence of ring organisation. Significance was calculated using an unpaired t-test between two conditions. * $p=0.01-0.05$; ** $p=0.001-0.01$.

4.3 Discussion

This chapter aimed to investigate the differences in the dynamics of immune synapse formation between BL6 and WAS DCs. Initial results (Fig 4.1) showed that in DC: T cell cocultures fixed at different time points, WAS DC were unable to form as many conjugates with OT-II T cells, suggesting that their contacts were not as stable or long-lasting as BL6 DC conjugates. Live imaging was also used to show decreased stability and contact length in WAS DCs conjugates (Fig 4.2). Although a longer live imaging period would be beneficial for both BL6 and WAS samples; this form of live imaging was not sensitive enough to detect ICAM-1-GFP polarisation towards the T cell interface and does not allow enough resolution to study the subtle molecular changes at the synapse.

A number of techniques were optimised to study the cell-cell interface in more detail. Z-plane reconstructions suggested that a bull's-eye organisation was formed in BL6 DC and this was incorrectly organised in the absence of WASp (Fig 4.9). Unfortunately, this could not be confirmed at higher resolution due to limitations of the micropit experiments for the DC: T cell system (Fig 4.11). A couple of different strategies could be adopted to optimise future experiments. Reducing the depth of the micropits used to 20 μ m (half the original depth) should reduce the time needed for DC seeding and may allow more efficient washing of unbound T cells from the substrates. Alternatively, micropits could be designed for T cell seeding. These would be much smaller in both depth and diameter in order to ensure only one T cell is present per pit. DCs could then be added to the top of the array substrate to allow interaction with seeded T cells.

The FRAP results shown here highlight several crucial points. First, the cortex of primary murine DCs contains two subpopulations of actin filaments, as recently reported in cell lines (Fritzsche et al., 2013). Second, the proportions of the two different subpopulations are not altered in the cortex beneath the synapse interface; however, in BL6 cells actin recovery after photobleaching is slower implicating distinct regulatory mechanisms during formation of the

IS. Third, the absence of WASp in DCs has no effect on the proportion of each filament subpopulation, nor does it affect the recovery of actin in the steady-state cortex. It does, however, increase the recovery rate of actin in the synaptic cortex, suggesting reduced stability and regulation of the actin network here. This provides strong evidence for a role of WASp as a scaffolding adaptor, perhaps through interaction with other partners such as Nck, talin or Fyn. One could make the case that FRAP data showing faster actin recovery in WAS DCs confirms the less stable adhesion and lack of podosomes seen in WAS.

Although these results provide useful insight into actin organisation at the synapse, there are limitations. FRAP across the synapse may encompass several types of actin networks, which would actually be spatially separate. For example, based on membrane protein composition, it has been suggested that the molecularly distinct areas of the synapse (cSMAC, pSMAC and dSMAC) are related to distinct regions in migrating T cells – the kinapse (lamellipodium, lamella and uropod) (Dustin, 2008b, Dustin, 2008a, Evans et al., 2009). More recently the model has gained momentum with recent publications showing distinct actin networks present in the comparable regions of the immune synapse and the migrating state of the T lymphocyte (Yi et al., 2012, Hammer and Burkhardt, 2013). Yi *et al* saw three zones with distinct actin content in Jurkat T cells interacting with supported planar bilayers – an outer, actin-rich zone, a middle zone formed of concentric arcs of F-actin and in inner/ central zone devoid of F-actin. Each of these networks should have different actin dynamics and thus different recovery rates after photobleaching. Although it is possible that the two different subpopulations identified in the FRAP experiments here correspond to the different actin networks described by Yi *et al*, the same spatial relationship cannot be inferred. The direction of imaging and bleaching in these experiments does not allow one to distinguish between these. The use of micropits or optical tweezers might make it possible to bleach different areas of the synapse and obtain good resolution of different actin networks.

Further, there is no evidence yet to suggest a similar organisation exists in DCs. Images of DCs on supported planar bilayers presented in this chapter do not show clear concentric arcs of F-actin. If these do exist on the DCs side of the synapse, they may be more difficult to image due to the much larger and less uniform cytoplasmic organisation in these cells, as well as the presence of podosome structures. Whether it is concentric arcs, podosomes, or both, the analysis of fluorescence recovery in the perpendicular direction to the synapse interface is complicated by the presence of distinct spatially regulated actin networks. It would be interesting to see whether future FRAP experiments can separate the contributions of different subpopulations in different areas of the synapse. Single molecule imaging would allow further characterisation of filaments at the synapse interface.

The synapse/kinapse comparison may be relevant for DCs and, as a model, is not mutually exclusive with the presence of podosomes. In migrating cells, podosomes are situated at the border between the lamellipodium and lamellum and further back through the lamellum (Calle et al., 2006a). In direct comparison, podosomes in DCs interacting with anti-MHC and anti-ICAM bilayers appear to form in a similar area (Fig 4.17, 4.20, 4.21). Thus although the podosome structures involved in these distinct cellular processes have different functions, the actin subpopulations and regulators involved may overlap. Questions remain about whether actin retrograde transport is involved on the DC side of the synapse, similarly to that described in T cells above, and if so, how this interacts with actin networks responsible for podosomes. Live imaging has shown that retrograde flux in migrating fibroblasts is inversely proportional to migration, i.e. flux was increased when fibroblasts were immobilised (Guo and Wang, 2007). If a similar mechanism is present in DCs, it could integrate mechanosensing into the surface organisation mechanism and downstream signalling.

F-actin intensities measured by confocal microscopy or flow cytometry suggest that WAS DCs contain less total polymerised actin. Taken together with the increased recovery rates of actin in FRAP, which suggest increased treadmilling and reduced stability, it is easy to see how a

deregulated, unstable actin network beneath the synapse would result in the poorer recruitment and concentration of MHC molecules seen in the bilayer experiments. This would be the case regardless of whether actin's role in synapse organisation involves retrograde flow, size exclusion or simply providing stability for membrane protein clusters.

The slower cSMAC formation seen in WAS DCs (Fig 4.14, 4.17, 4.18) might be expected to result in prolonged migration of microclusters through the pSMAC and thus increased signalling in the interacting T cell (Lee et al., 2003a, Ueda et al., 2011, Grakoui et al., 1999, Vardhana et al., 2010). It would be interesting to investigate this further by studying specifically phosphorylated proteins in the T cell activation pathway. An investigation of signalling on the DC side and the effects of slower cSMAC formation would also be beneficial.

Anti-MHCII bilayers did not induce podosome formation (Fig 4.14); instead half of control cells formed actin-rich dots at the centre of the synapse. It is unclear whether these are related to the podosomes seen on anti-ICAM-1 bilayers or why they appear only at later time points. Could these be the remnants of unsuccessful podosomes initially induced by inside-out integrin signalling during synapse formation?

The addition of anti-ICAM-1 alone was sufficient to induce podosomes, which is not as well described. It would be interesting to investigate the localisation of ICAM-1 itself in these structures; and also the specific necessity for ICAM-1 by testing whether podosomes form on bilayers targeting other ICAMs, integrins or costimulatory molecules.

Most of what is known about the lack of podosomes in the absence of WASp comes from studies of DCs or macrophages seeded on glass or fibronectin-coated coverslips (Linder and Kopp, 2005, Humphries et al., 2006, Monypenny et al., 2011, Linder et al., 1999). It is essential to note that lack of WASp abrogates podosome formation in a different adhesion setting, suggesting that it is crucial for the basic process of podosome formation rather than an upstream signal.

The presence of podosome-mediated adhesion in BL6 DCs may explain the larger contact surface measured on supported bilayers (Fig 4.18). It also supports previous observations using 3D EM reconstructions, which suggest that in a cell-cell system, BL6 DCs are able to induce much more extensive, intimate contacts (Fig 3.15 and 3.16). Protrusions from the DC into the T cell are quite commonly observed by EM. Although no prominent rings of these structures were noted during the EM imaging, these may be much more difficult to recognise in a cell-cell context compared to cell-bilayer interaction.

Podosomes shown here were confirmed using their basic morphology and staining for CD11a and capping protein. Stains for $\beta 2$ integrins and vinculin, which are normally used to characterise these structures (Linder and Kopp, 2005, Chou et al., 2006, Monypenny et al., 2011, Marchisio et al., 1987), were unsuccessful in several bilayer stains, though they rarely fail with fibronectin-bound cells. While this may reflect technical limitations specific to the bilayer set up, there is a possibility that podosomes formed at the synapse use a different array of actin binding and bundling proteins and adaptors. It would be interesting to further investigate the localisation of other adaptors and integrins, as well as the dependence of these podosomes on disassembly by calpain for correct dynamic organisation, as has been described in other cells (Calle et al., 2006b). Conversely, the presence of capping protein in migration-related podosomes has not been described; a recent paper showed no colocalisation of CapG to macrophage podosomes (De Clercq et al., 2013a). It would be interesting to see how this compares functionally with the colocalisation described here in synaptic podosomes.

The ring formation observed here is reminiscent of podosomes at the osteoclast interface with bone, which define the sealing zone (Babb et al., 1997, Destaing et al., 2003, Jurdic et al., 2006); with the exceptions of the pronounced outward ring expansion seen in osteoclasts at later time points. Whether formation of a fully functional sealing zone is dependent on podosomes is still under debate, though it has been suggested that podosomes evolve into a circular band of actin, which seals off the proteases secreted by actively resorbing osteoclasts

(Lakkakorpi et al., 1989, Vaananen et al., 2000). Similarly, although WAS DCs form some synapses, these are fewer and less organised and it would be interesting to investigate how their inability to form podosomes affects the function of the synapse.

Finally, it is interesting to highlight that podosomes have been shown in immature DCs and maturation is associated with a decrease in podosome-mediated adherence (Burns et al., 2004). DCs used for bilayer experiments were matured using LPS overnight and show characteristic maturation markers such as increased MHCII and CD80/86. This suggests maturation status may be less important for the formation of synaptic podosomes.

In summary, the decreased stability of the WAS DC actin cytoskeleton at the synapse interface results in smaller contacts, which are not as efficient in concentrating MHC molecules and show a less circular, symmetric organisation.

Chapter 5 – A disorganised immunological synapse is not sufficient for correct T cell activation

5.1 Introduction

The journey from a peripheral site of inflammation to the lymph node takes between 3-24 hours in humans (Macatonia et al., 1987, Cumberbatch and Kimber, 1992, Roake et al., 1995). During this, DCs process and present antigen (Banchereau and Steinman, 1998) and upregulate surface MHC-peptide complexes to allow optimal interaction with T cells (Sallusto and Lanzavecchia, 1994). The formation of a stable and functional IS is a crucial step in T cell activation as it allows recognition of antigen and other costimulatory molecules on the surface of the DC by rare T cell clones. It is important for the general lymphoproliferative response, but also for guiding CD4+ T cells to a suitable effector cell fate.

Results in previous chapters have shown that impaired actin polymerisation, caused by the loss of the actin regulator WASp, results in a malformed IS. This chapter aims to investigate whether this is sufficient to sustain intercellular signalling required for full T cell activation. T cell proliferation, surface marker expression (CD69) and IL-2 secretion were used as readouts of the DCs' ability to activate T cells.

As well as affecting signalling quantitatively, a malformed synapse may affect the quality of the message transduced to the T cell. Several groups have suggested that varying the strength of the contact, either through antigen dose or antigen affinity for TCR, can alter T helper differentiation (Hosken et al., 1995, Constant et al., 1995, Tao et al., 1997b) (see Introduction).

Data presented in the previous chapters has shown that WAS DC synapses are less stable, most likely due to incorrect actin and integrin organisation. How this affects T cell fate induction is investigated in this chapter using techniques including quantitative PCR, ELISA, microarray and in vivo models.

5.2 Results

5.2.1 CD69 upregulation

CD69 is a homodimeric cell surface protein and is one of the earliest markers of activation (reviewed in (Ziegler et al., 1994)). Previous work has shown that T cell activation results in rapid CD69 upregulation, with a peak around 8 hours post-stimulation, followed by decay and degradation. To test the ability of BL6 and WAS DCs to induce antigen-specific CD69 upregulation in T cells, DCs and T cells were cocultured overnight. DCs which were previously pulsed with either full OVA protein or the ova 323-339 peptide (class II epitope recognised by OT-II T cells) induced antigen-specific upregulation of CD69, compared to DCs pulsed with LPS only. No significant difference was observed between BL6 and WAS DCs in their ability to induce CD69 upregulation.

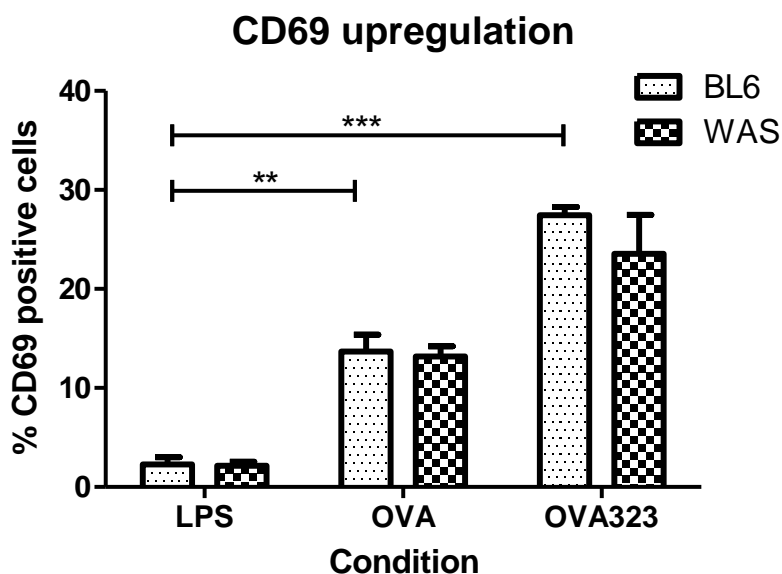


Figure 5.1 **No significant defect in CD69 upregulation in WAS DCs.** DCs were matured by overnight stimulation with LPS, with or without the addition of OVA or OVA323-339 antigen. 150 000 DCs were then cocultured with an equal number of T cells. CD69 expression was analysed 15hours later by flow cytometry (gating on the CD4 positive subpopulation). The graph represents mean values of 4 separate experiments. A t test was used to compare populations. *p = 0.01-0.05, **p = 0.001-0.01, *** p < 0.001

The ability of WAS DCs to induce normal CD69 upregulation in OT-II cells, despite IS malformation shown in the previous chapters, may be due to the pathways controlling CD69 expression. CD69 upregulation is a very early activation event, perhaps induced via TLR pathways and requiring very little stimulation. Flow cytometry analysis has shown that CD69 upregulation occurs even at low doses of antigen or short periods of stimulation (Caruso et al., 1997). Correct synapse formation may be unnecessary; the shorter, unstable and disorganised contacts formed with WAS DCs may be sufficient thus may not result in a functional defect in CD69 expression.

5.2.2 T cell proliferation

T cell proliferation induced by control and WAS DCs was also compared. LPS-matured DCs induce no proliferation (grey and black filled histograms), while OVA-pulsed DCs form antigen-specific contacts with OT-II cells and induce a large proliferative response (red and blue). There was no observable proliferation defect at a 1:1 cell ratio. At the 1:5 cell ratios, WAS DCs (red) consistently induced reduced antigen-specific proliferation in normal T cells compared to BL6. This was even more pronounced at lower DC: T cell ratios (1:8).

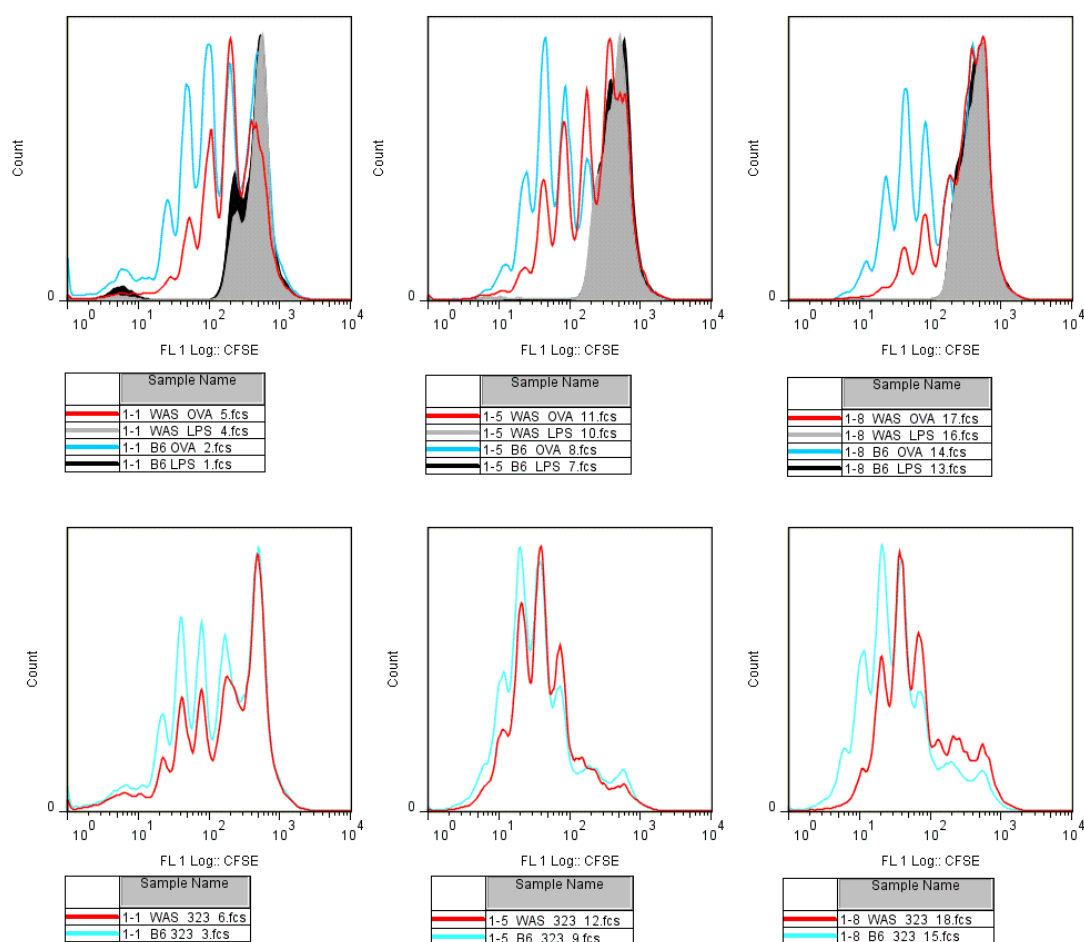


Figure 5.2 **Proliferation defect at lower levels of induction.** CD4⁺ OT-II cells stained with CFSE were mixed with dendritic cells at three different cell ratios of DC: T cells (1:1, 1:5 and 1:8). Cells were then co-cultured for 4 days, stained for CD3 and analysed on a CyAn ADP flow cytometer, gating on CD3⁺ cells only. Each peak represents a single cell division.

Proliferation ratios were calculated by dividing the number of daughter (proliferated) cells by the number of non-proliferated cells showing undiluted CFSE. This is quantified in Figure 5.3 Graph A. Due to large variation between experiments, the standard error means (SEM) appear very large and there was no significance between BL6 or WAS DC-induced T cell proliferation. The calculated ratios were then normalised relative to the BL6 OVA value of each respective experiment, effectively giving BL6 OVA a ratio of 1. Graph B shows the normalised results. Normalisation removed the variation arising from experimental differences and the significance of the different abilities of BL6 and WAS DCs to induce T cell proliferation becomes more apparent.

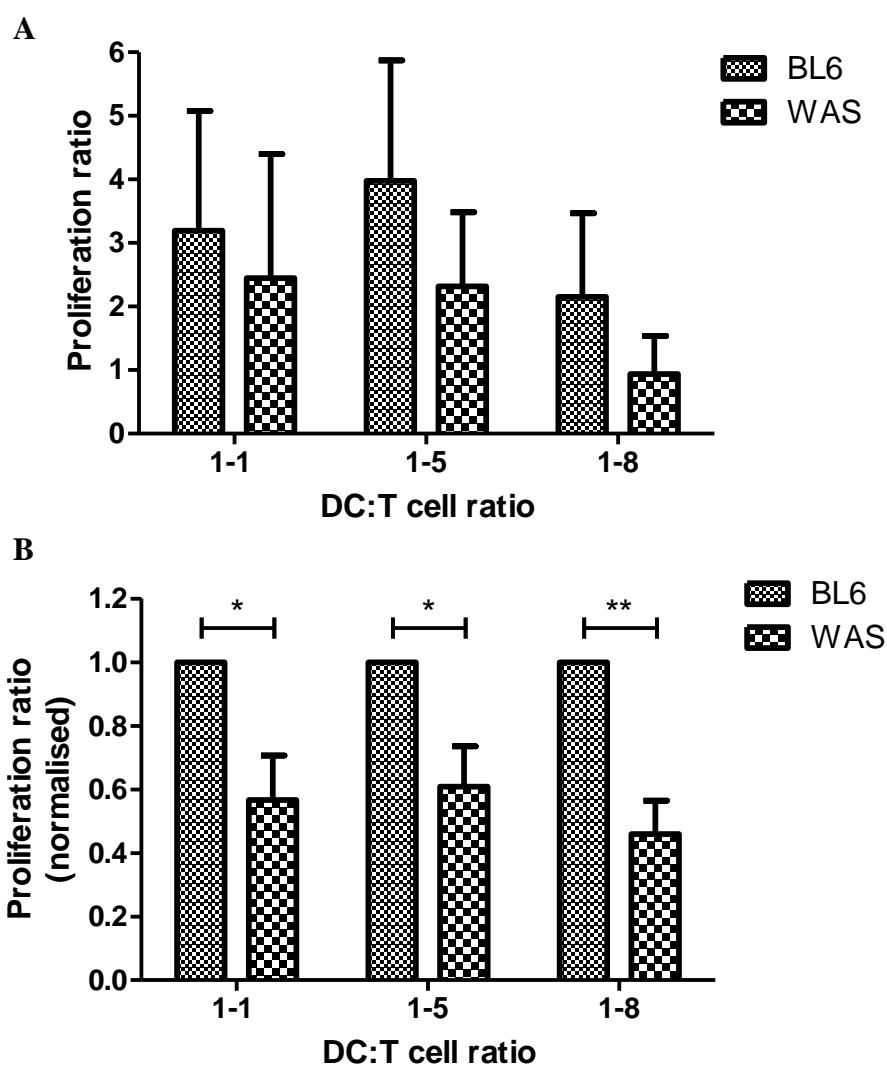


Figure 5.3 **Proliferation defect at lower levels of induction - normalised.** Top: Average and SEM of proliferation ratios (proliferated/non-proliferated cells). Bottom: proliferation ratios were divided by the BL6 OVA for each respective experiment to normalise. Results from 5 separate experiments were averaged. Significance was calculated using a paired t test. * $p = 0.01-0.05$, ** $p = 0.001-0.01$, *** $p < 0.001$.

5.2.3 IL-2 secretion

T cell activation also results in IL-2 production and secretion, which occurs later than CD69 upregulation and is necessary for T cell proliferation. WASp-deficient T cells exhibit reduced IL-2 production when induced by APCs (Cannon and Burkhardt, 2004). Here, IL-2 production was tested in normal T cells induced by either BL6 or WAS DCs.

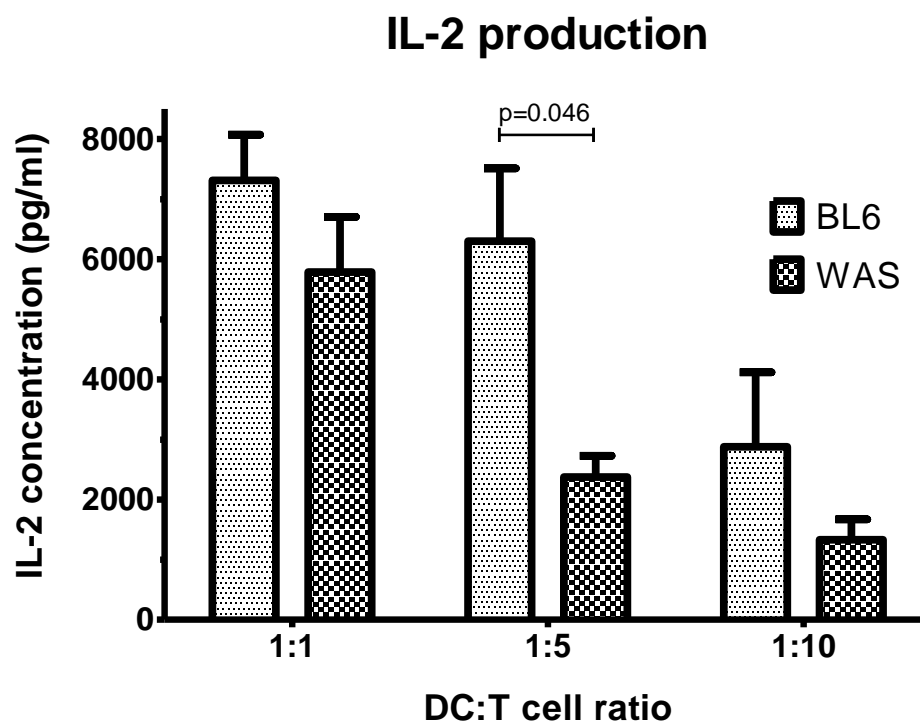


Figure 5.4 **Defective IL-2 production in T cells induced by WAS DCs.** IL-2 concentration in DC: T cells coculture supernatants was measured by ELISA 48hours after coculture. Each bar represents the average and SEM for 3 separate experiments, where IL-2 concentrations were measured in triplicate for each experiment. A two-tailed paired t-test was used to compare BL6 and WAS data sets for each cell ratio.

OT-II cells induced by WASp-deficient DCs do not achieve the same level of IL-2 production at any of the tested ratios. BL6 DCs appear to have sufficient inductive capacity to overcome a population stimulation threshold, achieving maximum IL-2 production even at lower DC: T cell ratio (1:5), although this is reduced at the lowest ratio (1:10). IL-2 production at this lowest ratio is comparable to WAS samples at the highest ratio, suggesting that even at a 10-times higher number, WAS DCs are incapable of producing enough signal to induce normal T cell activation.

5.2.4 QPCR

Factors such as strength of antigen-induced TCR signalling and costimulatory molecules present (Murphy and Reiner, 2002) may affect CD4 T cells differentiation into different subsets. As these factors may be affected by synaptic duration and organisation, it was interesting to investigate whether the abnormal synapses seen in WAS DC conjugates affect subsequent T cell differentiation. LPS-matured BL6 or WAS DCs were either pulsed with OVA or used without specific antigen in cocultures with OT-II T cells. Taqman murine gene expression assay were used in QPCR experiments designed to test for expression of the master regulators of the 4 major T helper cell subtypes- Tbx21 (Th1), GATA3 (Th2), FoxP3 (Treg) and Rorc (Th17). Due to variation between experiments and thus large standard error means, the differences observed were not statistically significant. Further, fold changes calculated for FoxP3 and Rorc were very low. Several refinements of the experimental design, discussed later, may result in a more accurate and sensitive assay.

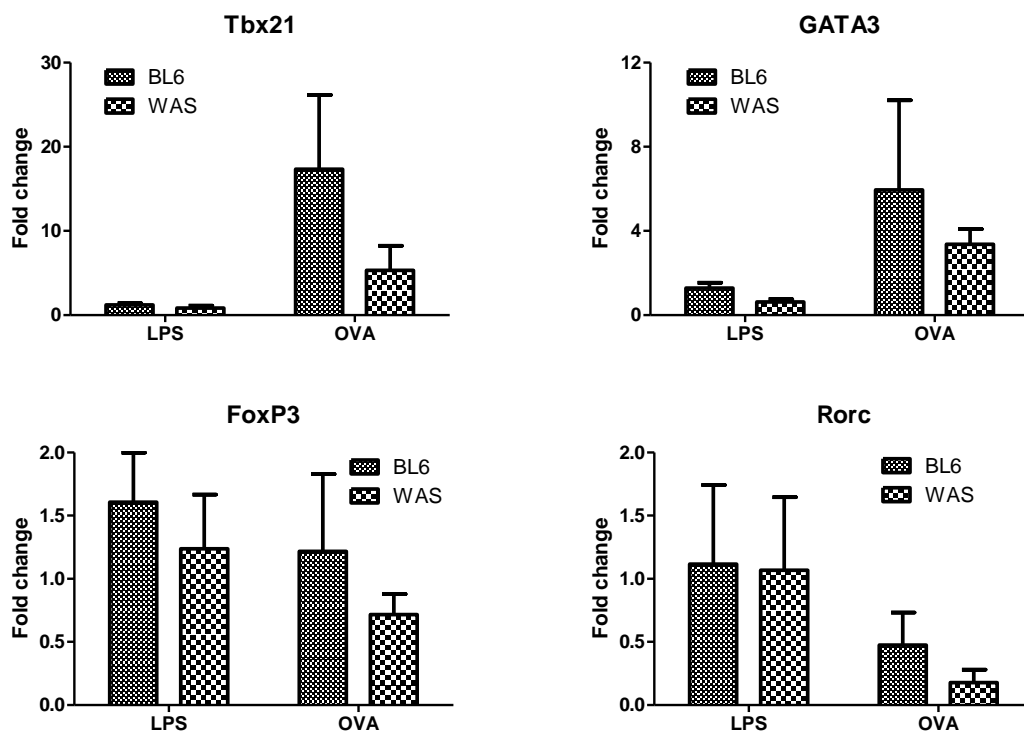


Figure 5.5 **T cell fate master regulators**. DCs and T cells were cocultured at a cell ratio of 1:5 for 48hrs. T cells were then purified using a murine CD4 isolation kit. Total mRNA was isolated, reverse transcribed and used, in triplicate, for real-time quantitative PCR. Replicate values were averaged; and results were normalised to murine GAPDH expression using $\Delta\Delta CT$ calculation (see Materials and Methods). Fold difference presented here shows mean and SEM from 4 separate experiments calculated relative to BL6 LPS value of each.

5.2.5 Cytokine ELISA

The supernatants from cocultures used for mRNA isolation (i.e. 48hrs after DC: T cell cocultures in 96-well plate) were used to determine the amount of different cytokines secreted by ELISA. Tbx21 has been shown to promote IFN γ production (Szabo et al., 2000), which in turn induces further Tbx21 expression (Lighvani et al., 2001), making IFN γ a suitable readout of Th1 differentiation. IFN γ has also been shown to express Th2 differentiation (Seder et al., 1992). Conversely, IL-4 signals through STAT6 to promote Th2 differentiation (Shimoda et al., 1996, Takeda et al., 1996, Kaplan et al., 1996). The anti-inflammatory cytokine IL-10 has also been shown to promote Th2 responses and inhibit Th1; it has been shown to promote IL-4 expression, and may itself be upregulated by IL-4 (Faith et al., 2012, Kosaka et al., 2011, Laouini et al., 2003, Moore et al., 2001, Schmidt-Weber et al., 1999). Th17 cells were identified as a subset of T helper cells which produce IL-17 (Park et al., 2005, Harrington et al., 2005, Bettelli et al., 2007). The graphs below show concentrations of these cytokines found in coculture supernatants.

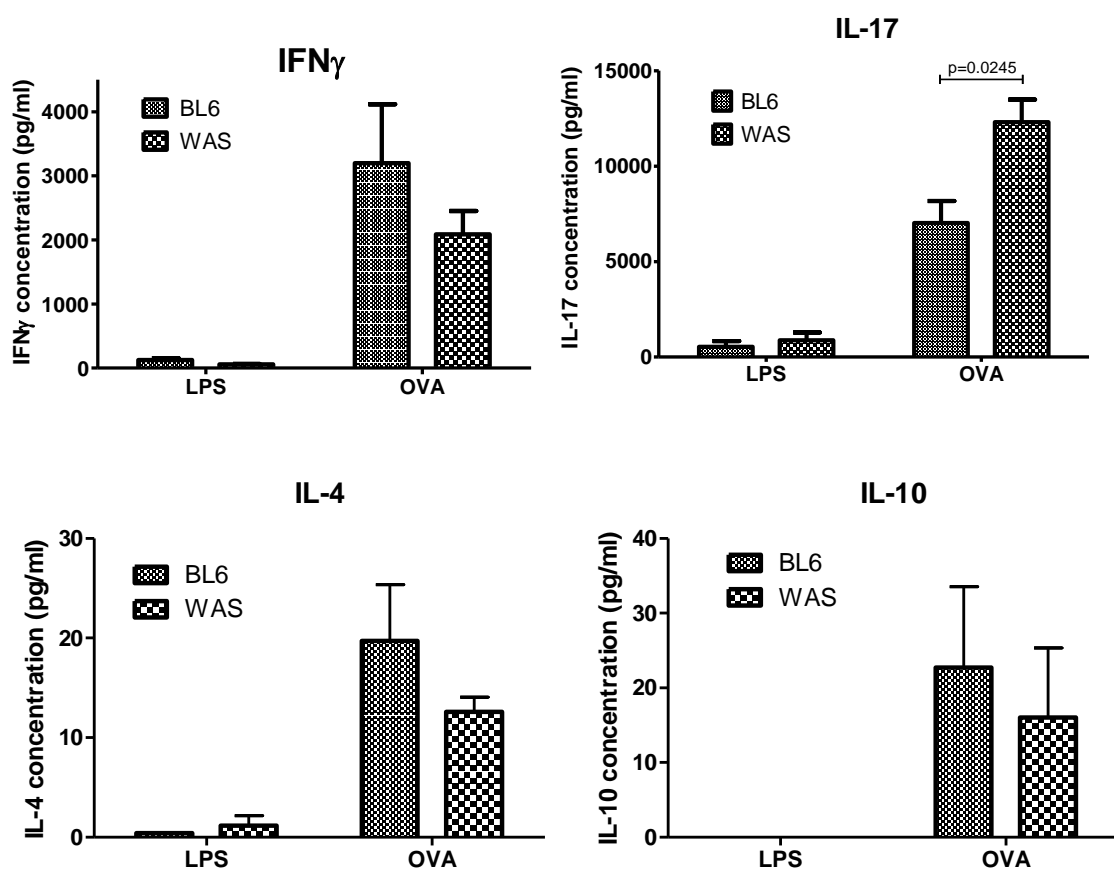


Figure 5.6 (previous page) **T helper cell cytokines.** Supernatants from DC: T cell cocultures were tested for the above cytokines using R&D systems ELISA kits. Concentrations were calculated using cytokine standard curves as per manufacturer's instructions. Samples were tested in triplicate and the graphs represent mean and SEM from 4 separate experiments. A paired t test was used to calculate significance.

Production or secretion of all cytokines was upregulated upon antigen-specific stimulation (OVA DCs) compared to LPS-only DCs. This suggests DCs are able to activate antigen-specific T cells in this in vitro model. Similar to Tbx21 expression, IFN γ production was reduced in T cells stimulated by WAS DCs compared to BL6; although the difference was not significant. GATA3, IL-4 and IL-10 presented a similar pattern, though again not statistically significant. Interestingly, while the Rorc signal was too low to detect any differences reliably, IL-17 showed robust, reproducible upregulation and this was significantly higher upon WAS DC-induced stimulation compared to control.

As OT-II cells were harvested from the same mice for coculture with both types of DCs, there is no genetic or environmental difference arising from these cells that would influence cytokine secretion or transcription factor expression. Any differences seen are likely to be the result of different stimulation by the DCs.

5.2.6 In vivo T cell fate induction

Trends seen in vitro, may combine in vivo to produce a more severe defect in cytokine secretion through their feedback loops and effects on other cell types. To test this, a DC adoptive transfer experiment was designed to investigate the ability of antigen-specific BL6 and WAS DCs to induce T cell activation and differentiation in vivo.

DCs were matured with LPS or pulsed with or without OVA to induce antigen presentation. 15hours later DCs were labelled with CFSE and 4×10^6 labelled cells were injected into the tail vein of OT-II mice. Two days after injection, mice were sacrificed and CD4⁺ cells were isolated from spleen and lymph nodes. CD4⁺ cells were incubated in PMA, ionomycin and brefeldin A for 5hours. Cells were washed and stained for several cytokines and analysed by flow cytometry.

Previous studies have shown impaired migration of WAS Langerhans cells or DCs, in vitro and in vivo, using methods such as skin painting and subcutaneous injections (Snapper et al., 2005, de Noronha et al., 2005, Bouma et al., 2007). To avoid confounding influences of poor DC migration on T cell activation, DC migration to spleen and lymph nodes was tested following i.v. injection. Aliquots of the spleen and lymph node cell suspensions were used to estimate efficiency of DC migration by quantifying CFSE-positive cells. Cell suspensions were stained for CD11c to select for DCs. Gating on CD11c-positive cells, CFSE-positive cells were quantified. Figure 5.7 shows DCs present in spleen (top) and lymph nodes (bottom). CFSE positive cells were low as a percentage of the total number of DCs, but were easily detected. Their presence was also confirmed by allowing cell suspensions to settle in culture dishes and checking for bright CFSE cells on a fluorescent microscope. Similar numbers were found in OT-II mice injected with either BL6 or WAS DCs, suggesting that abnormal migration in WAS DC would not distort differences in T cell activation in these experiments.

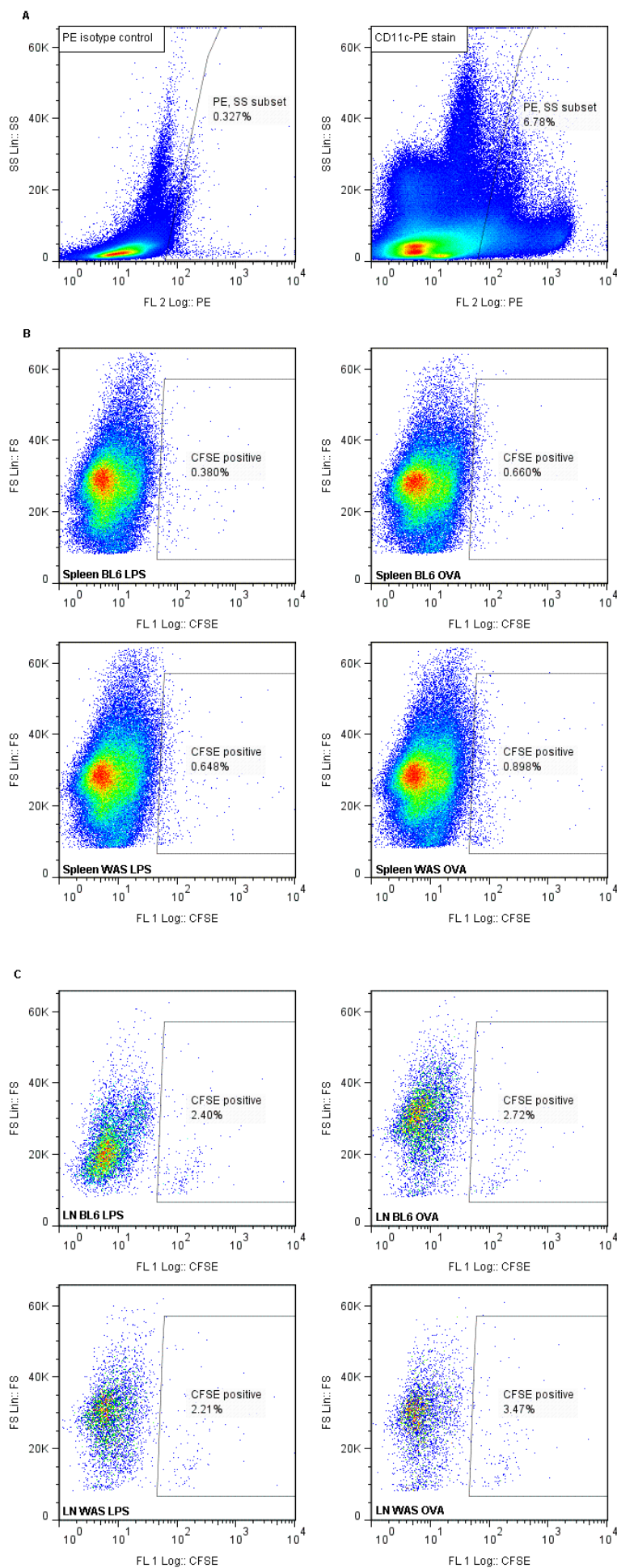
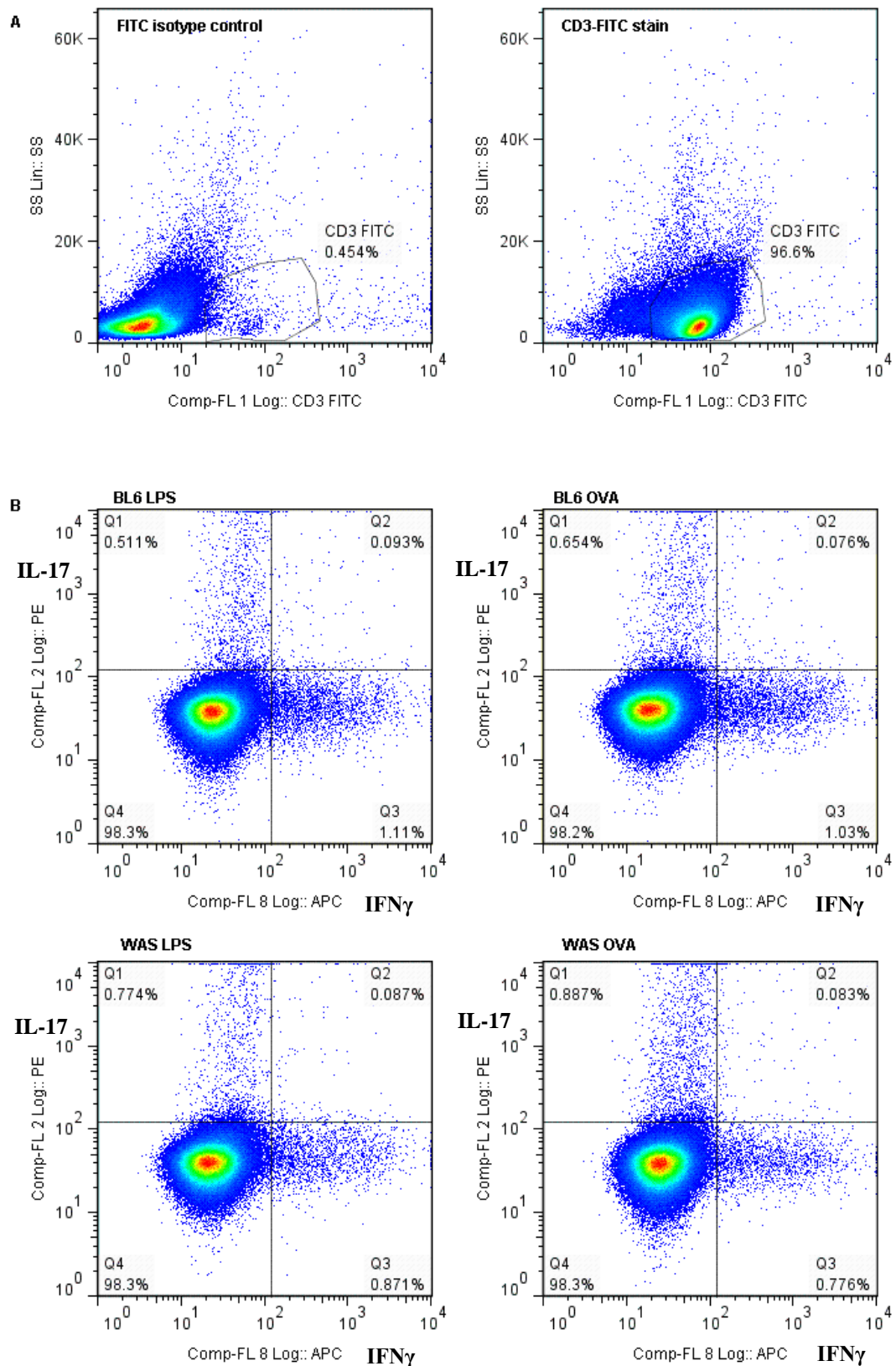


Figure 5.7 No significant difference in migration between BL6 and WAS DCs following IV injection. BL6 or WAS DCs were pulsed with LPS or LPS/OVA and stained with CFSE. The cells were injected i.v. into OT-II recipient mice. Two days post injection, cell suspensions from spleens and lymph nodes (LN) were immunostained for with anti-CD11c-PE and analysed by flow cytometry. Samples were gated for CD11c (A) and analysed for the presence of CFSE-positive cells in spleen (B) and lymph nodes (C).

Spleen and lymph node cell suspensions were mixed prior to T cell isolation. After the secondary stimulation (described above and in section 2.2.10), T cells were stained with fluorophore-conjugated antibodies CD3-FITC and either IL4-PE + IL-10-APC or IFN γ -APC + IL-17-PE. The CD3-FITC positive gate, in Figure 5.9A, shows that compared to an isotype control (left), CD3-FITC staining suggests that efficient T cell isolation was achieved, reaching over 96% of CD3 positive cells. These were gated on and analysed for cytokine expression. Figure 5.9B shows IFN γ (x-axis) and IL-17 (y-axis). Quadrant gates were set according to isotype control stains. Results suggest a slight decrease in IFN γ and increase in IL-17 in OT-II mice injected with WAS DCs compared to BL6 DCs. Although not significant, the differences were seen across all mice in this experiment. These supported the IFN γ and IL-17 results seen with cytokine ELISA analysis of in vitro cocultures (Fig 5.6).

Isotype controls for IL-4 and IL-10 showed higher than expected staining, making it difficult to set gates on positive cells. These were instead presented as histograms (Figure 5.9). No significant differences were seen between WAS and BL6 DC injections. Further, there was very little difference between the LPS and LPS+OVA conditions, suggesting either a technical error in the staining process or that OVA does not elicit a Th2 response in vivo.



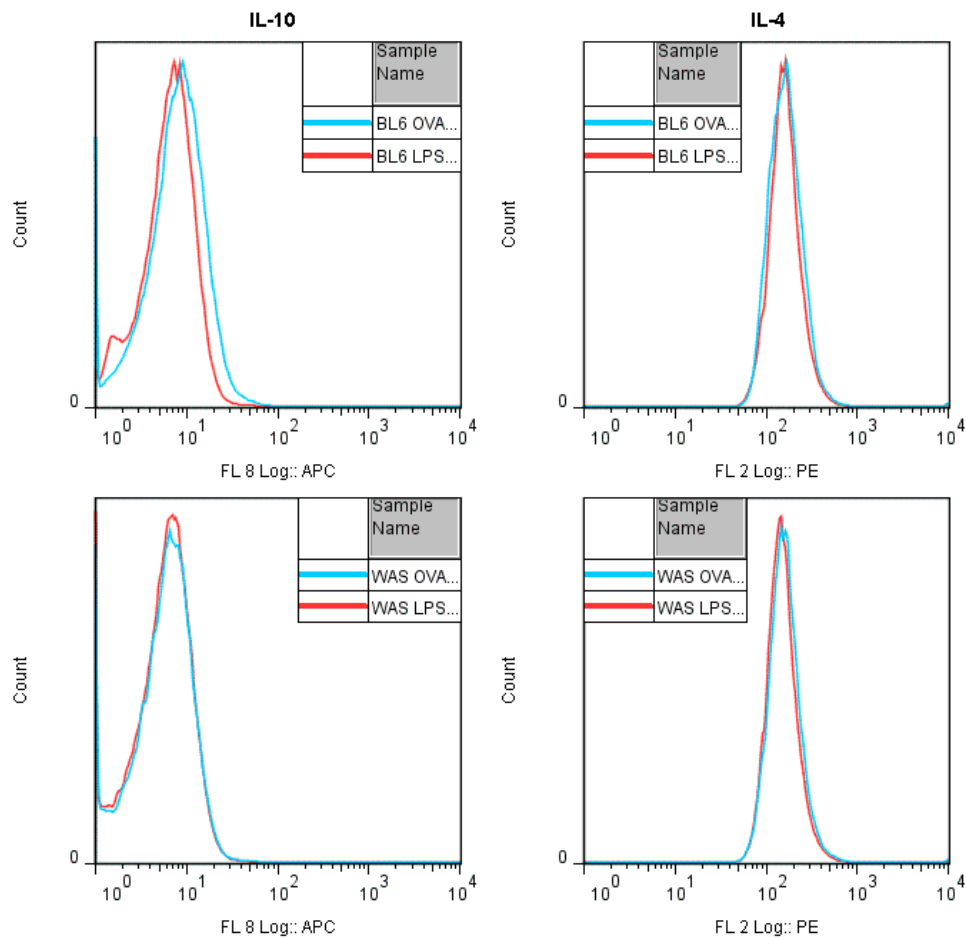


Figure 5.9 **IL-4 and IL-10 immunostaining**. Two days after DC i.v. injection, OT-II recipients were sacrificed and total CD4⁺ T cells were isolated using a Miltenyi Mouse CD4 T cell isolation kit and a secondary stimulation was performed in PMA, ionomycin and brefeldin A. T cells were stained for CD3 (FITC), IL-10 (APC) and IL-4 (PE). CD3-positive cells were gated on and histograms show IL-10 and IL-4 staining within the CD3 gate.

5.2.7 Microarray analysis

The data so far shows interesting trends though differences in T cell fate induction have been difficult to replicate, suggesting the responses involved may be more heterogeneous than expected. This led to the hypothesis that detecting differences in master regulators may not be sufficient to characterise such a complex immune response. Analysis of complete pathways should be more suited to this. Microarray analysis was chosen in order to build a more complete picture.

Similar to QPCR experiments described above, 48hour DC: T cell cocultures were split using a Miltenyi CD4 Isolation kit and RNA was isolation from the T cell fraction as described in section 2.2.8 of Materials and Methods. To check for potential RNA degradation or DNA contamination, samples were analysed on a Bioanalyser. This evaluates both RNA concentration and integrity. High quality RNA samples should show two strong peaks for the 18S and 28S ribosomal RNA with few low molecular weight peaks. Ideally, the 28S:18S ratio should be around 2 and the RNA Integrity Number (RIN) should be above 7. A representative electropherogram of BL6 OVA sample 1 (BO1) is shown in Figure 5.10. Any samples of poor quality or concentration were repeated, together with corresponding controls.

Samples were hybridised to an Affimetrix GeneChip Mouse Genome 2.0 Array. Data was imported into GeneSpring, where results were averaged for each condition and fold change analysis was performed (in collaboration with UCL Genomics facility). Fold change (FC) was calculated between pairs of data sets; gene lists were created of genes exhibiting a $FC \geq 1.3$ at significance level of $p \leq 0.05$. The number of genes differentially regulated to this level between different pairs of data sets are summarised in table 5.1 and presented as Venn diagrams in Figure 5.11.

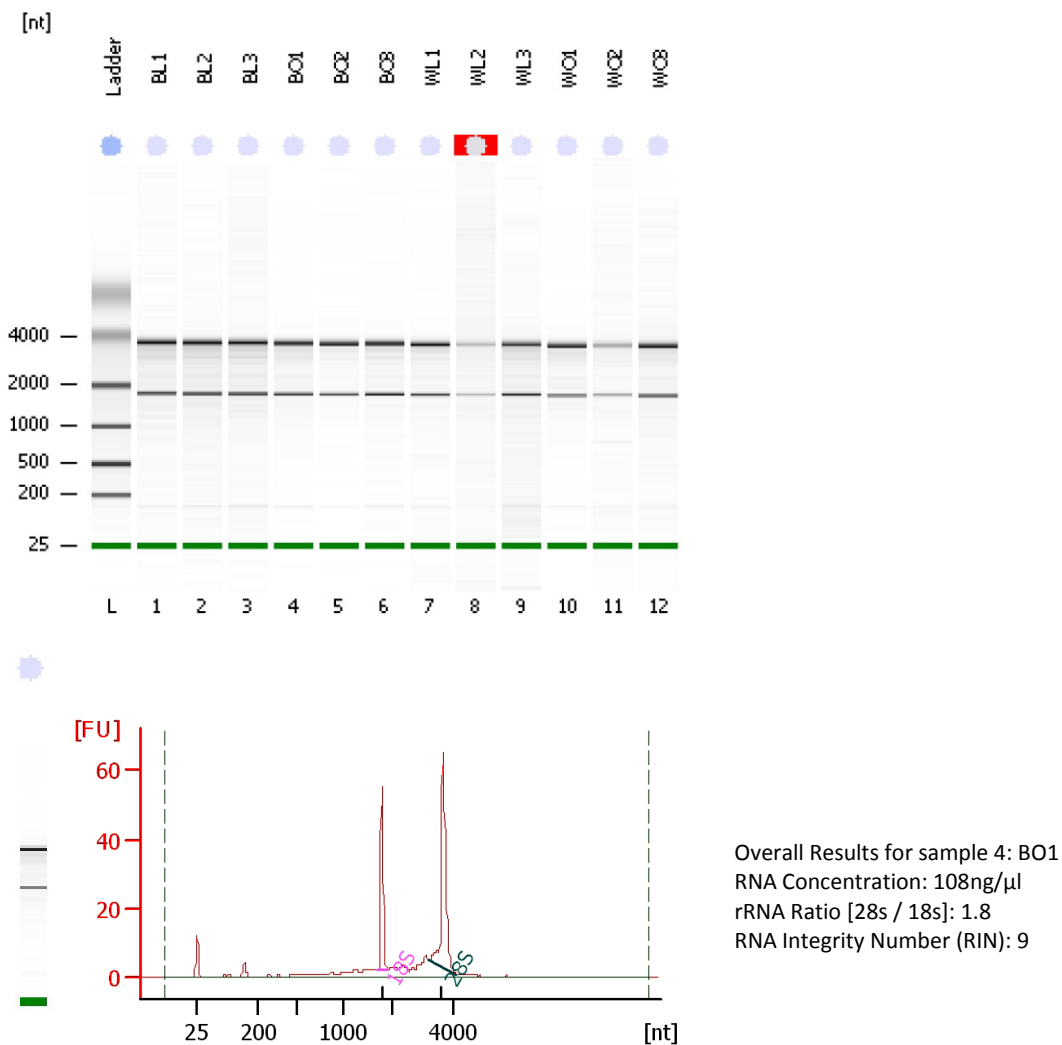


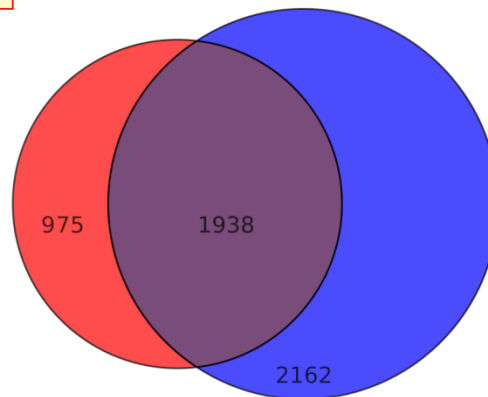
Figure 5.10 **Electropherograms of RNA samples.** RNA quality was analysed on 2100 Bioanalyser. Electropherograms are shown above with a summary of a representative sample BO1. Distinct 18s and 28s ribosomal RNA peaks can be seen.

Table 5.1

Data set pair	No of genes above cut off: FC1.3, p0.05
BOvsBL	2913
WOvsWL	4100
WLvsBL	113
WOvsBO	415

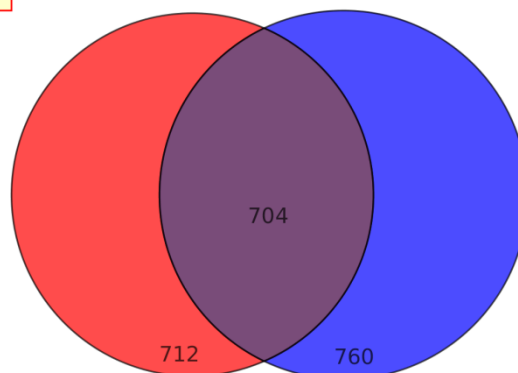
Entity List 1 : T Test
unpaired [BO] Vs [BL] P
<= 0.05 FC >=1.3
2913 entities

Entity List 2 : T Test
unpaired [WO] Vs [WL] P
<= 0.05 FC >=1.3
4100 entities



Entity List 1 : DOWN - FC
([BO] vs [BL])
1416 entities

Entity List 2 : DOWN - FC
([WO] vs [WL])
1464 entities



Entity List 1 : UP - FC ([BO]
vs [BL])
1497 entities

Entity List 2 : UP - FC
([WO] vs [WL])
2636 entities

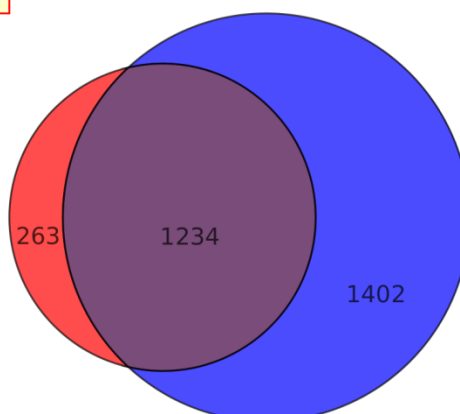


Figure 5.11 **Differentially regulated genes**. Genes which show a change (top), downregulation (middle) or upregulation (bottom) at fold change (FC) ≥ 1.3 with p value ≤ 0.05 . Genes differentially regulated in BL6 OVA (BO) compared to BL6 LPS (BL) samples are indicated in red; WAS OVA (WO) compared to WAS LPS (WL) are in blue.

Figure 5.11 compares the differences in gene lists summarised in Table 5.1. There are 2913 differentially expressed genes in BO compared to BL; and 4100 in WO compared to WL. The top Venn diagram in Figure 5.11 compares these two lists to illustrate that 1938 genes are shared, however there are differences in transcriptional regulation between antigen-specific stimulation by BL6 or WAS DCs. Of the 975 differentially regulated genes in BOvsBL, the majority (712) are downregulated (middle Venn diagram); while in WOvsWL, around two thirds of the differentially regulated genes (2162) are upregulated (bottom Venn diagram). Further, a Venn diagram comparing WLvsBL and WOvsBO clearly illustrates there is a larger difference in transcription upon OVA stimulation, confirming an antigen-specific response (Fig 5.12).

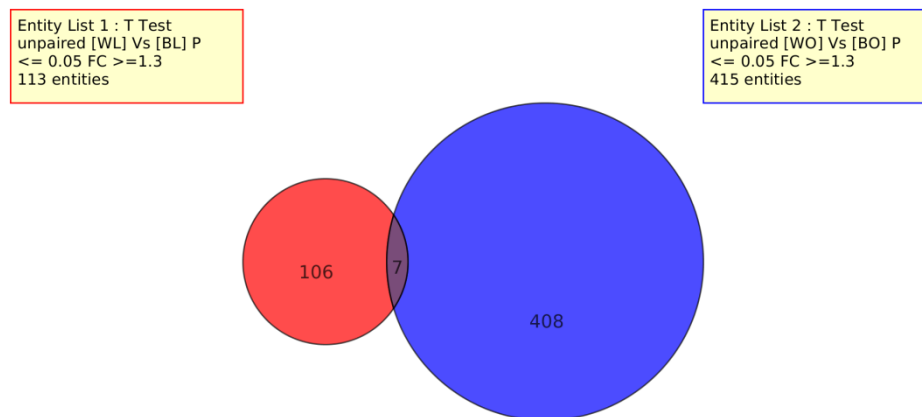


Figure 5.12 **Differentially regulated genes – antigen-specific response.** Venn diagram shows a comparison of total number of differentially regulated genes in WLvsBL compared to WOvsBO.

Gene lists (with FC values) were imported into Ingenuity Pathway Analysis (IPA) software. Differences between LPS and LPS/OVA samples mapped to several canonical pathways such as Cell Cycle Progression, EIF2 signalling and tRNA charging, confirming predicted increases in transcription, translation and proliferation upon antigen-specific T cell activation.

Comparison between BL6 and WAS showed some differences in protein ubiquitination and DNA double strand break repair pathways; however, for the purpose of this investigation, one pathway was selected for further examination – T helper cell differentiation. This is shown for BOvsBL and WOvsWL in Figure 5.13.

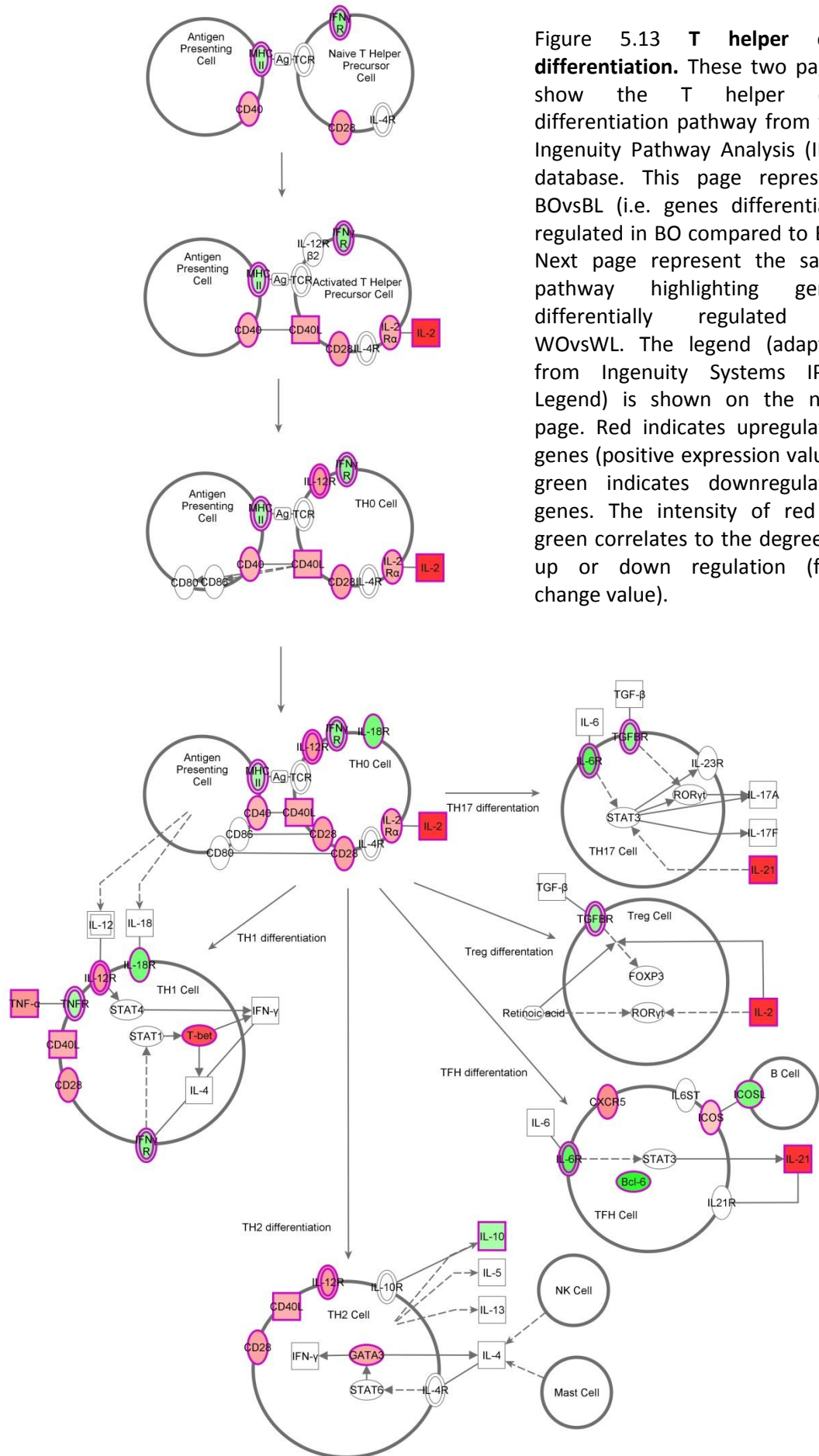
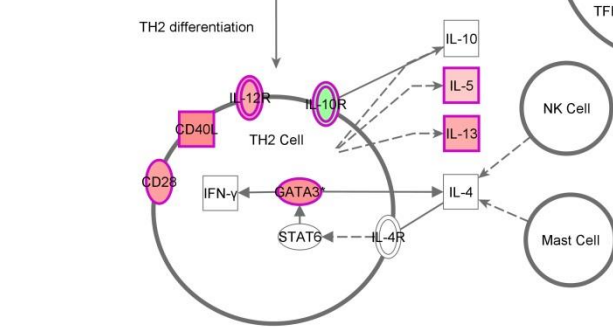
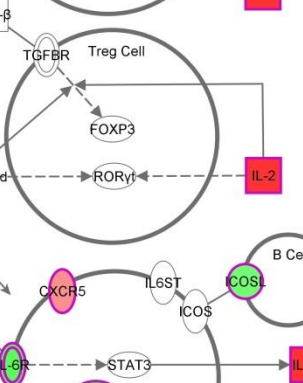
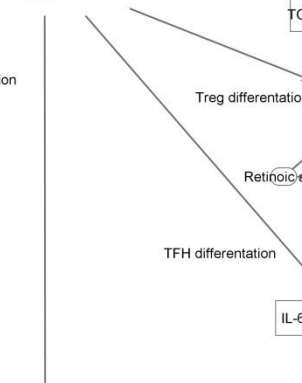
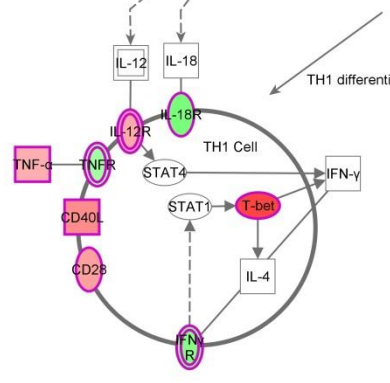
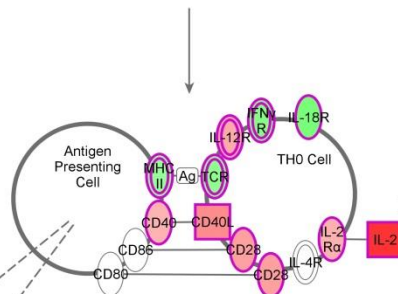
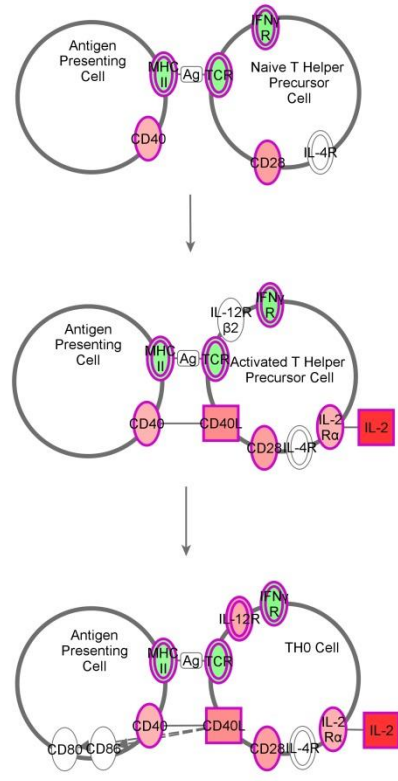


Figure 5.13 T helper cell differentiation. These two pages show the T helper cell differentiation pathway from the Ingenuity Pathway Analysis (IPA) database. This page represent BOvsBL (i.e. genes differentially regulated in BO compared to BL). Next page represent the same pathway highlighting genes differentially regulated in WOvsWL. The legend (adapted from Ingenuity Systems IPA8 Legend) is shown on the next page. Red indicates upregulated genes (positive expression value); green indicates downregulated genes. The intensity of red or green correlates to the degree of up or down regulation (fold change value).

T Helper Cell Differentiation



Network Shapes

- Cytokine
- ▤ Growth Factor
- ▭ Chemical / Drug / Toxicant
- ◇ Enzyme
- ▭ G-protein Coupled Receptor
- ▤ Ion Channel
- ▽ Kinase
- ▭ Ligand-dependent Nuclear Receptor
- ◇ Peptidase
- △ Phosphatase
- Transcription Regulator
- Translation Regulator
- Transmembrane Receptor
- ▽ Transporter
- ▽ microRNA
- Complex / Group
- Other

Relationships

- (A) — binding only — (B)
- (A) — inhibits — (B)
- (A) — acts on —> (B)
- (A) — inhibits AND acts on —> (B)
- (A) — leads to — (B)
- (A) — translocates to — (B)
- (A) — reaction —> (B)
- (A) — enzyme catalysis —> (B)
- (A) — reaction —> (B)

— direct interaction
- - - indirect interaction

Note: "Acts on" and "inhibits" edges may also include a binding event.

Several differences can be seen by comparing OVA responses from each cell type to their corresponding LPS only. For example, in BL6 there is upregulation of TNF α , and ICOS, which are either not present or are lower in the WAS response. ICOS (Inducible T cell costimulator) is upregulated in activated T cells and has been implicated in Th2 and TFH (follicular T helper cells) differentiation (Hutloff et al., 1999, Dong et al., 2001, Rudd and Schneider, 2003). It may also be important in initiating Th1 and Th2 responses in memory CD4 T cells (Khayyamian et al., 2002). Conversely, in WAS there is an increase in IL-5 and IL-13 cytokines, characteristic of a Th2 response (Mosmann et al., 2005, Wynn, 2003); and a small increase in IL-21, which is implicated in the development of T follicular and Th17 cells (Chtanova et al., 2004, Wei et al., 2007a).

The differences described above are seen in 'normalised' antigen-specific responses, where BL6 and WAS OVA DC induction of T cells is expressed in the context of their respective LPS only DC induction. Thus, any differences between BL6 and WAS which are present in both LPS and LPS/OVA conditions are overlooked. The largest interleukin difference however, was observed in a comparison between WLvsBL and WOVsBO. IL-12 showed significantly decreased expression in WAS compared to BL6 in both antigen-specific and LPS only conditions, with a FC of -2.08 (Fig 5.14). IL-12 is involved in the differentiation of Th1 cells (Hsieh et al., 1993) and may have a role in preventing food allergies (Ternblay et al., 2007). This result confirms previous observations of reduced IL-12 in WAS DCs by flow cytometry (Bouma et al., 2011). Another report also provided evidence for the requirement of the WASp-activator Cdc42 in polarised IL-12 secretion and immune synapse formation (Pulecio et al., 2010).

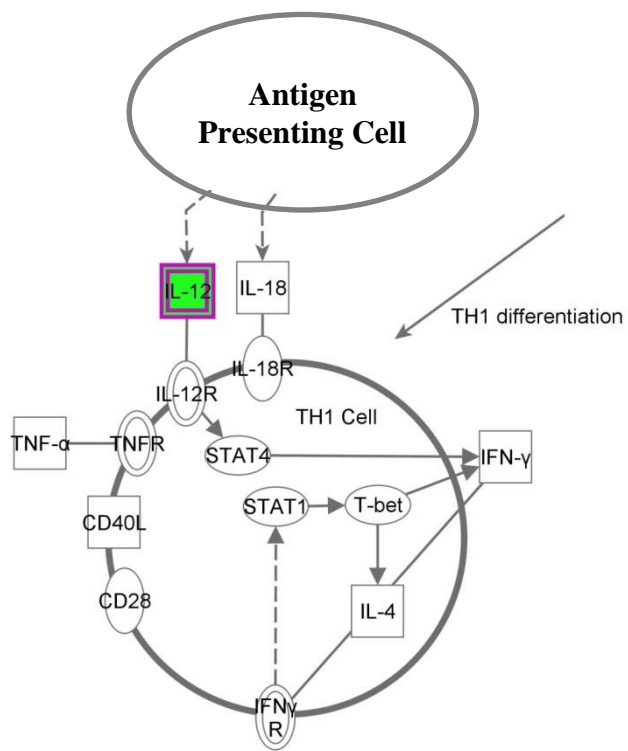


Figure 5.14 **T helper cell differentiation - WOsvsBO**. Part of the pathway in Fig 5.13, this pathway shows Th1 differentiation induced by an APC. Green indicates downregulated genes in WO compared to BO.

5.2.8 DC conditional WAS knockout model

To investigate the specific role of WASp in DCs, a cre-lox conditional WASp knockout mouse strain was created lacking WASp specifically in CD11c-positive cells (Baptista *et al*, manuscript submitted). WASp, flanked by LoxP sites, was removed by crossing animals with a CD11c-cre strain. This model can be used to study the role of DCs, and in particular their actin cytoskeleton, in several *in vivo* experiments. One of the clinical characteristics of WAS is autoimmunity and autoantibodies are present in both patients and WAS knockout mice (Schurman and Candotti, 2003, Nikolov *et al.*, 2010).

To test whether DCs play a role in the development of this autoimmunity, serum was collected from 25-week old mice and an autoantibody array chip was used to detect IgG and IgM isotype antibodies against 73 different autoantigens, as previously described (Ternblay *et al.*, 2007). Results are shown in Figure 5.15. Serum from the DC conditional WAS KO (DCcWKO) showed autoimmune responses, similar to WAS for IgG, and less severe for IgM though significantly higher than normal BL6. Particularly striking is the response to single- and double-stranded DNA (ssDNA and dsDNA). This suggests there may be a difference in plasmacytoid DC (PDC) responses, which express toll-like receptors (TLRs), specific in particular for ssDNA. Further investigation is required; however, this idea would support recent findings in the group using an LCMV infection model, which highlighted a defect in PDCs' ability to produce IFN α (K Lang, A Thrasher, personal communication).

The difference in IgG and IgM levels is also interesting. Different conditional WAS KO models show slightly different IgG and IgM patterns, for example, WAS KO specifically in Treg cells shows a less severe autoantibody response, with higher readouts for IgG than IgM (L Notarangelo, personal communication). This may reflect perturbations in a delicate balance, which would normally control B cell subtype polarisation, similar to T helper cell fluctuations. Thus, differences in antibody subsets produced during autoimmunity in different models may

be a read out of altered cytokine milieu. This assay highlighted the involvement of WAS and actin regulation specifically in DCs in preventing autoimmune disease.

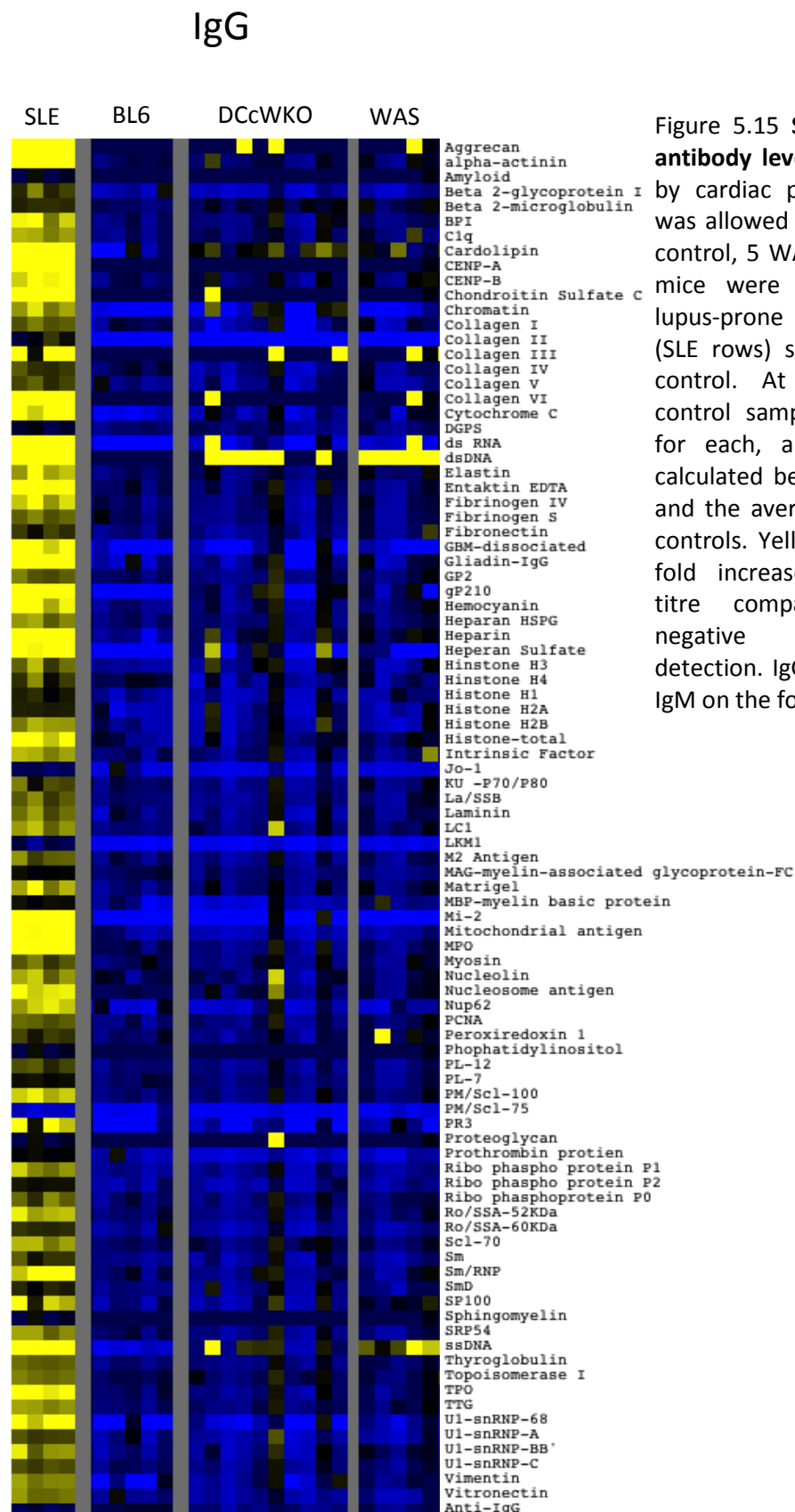
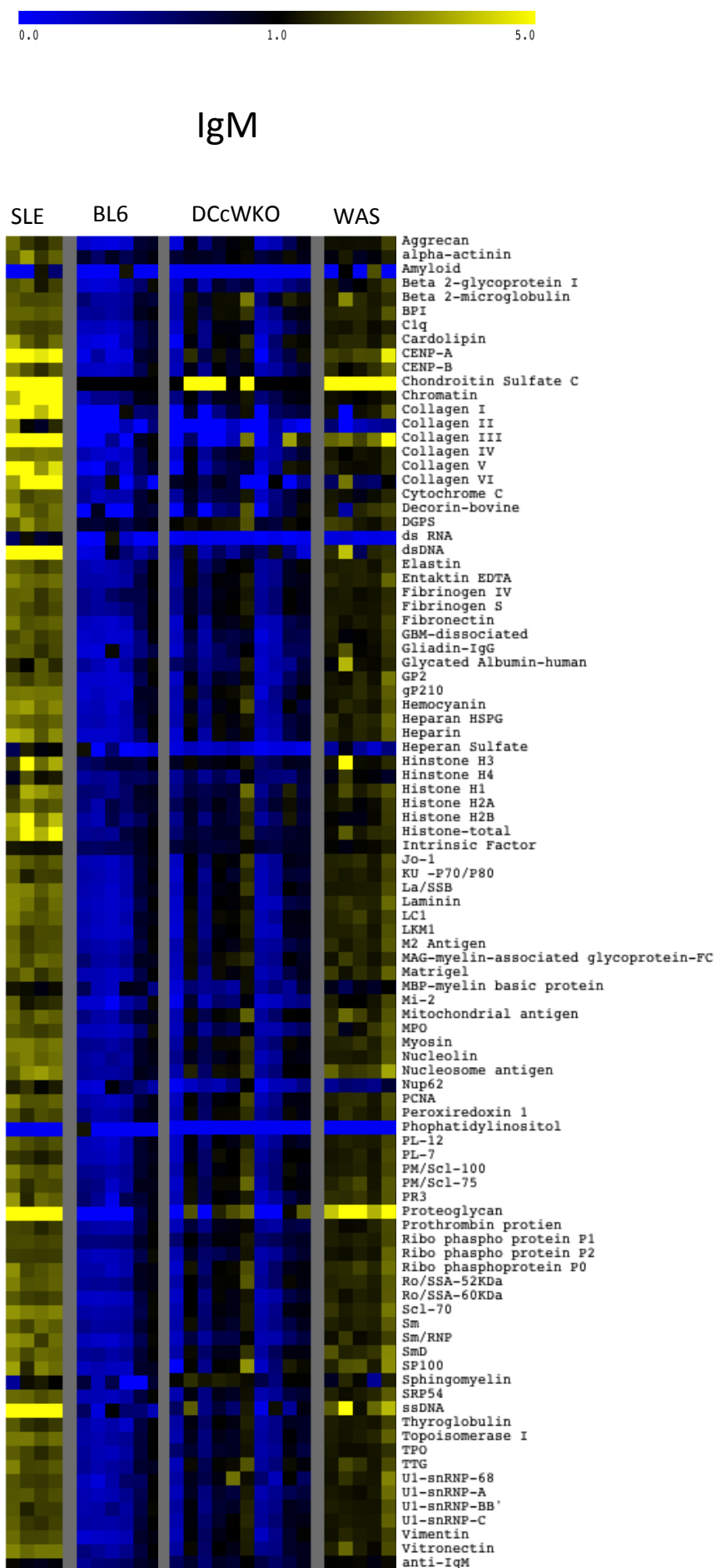


Figure 5.15 **Serum autoimmune antibody levels.** Mice were bled by cardiac puncture and blood was allowed to clot. Sera from 4 control, 5 WAS, and 10 DCcWKO mice were tested. Sera from lupus-prone MRL/NZM mouse (SLE rows) served as a positive control. At least 3 negative control samples were averaged for each, antigen ratios were calculated between each sample and the average of the negative controls. Yellow indicates a five-fold increase of autoantibody titre compared to average negative control sample detection. IgG is presented here, IgM on the following page.



5.2.9 Dynabead IP assay

In order to unravel the molecular pathway involved, an assay was developed using magnetic beads coated with anti-MHC class II and anti-ICAM-1. These were designed to mimic DC interaction with an antigen-specific primary T cell, using antibodies tested in bilayer experiments in Chapter 4. The model was validated by analysing cell-bead interactions by confocal microscopy.

As seen in Figure 5.16, BL6 DCs show a regular actin cytoskeleton around the cell cortex and an actin ring at the bead contact area, with an actin-free area in the centre. In contrast, WAS DCs exhibit abnormal, disorganised actin polymerisation. The frequency of normal cortical actin staining is quantified showing a significant reduction in WAS DCs ($p=0.0154$).

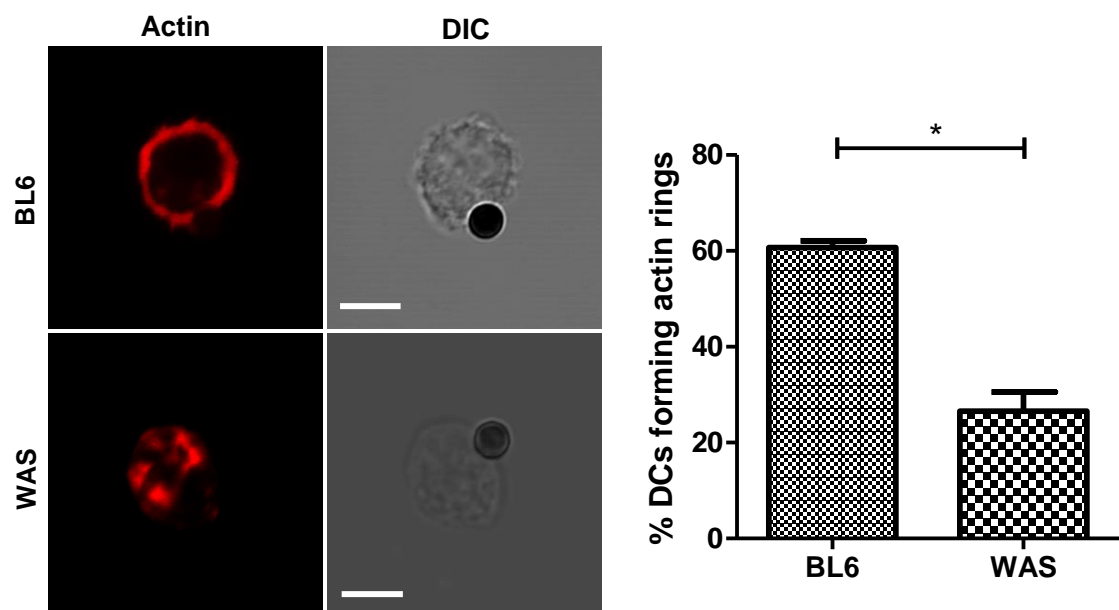


Figure 5.16 **Magnetic bead model.** DCs were incubated with beads coated with anti-MHCII and anti-ICAM-1 for 30min. The cell-bead suspension was resuspended gently and added to poly-L-lysine coated slides. These were fixed, stained using phalloidin-633 and analysed by confocal microscopy. Percentages of DCs showing actin rings beneath the bead were converted into arcsin values and a t test was performed. A minimum of 80 cells were examined in each of two experiments. * $p=0.0154$ Scale bars = $5\mu\text{m}$.

As the beads revealed a defect in actin organisation in WAS DCs, it was agreed they provided a reasonable model to replicate the defect seen in synapse formation. A further advantage of the bead model is the ability to isolate the interacting cells using a magnet; to lyse these and perform immunoprecipitation assays.

The first row in Fig 5.16 shows strong, specific pull down of WASp in IP samples compared to its level in whole cell lysates (around 63kDa). The second row however, highlights the presence of N-WASp in all samples (similar size). This does not seem to be specifically concentrated in IP samples, suggesting the α -WASp antibody used for IP has a higher affinity for WASp than N-WASp and is able to concentrate WASp to a greater extent. The presence of N-WASp however is worrying due to its homology with WASp and the overlap in interacting proteins. It would be difficult to distinguish between protein populations interacting with one or the other actin nucleator. For example, Nck (~47kDa), in the bottom panel, shows stronger pull down in BL6 compared to WAS samples, however it has also been described to interact with N-WASp (Donnelly et al., 2013) (and is present in WAS IP samples below), suggesting that the IP is not detecting synapse-specific interactions. It is possible that N-WASp may be recruited to the synapse, which may be able to bind some Nck, although not to the same level as BL6. However, the differences seen so far in IS structure, actin dynamics and function suggest N-WASp is unable to compensate for the lack of functional WASp.

WIP has recently been shown to link Nck and N-WASp during actin polymerisation (Donnelly et al., 2013); however, WIP does not appear to interact with WASp and N-WASp in the same way. It has been shown that WIP protects WASp from degradation as knockdown or overexpression of WIP results in decreased or increased levels of WASp respectively (Chou et al., 2006, Worth et al., 2013). This has not been seen for N-WASp (de la Fuente et al., 2007). IP samples probed for WIP, in Fig 5.16, show WIP (third panel; ~55kDa) interacts with WASp in BL6 cells (first two lanes), but no WIP is present in WAS IP samples. This may suggest WIP does not interact with N-WASp in these cells or this particular process. It could also reflect the reduced total WIP levels seen in whole cell lysates of WAS DCs (last two lanes). This contradicts previously published data, which suggests WIP levels are normal in WASp $-/-$ cells (Chou et al., 2006, Worth et al., 2013).

While the bead model is useful for highlighting difference in actin organisation between BL6 and WAS DCs, further optimisation is needed in order to use the cell: bead interactions to investigate WASp binding partners during IS formation.

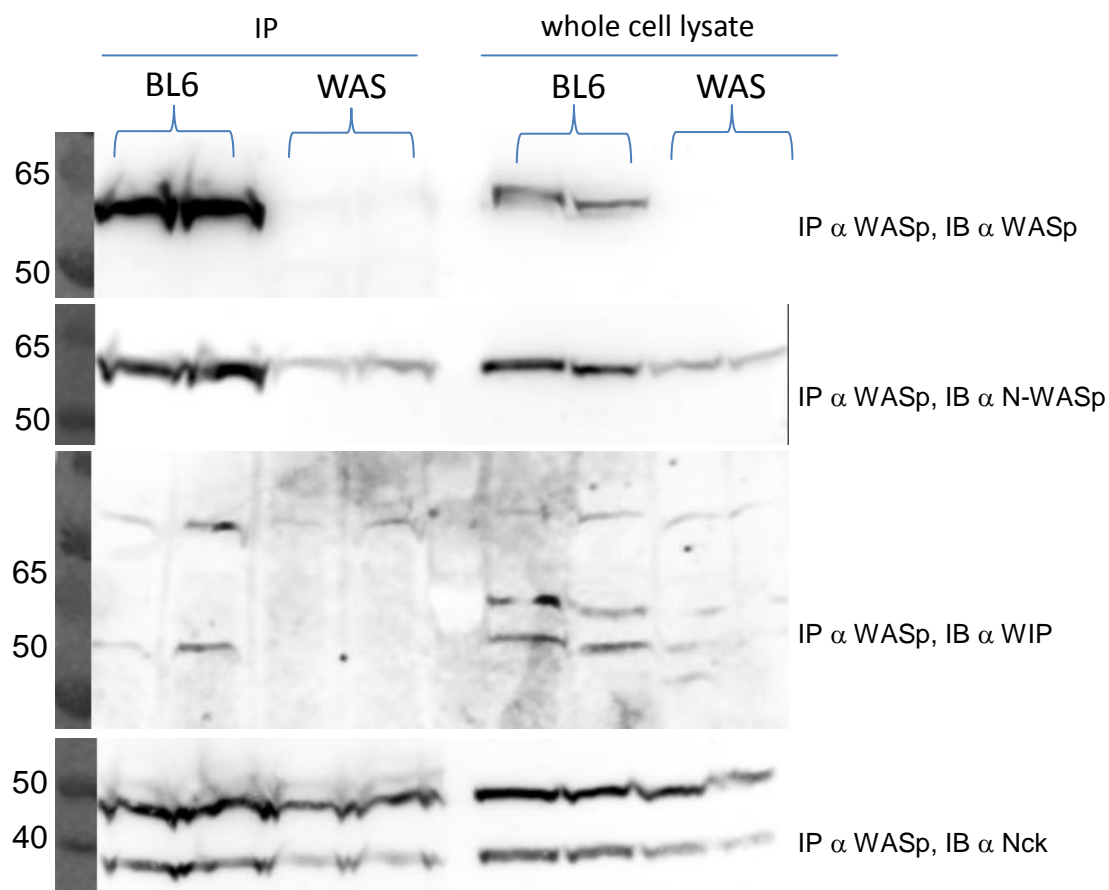


Figure 5.17 **Magnetic bead optimisation for immunoprecipitation.** DCs were incubated with beads coated with anti-MHCII and anti-ICAM-1 for 30min. The cell-bead suspension was resuspended gently and bead-bound cells were harvested using a Dynabead magnet. Cells were lysed and IP was performed according to protocol described in section 2.2.4. Denaturing elution was performed and samples were separated on a NUPAGE gel. Proteins were transferred to PVDF membranes, which were blocked in 5% milk and probed with antibodies against WASp, N-WASp, WIP and Nck. PreStained Page Ruler Protein ladder is used as size marker.

5.3 Discussion

This chapter aimed to investigate differences in DC capacity to induce T cell activation between BL6 and WAS DCs. Flow cytometry and IL-2 ELISA were used to show that WAS DCs were unable to induce the same level of T cell activation (Fig5.3 and 5.4). The greater difference in proliferation and IL-2 secretion at lower DC: T cell ratios suggest the DC actin cytoskeleton is especially important in conditions with lower DC-induced stimulation.

Results in the previous chapter showed slower “cSMAC” formation in WAS DCs compared to BL6. If this corresponds to slower cSMAC formation in an interacting T cell, might be expected to result in increased signalling in the T cell, due to prolonged TCR residence in the signalling-competent pSMAC rather than signal-terminating cSMAC (Lee et al., 2003a). Reduced proliferation and IL-2 production in WAS DC-induced T cells, however, suggest the opposite. It is unclear whether the cSMAC has a similar role in DCs, i.e. whether receptor uptake and degradation or recycling occurs in the same way in DCs. There is some evidence for MHCII-peptide complex recycling via a dynamin- and clathrin-independent pathway (Walseng et al., 2008). In this model, peptide-loaded MHCII molecules are quickly recycled back to the surface from early endocytic compartments, in a pathway distinct from that of newly-synthesised MHCII. However, it is unclear from this work whether this MHCII recycling is active at cell: cell synapses; and if so, where in the symmetric synapse structure the peptide-MHCII complexes would be targeted to. Further, in cell: cell contacts, both membranes are deformable and contain other surface molecules. Consequently, in vivo it is likely that other forces and interactions contribute to the control of downstream signalling. For example, the reduced number of microclusters, reduced MHC and lower cell spreading seen in WAS DCs (Fig 4.18) may all have confounding effects. Further optimisation of the micropit experiments shown in Chapter 4 may shed light on how signals for cSMAC formation are integrated from both sides of the IS.

The disorganised WAS synapse may affect T cell fate induction in several ways. If the strength of primary stimulation is important for fate induction, an asymmetric synapse may result in an imbalance between signalling microclusters and receptor uptake and recycling, resulting in inappropriate amplification or cessation of the signal. Maldonado *et al*, for example, show that co-polarisation of IFN γ receptor with the TCR to the IS leads to a Th1 response (Maldonado *et al.*, 2004). Tao *et al* suggest that the strength of the primary signal stimulation determines whether CD28 ligation is required for inducing Th2 differentiation ((Tao *et al.*, 1997a)).

Alternatively, if fate induction is dependent on activation of different costimulatory receptors, such as LFA-1, CD28 or CTLA-4 (Salomon and Bluestone, 1998, Smits *et al.*, 2002, Tao *et al.*, 1997b, Purvis *et al.*, 2010), abnormal spatial and/or temporal organisation of these could affect downstream signalling. For example, numerous studies have highlighted a role for LFA-1 ligation in Th1/Th2 balance (Salomon and Bluestone, 1998, Smits *et al.*, 2002, Perez *et al.*, 2003). Perez *et al* showed that LFA-1 induced downstream signalling through JAB-1 and cytohesin-1 (Perez *et al.*, 2003) and it would be interesting to see how these are affected by the improper organisation of LFA-1 in T cells activated by WAS DCs. Some groups have shown CD28 is important for inducing Th2 cell fate (Rodriguez-Palmero *et al.*, 1999, Tao *et al.*, 1997a). Others have shown a role for further surface factors, for example, Amsen *et al* express different Notch ligands to induce either Th1 or Th2 differentiation, with Delta inducing Th1 cells and Jagged inducing Th2 cell fate, independently of IL-4/STAT6 (Amsen *et al.*, 2004). It would be interesting to investigate how these ligands are organised at the IS. Thus, although the exact intercellular signalling determinants of T cell fate are unknown, it is easy to see how an unstable DC actin network may not be able to stabilise the necessary interactions.

QPCR and DC adoptive transfer experiments showed very small differences in the master regulators of T cell fates between T cell induced by BL6 or WAS DCs. In the *in vivo* experiments in particular, there were very small differences between LPS only and OVA-pulsed DCs. Several attempts were made at improving the protocol, including increasing the number of DCs

injected or the ovalbumin dose, or testing different time points post-injection. Most of these were unsuccessful, with several animals dying, thus an insufficient number for statistical analysis. CFSE staining of live cells is a well-established protocol. Although it is unlikely the CFSE staining of the DCs affected their function, it has previously been noted in the lab that some CFSE staining protocols result in a type of anergy in T cells where cells remained viable but did not proliferate in antigen-specific settings for 4 days (own observations). One further improvement to the experimental design for DC adoptive transfer may be to use DCs from control or WAS-deficient mice expressing a reporter, instead of relying on CFSE staining to follow migration. One such model is the DC-GLOWS mouse strain, which is WASp-deficient and expresses YFP under the CD11c promoter. A control, WASp-expressing CD11c-YFP, mouse strain is also available.

Using QPCR, any significant differences were difficult to replicate, suggesting that a complex or heterogeneous response was involved and detection of master regulator differences alone would not be sufficient to describe the complex response. Microarrays should compile data from different genes and detect pathways involved in different T helper cell differentiation. Even using this technique, only small differences in T cell activation and differentiation were observed and these are highlighted in Fig 5.13. In vivo, one reason for this may be the fact that a very small proportion of T cells show a strong cytokine response, as seen in the FACS plots in Fig 5.8, so the response may be quickly diluted across the population.

To test the initial hypothesis fully, it would be advantageous to test standard responses to a variety of pathogens or peptides that polarise T cell responses to each of the different effector T cell fates; then investigate how these differ in the context of WAS. Furthermore, characterisation of FYN DC's capacity for T cell inductions would shed light on the requirement of WASp phosphorylation for a functional, signalling-competent synapse.

Despite limitations, and although Rorc upregulation was too low to detect reliably above LPS signal, the significant increase in IL-17 secreted in vitro agree with increased IL-17 production

observed in vivo. This is also supported by recent findings in the lab using an antigen-induced arthritis model. Arthritis appears to be exacerbated in WAS knockout mice, with a significant increase in Th17 (CD4+IL17+) cells (Bouma, personal communication). Further, the severity of the disease correlates with increased Th17 and decreased Treg and Breg cell numbers.

The differences seen here, although small, highlight interesting trends and point to defects in IS function in WAS DCs. In WAS patients, all immune cells are WASp-deficient, which results in even poorer cell-cell communication and a lower capacity to induce the correct immune response. Data presented here highlights the essential role DCs, and in particular the DC actin cytoskeleton, play in functionally relevant cell-cell communication.

Chapter 6 – Abnormal actin regulation in novel primary immunodeficiencies

6.1 Introduction

Correct actin structure and function depends on a delicate balance of feedback mechanisms and regulators. Its importance is highlighted by the existence of several actin regulating proteins exclusively expressed in cells of the immune system; and by the fact that several primary immunodeficiencies are caused by defects in actin regulation.

It was hypothesised that lack of functional actin regulating proteins results in abnormal basic cellular processes, which could be the result of both increased or decreased actin polymerisation. First, the state of the actin cytoskeletal network was investigated in two novel Primary Immunodeficiencies (PIDs).

Megakaryoblastic acute leukemia 1 (MAL; also termed MKL-1, MRTF-A, BSAC) was originally identified due to its involvement in acute megakaryoblastic leukaemias, resulting from a chromosome translocation which produced the oncogenic RBM15-MKL-1 fusion protein (Ma et al., 2001, Mercher et al., 2001).

MKL-1 belongs to the MRTF (myocardin-related transcription factors) family of transcription factors, with conserved domains for actin binding, dimerisation and transcriptional activation. Unlike myocardin, which is specifically expressed in the heart, MKL-1 is ubiquitously expressed and thus could be a common regulator of growth factor-induced immediate-early genes (Ma et al., 2001, Mercher et al., 2001, Wang et al., 2002).

MKL-1 has been shown to interact with serum response factor (SRF) to activate transcription of a number of genes with a role in actin organisation (Cen et al., 2003, Selvaraj and Prywes, 2003, Miralles et al., 2003). SRF activity is related to cellular G actin content and changes in actin dynamics by Rho GTPase result in SRF activation (Hill et al., 1995, Sotiropoulos et al., 1999). Expression of dominant negative forms of actin nucleators, or overexpression of wild-type or non-polymerisable actin, inhibit SRF activation (Geneste et al., 2002, Grosse et al., 2003, Posern et al., 2002). These results suggested that actin polymerisation or stabilisation, and thus G actin pool depletion, enhances SRF activity.

The precise mechanism between G-actin and MKL-1 activation is unclear. Loss of *MKL-1* expression has been shown to affect megakaryocyte migration and platelet formation (Gilles et al., 2009). Its effects on other cellular functions have not been studied and the experiments shown in this chapter aimed to investigate the effect of MKL-1 mutation on total cellular actin and consequently myeloid cell adhesion, spreading and podosome formation.

The second novel immunodeficiency was found to be caused by a previously undescribed mutation in Actin-Interacting Protein (AIP1). In a yeast two-hybrid screen, AIP1 was originally identified as an actin-interacting protein (Amberg et al., 1995). It has been shown to interact with ADF (actin-depolymerising factor)/cofilin by affinity chromatography (Okada et al., 1999) and yeast two-hybrid systems (Rodal et al., 1999). Cofilin severs actin filaments by changing the conformation of the filament and weakening forces of the lateral contacts within filaments (McGough et al., 1997, Galkin et al., 2001). Although, it severs filaments, it does not cap their ends, thus increasing the availability of free filament ends for further polymerisation or depolymerisation (Mabuchi, 1983, Hawkins et al., 1993, Hayden et al., 1993, Blanchoin and Pollard, 1999, Ichetovkin et al., 2000). Consequently, it plays a crucial role in actin filament turnover (Bamburg et al., 1999, Maciver and Hussey, 2002).

AIP1 alone has no significant effect on actin filaments; however, it has been shown to accelerate cofilin's severing activity on actin filaments by capping severed filament ends to

prevent elongation or reannealing (Okada et al., 1999, Aizawa et al., 1999, Okada et al., 2002) and weakening interactions between actin monomers within a filament. Although cofilin and AIP1 have been shown to be important for migration, in *Drosophila* as well as *Dictyostelium*, very little is known about how this is regulated (Konzok et al., 1999, Ono, 2003, Chen et al., 2001, Zhang et al., 2011). The mutation of the mammalian homologue of AIP1, WDR1, has been shown to result in cytoskeletal defects in neutrophils (Kile et al., 2007). Although complete loss of function of WDR1 is embryonically lethal, hypomorphic mutations result in macrothrombocytopaenia and autoinflammatory disease (Kile et al., 2007).

A non-synonymous base change in WDR1 was identified in a pair of siblings with episodes of unprovoked inflammation and thrombocytopaenia. The experiments presented here aimed to investigate how this mutation in WDR1 affects the cellular actin network.

Finally, DOCK8 was investigated as another player in the Arp2/3 actin polymerisation pathway. Mutations in the gene *DOCK8* (dedicator of cytokinesis 8) have recently been shown to be the cause of a human immunodeficiency associated with recurrent viral infections, allergic disease, malignancy and hyper IgE previously known as autosomal hyper IgE syndrome. This suggests that at the cellular level, DOCK8 patients have multiple abnormalities in all lineages of the immune system. This includes reduced numbers of T cells (both CD4 and CD8) which deteriorates with age, with some loss of B and NK cells. Furthermore, these cells fail to proliferate in response to antigen with a reduction in the production of antiviral cytokines. In addition, antibody levels are often abnormal with elevated IgE and low IgM (Su, 2010, Moulding et al., 2013).

DOCK8 is a member of a family of guanine nucleotide exchange factors (GEFs), many of which interact with CDC42 to facilitate the switching between GDP and GTP bound forms. CDC42 is a Rho GTPase known to be important for regulation of the actin cytoskeleton, including WASp activation (see Introduction). Actin's crucial role in the formation of the DC immune synapse is highlighted in the previous chapters. DOCK8 has been shown to be important in the formation

of B cell and NK cell immunological synapses (Ham et al., 2013). DOCK8 NK cells showed defective conjugate formation and impaired polarisation of F-actin, LFA-1 and cytolytic granule towards target cells. Further, DOCK8 was shown to interact directly with WASp and the integrin regulator talin, and contribute to their polarisation towards the IS (Ham et al., 2013). Little is known about how mutations in DOCK8 affect dendritic cell (DC) function during synapse formation.

This part of the project aimed to use a DOCK8 mutant murine model (Randall et al., 2009) to investigate the role in actin regulation in dendritic cells and its functional effect on the DC: T cell immune synapse.

6.2 Results

6.2.1 Megakaryoblastic leukaemia (MKL-1)

A girl born to second cousin consanguineous parents presented in the first year of life with *Pseudomonas* septic shock associated with meningitis, otitis media, and multiple subcutaneous abscesses. Whole exome sequencing identified a mutation in Megakaryoblastic leukemia 1 (*MKL-1*), a co-factor of the transcription serum-response factor (SRF) that binds to the promoters of several actin-regulating genes. Therefore the role of MKL-1 in actin-mediated functions of immune cells was investigated.

An EBV-immortalised B cell line was made from patient cells and lysates were made for Western blot analysis. MKL-1 is predicted to have a size of around 160kDa although on 4-12% percent acrylamide gel it appears to migrate to 140kDa (as previously published (Gilles et al., 2009)). As Figure 6.1 shows, MKL-1 expression was severely reduced in patient cells. An antibody against the N-terminus, which also appeared to recognise MKL-2, showed no difference in MKL-2 (~118kDa) expression between patient and control cells (not shown). This suggests MKL-2 is unable to compensate for the lack of MKL-1 function in the immune system.

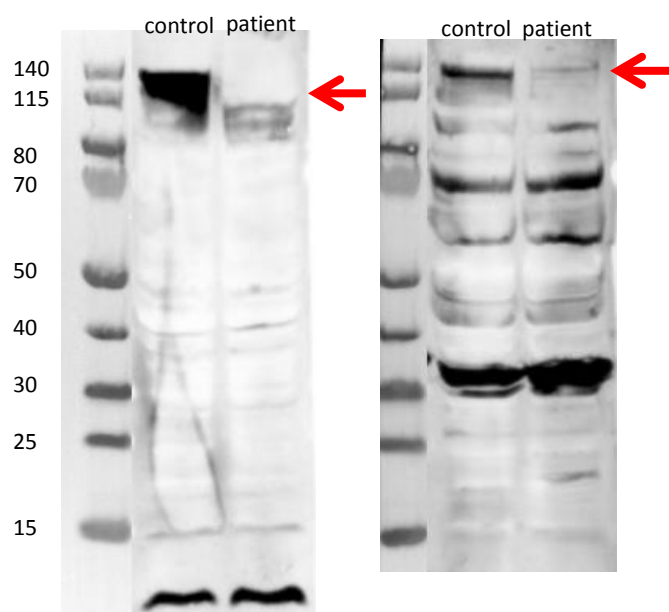


Figure 6.1 **Mutation in MKL-1 resulting in loss of protein expression.** Using two separate antibodies (left = Sigma; right = SantaCruz), lysates from control and patient EBV-immortalised B cell lines were separated by SDS-PAGE and probed for MKL-1.

Peripheral blood mononuclear cells (PBMCs) were isolated from control or patient blood and a CD14-selection was performed. CD14-positive monocytic cells were cultured for 5 days in the presence of IL-4 and GM-CSF to induce DC differentiation. Figure 6.2 shows the morphology of DCs after 5 days in culture. Control DCs showed good adhesion to culture dishes, spreading and polarisation. Patient DCs remained rounded and showed a severely reduced ability to adhere, spread and polarise.

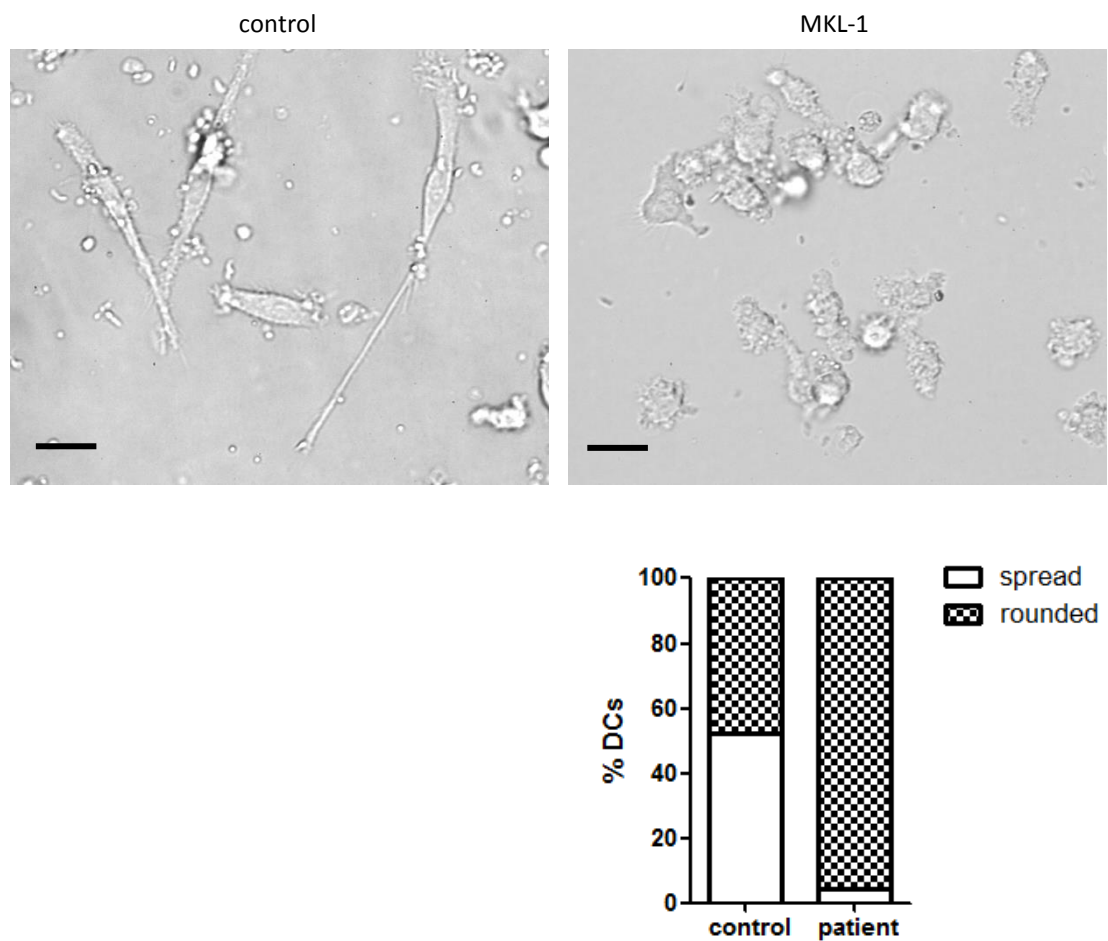


Figure 6.2 **DC morphology 5 days post isolation**. Over 500 cells were observed and characterised as either adhered, spread and polarised or rounded and floating. This is quantified in the graph. Scale bar = 20 μ m.

CD14-positive myeloid cells and the remaining (CD14⁻) lymphoid fraction were assessed for total F-actin content. As phalloidin staining can be very variable and it binds to filamentous actin stoichiometrically, to directly assess the total actin content, control and patient cells were stained together as a mixed sample population. Patient cells were stained with CFSE and washed twice to prevent dye transfer to other cells. They were then mixed with an equal number of control cells, fixed, permeabilised and stained with 647-conjugated Phalloidin. Figure 6.3 shows analysis of these by both flow cytometry and confocal microscopy. These histograms indicate that control cells contain more total polymerised actin; which can also be seen in the confocal images where CFSE-positive (green) patient cells stained less brightly with phalloidin-647 than unstained control cells. The dot plot represents MFIs of individual cells, calculated by measuring the average intensity of each cell in the phalloidin channel of confocal images. This shows that control cells contain significantly more total polymerised actin. Similar results were obtained when CFSE-stained control cells were mixed with unstained patient cells.

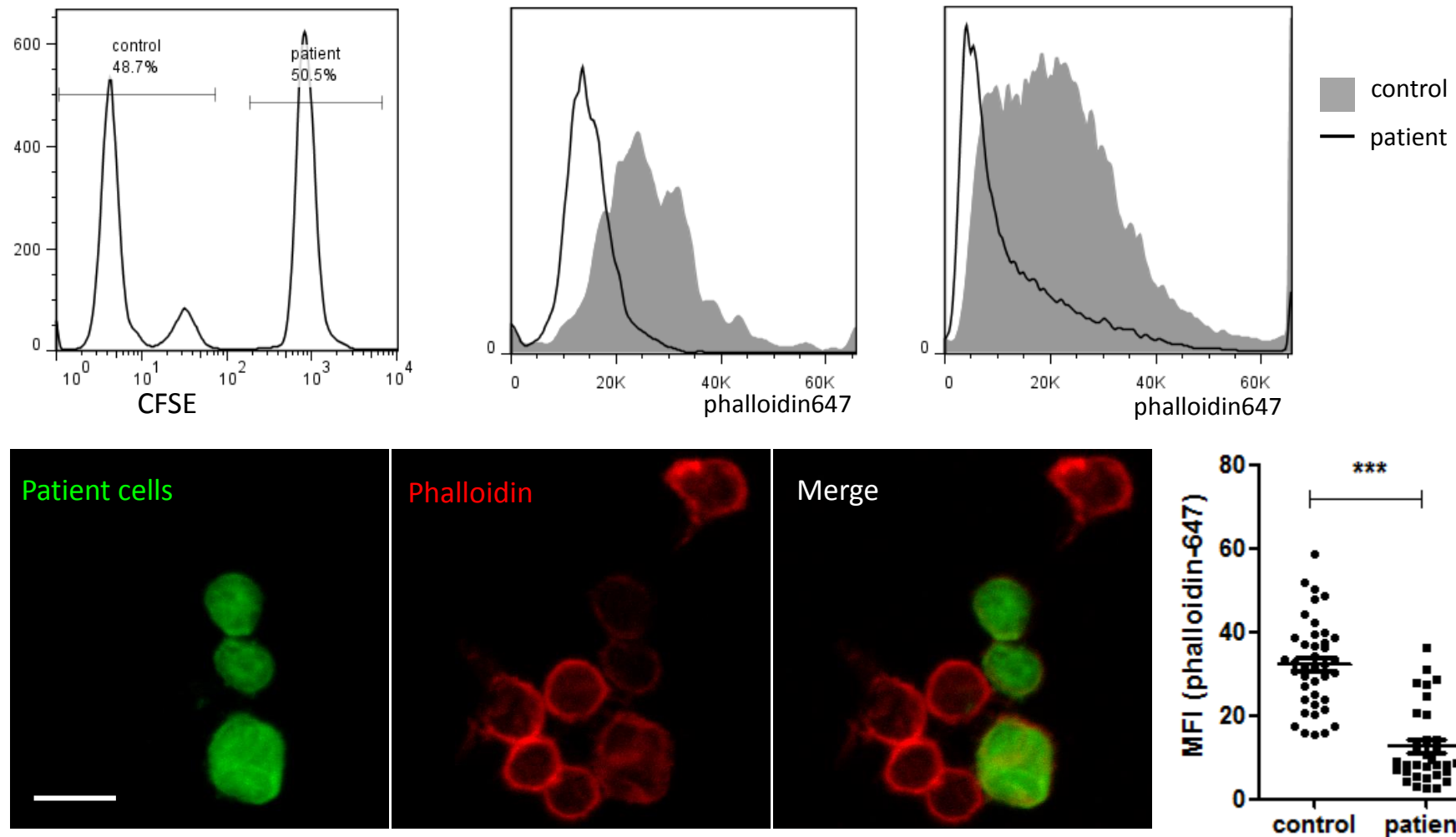


Figure 6.3. **Total polymerised actin is reduced in MKL-1 patient cells.** Mixed population phalloidin stains were performed on cells of both the myeloid and lymphoid lineages. Patient cells are CFSE stained in the FACS histograms and confocal images. Confocal images show control and patient lymphocyte populations. Scale bar = 8 μ m. MFI of individual cells were calculated in ImageJ. Significance level was calculated using an unpaired t test. *** $p < 0.0001$

To further investigate MKL-1 deficiency, a monocytic THP1 knockdown (KD) cell line was created. THP1 were infected with lentivirus encoding either scrambled (SCR) control shRNA or a shRNA sequence previously described to specifically silence *MKL-1*. After 3 days in culture, the cells were sorted for high GFP expression and a stable cell line was propagated. Knockdown of MKL-1 at protein level was confirmed by western (Figure 6.4a).

To confirm the actin defects seen in patient cells, THP1 cell lines were stained for phalloidin using a similar mixed population protocol, substituting CFSE with a far red DDAO dye. In Figure 6.4b, MKL-1 KD THP1 are DDAO-positive and SCR THP1 are unstained. Phalloidin-564 staining shows MKL-1 KD results in decreased amount of total polymerised actin.

The THP1 cell line was cultured in the presence of rhIL-4 (10ng/ml) and rhGM-CSF (10ng/ml) to induce differentiation into DCs (THP1DCs). Figure 6.4d shows these GFP-positive, shRNA-expressing THP1 cells after 5 days in culture. MKL-1 knockdown cells exhibit reduced spreading and adhesion compared to SCR. This is quantified in Figure 6.4c.

Consistent with the adhesion and spreading defect, MKL-1 knockdown THP1DCs were unable to form podosomes when seeded on fibronectin (Figure 6.4e). This was also observed in primary monocytes from the patient (D Moulding, personal communication). This suggests that MKL-1 plays an important role in podosome formation or maintenance, which is likely to have a severe adverse impact on immune function given the importance of podosomes for cell migration in vivo (Calle et al., 2006b, Chou et al., 2006, Linder and Aepfelbacher, 2003, Klos Dehring et al., 2011, Isaac et al., 2010).

These experiments show that a mutation which disrupts MKL-1 expression reduces the amount of total polymerised actin and affects myeloid cell adhesion, spreading and podosome formation.

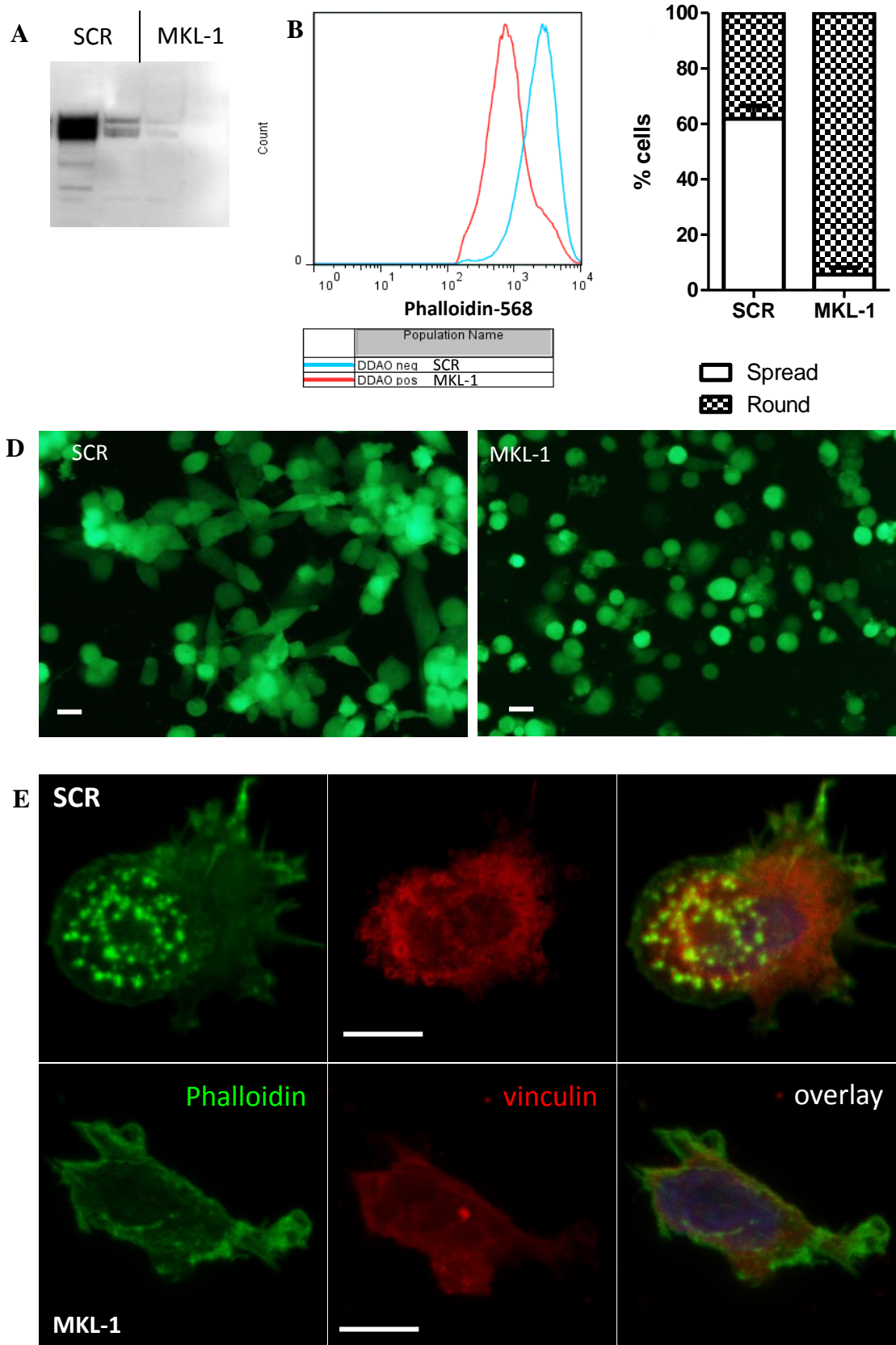


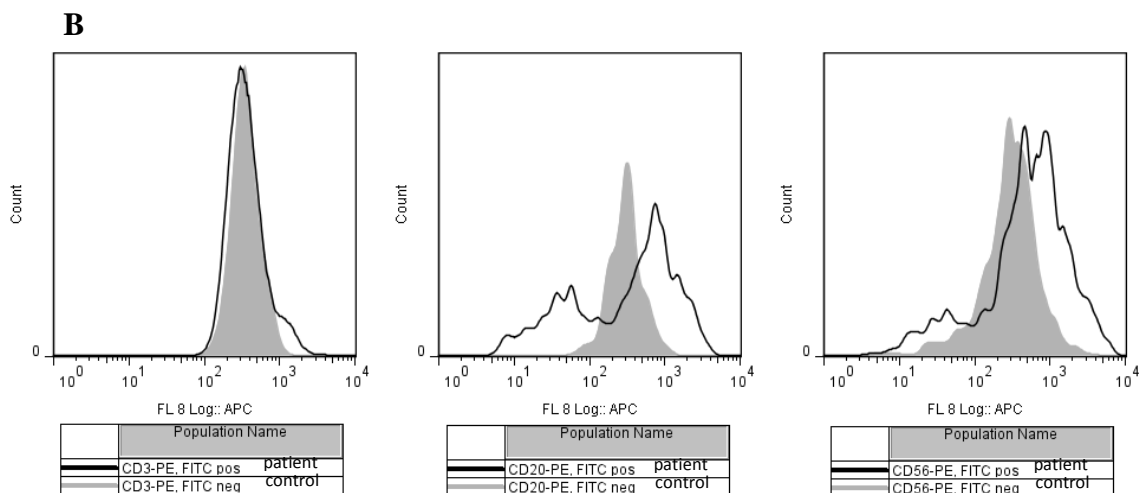
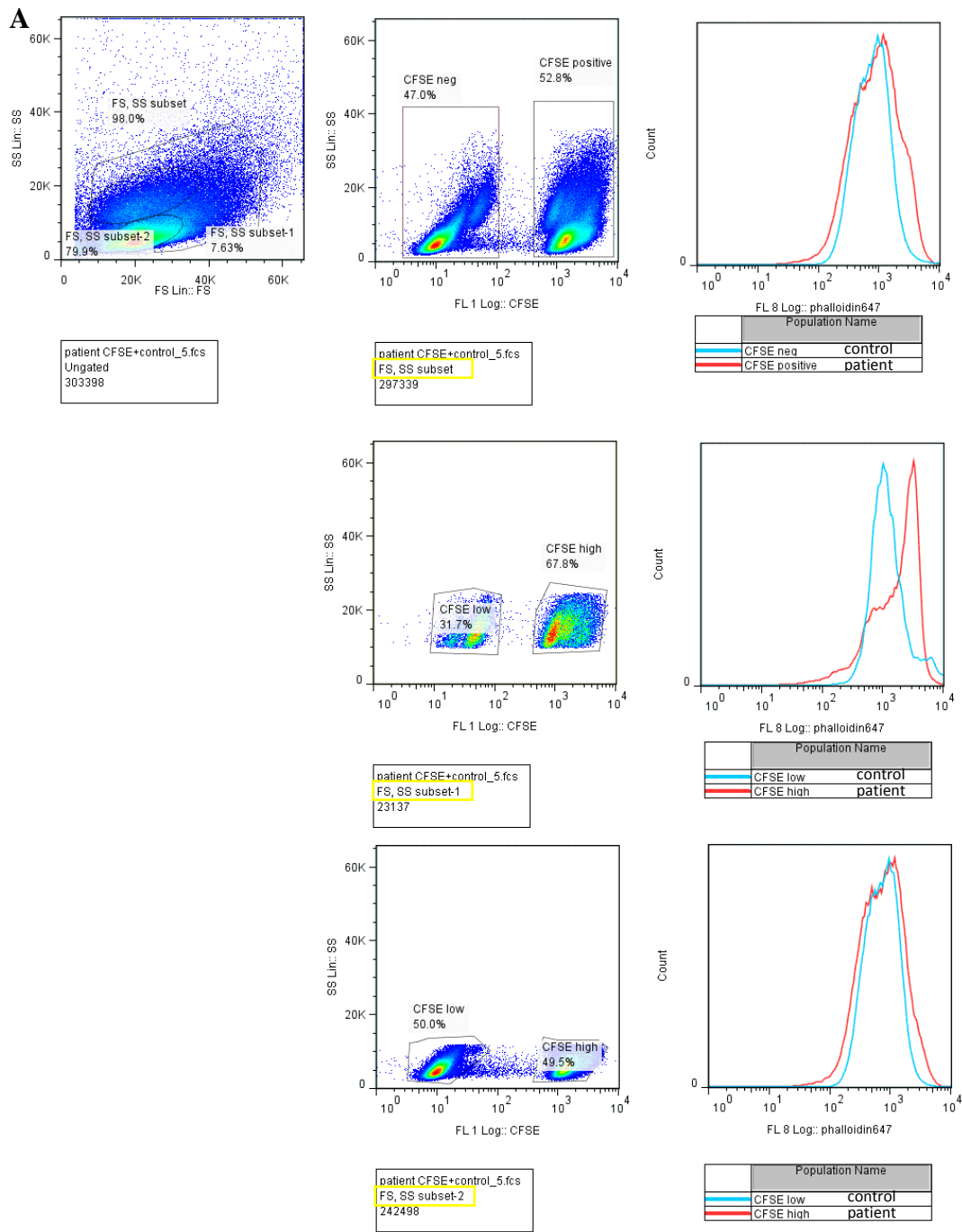
Figure 6.4 **MKL-1 knockdown THP1 cell line.** A) Western showing reduced MKL-1 (~98kDa) protein expression in cells treated with MKL-1 specific shRNA compared to SCR control shRNA. B) Mixed population actin stain showing decreased polymerised actin in MKL-1 cells. C and D) THP1 at day 5 of DC differentiation culture. Spread and rounded cells quantified as before. E) THP1DCs seeded on fibronectin to analyse podosome formation. Scale bars = 10µm.

6.2.2 Actin-interacting protein 1 (AIP1)

A non-synonymous base change in *WDR1* was identified in a pair of siblings with episodes of unprovoked inflammation and thrombocytopaenia (N Klein and P Brogan, personal communication). Western blot analysis has revealed the presence of a smaller sized protein, however, it is unclear whether the mutation results in a truncated protein or expression of a splice variant (A Standing, personal communication). The following experiments aimed to determine the effect of this mutation on the actin cytoskeleton of immune cells.

As before, Ficoll and CD14 magnetic cell purification was performed on patient and control peripheral blood samples. CD14-negative PBMCs were stained with phalloidin-647 in a mixed population sample and analysed by flow cytometry. The forward scatter (FS)/ side scatter (SS) plot showed several populations with distinct differences between control and patient cells (Fig 6.5a). To characterise these further, cells were stained for surface markers for T cells (CD3), B cells (CD20) and NK cells (CD56), before fixing, permeabilising and staining for actin. CD3-positive cells show no difference in total polymerised actin between control and patient; however, in both CD20- and CD56-positive populations, patient cells were more strongly stained for phalloidin than control cells (Fig 6.5b). This suggests the *WDR1* mutation results in increased actin polymerisation in B and NK cell populations.

Figure 6.5 **WDR1 patient lymphocyte actin.** Patient B cells and NK cells contain more total polymerised actin. Patient lymphocytes were stained with CFSE and mixed with unstained control lymphocytes. A) The mixed population was permeabilised and stained with phalloidin. B) Cells were first stained for surface CD3, CD20 or CD56 with PE-conjugated antibodies, followed by fixing and permeabilisation.



CD14-positive cells were differentiated into DCs and also stained with phalloidin in a mixed population sample. Figure 6.6 shows that patient cells (black line) from the myeloid lineage also contain more polymerised actin than control cells at steady state. Further, upon activation with LPS or LPS/ATP for 4 hours, actin polymerisation in patient cells appears to be upregulated to a much greater extent than in control cells, as illustrated by their mean fluorescent intensities (MFI). Patient cell MFIs are double those of control cells. Stains for each treatment were performed in a mixed population sample; however, comparison of MFIs across treatments is not valid as untreated cells were stained separately and may have been stained for longer, which could explain the elevated phalloidin intensity in these cells compared to cells post treatment. Results for separate treatments were normalised against control and presented in the bar graph.

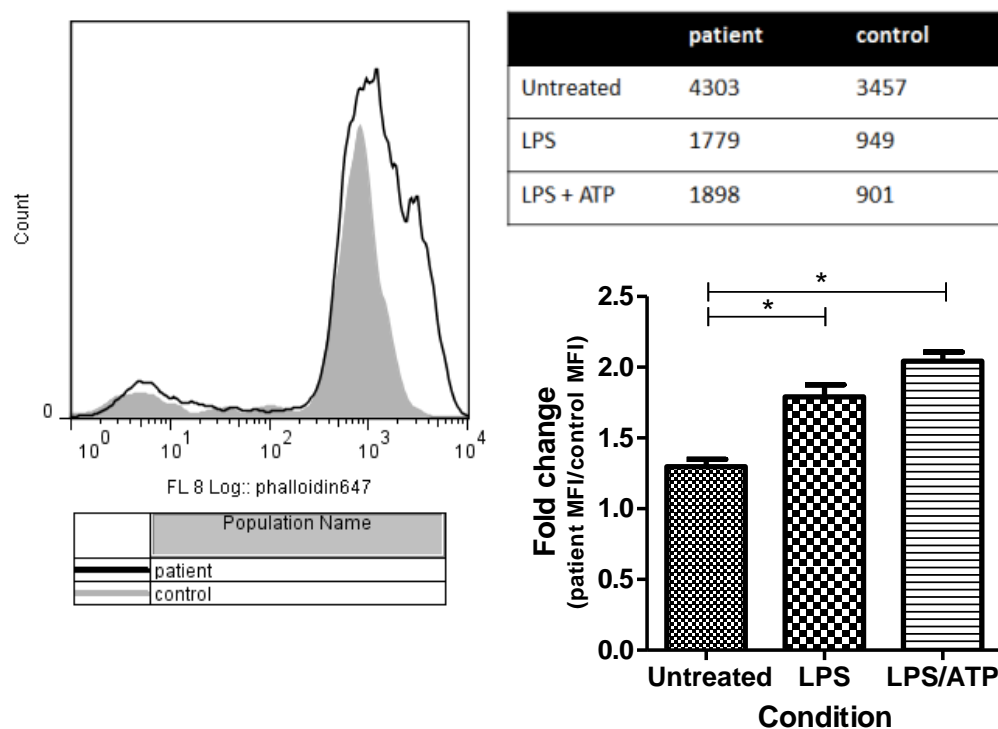


Figure 6.6 **Total polymerised actin in DCs**. Grey histogram represents untreated patient and control DCs, permeabilised and stained for phalloidin in a mixed population sample. On the right, the table summarises MFIs of cell populations following LPS or LPS/ATP treatment. MFIs from two separate experiments are normalised against control values in the bar chart. An unpaired t test was performed.

* $p = 0.05-0.01$

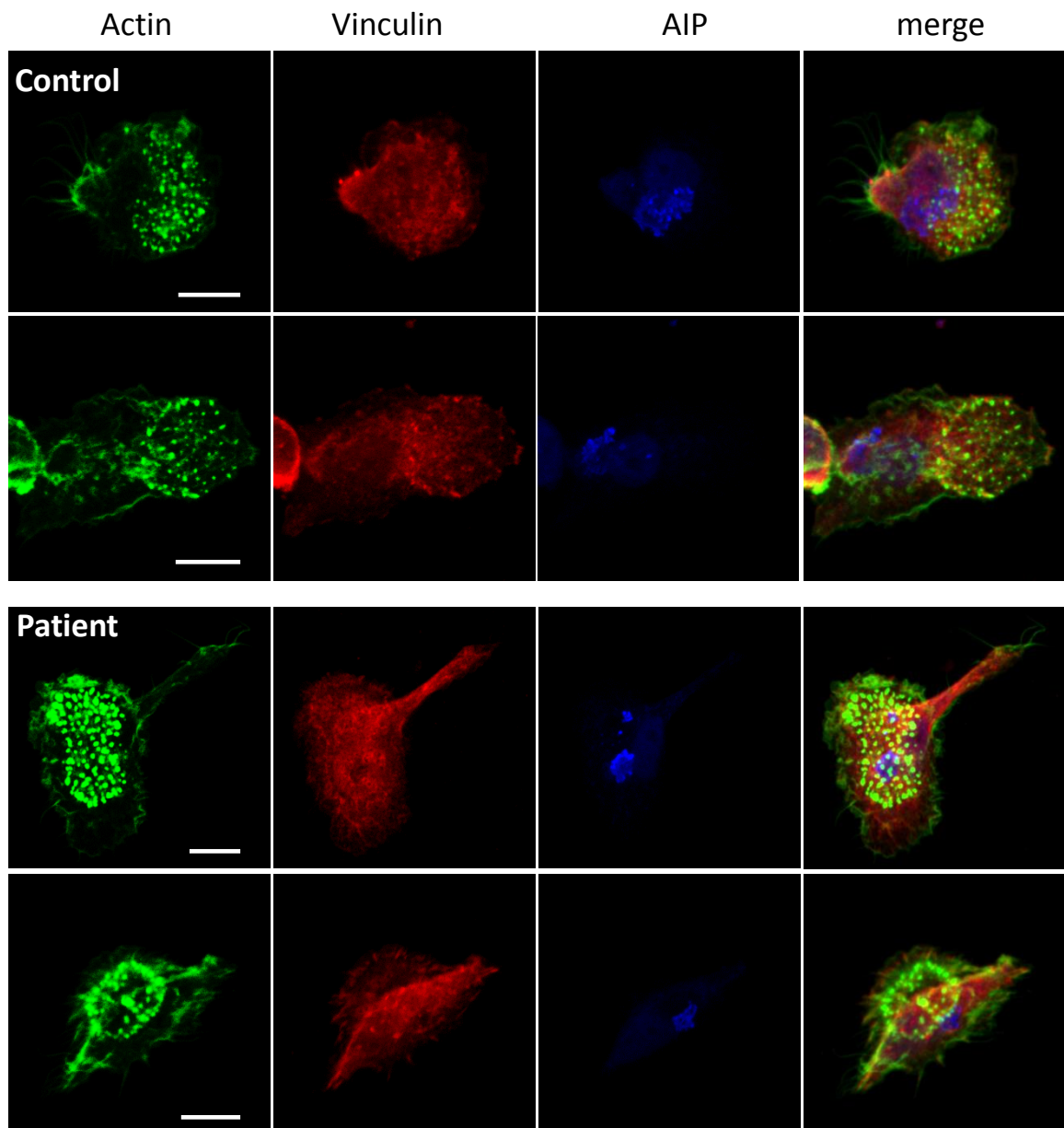


Figure 6.7 **Podosome formation.** Patient and control cells were seeded on fibronectin-coated coverslips for 4 hours, fixed and stained for actin (phalloidin-488), vinculin and WDR1. Coverslips were mounted on glass slides and analysed by confocal microscopy. Scale bars = 10 μ m

To investigate whether the WDR1 mutation affects cell adhesion, patient and control DCs were seeded on fibronectin-coated coverslips and stained (Fig 6.7). Actin and vinculin stains showed patient cells formed podosomes which, unlike WAS or MKL-1, appeared larger than control cell podosomes in both the xy and the z plane. To take into account both dimensions, podosome volumes were measured using threshold and measurement functions in Volocity. These are shown in Figure 6.8. Although the number of podosomes per cell was not significantly

different, podosomes formed by patient cells were significantly larger than control. This suggests that the mutation in *WDR1* either increases actin polymerisation at podosome structures or results in decreased podosome turnover through stabilisation or reduced depolymerisation.

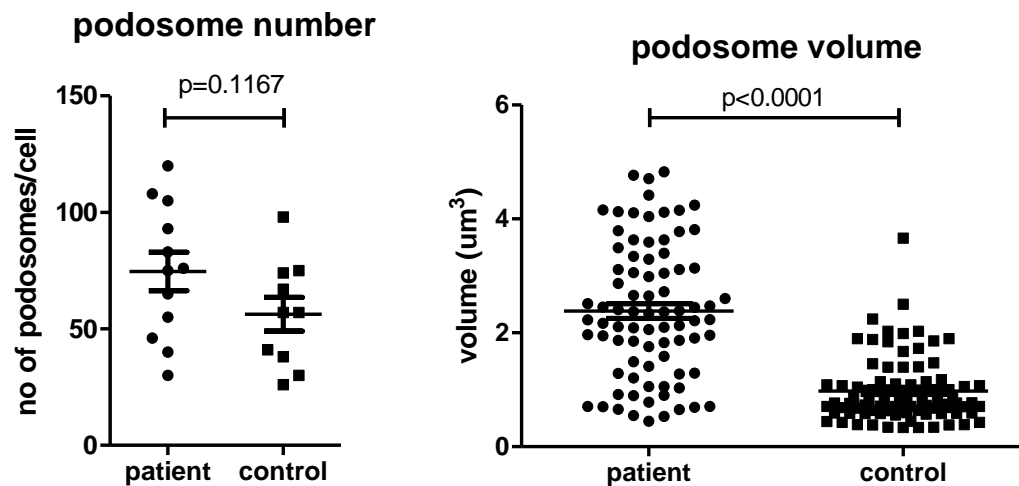


Figure 6.8 **Podosome volumes.** Podosomes in patient and control cells were counted and size was analysed using Threshold and Measure functions in Velocity. A minimum of 10 cells were measured from each sample. An unpaired t test was used to test for significance.

A THP1 *WDR1* knockdown cell line was created to investigate the effect of lack of *WDR1* protein expression. The Western blot in Figure 6.9 shows *WDR1* expression in untransduced THP1s and those infected with SCR control virus. *WDR1* expression is severely decreased in THP1s expressing hairpin (HP) 4 or 5 shRNA constructs.

WDR1 knockdown was unable to reproduce the abnormalities seen in patient cells, including increased F-actin and increased podosome volumes (not shown), as well as altered cell migration (J Record, personal communication). This suggests that defects seen in patient cells result from the abnormal regulation or localisation of the splice variant or truncated protein expressed, rather than complete loss of its function. It would be interesting the further

investigate the nature of the mutation and introduce this mutated WDR1 into the knockdown cell line.

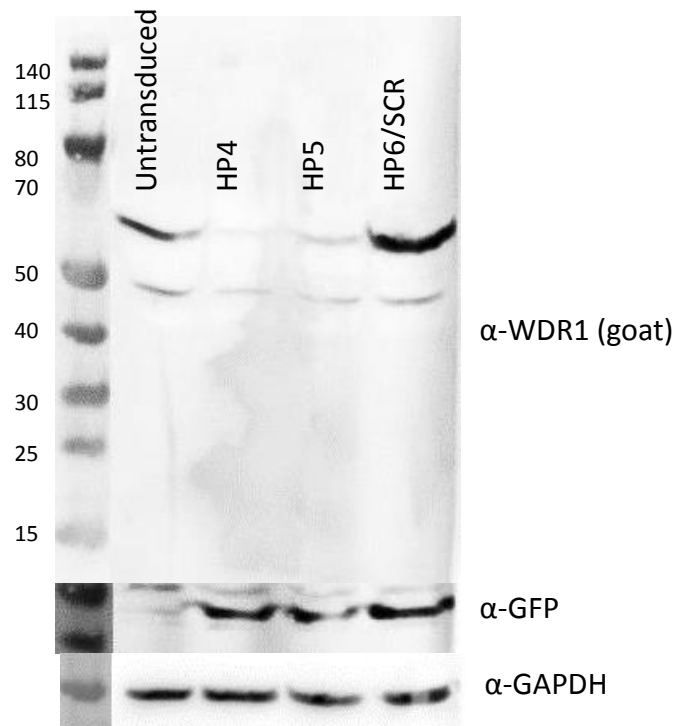


Figure 6.9 **WDR1 knockdown cell line.** Prestained PageRuler Protein ladder was used as a size marker. PVDF membrane was probed with a rabbit anti-WDR1 antibody, followed by an anti-rabbit-HRP conjugated secondary. GAPDH is used as a loading control to show similar loading in all samples. GFP expression confirms shRNA construct expression.

6.2.3 Deducator of cytokinesis (DOCK) 8

DOCK8 is a guanine nucleotide exchange factor, which has been shown to interact with several Rho GTPases, including Cdc42 (Ruusala and Aspenstrom, 2004). WASp, as the best understood effector of the Rho GTPase pathway, can be regulated by Cdc42 (Thrasher and Burns, 2010). The following experiments aimed to investigate how disrupting the function of DOCK8, an upstream member of this pathway, affects immune synapse formation described in Chapter 3. Dock8 deficient mice (Randall et al., 2009) were bred in house, bone marrow was isolated from femurs and cells were cultured in 20ng/ml GMCSF to generate BMDCs. As previously described for WAS DCs, these were matured and pulsed with OVA; and cocultured with OTII CD4 cells. To investigate the stability of the DOCK8 DC synapses, conjugate numbers were analysed by confocal microscopy.

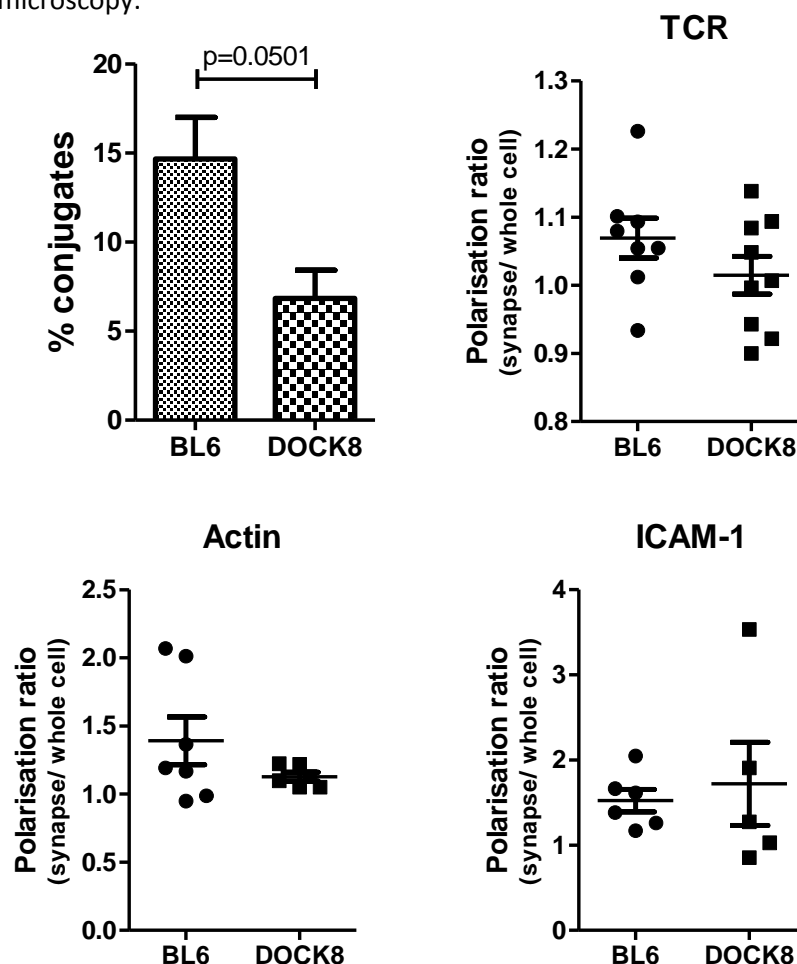


Figure 6.10 **Stable conjugate formation and polarisation of synapse markers.** DC: T cell cocultures, seeded on poly-L-lysine slides, were stained for ICAM-1, actin and TCR. These were analysed by confocal microscopy and DCs forming conjugates were quantified as a percentage of total DC number. Percentages from 2 separate experiments were converted to arcsin numbers and a paired t test was used to analyse significance. Polarisation ratios were calculated as described before in Fig3.8.

DOCK8 DCs form fewer stable conjugates than BL6, as seen in Fig 6.10 (top left). This suggests that disrupting Cdc42-mediated pathways affects the stability of cell: cell contacts. Interestingly, unlike WAS DC conjugates, in DOCK8 DCs polarisation of ICAM-1 appears normal, suggesting that this integrin is regulated normally and is not responsible for the differences in stable synapse numbers. Due to the variability of these results (large SEM on the dot plots in Fig6.10) it would be beneficial to repeat these with a larger number of cells.

Similar to the WAS conjugates, immunofluorescent staining for γ -tubulin showed that the T cell MTOC did not polarise towards the IS interface (Fig 6.11). This was almost as severe as the defect seen in T cells contacting WAS DCs; the mean distance between the T cell MTOC and the IS was 2.55 μ m in Dock8 and 2.86 μ m in WAS conjugates.

MTOC polarisation

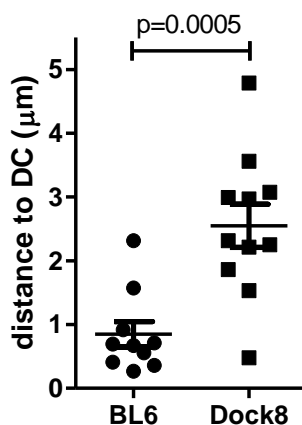
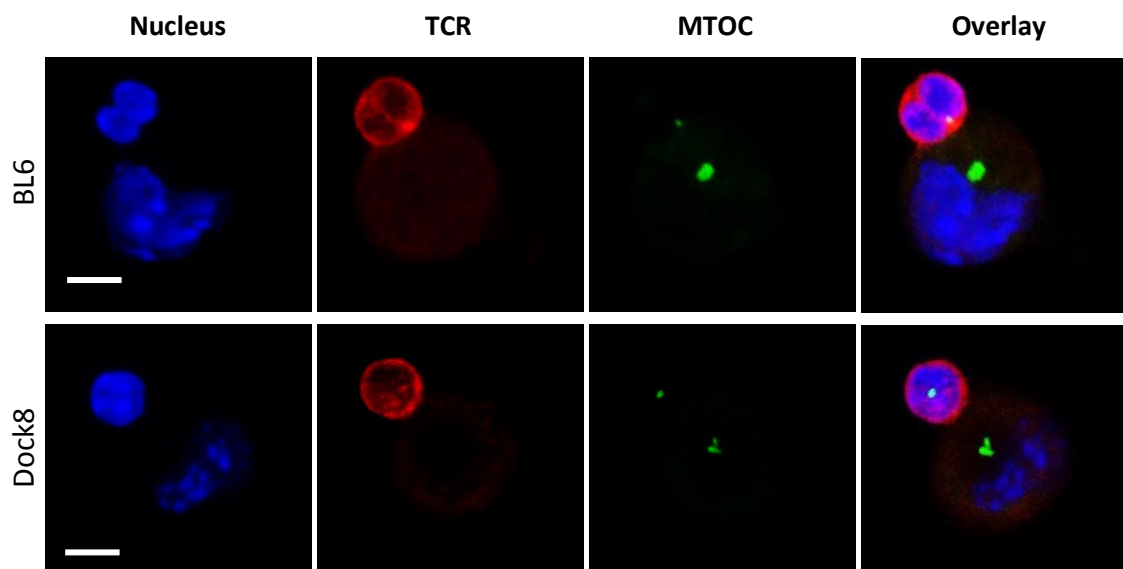


Figure 6.11 **MTOC polarisation**. DC: T cell cocultures, seeded on poly-L-lysine slides, were stained for TCR (red), γ -tubulin (green) and the nucleus (DAPI; blue). These were analysed by confocal microscopy and the distance between the T cell MTOC and the DC interface was measured in ImageJ. Scale bar = 5 μ m. A minimum of 10 cells was and an unpaired t test was used to analyse significance.



Although no differences in integrin localisation were observed, the reduced number of stable conjugates and severely disrupted MTOC translocation induced by DOCK8 DCs suggest there may still be quantitative and qualitative abnormalities in functional IS formation as a result of DOCK8 deficiency. To investigate this, concentrations of secreted cytokines in DC: T cell coculture supernatants were measured by ELISA.

Figure 6.12 shows the results from IL-2, IFN γ and IL-17 ELISA analyses, which previously showed the largest differences in WAS DC cocultures compared to BL6 (Fig 5.4- 5.6). DOCK8 DCs were unable to induce the same IL-2 secretion as BL6 at a 1:1 cell ratio, similar to what was observed in WAS. At 1:5 ratio however, both types of DCs induced less IL-2 production and there was no significant difference between them. It would be interesting to investigate whether these differences reflect altered T cell proliferation.

IFN γ secretion was significantly lower in T cells induced by DOCK8 DCs, compared to BL6, at both cell ratios. Similar to the difference seen in WAS, this suggests there may be a defect in Th1 cell fate specification. However, IL-17 secretion appeared normal in T cells induced by DOCK8 DCs, suggesting Th17 development is normal. Further QPCR or in vivo cytokine assays are required to confirm these differences.

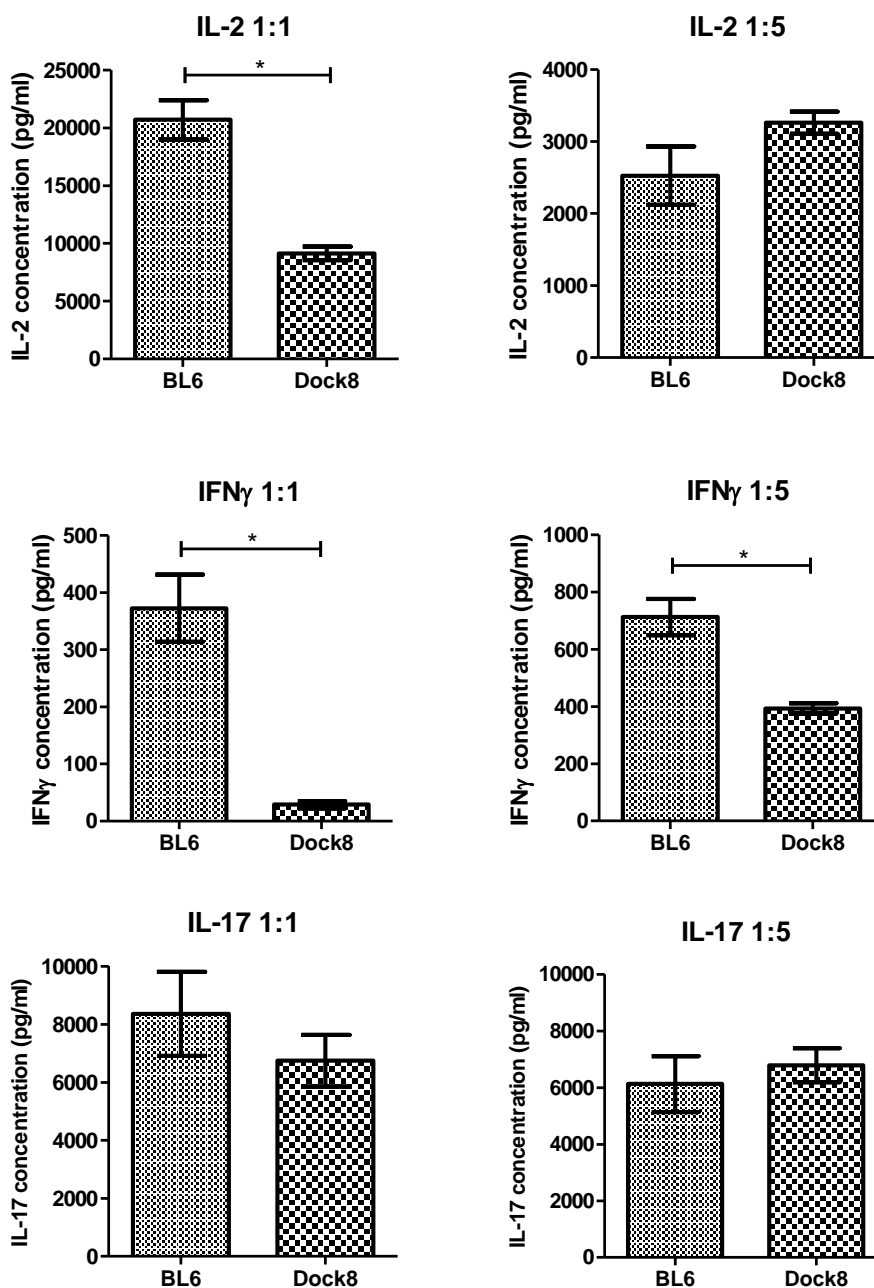


Figure 6.12 **Coculture cytokine secretion.** BL6 or Dock8 BMDCs were pulsed with OVA and cocultured with T cells at 1:1 and 1:5 DC: T cell ratios. 48hrs after coculture, supernatants were collected and analysed using R&D systems ELISAs. Each graph represents an average from 3 separate experiments, each of which was measured in triplicate. A paired t test was used to determine significance. *p=0.01-0.05

6.3 Discussion

This chapter aimed to investigate the role of several actin regulators in the steady state maintenance of the actin cytoskeleton, as well as during adhesion and synapse formation as described for WASp in previous chapters.

First, two novel PIDs were described, MKL-1 and WDR1; both of which result from mutations in actin-regulating proteins. Loss of *MKL-1* expression, in patient and THP1 knockdown cells, resulted in significant loss of cellular polymerised actin. This resulted in poor cellular adhesion, spreading and migration (not shown, J Record). The reduction in F-actin would be expected to affect other fundamental processes, such as cell division. Indeed, the MKL-1 THP1 cell line appeared to expand slower in culture, compared to SCR cell lines. A separate investigation of actin dynamics throughout the cell cycle in the context of MKL-1 would be interesting, including live imaging of MKL-1-deficient cells during cell division. Abnormal cell division may correlate with some clinical findings, such as neutropenia.

In terms of MKL-1's role in transcription regulation, the planned future work for this project includes a complete transcriptome analysis using RNA Sequencing. For example, some of the genes known to be regulated by MKL-1 are the myosin heavy and light chains (Sun et al., 2006, Gilles et al., 2009). Myosin has a role in both migration and podosome formation (Bhuwania et al., 2012, Vicente-Manzanares et al., 2009). Thus defects seen above may be the result of perturbed non-muscle myosin function. However, a full transcriptional analysis is important as it is likely that the complex disease results from the abnormal regulation of several actin modulators, including vinculin and N-WASp (Gilles et al., 2009).

The second immunodeficiency described was shown to be related to a homozygous mutation in *WDR1*. This was shown to result in an increase in polymerised actin, abnormal podosome formation and impaired phagocytosis by dendritic cells (A Standing). Thus, similar to the effects of decreased F-actin described above, an increase in F-actin also has detrimental effects on basic cell processes. This highlights the crucial role of actin regulators in controlling the

delicate balance between actin assembly and disassembly, particularly in the immune system. As the defects are present in several cell lineages, it is likely that these regulators play similar roles across a number of cell types. Many questions remain unanswered. The precise nature of the *WDR1* patient mutation is still unknown and characterising this may allow expression of the variant protein in a THP1 cell line in order to reconstitute the defect more completely on a cellular level. The increased podosome volume phenotype also needs further characterisation. Increased F-actin content has been described for the constitutively active WASp-I294T (Moulding et al., 2007), however podosomes in these cells, although deregulated, were not significantly larger. This highlights the importance of filament severing and depolymerisation, as well as nucleation, in the maintenance of podosomes. Live imaging and FRAP should provide useful insight into the turnover dynamics of these altered adhesion structures. As the loss of functional *WDR1* results in an increased F-actin network, the results presented here agree with previous findings using electron microscopy showing that AIP1 and cofilin increase the population of short filaments (Okada et al., 1999, Aizawa et al., 1999). Characterisation of the distinct actin subpopulations, similar to that conducted for WAS DCs in Chapter 4, would be valuable.

Imaging migration in vivo or cell adhesion under flow, for example using flow chambers, may be helpful for both *MKL-1* and *WDR1* studies, to provide more physiologically relevant quantification of these processes. Further, mouse models, such as the *MKL1*^{-/-} model developed by Li *et al* (Li et al., 2006), would be useful for more regular investigations into other cellular processes, including NK or CD8 cell killing, macrophage phagocytosis, humoral immunity, as well as antigen presentation and IS formation.

Finally, *Dock8* deficiency is the best described of the three immunodeficiencies presented in this chapter. In 2009, *DOCK8* was independently described as the cause of severe immune deficiency in both humans and mice (Randall et al., 2009, Zhang et al., 2009, Engelhardt et al., 2009). Initially, yeast two-hybrid screens showed *DOCK8* interaction with Cdc42 (Ruusala and

Aspenstrom, 2004). More recently, this has been confirmed using pull down experiments and was shown to be important for DC migration (Harada et al., 2012). As Cdc42 is a potential WASp activator, DOCK8 deficiency is interesting to study as an example of an upstream defect or disruption in the Arp2/3-dependent actin polymerisation pathway.

In contrast to WAS conjugates, in which ICAM-1 polarisation was defective (Fig 3.11), in DOCK8 DCs this was shown to be normal, albeit in very few cells (Fig 6.10). This suggests that WASp is essential for ICAM-1 localisation; however WASp, or Cdc42, may be activated via a DOCK8-independent pathway. For example, Cdc42 could be activated by other GEFs such as Dbp and Vav1 (Schmidt and Hall, 2002), or WASp activation may be unnecessary for correct ICAM-1 polarisation. The latter argument supports results obtained from FYN DC in Chapter 3, where it appears the presence of WASp alone, without activation through phosphorylation, is enough to restore most ICAM-1 polarisation (see Chapter 3 discussion).

Furthermore, although the Dock8 DCs show normal ICAM-1 polarisation, they are unable to induce correct T cell MTOC polarisation in the interacting T cell. This suggests that the ICAM-1-LFA-1 interaction is not essential for this process, although an LFA-1 stain of the Dock8 conjugates would be required to confirm that ICAM-1 polarisation in Dock8 DCs leads to LFA-1 polarisation in T cells, similar to that seen in BL6 conjugates. Although LFA-1 has been suggested to play a role in MTOC docking (De Clercq et al., 2013b), results presented here show there is some uncoupling between the ICAM-1-LFA-1 interaction and MTOC translocation. This is the case in Dock8 DCs in this chapter; as well as FYN DCs in Chapter 3, which polarise ICAM-1 correctly but show only limited recovery of MTOC polarisation (Fig 3.11, 3.12).

Despite correct ICAM-1 localisation, Dock8 DCs do form fewer conjugates with T cells in vitro (Fig 6.10), suggesting there is some defect in the stability of the conjugates. It would be interesting to examine this further using serial block face SEM (similar to WAS in Fig 3.15) to determine whether the size of the adhesion area between the two cells is affected. Further,

since ICAM-1 polarisation, and presumably its synapse function, are normal in Dock8 DCs, it would also be intriguing to study their interaction with lipid bilayers to see if ICAM-1-dependent podosomes are formed and organised as described for BL6.

In summary, the data presented here provides strong support for the crucial role of actin regulators in the immune system. The MKL-1 patient presented with *Pseudomonas* septic shock associated with meningitis, otitis media, and multiple cutaneous and subcutaneous abscesses. The *WDR1* mutation appears to lead to episodes of unprovoked inflammation and thrombocytopenia. The defective cytoskeletal function in both these patients results in abnormal migration, cell-cell interaction and phagocytosis, all of which can be related to the clinical symptoms observed.

The clinical characteristics of Dock8 deficiency include severe food or environmental allergies, otitis media, pneumonia or bronchitis and cutaneous viral infections (Zhang et al., 2009, Chu et al., 2012). Susceptibility to viral infections is also seen in other PIDs such as WAS (Modiano et al., 1995, Saijo et al., 1998, Artac et al., 2010). As in WAS, the increased susceptibility to viral infections could be the result of a combination of factors including defective skin barrier, reduced numbers of T cell, impaired T cell proliferation and antiviral cytokine production, and abnormal migration into infected tissues (Zhang et al., 2010). Other symptoms described in Dock8 deficiency, such as rash, elevated IgE and susceptibility to autoimmunity, are very similar to those described in WAS (Thrasher and Burns, 2010). Similar to WAS, the disease pathology is likely to be the result of a combination of cellular defects including the inability of B cells to generate high-affinity antibodies; the absence of T cell memory; defects in DC migration and capacity to prime T cells; as well as reduced NK cell cytotoxicity. As an effector of the Rho GTPase Cdc42, WASp presumably acts downstream of DOCK8 and the similar clinical manifestations may reflect the overlapping signalling pathways. While WASp function may also be diminished in DOCK8 patients, this cannot explain the complete phenotype of DOCK8 patients and data presented in this chapter suggests that WASp can be activated by

Dock8-independent pathways. Unlike WAS, DOCK8 expression is not restricted to the haematopoietic system, it would be interesting to see whether reconstitution of the immune system would correct disease pathology. Further, in mice DOCK8 mutations replicate many of the cellular defects described while the animals show no obvious clinical phenotype, similar to WAS knockout animals (Snapper et al., 1998, Zhang et al., 1999).

Deficiencies in all three major components of Rho GTPase signalling have been described: the effectors, such as WASp, the GTPases, such as Rac2, and the upstream modulators, such as DOCK8 (actin-related PIDs reviewed in (Moulding et al., 2013)). While this pathway appears essential, novel immunodeficiencies have been described to results from mutations in other pathways, such as MKL-1 and WDR1 presented here. These two actin regulating proteins, through their roles in controlling actin dynamics, are crucial to the normal functioning of immune cells and themselves provide unique opportunities for research to better understand the role of the actin cytoskeleton in immunity.

Chapter 7 – Discussion

Our knowledge of the immunological synapse and its role in T cell activation has improved greatly over the last couple of decades (Smith-Garvin et al., 2009). How cells form stable interactions, which have a role in intercellular signalling, is an important question in cell biology and the field of immunology in particular. The actin and microtubule arms of the cytoskeleton play key roles in IS formation in the obligatorily mobile immune cells. Most studies have focused on the T cell side and several groups have shown the importance of the actin cytoskeleton in this process (Bunnell et al., 2001, Babich et al., 2012, Beemiller et al., 2012). Although many of the cytoskeletal regulators are conserved, their precise interactions, effectors and functions may differ between cell types.

WASp deficiency results in a more fluid, unstable DC synapse

In T cells, it has been suggested that L-plastin, a leukocyte-specific actin bundling protein, interacts with LFA-1 and through its recruitment to the IS and F-actin bundling activities is able to stabilise and cluster LFA-1 at this site. Disrupting L-plastin function led to a decrease in LFA-1 phosphorylation and synaptic localisation; thus leading to abnormal MTOC docking, IL-2 secretion and proliferation (De Clercq et al., 2013b). This supported previous evidence that L-plastin plays a crucial role in recruitment of LFA-1 and full T cell activation (Wang et al., 2010, Wabnitz et al., 2010). De Clercq *et al* suggest that L-plastin may be involved in converting the diffuse cSMAC cytoskeleton into the longer-filament, tightly-bundled network required in the pSMAC (De Clercq et al., 2013b). L-plastin phosphorylation enhances its bundling activity,

resulting in an increasingly 'opaque' actin network, which increases LFA-1 stabilisation and activation (De Clercq et al., 2013b). In agreement with this, they show a reduction in IS length and surface area in T cells with disrupted L-plastin function, suggesting that T cells are unable to generate a normal pSMAC. The authors however, do not investigate distinct c- and p-SMAC compositions in these synapses.

Their results are remarkably similar to the reduced LFA-1 polarisation and decreased IS contact area in WAS DCs, presented here in Chapter 3. Similarly functional differences, including MTOC docking, IL-2 secretion and proliferation, were also seen as a result of poor IS formation by WAS DC, as described in Chapter 5. This clearly highlights a role for LFA-1 in the correct organisation of the synapse interface during T cell activation; incorrect localisation of LFA-1, whether through a cell-intrinsic mechanism (L-plastin dysregulation) or an external driving force (incorrect ICAM-1 localisation) leads to abnormal synapse formation and function.

It is possible that the two pathways interact across the cell interface. If WASp-deficiency disrupts ICAM-1 localisation in the DC and this results in fewer, less organised LFA-1 interactions, less L-plastin may be recruited on the T cell side of the synapse leading to a less bundled actin and less LFA-1 clustering and stabilisation. Results presented in Chapter 4 only consider the dynamics of the actin cytoskeleton in the dendritic cell though it would be interesting to further investigate cytoskeletal dynamics in the WAS DC-induced T cells. As LFA-1 has been highlighted as a crucial player in both adhesion and signalling between T cells and APCs, for example through JAB-1 and cytohesin-1 (Perez et al., 2003), it would also be beneficial to study the integrity of these pathways in T cells induced by WAS DCs.

The results in Chapter 3 confirm previous observations from the group. WAS DCs were shown to form shorter-lasting contacts with OT-II T cells and induce less proliferation and calcium fluctuation of T cells compared to control BL6 DCs (Fig 4.2, 5.2, (Bouma et al., 2011)). Some differences in MTOC polarisation were also previously observed (Bouma et al., 2011), though these were not significant. Improved staining protocols in this thesis have confirmed this

difference and allowed analysis of statistical significance (Fig 3.12). The decreased IL-12 production by WAS DCs reported by FACS (Bouma et al., 2011) has also been confirmed using microarray analysis (Fig 5.14); though the paper also considers IL-12 in FYN DC samples, which was not analysed by microarrays here. Finally, the defects in LFA-1 polarisation and bulls eye pattern formation were also affirmed (Fig 3.9, 4.9 and (Bouma et al., 2011)).

Further to these findings, results in Chapter 3 show defective ICAM-1 polarisation in WAS DCs (Fig 3.11), which is implicated in the abnormal organisation of its ligand LFA-1 and the symmetric IS interface. Experiments in Chapter 3 also utilised electron microscopy to improve imaging resolution and allow the quantification of contact surface area between the T cell and DC, which is severely reduced in WAS (Fig 3.16).

The reduced contact area and defect in integrin polarisation towards the synapse in WAS DCs are in agreement with a less stable actin network (as shown by FRAP, Fig 4.8) and the inability of WAS DCs to form stable adhesion structures using dynamic podosomes (Fig 4.20). On a molecular level, these results suggest that WASp stabilises the actin cytoskeleton upon IS formation, in a manner exhibiting dynamics distinct from the steady state cortex (see FRAP results and discussion). This of course could translate into defects in macromolecular organisation in WAS DCs, for example, an inability of this fluid, disorganised actin network to stabilise molecular complexes and clusters required for signal transduction. Eventually, at the cellular level, this could result in reduced adhesion forces (due to decreased integrin clustering) and/or reduced signalling (due to lower local concentration and stability of peptide-MHC complexes or costimulatory molecules).

As discussed in Chapter 3, LFA-1 may also play a role in MTOC polarisation towards the IS (Yi et al., 2013), both of which are abnormal in T cells contacting WAS DCs. In contact with FYN DCs however, T cells are able to polarise LFA-1 and form extensive contacts with the DC, yet MTOC polarisation is not recovered completely, suggesting an LFA-1-independent mechanism may also be required.

It should be noted that CD4 cells also show some directional secretion, similar to CD8 and NK cells (Huse et al., 2006). IFN γ secretion was microtubule-dependent and polarised towards the synapse; this may serve to activate APC in antigen-specific manner (Boehm et al., 1997). By contrast, TNF secretion was multidirectional as TNF can act on a range of cell types to induce an inflammatory response (Locksley et al., 2001). The directional secretion pathway may be regulated by MTOC docking. WASp-deficient Th1 cells (which are unable to polarise their MTOC towards the IS) have been shown to secrete chemokines but not IFN γ (Morales-Tirado et al., 2004). It would be interesting to see if this is also the case in T cells where lack of MTOC polarisation is not the result of intrinsic WASp deficiency but that of irregular IS organisation. Combined, these results highlight a synapse-specific link between the actin and microtubule cytoskeletons.

Despite slower 'cSMAC' formation by WAS DCs (Fig 4.14, 4.17, 4.18), their T cell inductive capacity was lower. T cell induced by WAS DCs exhibited less proliferation and IL-2 secretion (Fig 5.3 and 5.4), suggesting lower levels of successful TCR activation and downstream signalling, though specific signalling complexes or phosphorylation were not investigated. This may be the result of asymmetric pSMAC organisation, or the macromolecular interface instability and fluidity discussed earlier. If one assumes that TCR organisation mirrors that of peptide-MHC observed, these results confirm that speed of TCR microcluster translocation, or their maintenance in the periphery are not the only determinants of downstream signalling. Further, differences in IS organisation clearly have a functional impact on T cell activation; and show small but measurable effects on T helper cell differentiation (Chapter 5).

Novel adhesive structures at the IS

The presence of podosomes in the DC: bilayer model interface was unexpected. Podosomes are cylindrical protrusions, formed on the ventral side of adherent cells. They are around 0.2-1 μ m in diameter with a central core of F-actin and a characteristic ring of vinculin, talin and β 2

or $\beta 3$ integrins (Gavazzi et al., 1989, DeFife et al., 1999, Linder and Aepfelbacher, 2003). These structures are known to be highly dynamic, with a turnover rate measured in seconds or minutes (Stickel and Wang, 1987, Kanehisa et al., 1990). Their precise function is less clear though they have been implicated in cell adhesion to some substrates, providing friction forces to allow migration, or linking intracellular cytoskeletal components to ECM and cell-cell adhesions (Gaidano et al., 1990, Burns et al., 2004). Although, podosomes have mainly been described in cells of the myeloid lineage, such as macrophages, DCs and osteoclasts; it is likely that in vivo, these structures have much more varied roles, in a large range of cell lineages. For example, lymphocytes have been shown to form podosomes, both in vitro and in vivo, followed by more extensive “invasive podosomes”, which were required for transcellular diapedesis (through individual microvascular endothelial cells) (Carman et al., 2007). Although, it could be argued that these are similar to invadopodia, their average size as well as highly dynamic assembly and disassembly (tens of seconds) is more consistent with podosomes. It is unclear whether podosomes have a precursor role in invadopodia formation, or whether podosomes are required at the site of invadopodia formation (perhaps to stabilise cell-cell interaction while the invading cell finds the path of least resistance for pore formation and diapedesis). The authors suggest that the sizes of protrusions exhibit a continuous rather than bimodal distribution, which would suggest a “continuum of related protrusive structures rather than the existence of categorically distinct ones” (Carman et al., 2007).

Carman *et al* also found an enrichment of vesicles in endothelial cells adjacent to sites of podosome formation (Carman et al., 2007). It is possible that podosome formation, and the subsequent downstream signalling e.g. tyrosine phosphorylation (Gavazzi et al., 1989), may play a role in vesicle transport or recruitment/ activation of fusogenic proteins. Vesicles, in turn, may play distinct roles in different cell-cell contacts, for example, increasing plasma membrane surface area to allow pore formation during diapedesis. It would be interesting to investigate where similar vesicle clustering occurs beneath the DC synapse interface and whether these are involved in the release of cytokines for optimal T cell activation.

Confocal imaging studies of DC: T cell conjugates presented here do not provide evidence for the existence of podosomes at the interface, though this may be explained by the insufficient resolution achieved by z-stack interface reconstructions. There is evidence however, for extensive “invasive podosomes” from the T cell into the DC (own EM data, (Ueda et al., 2011)). One possibility is that this type of adhesion is more common than expected and is in fact what mediates the initial contact for several cell-cell interactions, including the immunological synapse. Further signals such as, costimulatory receptors and cytokines may be responsible for organising the final functional structure. Cell: cell contacts may not require formation of a stabilising podosome structure *in vitro*; which may be crucial for cell interactions between DCs and T cells migrating through the lymphatics and lymph node structures. Alternatively, podosomes may not be required *in vivo* but may be an artefact of interaction with a non-deformable membrane. Optimisation of imaging techniques including micropits, optical tweezers or multi-photon microscopy may shed light on the relevance of these structures *in vivo* (or *in vitro* in cell: cell contacts).

Microtubules have been implicated in the regulation of podosome formation and patterning (Linder et al., 2000, Babb et al., 1997, Destaing et al., 2003). Destaing *et al* suggest that microtubules promote stability of the mature podosome belt in osteoclasts but are not required for the initial podosome ring or cluster formation (Destaing et al., 2003). The authors use reversible nocodazole-mediated microtubule disruption to show podosome belt collapse but do not investigate the localisation of the osteoclast MTOC. It is interesting to note that the DC MTOC does not polarise towards the IS in DC: T cell conjugates. Future experiments could probe MTOC localisation in DCs interacting with supported bilayers, or the effects of nocodazole treatment on synaptic podosome rings.

The synapse/ kinapse model has been a key to understanding how migrating T cells reorganise their cytoskeleton and surface receptors to produce symmetric contact interfaces (Dustin, 2007). In keeping with this model, Dock2 has been shown to play a role both at the leading

edge, during leukocyte migration (Fukui et al., 2001, Nishikimi et al., 2009), and at the IS, during T cell activation (Le Floc'h et al., 2013). Interestingly, the different mechanisms have been proposed for Dock2 accumulation at the two distinct locations. At the leading edge, Dock2 is regulated by phosphatidic acid (Nishikimi et al., 2009), while at the IS, the majority of Dock2 recruitment is through interaction with PIP3. This is one example of different activators or signal transducers used to differentiate between cellular processes that may use similar pathways or effectors. A similar strategy may be at play on the DC side, where talin and vinculin rings (characteristic of adhesive podosomes) did not show the same organisation in the synapse (Chapter 4). As podosomes may be crucial for both migration and adhesion during IS formation, their structural proteins may be the same (actin, WASp, β 2 integrins), but their activators or binding partners (e.g. vinculin) may differ. Podosomes at the IS have a different, annular organisation compared to the clusters found at the leading edge, which is consistent with the formation of a symmetrical structure.

As discussed earlier, podosomes have been described primarily in the context of myeloid cells, however, there is evidence for their existence in other cells, including primary lymphocytes (Carman et al., 2007) and B cell lines (Redondo-Munoz et al., 2006). Further investigation is required into the structure, dynamics, regulators, effectors and other components of these podosomes. Based on podosomal structures seen at the synapse, these results strongly suggest that podosomes are more versatile in structure and function than originally expected and that they may be differentially regulated depending on the cell lineage, environment cues or cellular context and other surface molecules or downstream signalling present.

Several groups have reported that organised assembly of podosome components is strongly dependent on WASp (Linder et al., 1999, Burns et al., 2001, Jones et al., 2002, Calle et al., 2004, Linder and Aepfelbacher, 2003, Olivier et al., 2006). In agreement with this, no podosomes were observed in WAS-deficient primary murine DCs on supported lipid bilayers.

More to achieve at the IS

In an organism, T cell motility is most likely irregular and not as uniform as predicted; some T cells may meet a DC presenting sufficient antigen and form a stable attachment immediately, others may remain dynamic for a much longer time. The precise interactions are most likely dependent on many factors including the initial speed of T cell migration, the number of specific TCRs present on its surface, the polarity/orientation of the T cell, the number of pMHCs available, the flexibility of the DC membrane, integrin activation status, the location within the lymph node and the cytokine milieu. Such a heterogeneous response may explain why different studies observe different interactions or requirements over time both *in vitro* and *in vivo*.

A complete picture of immunological synapses would require the localisation of many other actin-regulating proteins such as capping or severing proteins, bundling proteins, polymerisation and depolymerisation regulators. Further, most IS studies consider actin as 2D network, for example focusing on filaments running in the plane of the interface only, which does not take into account the dynamics or function of other actin subpopulations. Improvements in super resolution microscopy allow researchers to probe these more deeply and investigate actin directionality or the contribution of different molecular populations to overall structure and function (Smith et al., 2013b, Oddos et al., 2008, Williamson et al., 2011).

Further investigation of lipid composition is also required. The involvement of lipid messengers in IS organisation is apparent, for example the DAG-dependent polarisation of the MTOC or the recruitment of Dock2 by PIP3 (Quann et al., 2009, Le Floc'h et al., 2013). These mechanisms can provide quick gradients of the messenger required, which are sensitive to change and thus ideal for regulating dynamic cytoskeletal structures.

More questions remain regarding the MTOC polarisation and docking signals as well as the cooperation between the actin and microtubule cytoskeletons at the IS. It is clear however that many dynamic regulators are involved to achieve spatial and temporal regulation.

Wiskott-Aldrich syndrome

The IS has been described as a 'knowledge' transfer facility, which can transfer information through its structure, its dynamics and the context (Xie et al., 2013). Results presented here strongly support this idea and show that the transfer of information is disrupted as a result of deregulated actin in WAS cells.

Although it is helpful and necessary to focus on individual cell-cell contacts, it is important to remember that the immune system involves a complicated range of different cell interactions (previously described as 'immunological circuits' – (Gerard et al., 2013)). There is evidence for autocrine and paracrine stimulation of T cells, B cells and DCs (Sabatos et al., 2008, Tadokoro et al., 2006, Okada et al., 2005, Itano et al., 2003). This suggests many other cell-cell interactions are involved in determining the overall immune response.

Deregulated DC actin and poorly formed conjugates are also likely to affect T cell repriming directly, as well as T cell clustering, T:T communication or downregulation of T cell responses. If WAS DCs are unable to stably interact with several T cells and cluster these as seen in normal DCs (Bousso and Robey, 2003), T:T cell interactions may have altered efficiency or capacity for activation. T:T synapses are considered to play a role in T cell expansion, activation and differentiation; as well as the regulation of a balanced immune response by inducing T cell suppression or apoptosis (Thummler et al., 2010, Collison et al., 2009, Helft et al., 2008, Lenardo, 1991, Mempel et al., 2006).

Other cells also play a role in augmenting the response. It is known that innate signals are crucial for both optimal activation and pathogen-specific priming of DCs, which in turn determines the precise adaptive immune response initiated (Kapsenberg, 2003, Corthay, 2006). As WASp-deficiency affects both the innate and adaptive arms of an immune response, it is likely that many cell-intrinsic and externally-activated pathways are disturbed, resulting in the complex disease. Thus the reduced priming capacity of WAS DCs, resulting in poor

activation and disturbed helper cell fate balance of T cells is only one component of the deregulated circuit.

Cellular defects in WAS are often not clear cut in vitro. Phagocytosis, particular antigen presentation and humoral immunity are all decreased but not abolished (Leverrier et al., 2001, Westerberg et al., 2003, Westerberg et al., 2005). Similarly, in this thesis, WAS DCs are shown to form some synapses, albeit fewer, shorter and more disorganised. This suggests there may be some redundancy in regulatory pathways, for example, some functions may be compensated by proteins such as N-WASp; however this is insufficient to restore individual cell function and, as discussed above, small cellular defects would be compounded in the whole organism immune response.

Reconstitution of WASp expression in several cell lineages, including T, NKT and B cells but not myeloid cells, has been shown to confer a selective survival or homing advantage to the WASp-expressing cells compared to their deficient counterparts (Meyer-Bahlburg et al., 2008, Westerberg et al., 2008). Studies into the myeloid functions of WAS therefore are crucial as they may have important consequences for patients who show limited myeloid reconstitution after gene therapy or bone marrow transplants.

Actin in the immune system

The importance of actin in the immune system is highlighted by the number of actin-related immunodeficiencies and by the fact that several actin regulators or adhesion proteins are expressed exclusively in immune cells.

Deficiencies in all three major components of Rho GTPase signalling pathway have been described: the effectors, such as WASp, the GTPases, such as Rac2, and the upstream modulators, such as DOCK8 (Moulding et al., 2013). The murine Dock8 deficiency investigated in Chapter 6 shows many cellular defects similar to WAS. Dock8 DCs form fewer stable

conjugates and are unable to induce T cell MTOC polarisation. In contrast to WAS DCs, cells deficient in this upstream regulator are able to polarise ICAM-1 to the IS, suggesting that WASp, or Cdc42, in these cells may be activated by a different mechanism. Alternatively, ICAM-1 polarisation may require WASp expression but not its function in actin nucleation. Although Dock8 DCs show normal ICAM-1 polarisation, and T cell LFA-1 polarisation would be expected to mimic this, MTOC migration is not restored, suggesting the requirement of an LFA-1-independent mechanism in this process.

Although much remains to be characterised in the Dock8-deficient mice, results here show that, similar to WAS, the abnormal synapse formed by Dock8 DCs results in perturbed cytokine secretion, in particular affecting IL-2 and IFN γ . This highlights a role for DCs in correct synapse organisation and function, which depends on actin regulation through the WASp and Rho GTPase pathway.

Chapter 6 also presents results from two other actin-related immune defects – MKL-1 and AIP1. These have shown that actin deregulation, whether through increased or decreased total F-actin content, can have very severe adverse effects on basic immune cell functions. These mutations highlight the large number and diversity of actin-regulating pathways involved in dendritic cell migration and adhesion; and provide useful models for studying actin dynamics and contribution to many other cellular processes.

References

- ABDI, K. 2002. IL-12: The role of p40 versus p75. *Scandinavian Journal of Immunology*, 56, 1-11.
- ABDI, K., SINGH, N. & MATZINGER, P. 2006. T-cell control of IL-12p75 production. *Scandinavian Journal of Immunology*, 64, 83-92.
- ABDUL-MANAN, N., AGHAZADEH, B., LIU, G. A., MAJUMDAR, A., OUERFELLI, O., SIMINOVITCH, K. A. & ROSEN, M. K. 1999. Structure of Cdc42 in complex with the GTPase-binding domain of the 'Wiskott-Aldrich syndrome' protein. *Nature*, 399, 379-383.
- ABRAHAM, C., GRIFFITH, J. & MILLER, J. 1999. The dependence for leukocyte function-associated antigen-1/ICAM-1 interactions in T cell activation cannot be overcome by expression of high density TCR ligand. *Journal of Immunology*, 162, 4399-4405.
- ABRAM, C. L. & LOWELL, C. A. 2007. The expanding role for ITAM-based signaling pathways in immune cells. *Sci STKE*, 2007, re2.
- ACHARD, V., MARTIEL, J. L., MICHELOT, A., GUERIN, C., REYMANN, A. C., BLANCHOIN, L. & BOUJEMAA-PATERSKI, R. 2010. A "Primer"-Based Mechanism Underlies Branched Actin Filament Network Formation and Motility. *Current Biology*, 20, 423-428.
- ACUTO, O. & MICHEL, F. 2003. CD28-mediated co-stimulation: A quantitative support for TCR signalling. *Nature Reviews Immunology*, 3, 939-951.
- AHMED, K. A., MUNEGOWDA, M. A., XIE, Y. & XIANG, J. 2008. Intercellular trogocytosis plays an important role in modulation of immune responses. *Cellular & molecular immunology*, 5, 261-9.
- AIZAWA, H., KATADAE, M., MARUYA, M., SAMESHIMA, M., MURAKAMI-MUROFUSHI, K. & YAHARA, I. 1999. Hyperosmotic stress-induced reorganization of actin bundles in Dictyostelium cells over-expressing cofilin. *Genes to Cells*, 4, 311-324.
- AKIN, O. & MULLINS, R. D. 2008. Capping protein increases the rate of actin-based motility by promoting filament nucleation by the Arp2/3 complex. *Cell*, 133, 841-851.
- AL-ALWAN, M. M., ROWDEN, G., LEE, T. D. & WEST, K. A. 2001. The dendritic cell cytoskeleton is critical for the formation of the immunological synapse. *J Immunol*, 166, 1452-6.
- AL KHATIB, S., KELES, S., GARCIA-LLORET, M., KARAKOC-AYDINER, E., REISLI, I., ARTAC, H., CAMCIOGLU, Y., COKUGRAS, H., SOMER, A., KUTUKCULER, N., YILMAZ, M., IKINCIOLLARI, A., YEGIN, O., YUKSEK, M., GENEL, F., KUCUKOSMANOGLU, E., BAKI, A., BAHCECILER, N. N., RAMBHATLA, A., NICKERSON, D. W., MCGHEE, S., BARLAN, I. B. & CHATILA, T. 2009. Defects along the T(H)17 differentiation

- pathway underlie genetically distinct forms of the hyper IgE syndrome. *J Allergy Clin Immunol*, 124, 342-8, 348 e1-5.
- ALAKOSKELA, J. M., KONER, A. L., RUDNICKA, D., KOHLER, K., HOWARTH, M. & DAVIS, D. M. 2011. Mechanisms for Size-Dependent Protein Segregation at Immune Synapses Assessed with Molecular Rulers. *Biophysical Journal*, 100, 2865-2874.
- ALARCON, B., MESTRE, D. & MARTINEZ-MARTIN, N. 2011. The immunological synapse: a cause or consequence of T-cell receptor triggering? *Immunology*, 133, 420-5.
- ALBERT, M. H., BITTNER, T. C., NONOYAMA, S., NOTARANGELO, L. D., BURNS, S., IMAI, K., ESPANOL, T., FASTH, A., PELLIER, I., STRAUSS, G., MORIO, T., GATHMANN, B., NOORDZIJ, J. G., FILLAT, C., HOENIG, M., NATHRATH, M., MEINDL, A., PAGEL, P., WINTERGERST, U., FISCHER, A., THRASHER, A. J., BELOHRADSKY, B. H. & OCHS, H. D. 2010. X-linked thrombocytopenia (XLT) due to WAS mutations: clinical characteristics, long-term outcome, and treatment options. *Blood*, 115, 3231-3238.
- ALTIN, J. G. & SLOAN, E. K. 1997. The role of CD45 and CD45-associated molecules in T cell activation. *Immunology and Cell Biology*, 75, 430-445.
- AMBERG, D. C., BASART, E. & BOTSTEIN, D. 1995. Defining Protein Interactions with Yeast Actin in-Vivo. *Nature Structural Biology*, 2, 28-35.
- AMSEN, D., BLANDER, J. M., LEE, G. R., TANIGAKI, K., HONJO, T. & FLAVELL, R. A. 2004. Instruction of distinct CD4 T helper cell fates by different notch ligands on antigen-presenting cells. *Cell*, 117, 515-526.
- ANCLIFF, P. J., BLUNDELL, M. P., CORY, G. O., CALLE, Y., WORTH, A., KEMPSKI, H., BURNS, S., JONES, G. E., SINCLAIR, J., KINNON, C., HANN, I. M., GALE, R. E., LINCH, D. C. & THRASHER, A. J. 2006. Two novel activating mutations in the Wiskott-Aldrich syndrome protein result in congenital neutropenia. *Blood*, 108, 2182-9.
- ANDZELM, M. M., CHEN, X., KRZEWSKI, K., ORANGE, J. S. & STROMINGER, J. L. 2007. Myosin IIA is required for cytolytic granule exocytosis in human NK cells. *Journal of Experimental Medicine*, 204, 2285-2291.
- ANIKEEVA, N., SOMERSALO, K., SIMS, T. N., THOMAS, V. K., DUSTIN, M. L. & SYKULEV, Y. 2005. Distinct role of lymphocyte function-associated antigen-1 in mediating effective cytolytic activity by cytotoxic T lymphocytes. *Proceedings of the National Academy of Sciences of the United States of America*, 102, 6437-6442.
- ANTON, I. M., LU, W. G., MAYER, B. J., RAMESH, N. & GEHA, R. S. 1998. The Wiskott-Aldrich syndrome protein-interacting protein (WIP) binds to the adaptor protein Nck. *Journal of Biological Chemistry*, 273, 20992-20995.
- ARTAC, H., GOKTURK, B., BOZDEMIR, S. E., TOY, H., VAN DER BURG, M., SANTISTEBAN, I., HERSHFELD, M. & REISLI, I. 2010. Late-onset adenosine deaminase deficiency presenting with Heck's disease. *Eur J Pediatr*, 169, 1033-6.
- ASPENSTROM, P., LINDBERG, U. & HALL, A. 1996. Two GTPases, cdc42 and rac, bind directly to a protein implicated in the immunodeficiency disorder Wiskott-Aldrich syndrome. *Current Biology*, 6, 70-75.

- AZUMA, M., CAYABYAB, M., BUCK, D., PHILLIPS, J. H. & LANIER, L. L. 1992. Cd28 Interaction with B7-Costimulates Primary Allogeneic Proliferative Responses and Cytotoxicity Mediated by Small, Resting Lymphocytes-T. *Journal of Experimental Medicine*, 175, 353-360.
- BABB, S. G., MATSUDAIRA, P., SATO, M., CORREIA, I. & LIM, S. S. 1997. Fimbrin in podosomes of monocyte-derived osteoclasts. *Cell Motility and the Cytoskeleton*, 37, 308-325.
- BABICH, A., LI, S. X., O'CONNOR, R. S., MILONE, M. C., FREEDMAN, B. D. & BURKHARDT, J. K. 2012. F-actin polymerization and retrograde flow drive sustained PLC gamma 1 signaling during T cell activation. *Journal of Cell Biology*, 197, 775-787.
- BADOUR, K., ZHANG, J., SHI, F., LENG, Y., COLLINS, M. & SIMINOVITCH, K. A. 2004. Fyn and PTP-PEST-mediated regulation of Wiskott-Aldrich syndrome protein (WASp) tyrosine phosphorylation is required for coupling T cell antigen receptor engagement to WASp effector function and T cell activation. *J Exp Med*, 199, 99-112.
- BADOUR, K., ZHANG, J., SHI, F., MCGAVIN, M. K., RAMPERSAD, V., HARDY, L. A., FIELD, D. & SIMINOVITCH, K. A. 2003. The Wiskott-Aldrich syndrome protein acts downstream of CD2 and the CD2AP and PSTPIP1 adaptors to promote formation of the immunological synapse. *Immunity*, 18, 141-54.
- BAI, M., MISSEL, A. R., LEVINE, A. J. & KLUG, W. S. 2011. On the role of the filament length distribution in the mechanics of semiflexible networks. *Acta Biomaterialia*, 7, 2109-2118.
- BALAGOPALAN, L., BARR, V. A., KORTUM, R. L., PARK, A. K. & SAMELSON, L. E. 2013. Cutting Edge: Cell Surface Linker for Activation of T Cells Is Recruited to Microclusters and Is Active in Signaling. *Journal of Immunology*, 190, 3849-3853.
- BAMBURG, J. R., MCGOUGH, A. & ONO, S. 1999. Putting a new twist on actin: ADF/cofilins modulate actin dynamics. *Trends in Cell Biology*, 9, 364-370.
- BANCHEREAU, J. & STEINMAN, R. M. 1998. Dendritic cells and the control of immunity. *Nature*, 392, 245-52.
- BANERJEE, P. P., PANDEY, R., ZHENG, R., SUHOSKI, M. M., MONACO-SHAWVER, L. & ORANGE, J. S. 2007. Cdc42-interacting protein-4 functionally links actin and microtubule networks at the cytolytic NK cell immunological synapse. *Journal of Experimental Medicine*, 204, 2305-2320.
- BANIN, S., TRUONG, O., KATZ, D. R., WATERFIELD, M. D., BRICKELL, P. M. & GOUT, I. 1996. Wiskott-Aldrich syndrome protein (WASp) is a binding partner for c-Src family protein-tyrosine kinases. *Current Biology*, 6, 981-988.
- BARDA-SAAD, M., BRAIMAN, A., TITERENCE, R., BUNNELL, S. C., BARR, V. A. & SAMELSON, L. E. 2005. Dynamic molecular interactions linking the T cell antigen receptor to the actin cytoskeleton. *Nature Immunology*, 6, 80-89.
- BARDA-SAAD, M., SHIRASU, N., PAUKER, M. H., HASSAN, N., PERL, O., BALBO, A., YAMAGUCHI, H., HOUTMAN, J. C., APPELLA, E., SCHUCK, P. & SAMELSON, L. E.

2010. Cooperative interactions at the SLP-76 complex are critical for actin polymerization. *The EMBO journal*, 29, 2315-28.
- BARTOLINI, F., MOSELEY, J. B., SCHMORANZER, J., CASSIMERIS, L., GOODE, B. L. & GUNDERSEN, G. G. 2008. The formin mDia2 stabilizes microtubules independently of its actin nucleation activity. *Journal of Cell Biology*, 181, 523-536.
- BATISTA, F. D., IBER, D. & NEUBERGER, M. S. 2001. B cells acquire antigen from target cells after synapse formation. *Nature*, 411, 489-494.
- BEAL, A. M., ANIKEEVA, N., VARMA, R., CAMERON, T. O., VASILIVER-SHAMIS, G., NORRIS, P. J., DUSTIN, M. L. & SYKULEV, Y. 2009. Kinetics of Early T Cell Receptor Signaling Regulate the Pathway of Lytic Granule Delivery to the Secretory Domain. *Immunity*, 31, 632-642.
- BEDFORD, P. A., BURKE, F., STAGG, A. J. & KNIGHT, S. C. 2008. Dendritic cells derived from bone marrow cells fail to acquire and present major histocompatibility complex antigens from other dendritic cells. *Immunology*, 124, 542-552.
- BEMILLER, P., JACOBELLI, J. & KRUMMEL, M. F. 2012. Integration of the movement of signaling microclusters with cellular motility in immunological synapses. *Nature Immunology*, 13, 787-+.
- BEGG, D. A., RODEWALD, R. & REBHUN, L. I. 1978. Visualization of Actin Filament Polarity in Thin-Sections - Evidence for Uniform Polarity of Membrane-Associated Filaments. *Journal of Cell Biology*, 79, 846-852.
- BELTZNER, C. C. & POLLARD, T. D. 2008. Pathway of actin filament branch formation by Arp2/3 complex. *Journal of Biological Chemistry*, 283, 7135-7144.
- BENVENUTI, F., HUGUES, S., WALMSLEY, M., RUF, S., FETLER, L., POPOFF, M., TYBULEWICZ, V. L. J. & AMIGORENA, S. 2004a. Requirement of Rac1 and Rac2 expression by mature dendritic cells for T cell priming. *Science*, 305, 1150-1153.
- BENVENUTI, F., LAGAUDRIERE-GESBERT, C., GRANDJEAN, I., JANCIC, C., HIVROZ, C., TRAUTMANN, A., LANTZ, O. & AMIGORENA, S. 2004b. Dendritic cell maturation controls adhesion, synapse formation, and the duration of the interactions with naive T lymphocytes. *Journal of immunology*, 172, 292-301.
- BERTHIER, R., MARTINON-EGO, C., LAHARIE, A. M. & MARCHE, P. N. 2000. A two-step culture method starting with early growth factors permits enhanced production of functional dendritic cells from murine splenocytes. *Journal of Immunological Methods*, 239, 95-107.
- BERTRAND, F., ESQUERRE, M., PETIT, A. E., RODRIGUES, M., DUCHEZ, S., DELON, J. & VALITUTTI, S. 2010. Activation of the Ancestral Polarity Regulator Protein Kinase C zeta at the Immunological Synapse Drives Polarization of Th Cell Secretory Machinery toward APCs. *Journal of Immunology*, 185, 2887-2894.
- BETTELLI, E., KORN, T. & KUCHROO, V. K. 2007. Th17: the third member of the effector T cell trilogy. *Current Opinion in Immunology*, 19, 652-657.
- BHUWANIA, R., CORNFINE, S., FANG, Z. Y., KRUGER, M., LUNA, E. J. & LINDER, S. 2012. Supervillin couples myosin-dependent contractility to podosomes and enables their turnover. *Journal of Cell Science*, 125, 2300-2314.

- BIANCHI, E., DENTI, S., GRANATA, A., BOSSI, G., GEGINAT, J., VILLA, A., ROGGE, L. & PARDI, R. 2000. Integrin LFA-1 interacts with the transcriptional co-activator JAB1 to modulate AP-1 activity. *Nature*, 404, 617-+.
- BIGGS, M. J., MILONE, M. C., SANTOS, L. C., GONDARENKO, A. & WIND, S. J. 2011. High-resolution imaging of the immunological synapse and T-cell receptor microclustering through microfabricated substrates. *J R Soc Interface*.
- BILLADEAU, D. D., NOLZ, J. C. & GOMEZ, T. S. 2007. Regulation of T-cell activation by the cytoskeleton. *Nature reviews. Immunology*, 7, 131-43.
- BINDSCHADLER, M., OSBORN, E. A., DEWEY, C. F. & MCGRATH, J. L. 2004. A mechanistic model of the actin cycle. *Biophysical Journal*, 86, 2720-2739.
- BLANCHOIN, L., AMANN, K. J., HIGGS, H. N., MARCHAND, J. B., KAISER, D. A. & POLLARD, T. D. 2000. Direct observation of dendritic actin filament networks nucleated by Arp2/3 complex and WASP/Scar proteins. *Nature*, 404, 1007-11.
- BLANCHOIN, L. & POLLARD, T. D. 1999. Mechanism of interaction of Acanthamoeba actophorin (ADF/cofilin) with actin filaments. *Journal of Biological Chemistry*, 274, 15538-15546.
- BLUESTONE, J. A. 1995. New Perspectives of Cd28-B7-Mediated T-Cell Costimulation. *Immunity*, 2, 555-559.
- BLUNDELL, M. P., BOUMA, G., METELO, J., WORTH, A., CALLE, Y., COWELL, L. A., WESTERBERG, L. S., MOULDING, D. A., MIRANDO, S., KINNON, C., CORY, G. O., JONES, G. E., SNAPPER, S. B., BURNS, S. O. & THRASHER, A. J. 2009. Phosphorylation of WASp is a key regulator of activity and stability in vivo. *Proc Natl Acad Sci U S A*, 106, 15738-43.
- BLUNDELL, M. P., WORTH, A., BOUMA, G. & THRASHER, A. J. 2010. The Wiskott-Aldrich syndrome: The actin cytoskeleton and immune cell function. *Dis Markers*, 29, 157-75.
- BOEHM, U., KLAMP, T., GROOT, M. & HOWARD, J. C. 1997. Cellular responses to interferon-gamma. *Annual Review of Immunology*, 15, 749-795.
- BOGUSKI, M. S. & MCCORMICK, F. 1993. Proteins Regulating Ras and Its Relatives. *Nature*, 366, 643-654.
- BOUGUERMOUH, S., FORTIN, G., BABA, N., RUBIO, M. & SARFATI, M. 2009. CD28 Co-Stimulation Down Regulates Th17 Development. *Plos One*, 4.
- BOUMA, G., BURNS, S. & THRASHER, A. J. 2007. Impaired T-cell priming in vivo resulting from dysfunction of WASp-deficient dendritic cells. *Blood*, 110, 4278-84.
- BOUMA, G., BURNS, S. O. & THRASHER, A. J. 2009. Wiskott-Aldrich Syndrome: Immunodeficiency resulting from defective cell migration and impaired immunostimulatory activation. *Immunobiology*, 214, 778-90.
- BOUMA, G., MENDOZA-NARANJO, A., BLUNDELL, M. P., DE FALCO, E., PARSLEY, K. L., BURNS, S. O. & THRASHER, A. J. 2011. Cytoskeletal remodeling mediated by WASp in dendritic cells is necessary for normal immune synapse formation and T-cell priming. *Blood*, 118, 2492-2501.

- BOUSSO, P., BHAKTA, N. R., LEWIS, R. S. & ROBEY, E. 2002. Dynamics of thymocyte-stromal cell interactions visualized by two-photon microscopy. *Science*, 296, 1876-1880.
- BOUSSO, P. & ROBEY, E. 2003. Dynamics of CD8(+) T cell priming by dendritic cells in intact lymph nodes. *Nature Immunology*, 4, 579-585.
- BRASEL, K., DE SMEDT, T., SMITH, J. L. & MALISZEWSKI, C. R. 2000. Generation of murine dendritic cells from flt3-ligand-supplemented bone marrow cultures. *Blood*, 96, 3029-3039.
- BROSSARD, C., FEUILLET, V., SCHMITT, A., RANDRIAMAMPITA, C., ROMAO, M., RAPOSO, G. & TRAUTMANN, A. 2005. Multifocal structure of the T cell - dendritic cell synapse. *European journal of immunology*, 35, 1741-53.
- BROWN, A. C. N., ODDOS, S., DOBBIE, I. M., ALAKOSKELA, J. M., PARTON, R. M., EISSMANN, P., NEIL, M. A. A., DUNSBY, C., FRENCH, P. M. W., DAVIS, I. & DAVIS, D. M. 2011. Remodelling of Cortical Actin Where Lytic Granules Dock at Natural Killer Cell Immune Synapses Revealed by Super-Resolution Microscopy. *Plos Biology*, 9.
- BRUNNER, M. C., CHAMBERS, C. A., CHAN, F. K. M., HANKE, J., WINOTO, A. & ALLISON, J. P. 1999. CTLA-4-mediated inhibition of early events of T cell proliferation. *Journal of Immunology*, 162, 5813-5820.
- BUNNELL, S. C., KAPOOR, V., TRIBLE, R. P., ZHANG, W. G. & SAMELSON, L. E. 2001. Dynamic actin polymerization drives T cell receptor-induced spreading: A role for the signal transduction adaptor LAT. *Immunity*, 14, 315-329.
- BURNS, S., HARDY, S. J., BUDDLE, J., YONG, K. L., JONES, G. E. & THRASHER, A. J. 2004. Maturation of DC is associated with changes in motile characteristics and adherence. *Cell Motility and the Cytoskeleton*, 57, 118-132.
- BURNS, S., THRASHER, A. J., BLUNDELL, M. P., MACHESKY, L. & JONES, G. E. 2001. Configuration of human dendritic cell cytoskeleton by Rho GTPases, the WAS protein, and differentiation. *Blood*, 98, 1142-1149.
- CALDWELL, J. E., HEISS, S. G., MERMALL, V. & COOPER, J. A. 1989. Effects of Capz, an Actin Capping Protein of Muscle, on the Polymerization of Actin. *Biochemistry*, 28, 8506-8514.
- CALLE, Y., BURNS, S., THRASHER, A. J. & JONES, G. E. 2006a. The leukocyte podosome. *European Journal of Cell Biology*, 85, 151-157.
- CALLE, Y., CARRAGHER, N. O., THRASHER, A. J. & JONES, G. E. 2006b. Inhibition of calpain stabilises podosomes and impairs dendritic cell motility. *Journal of Cell Science*, 119, 2375-2385.
- CALLE, Y., CHOU, H. C., THRASHER, A. J. & JONES, G. E. 2004. Wiskott-Aldrich syndrome protein and the cytoskeletal dynamics of dendritic cells. *Journal of Pathology*, 204, 460-469.
- CALVEZ, R., LAFOURESSE, F., DEMEESTER, J., GALY, A., VALITUTTI, S. & DUPRE, L. 2011. The Wiskott-Aldrich syndrome protein permits the assembly of a focused immunological synapse enabling sustained TCR signalling. *Haematologica*.

- CAMBI, A., JOOSTEN, B., KOOPMAN, M., DE LANGE, F., BEEREN, I., TORENSMA, R., FRANSEN, J. A., GARCIA-PARAJO, M., VAN LEEUWEN, F. N. & FIGDOR, C. G. 2006. Organization of the integrin LFA-1 in nanoclusters regulates its activity. *Mol Biol Cell*, 17, 4270-81.
- CAMPELLONE, K. G. & WELCH, M. D. 2010. A nucleator arms race: cellular control of actin assembly. *Nature Reviews Molecular Cell Biology*, 11, 237-251.
- CAMPI, G., VARMA, R. & DUSTIN, M. L. 2005. Actin and agonist MHC-peptide complex-dependent T cell receptor microclusters as scaffolds for signaling. *The Journal of experimental medicine*, 202, 1031-6.
- CANNON, J. L. & BURKHARDT, J. K. 2004. Differential roles for Wiskott-Aldrich syndrome protein in immune synapse formation and IL-2 production. *J Immunol*, 173, 1658-62.
- CANNON, J. L., LABNO, C. M., BOSCO, G., SETH, A., MCGAVIN, M. H., SIMINOVITCH, K. A., ROSEN, M. K. & BURKHARDT, J. K. 2001. Wasp recruitment to the T cell:APC contact site occurs independently of Cdc42 activation. *Immunity*, 15, 249-59.
- CANTOR, J., BROWNE, C. D., RUPPERT, R., FERAL, C. C., FASSLER, R., RICKERT, R. C. & GINSBERG, M. H. 2009. CD98hc facilitates B cell proliferation and adaptive humoral immunity. *Nat Immunol*, 10, 412-9.
- CANTRELL, D. 1996. T cell antigen receptor signal transduction pathways. *Annual Review of Immunology*, 14, 259-274.
- CARLIER, M. F., NIOCHE, P., BROUTIN-L'HERMITE, I., BOUJEMAA, R., LE CLAINCHE, C., EGILE, C., GARBAY, C., DUCRUIX, A., SANSONETTI, P. & PANTALONI, D. 2000. GRB2 links signaling to actin assembly by enhancing interaction of neural Wiskott-Aldrich syndrome protein (N-WASp) with actin-related protein (ARP2/3) complex. *Journal of Biological Chemistry*, 275, 21946-21952.
- CARLIER, M. F. & PANTALONI, D. 1997. Control of actin dynamics in cell motility. *Journal of Molecular Biology*, 269, 459-467.
- CARLSSON, L., NYSTROM, L. E., SUNDKVIST, I., MARKEY, F. & LINDBERG, U. 1977. Actin Polymerizability Is Influenced by Profilin, a Low-Molecular Weight Protein in Non-Muscle Cells. *Journal of Molecular Biology*, 115, 465-483.
- CARMAN, C. V., SAGE, P. T., SCIUTO, T. E., DE LA FUENTE, M. A., GEHA, R. S., OCHS, H. D., DVORAK, H. F., DVORAK, A. M. & SPRINGER, T. A. 2007. Transcellular diapedesis is initiated by invasive podosomes. *Immunity*, 26, 784-797.
- CARRASCO, Y. R., FLEIRE, S. J., CAMERON, T., DUSTIN, M. L. & BATISTA, F. D. 2004. LFA-1/ICAM-1 interaction lowers the threshold of B cell activation by facilitating B cell adhesion and synapse formation. *Immunity*, 20, 589-99.
- CARUSO, A., LICENZIATI, S., CORULLI, M., CANARIS, A. D., DE FRANCESCO, M. A., FIORENTINI, S., PERONI, L., FALLACARA, F., DIMA, F., BALSARI, A. & TURANO, A. 1997. Flow cytometric analysis of activation markers on stimulated T cells and their correlation with cell proliferation. *Cytometry*, 27, 71-6.
- CASTRILLON, D. H. & WASSERMAN, S. A. 1994. Diaphanous Is Required for Cytokinesis in Drosophila and Shares Domains of Similarity with the Products of the Limb Deformity Gene. *Development*, 120, 3367-3377.

- CEMERSKI, S., DAS, J., LOCASALE, J., ARNOLD, P., GIURISATO, E., MARKIEWICZ, M. A., FREMONT, D., ALLEN, P. M., CHAKRABORTY, A. K. & SHAW, A. S. 2007. The stimulatory potency of T cell antigens is influenced by the formation of the immunological synapse. *Immunity*, 26, 345-355.
- CEN, B., SELVARAJ, A., BURGESS, R. C., HITZLER, J. K., MA, Z. G., MORRIS, S. W. & PRYWES, R. 2003. Megakaryoblastic leukemia 1, a potent transcriptional coactivator for serum response factor (SRF), is required for serum induction of SRF target genes. *Molecular and Cellular Biology*, 23, 6597-6608.
- CHAMBERS, C. A., SULLIVAN, T. J. & ALLISON, J. P. 1997. Lymphoproliferation in CTLA-4-deficient mice is mediated by costimulation-dependent activation of CD4(+) T cells. *Immunity*, 7, 885-895.
- CHAN, A. C., DESAI, D. M. & WEISS, A. 1994. The Role of Protein-Tyrosine Kinases and Protein-Tyrosine Phosphatases in T-Cell Antigen Receptor Signal-Transduction. *Annual Review of Immunology*, 12, 555-592.
- CHAN, A. C., IWASHIMA, M., TURCK, C. W. & WEISS, A. 1992. ZAP-70: a 70 kd protein-tyrosine kinase that associates with the TCR zeta chain. *Cell*, 71, 649-62.
- CHANG, J. T., PALANIVEL, V. R., KINJYO, I., SCHAMBACH, F., INTLEKOFER, A. M., BANERJEE, A., LONGWORTH, S. A., VINUP, K. E., MRASS, P., OLIARO, J., KILLEEN, N., ORANGE, J. S., RUSSELL, S. M., WENINGER, W. & REINER, S. L. 2007. Asymmetric T lymphocyte division in the initiation of adaptive immune responses. *Science*, 315, 1687-91.
- CHEMIN, K., BOHINEUST, A., DOGNIAUX, S., TOURRET, M., GUEGAN, S., MIRO, F. & HIVROZ, C. 2012. Cytokine Secretion by CD4(+) T Cells at the Immunological Synapse Requires Cdc42-Dependent Local Actin Remodeling but Not Microtubule Organizing Center Polarity. *Journal of Immunology*, 189, 2159-2168.
- CHEN, C. Y., FAHERTY, D. A., GAULT, A., CONNAUGHTON, S. E., POWERS, G. D., GODFREY, D. I. & NABAVI, N. 1994. Monoclonal-Antibody 2d10 Recognizes a Novel T-Cell Costimulatory Molecule on Activated Murine B-Lymphocytes. *Journal of Immunology*, 152, 2105-2114.
- CHEN, J., GODT, D., GUNSALUS, K., KISS, I., GOLDBERG, M. & LASKI, F. A. 2001. Cofilin/ADF is required for cell motility during Drosophila ovary development and oogenesis. *Nature Cell Biology*, 3, 204-209.
- CHEREAU, D., KERFF, F., GRACEFFA, P., GRABAREK, Z., LANGSETMO, K. & DOMINGUEZ, R. 2005. Actin-bound structures of Wiskott-Aldrich syndrome protein (WASP)-homology domain 2 and the implications for filament assembly. *Proceedings of the National Academy of Sciences of the United States of America*, 102, 16644-16649.
- CHESARONE, M., GOULD, C. J., MOSELEY, J. B. & GOODE, B. L. 2009. Displacement of Formins from Growing Barbed Ends by Bud14 Is Critical for Actin Cable Architecture and Function. *Developmental Cell*, 16, 292-302.

- CHICHA, L., JARROSSAY, D. & MANZ, M. G. 2004. Clonal type I interferon-producing and dendritic cell precursors are contained in both human lymphoid and myeloid progenitor populations. *Journal of Experimental Medicine*, 200, 1519-1524.
- CHOU, H.-C., ANTÓN, I. M., HOLT, M. R., CURCIO, C., LANZARDO, S., WORTH, A., BURNS, S., THRASHER, A. J., JONES, G. E. & CALLE, Y. 2006. WIP Regulates the Stability and Localization of WASP to Podosomes in Migrating Dendritic Cells. *Current Biology*, 16, 2337-2344.
- CHOUDHURI, K., WISEMAN, D., BROWN, M. H., GOULD, K. & VAN DER MERWE, P. A. 2005. T-cell receptor triggering is critically dependent on the dimensions of its peptide-MHC ligand. *Nature*, 436, 578-82.
- CHTANOVA, T., TANGYE, S. G., NEWTON, R., FRANK, N., HODGE, M. R., ROLPH, M. S. & MACKAY, C. R. 2004. T follicular helper cells express a distinctive transcriptional profile, reflecting their role as non-Th1/Th2 effector cells that provide help for B cells. *Journal of Immunology*, 173, 68-78.
- CHU, E. Y., FREEMAN, A. F., JING, H., COWEN, E. W., DAVIS, J., SU, H. C., HOLLAND, S. M. & TURNER, M. L. 2012. Cutaneous manifestations of DOCK8 deficiency syndrome. *Arch Dermatol*, 148, 79-84.
- COLF, L. A., BANKOVICH, A. J., HANICK, N. A., BOWERMAN, N. A., JONES, L. L., KRANZ, D. M. & GARCIA, K. C. 2007. How a single T cell receptor recognizes both self and foreign MHC. *Cell*, 129, 135-146.
- COLLISON, L. W., PILLAI, M. R., CHATURVEDI, V. & VIGNALI, D. A. A. 2009. Regulatory T Cell Suppression Is Potentiated by Target T Cells in a Cell Contact, IL-35-and IL-10-Dependent Manner. *Journal of Immunology*, 182, 6121-6128.
- COMBS, J., KIM, S. J., TAN, S., LIGON, L. A., HOLZBAUR, E. L., KUHN, J. & POENIE, M. 2006. Recruitment of dynein to the Jurkat immunological synapse. *Proceedings of the National Academy of Sciences of the United States of America*, 103, 14883-8.
- CONSTANT, S., PFEIFFER, C., WOODARD, A., PASQUALINI, T. & BOTTOMLY, K. 1995. Extent of T cell receptor ligation can determine the functional differentiation of naive CD4+ T cells. *The Journal of experimental medicine*, 182, 1591-6.
- COOPER, J. A. & SEPT, D. 2008. New insights into mechanism and regulation of actin capping protein. *International Review of Cell and Molecular Biology*, Vol 267, 267, 183-+.
- COPELAND, J. W., COPELAND, S. J. & TREISMAN, R. 2004. Homo-oligomerization is essential for F-actin assembly by the formin family FH2 domain. *Journal of Biological Chemistry*, 279, 50250-50256.
- CORBI, A. L. & LOPEZ-RODRIGUEZ, C. 1997. CD11c integrin gene promoter activity during myeloid differentiation. *Leuk Lymphoma*, 25, 415-25.
- CORDOBA, S. P., CHOUDHURI, K., ZHANG, H., BRIDGE, M., BASAT, A. B., DUSTIN, M. L. & VAN DER MERWE, P. A. 2013. The large ectodomains of CD45 and CD148 regulate their segregation from and inhibition of ligated T-cell receptor. *Blood*, 121, 4295-4302.

- CORTHAY, A. 2006. A three-cell model for activation of naive T helper cells. *Scandinavian Journal of Immunology*, 64, 93-96.
- CORY, G. O., GARG, R., CRAMER, R. & RIDLEY, A. J. 2002. Phosphorylation of tyrosine 291 enhances the ability of WASp to stimulate actin polymerization and filopodium formation. Wiskott-Aldrich Syndrome protein. *The Journal of biological chemistry*, 277, 45115-21.
- COTE, J. F. & VUORI, K. 2007. GEF what? Dock180 and related proteins help Rac to polarize cells in new ways. *Trends Cell Biol*, 17, 383-93.
- COUDRONNIERE, N., VILLALBA, M., ENGLUND, N. & ALTMAN, A. 2000. NF-kappa B activation induced by T cell receptor/CD28 costimulation is mediated by protein kinase C-theta. *Proceedings of the National Academy of Sciences of the United States of America*, 97, 3394-3399.
- CUMBERBATCH, M. & KIMBER, I. 1992. Dermal Tumor-Necrosis-Factor-Alpha Induces Dendritic Cell-Migration to Draining Lymph-Nodes, and Possibly Provides One Stimulus for Langerhans Cell-Migration. *Immunology*, 75, 257-263.
- CURTSINGER, J. M., LINS, D. C. & MESCHER, M. F. 2003. Signal 3 determines tolerance versus full activation of naive CD8 T cells: Dissociating proliferation and development of effector function. *Journal of Experimental Medicine*, 197, 1141-1151.
- CURTSINGER, J. M., SCHMIDT, C. S., MONDINO, A., LINS, D. C., KEDL, R. M., JENKINS, M. K. & MESCHER, M. F. 1999. Inflammatory cytokines provide a third signal for activation of naive CD4(+) and CD8(+) T cells. *Journal of Immunology*, 162, 3256-3262.
- DASOUKI, M., OKONKWO, K. C., RAY, A., FOLMSBEEL, C. K., GOZALES, D., KELES, S., PUCK, J. M. & CHATILA, T. 2011. Deficient T Cell Receptor Excision Circles (TRECs) in autosomal recessive hyper IgE syndrome caused by DOCK8 mutation: implications for pathogenesis and potential detection by newborn screening. *Clin Immunol*, 141, 128-32.
- DAVIDSON, T. S., DIPAOLO, R. J., ANDERSSON, J. & SHEVACH, E. M. 2007. Cutting edge: IL-2 is essential for TGF-beta-mediated induction of Foxp(3+) T regulatory cells. *Journal of Immunology*, 178, 4022-4026.
- DAVIS, D. M., CHIU, I., FASSETT, M., COHEN, G. B., MANDELBOIM, O. & STROMINGER, J. L. 1999. The human natural killer cell immune synapse. *Proceedings of the National Academy of Sciences of the United States of America*, 96, 15062-15067.
- DAVIS, S. J., IKEMIZU, S., EVANS, E. J., FUGGER, L., BAKKER, T. R. & VAN DER MERWE, P. A. 2003. The nature of molecular recognition by T cells. *Nature Immunology*, 4, 217-224.
- DAVIS, S. J. & VANDERMERWE, P. A. 1996. The structure and ligand interactions of CD2: Implications for T-cell function. *Immunology Today*, 17, 177-187.
- DE CLERCQ, S., BOUCHERIE, C., VANDEKERCKHOVE, J., GETTEMANS, J. & GUILLABERT, A. 2013a. L-Plastin Nanobodies Perturb Matrix Degradation, Podosome Formation, Stability and Lifetime in THP-1 Macrophages. *Plos One*, 8.

- DE CLERCQ, S., ZWAENEPOEL, O., MARTENS, E., VANDEKERCKHOVE, J., GUILLABERT, A. & GETTEMANS, J. 2013b. Nanobody-induced perturbation of LFA-1/L-plastin phosphorylation impairs MTOC docking, immune synapse formation and T cell activation. *Cellular and Molecular Life Sciences*, 70, 909-922.
- DE LA FUENTE, M. A., SASAHARA, Y., CALAMITO, M., ANTON, I. M., ELKHAL, A., GALLEGO, M. D., SURESH, K., SIMINOVITCH, K., OCHS, H. D., ANDERSON, K. C., ROSEN, F. S., GEHA, R. S. & RAMESH, N. 2007. WIP is a chaperone for Wiskott-Aldrich syndrome protein (WASP). *Proceedings of the National Academy of Sciences of the United States of America*, 104, 926-931.
- DE NORONHA, S., HARDY, S., SINCLAIR, J., BLUNDELL, M. P., STRID, J., SCHULZ, O., ZWIRNER, J., JONES, G. E., KATZ, D. R., KINNON, C. & THRASHER, A. J. 2005. Impaired dendritic-cell homing in vivo in the absence of Wiskott-Aldrich syndrome protein. *Blood*, 105, 1590-7.
- DEDHAR, S. & HANNIGAN, G. E. 1996. Integrin cytoplasmic interactions and bidirectional transmembrane signalling. *Current Opinion in Cell Biology*, 8, 657-669.
- DEFIFE, K. M., JENNEY, C. R., COLTON, E. & ANDERSON, J. M. 1999. Cytoskeletal and adhesive structural polarizations accompany IL-13-induced human macrophage fusion. *Journal of Histochemistry & Cytochemistry*, 47, 65-74.
- DELON, J. & GERMAIN, R. N. 2000. Information transfer at the immunological synapse. *Current Biology*, 10, R923-R933.
- DELON, J., KAIBUCHI, K. & GERMAIN, R. N. 2001. Exclusion of CD43 from the immunological synapse is mediated by phosphorylation-regulated relocation of the cytoskeletal adaptor moesin. *Immunity*, 15, 691-701.
- DEMOND, A. L., MOSSMAN, K. D., STARR, T., DUSTIN, M. L. & GROVES, J. T. 2008. T cell receptor microcluster transport through molecular mazes reveals mechanism of translocation. *Biophysical Journal*, 94, 3286-3292.
- DENK, W. & HORSTMANN, H. 2004. Serial block-face scanning electron microscopy to reconstruct three-dimensional tissue nanostructure. *PLoS biology*, 2, e329.
- DEPOIL, D., ZARU, R., GUIRAUD, M., CHAUVEAU, A., HARRIAGUE, J., BISMUTH, G., UTZNY, C., MULLER, S. & VALITUTTI, S. 2005. Immunological synapses are versatile structures enabling selective T cell polarization. *Immunity*, 22, 185-94.
- DERRY, J. M., OCHS, H. D. & FRANCKE, U. 1994. Isolation of a novel gene mutated in Wiskott-Aldrich syndrome. *Cell*, 79, following 922.
- DESTAING, O., SALTEL, F., GEMINARD, J. C., JURDIC, P. & BARD, F. 2003. Podosomes display actin turnover and dynamic self-organization in osteoclasts expressing actin-green fluorescent protein. *Molecular Biology of the Cell*, 14, 407-416.
- DEVRIENDT, K., KIM, A. S., MATHIJS, G., FRINTS, S. G. M., SCHWARTZ, M., VAN DEN OORD, J. J., VERHOEF, G. E. G., BOOGAERTS, M. A., FRYNS, J. P., YOU, D. Q., ROSEN, M. K. & VANDENBERGHE, P. 2001. Constitutively activating mutation in WASP causes X-linked severe congenital neutropenia. *Nature Genetics*, 27, 313-317.
- DINARELLO, C. A. 1988. Biology of Interleukin-1. *Faseb Journal*, 2, 108-115.

- DOHERTY, G. J. & MCMAHON, H. T. 2008. Mediation, modulation, and consequences of membrane-cytoskeleton interactions. *Annual Review of Biophysics*, 37, 65-95.
- DOMINGUEZ, R. 2004. Actin-binding proteins - a unifying hypothesis. *Trends in Biochemical Sciences*, 29, 572-578.
- DOMINGUEZ, R. & HOLMES, K. C. 2011. Actin Structure and Function. *Annual Review of Biophysics*, Vol 40, 40, 169-186.
- DONG, C., JUEDES, A. E., TEMANN, U. A., SHRESTA, S., ALLISON, J. P., RUDDLE, N. H. & FLAVELL, R. A. 2001. ICOS costimulatory receptor is essential for T-cell activation and function. *Faseb Journal*, 15, A345-A345.
- DONNADIEU, E., BISMUTH, C. & TRAUTMANN, A. 1994. Antigen Recognition by Helper T-Cells Elicits a Sequence of Distinct Changes of Their Shape and Intracellular Calcium. *Current Biology*, 4, 584-595.
- DONNELLY, S. K., WEISSWANGE, I., ZETTL, M. & WAY, M. 2013. WIP Provides an Essential Link between Nck and N-WASP during Arp2/3-Dependent Actin Polymerization. *Current Biology*, 23, 999-1006.
- DUPLAY, P., ALCOVER, A., FARGEAS, C., SEKALY, R. P. & BRANTON, P. E. 1996. An activated epidermal growth factor receptor/Lck chimera restores early T cell receptor-mediated calcium response in a CD45-deficient T cell line. *Journal of Biological Chemistry*, 271, 17896-17902.
- DUPRE, L., AIUTI, A., TRIFARI, S., MARTINO, S., SARACCO, P., BORDIGNON, C. & RONCAROLO, M. G. 2002. Wiskott-Aldrich syndrome protein regulates lipid raft dynamics during immunological synapse formation. *Immunity*, 17, 157-66.
- DUSTIN, M. L. 2007. Cell adhesion molecules and actin cytoskeleton at immune synapses and kinapses. *Current Opinion in Cell Biology*, 19, 529-533.
- DUSTIN, M. L. 2008a. T-cell activation through immunological synapses and kinapses. *Immunological Reviews*, 221, 77-89.
- DUSTIN, M. L. 2008b. Visualization of Cell-Cell Interaction Contacts-Synapses and Kinapses. *Multichain Immune Recognition Receptor Signaling: From Spatiotemporal Organization to Human Disease*, 640, 164-182.
- DUSTIN, M. L. 2009a. The cellular context of T cell signaling. *Immunity*, 30, 482-92.
- DUSTIN, M. L. 2009b. Modular Design of Immunological Synapses and Kinapses. *Cold Spring Harbor Perspectives in Biology*, 1.
- DUSTIN, M. L., BROMLEY, S. K., KAN, Z. Y., PETERSON, D. A. & UNANUE, E. R. 1997. Antigen receptor engagement delivers a stop signal to migrating T lymphocytes. *Proceedings of the National Academy of Sciences of the United States of America*, 94, 3909-3913.
- DUSTIN, M. L., CHAKRABORTY, A. K. & SHAW, A. S. 2010. Understanding the Structure and Function of the Immunological Synapse. *Cold Spring Harbor Perspectives in Biology*, 2.
- DUSTIN, M. L., OLSZOWY, M. W., HOLDORF, A. D., LI, J., BROMLEY, S., DESAI, N., WIDDER, P., ROSENBERGER, F., VAN DER MERWE, P. A., ALLEN, P. M. & SHAW, A. S. 1998. A novel adaptor protein orchestrates receptor patterning and cytoskeletal polarity in T-cell contacts. *Cell*, 94, 667-677.

- DUSTIN, M. L., ROTHLEIN, R., BHAN, A. K., DINARELLO, C. A. & SPRINGER, T. A. 1986. Induction by IL-1 and Interferon-Gamma - Tissue Distribution, Biochemistry, and Function of a Natural Adherence Molecule (Icam-1). *Journal of Immunology*, 137, 245-254.
- DUTARTRE, H., DAVOUST, J., GORVEL, J. P. & CHAVRIER, P. 1996. Cytokinesis arrest and redistribution of actin-cytoskeleton regulatory components in cells expressing the Rho GTPase CDC42Hs. *Journal of Cell Science*, 109, 367-377.
- EGILE, C., ROUILLER, I., XU, X. P., VOLKMANN, N., LI, R. & HANEIN, D. 2005. Mechanism of filament nucleation and branch stability revealed by the structure of the Arp2/3 complex at actin branch junctions. *Plos Biology*, 3, 1902-1909.
- EIBERT, S. M., LEE, K. H., PIPKORN, R., SESTER, U., WABNITZ, G. H., GIESE, T., MEUER, S. C. & SAMSTAG, Y. 2004. Cofilin peptide homologs interfere with immunological synapse formation and T cell activation. *Proceedings of the National Academy of Sciences of the United States of America*, 101, 1957-1962.
- ENGELHARDT, K. R., MCGHEE, S., WINKLER, S., SASSI, A., WOELLNER, C., LOPEZ-HERRERA, G., CHEN, A., KIM, H. S., LLORET, M. G., SCHULZE, I., EHL, S., THIEL, J., PFEIFER, D., VEELKEN, H., NIEHUES, T., SIEPERMANN, K., WEINSPACH, S., REISLI, I., KELES, S., GENEL, F., KUTUKCULER, N., CAMCIOGLU, Y., SOMER, A., KARAKOC-AYDINER, E., BARLAN, I., GENNERY, A., METIN, A., DEGERLIYURT, A., PIETROGRANDE, M. C., YEGANEH, M., BAZ, Z., AL-TAMEMI, S., KLEIN, C., PUCK, J. M., HOLLAND, S. M., MCCABE, E. R., GRIMBACHER, B. & CHATILA, T. A. 2009. Large deletions and point mutations involving the dedicator of cytokinesis 8 (DOCK8) in the autosomal-recessive form of hyper-IgE syndrome. *J Allergy Clin Immunol*, 124, 1289-302 e4.
- ETIENNE-MANNEVILLE, S. & HALL, A. 2002. Rho GTPases in cell biology. *Nature*, 420, 629-635.
- EVANS, J. G., CORREIA, I., KRASAVINA, O., WATSON, N. & MATSUDAIRA, P. 2003. Macrophage podosomes assemble at the leading lamella by growth and fragmentation. *Journal of Cell Biology*, 161, 697-705.
- EVANS, R., PATZAK, I., SVENSSON, L., DE FILIPPO, K., JONES, K., MCDOWALL, A. & HOGG, N. 2009. Integrins in immunity. *Journal of Cell Science*, 122, 215-225.
- FAITH, A., SINGH, N., FAROOQUE, S., DIMELOE, S., RICHARDS, D. F., LU, H., ROBERTS, D., CHEVRETTON, E., LEE, T. H., CORRIGAN, C. J. & HAWRYLOWICZ, C. M. 2012. T cells producing the anti-inflammatory cytokine IL-10 regulate allergen-specific Th2 responses in human airways. *Allergy*, 67, 1007-1013.
- FELIX, N. J., DONERMEYER, D. L., HORVATH, S., WALTERS, J. J., GROSS, M. L., SURI, A. & ALLEN, P. M. 2007. Alloreactive T cells respond specifically to multiple distinct peptide-MHC complexes. *Nature Immunology*, 8, 388-397.
- FERRON, F., REBOWSKI, G., LEE, S. H. & DOMINGUEZ, R. 2007. Structural basis for the recruitment of profilin-actin complexes during filament elongation by Ena/VASP. *Embo Journal*, 26, 4597-4606.
- FINCK, B. K., LINSLEY, P. S. & WOFSY, D. 1994. Treatment of Murine Lupus with Ctl4ig. *Science*, 265, 1225-1227.

- FREEMAN, G. J., BOUSSIOTIS, V. A., ANUMANTHAN, A., BERNSTEIN, G. M., KE, X. Y., RENNERT, P. D., GRAY, G. S., GRIBBEN, J. G. & NADLER, L. M. 1995. B7-1 and B7-2 Do Not Deliver Identical Costimulatory Signals, since B7-2 but Not B7-1 Preferentially Costimulates the Initial Production of Il-4. *Immunity*, 2, 523-532.
- FREEMAN, G. J., LOMBARD, D. B., GIMMI, C. D., BROD, S. A., LEE, K., LANING, J. C., HAFLER, D. A., DORF, M. E., GRAY, G. S., REISER, H., JUNE, C. H., THOMPSON, C. B. & NADLER, L. M. 1992. Ctl-4 and Cd28 Messenger-Rna Are Coexpressed in Most T-Cells after Activation - Expression of Ctl-4 and Cd28 Messenger-Rna Does Not Correlate with the Pattern of Lymphokine Production. *Journal of Immunology*, 149, 3795-3801.
- FRIEDMAN, R. S., BEEMILLER, P., SORENSEN, C. M., JACOBELLI, J. & KRUMMEL, M. F. 2010. Real-time analysis of T cell receptors in naive cells in vitro and in vivo reveals flexibility in synapse and signaling dynamics. *Journal of Experimental Medicine*, 207, 2733-2749.
- FRITZSCHE, M., LEWALLE, A., DUKE, T., KRUSE, K. & CHARRAS, G. 2013. Analysis of turnover dynamics of the submembranous actin cortex. *Molecular Biology of the Cell*, 24, 757-767.
- FUKATA, Y., AMANO, M. & KAIBUCHI, K. 2001. Rho-Rho-kinase pathway in smooth muscle contraction and cytoskeletal reorganization of non-muscle cells. *Trends in Pharmacological Sciences*, 22, 32-39.
- FUKUI, Y., HASHIMOTO, O., SANUI, T., OONO, T., KOGA, H., ABE, M., INAYOSHI, A., NODA, M., OIKE, M., SHIRAI, T. & SASAZUKI, T. 2001. Haematopoietic cell-specific CDM family protein DOCK2 is essential for lymphocyte migration. *Nature*, 412, 826-831.
- FURUKAWA, T., ITOH, M., KRUEGER, N. X., STREULI, M. & SAITO, H. 1994. Specific Interaction of the Cd45 Protein-Tyrosine-Phosphatase with Tyrosine-Phosphorylated Cd3 Zeta-Chain. *Proceedings of the National Academy of Sciences of the United States of America*, 91, 10928-10932.
- GAIDANO, G., BERGUI, L., SCHENA, M., GABOLI, M., CREMONA, O., MARCHISIO, P. C. & CALIGARISCAPPIO, F. 1990. Integrin Distribution and Cytoskeleton Organization in Normal and Malignant Monocytes. *Leukemia*, 4, 682-687.
- GALKIN, V. E., ORLOVA, A., LUKOYANOVA, N., WRIGGERS, W. & EGELMAN, E. H. 2001. Actin depolymerizing factor stabilizes an existing state of F-actin and can change the tilt of F-actin subunits. *Journal of Cell Biology*, 153, 75-86.
- GARBOCZI, D. N., GHOSH, P., UTZ, U., FAN, Q. R., BIDDISON, W. E. & WILEY, D. C. 1996. Structure of the complex between human T-cell receptor, viral peptide and HLA-A2. *Nature*, 384, 134-141.
- GARCIA, K. C., DEGANI, M., STANFIELD, R. L., BRUNMARK, A., JACKSON, M. R., PETERSON, P. A., TEYTON, L. & WILSON, I. A. 1996. An alpha beta T cell receptor structure at 2.5 angstrom and its orientation in the TCR-MHC complex. *Science*, 274, 209-219.

- GARDEL, M. L., SCHNEIDER, I. C., ARATYN-SCHAUS, Y. & WATERMAN, C. M. 2010. Mechanical Integration of Actin and Adhesion Dynamics in Cell Migration. *Annual Review of Cell and Developmental Biology*, Vol 26, 26, 315-333.
- GARDEL, M. L., SHIN, J. H., MACKINTOSH, F. C., MAHADEVAN, L., MATSUDAIRA, P. & WEITZ, D. A. 2004. Elastic Behavior of cross-linked and bundled actin networks. *Science*, 304, 1301-1305.
- GARRIGAN, K., MORONIRAWSON, P., MCMURRAY, C., HERMANS, I., ABERNETHY, N., WATSON, J. & RONCHESE, F. 1996. Functional comparison of spleen dendritic cells and dendritic cells cultured in vitro from bone marrow precursors. *Blood*, 88, 3508-3512.
- GAVAZZI, I., NERMUT, M. V. & MARCHISIO, P. C. 1989. Ultrastructure and Gold-Immunolabeling of Cell Substratum Adhesions (Podosomes) in Rsv-Transformed Bhk Cells. *Journal of Cell Science*, 94, 85-99.
- GEIGER, B., ROSEN, D. & BERKE, G. 1982. Spatial Relationships of Microtubule-Organizing Centers and the Contact Area of Cyto-Toxic Lymphocytes-T and Target-Cells. *Journal of Cell Biology*, 95, 137-143.
- GENESTE, O., COPELAND, J. W. & TREISMAN, R. 2002. LIM kinase and Diaphanous cooperate to regulate serum response factor and actin dynamics. *Journal of Cell Biology*, 157, 831-838.
- GERARD, A., BEEMILLER, P., FRIEDMAN, R. S., JACOBELLI, J. & KRUMMEL, M. F. 2013. Evolving immune circuits are generated by flexible, motile, and sequential immunological synapses. *Immunological Reviews*, 251, 80-96.
- GHIMIRE, T. R., BENSON, R. A., GARSIDE, P. & BREWER, J. M. 2012. Alum increases antigen uptake, reduces antigen degradation and sustains antigen presentation by DCs in vitro. *Immunology Letters*, 147, 55-62.
- GILLES, L., BLUTEAU, D., BOUKOUR, S., CHANG, Y. H., ZHANG, Y. Y., ROBERT, T., DESSEN, P., DEBILI, N., BERNARD, O. A., VAINCHENKER, W. & RASLOVA, H. 2009. MAL/SRF complex is involved in platelet formation and megakaryocyte migration by regulating MYL9 (MLC2) and MMP9. *Blood*, 114, 4221-4232.
- GILLIET, M., BOONSTRA, A., PATUREL, C., ANTONENKO, S., XU, X. L., TRINCHIERI, G., O'GARRA, A. & LIU, Y. J. 2002. The development of murine plasmacytoid dendritic cell precursors is differentially regulated by FLT3-ligand and granulocyte/macrophage colony-stimulating factor. *Journal of Experimental Medicine*, 195, 953-958.
- GOMEZ, T. S. & BILLADEAU, D. D. 2008. T cell activation and the cytoskeleton: you can't have one without the other. *Advances in immunology*, 97, 1-64.
- GOODRIDGE, H. S., REYES, C. N., BECKER, C. A., KATSUMOTO, T. R., MA, J., WOLF, A. J., BOSE, N., CHAN, A. S. H., MAGEE, A. S., DANIELSON, M. E., WEISS, A., VASILAKOS, J. P. & UNDERHILL, D. M. 2011. Activation of the innate immune receptor Dectin-1 upon formation of a phagocytic synapse. *Nature*, 472, 471-475.

- GRACEFFA, P. & DOMINGUEZ, R. 2003. Crystal structure of monomeric actin in the ATP state - Structural basis of nucleotide-dependent actin dynamics. *Journal of Biological Chemistry*, 278, 34172-34180.
- GRAF, B., BUSHNELL, T. & MILLER, J. 2007. LFA-1-mediated T cell costimulation through increased localization of TCR/class II complexes to the central supramolecular activation cluster and exclusion of CD45 from the immunological synapse. *J Immunol*, 179, 1616-24.
- GRAHAM, D. B., CELLA, M., GIURISATO, E., FUJIKAWA, K., MILETIC, A. V., KLOEPEL, T., BRIM, K., TAKAI, T., SHAW, A. S., COLONNA, M. & SWAT, W. 2006. Vav1 controls DAP10-mediated natural cytotoxicity by regulating actin and microtubule dynamics. *Journal of Immunology*, 177, 2349-2355.
- GRAKOU, A., BROMLEY, S. K., SUMEN, C., DAVIS, M. M., SHAW, A. S., ALLEN, P. M. & DUSTIN, M. L. 1999. The immunological synapse: A molecular machine controlling T cell activation. *Science*, 285, 221-227.
- GRIGGS, B. L., LADD, S., SAUL, R. A., DUPONT, B. R. & SRIVASTAVA, A. K. 2008. Deducator of cytokinesis 8 is disrupted in two patients with mental retardation and developmental disabilities. *Genomics*, 91, 195-202.
- GROSS, J. A., CALLAS, E. & ALLISON, J. P. 1992. Identification and Distribution of the Costimulatory Receptor Cd28 in the Mouse. *Journal of Immunology*, 149, 380-388.
- GROSSE, R., COPELAND, J. W., NEWSOME, T. P., WAY, M. & TREISMAN, R. 2003. A role for VASP in RhoA-diaphanous signalling to actin dynamics and SRF activity. *Embo Journal*, 22, 3050-3061.
- GROVES, J. T. & DUSTIN, M. L. 2003. Supported planar bilayers in studies on immune cell adhesion and communication. *J Immunol Methods*, 278, 19-32.
- GUO, W. H. & WANG, Y. L. 2007. Retrograde fluxes of focal adhesion proteins in response to cell migration and mechanical signals. *Molecular Biology of the Cell*, 18, 4519-4527.
- GUY, C. S., VIGNALI, K. M., TEMIROV, J., BETTINI, M. L., OVERACRE, A. E., SMELTZER, M., ZHANG, H., HUPPA, J. B., TSAI, Y. H., LOBRY, C., XIE, J. M., DEMPSEY, P. J., CRAWFORD, H. C., AIFANTIS, I., DAVIS, M. M. & VIGNALI, D. A. A. 2013. Distinct TCR signaling pathways drive proliferation and cytokine production in T cells. *Nature Immunology*, 14, 262-270.
- HALL, A. 2005. Rho GTPases and the control of cell behaviour. *Biochemical Society Transactions*, 33, 891-895.
- HAM, H., GUERRIER, S., KIM, J., SCHOON, R. A., ANDERSON, E. L., HAMANN, M. J., LOU, Z. & BILLADEAU, D. D. 2013. Deducator of Cytokinesis 8 Interacts with Talin and Wiskott-Aldrich Syndrome Protein To Regulate NK Cell Cytotoxicity. *J Immunol*.
- HAMMER, J. A. & BURKHARDT, J. K. 2013. Controversy and consensus regarding myosin II function at the immunological synapse. *Current Opinion in Immunology*, 25, 300-306.
- HARADA, Y., TANAKA, Y., TERASAWA, M., PIECZYK, M., HABIRO, K., KATAKAI, T., HANAWA-SUETSUGU, K., KUKIMOTO-NIINO, M., NISHIZAKI, T., SHIROUZU, M.,

- DUAN, X., URUNO, T., NISHIKIMI, A., SANEMATSU, F., YOKOYAMA, S., STEIN, J. V., KINASHI, T. & FUKUI, Y. 2012. DOCK8 is a Cdc42 activator critical for interstitial dendritic cell migration during immune responses. *Blood*, 119, 4451-61.
- HARRINGTON, L. E., HATTON, R. D., MANGAN, P. R., TURNER, H., MURPHY, T. L., MURPHY, K. M. & WEAVER, C. T. 2005. Interleukin 17-producing CD4(+) effector T cells develop via a lineage distinct from the T helper type 1 and 2 lineages. *Nature Immunology*, 6, 1123-1132.
- HARRIS, E. S., LI, F. & HIGGS, H. N. 2004. The mouse formin, FRL alpha, slows actin filament barbed end elongation, competes with capping protein, accelerates polymerization from monomers, and severs filaments. *Journal of Biological Chemistry*, 279, 20076-20087.
- HARTMAN, N. C., NYE, J. A. & GROVES, J. T. 2009. Cluster size regulates protein sorting in the immunological synapse. *Proc Natl Acad Sci U S A*, 106, 12729-34.
- HASHIMOTO-TANE, A., YOKOSUKA, T., SAKATA-SOGAWA, K., SAKUMA, M., ISHIHARA, C., TOKUNAGA, M. & SAITO, T. 2011. Dynein-driven transport of T cell receptor microclusters regulates immune synapse formation and T cell activation. *Immunity*, 34, 919-31.
- HASKINS, K., KAPPLER, J. & MARRACK, P. 1984. The Major Histocompatibility Complex Restricted Antigen Receptor on T-Cells. *Annual Review of Immunology*, 2, 51-66.
- HAWKINS, M., POPE, B., MACIVER, S. K. & WEEDS, A. G. 1993. Human Actin Depolymerizing Factor Mediates a Ph-Sensitive Destruction of Actin-Filaments. *Biochemistry*, 32, 9985-9993.
- HAYDEN, S. M., MILLER, P. S., BRAUWEILER, A. & BAMBURG, J. R. 1993. Analysis of the Interactions of Actin Depolymerizing Factor with G-Actin and F-Actin. *Biochemistry*, 32, 9994-10004.
- HEIM, M. H. 1999. The Jak-STAT pathway: cytokine signalling from the receptor to the nucleus. *Journal of receptor and signal transduction research*, 19, 75-120.
- HELFT, J., JACQUET, A., JONCKER, N. T., GRANDJEAN, I., DOROTHEE, G., KISSENFENNIG, A., MALISSEN, B., MATZINGER, P. & LANTZ, O. 2008. Antigen-specific T-T interactions regulate CD4 T-cell expansion. *Blood*, 112, 1249-1258.
- HENRICKSON, S. E., MEMPEL, T. R., MAZO, I. B., LIU, B., ARTYOMOV, M. N., ZHENG, H., PEIXOTO, A., FLYNN, M. P., SENMAN, B., JUNT, T., WONG, H. C., CHAKRABORTY, A. K. & VON ANDRIAN, U. H. 2008. T cell sensing of antigen dose governs interactive behavior with dendritic cells and sets a threshold for T cell activation. *Nature Immunology*, 9, 282-291.
- HIGGS, H. N. & POLLARD, T. D. 2000. Activation by Cdc42 and PIP(2) of Wiskott-Aldrich syndrome protein (WASp) stimulates actin nucleation by Arp2/3 complex. *The Journal of cell biology*, 150, 1311-20.
- HILL, C. S., WYNNE, J. & TREISMAN, R. 1995. The Rho-Family Gtpases Rhoa, Rac1, and Cdc42hs Regulate Transcriptional Activation by Srf. *Cell*, 81, 1159-1170.

- HO, I. C., TAI, T. S. & PAI, S. Y. 2009. GATA3 and the T-cell lineage: essential functions before and after T-helper-2-cell differentiation. *Nature reviews. Immunology*, 9, 125-35.
- HOGG, N., PATZAK, I. & WILLENBROCK, F. 2011. The insider's guide to leukocyte integrin signalling and function. *Nature Reviews Immunology*, 11, 416-426.
- HOSKEN, N. A., SHIBUYA, K., HEATH, A. W., MURPHY, K. M. & O'GARRA, A. 1995. The effect of antigen dose on CD4+ T helper cell phenotype development in a T cell receptor-alpha beta-transgenic model. *The Journal of experimental medicine*, 182, 1579-84.
- HOSSEINI, B. H., LOUBAN, I., DJANDJI, D., WABNITZ, G. H., DEEG, J., BULBUC, N., SAMSTAG, Y., GUNZER, M., SPATZ, J. P. & HAMMERLING, G. J. 2009. Immune synapse formation determines interaction forces between T cells and antigen-presenting cells measured by atomic force microscopy. *Proceedings of the National Academy of Sciences of the United States of America*, 106, 17852-17857.
- HOUTMAN, J. C. D., YAMAGUCHI, H., BARDA-SAAD, M., BRAIMAN, A., BOWDEN, B., APPELLA, E., SCHUCK, P. & SAMELSON, L. E. 2006. Oligomerization of signaling complexes by the multipoint binding of GRB2 to both LAT and SOS1. *Nature Structural & Molecular Biology*, 13, 798-805.
- HSIEH, C. S., MACATONIA, S. E., TRIPP, C. S., WOLF, S. F., OGARRA, A. & MURPHY, K. M. 1993. Development of Th1 Cd4+ T-Cells through Il-12 Produced by Listeria-Induced Macrophages. *Science*, 260, 547-549.
- HUANG, J., ZARNITSYNA, V. I., LIU, B. Y., EDWARDS, L. J., JIANG, N., EVAVOLD, B. D. & ZHU, C. 2010. The kinetics of two-dimensional TCR and pMHC interactions determine T-cell responsiveness. *Nature*, 464, 932-U156.
- HUANG, J. Y., LO, P. F., ZAL, T., GASCOIGNE, N. R. J., SMITH, B. A., LEVIN, S. D. & GREY, H. M. 2002. CD28 plays a critical role in the segregation of PKC theta within the immunologic synapse. *Proceedings of the National Academy of Sciences of the United States of America*, 99, 9369-9373.
- HUANG, W., OCHS, H. D., DUPONT, B. & VYAS, Y. M. 2005. The Wiskott-Aldrich syndrome protein regulates nuclear translocation of NFAT2 and NF-kappa B (RelA) independently of its role in filamentous actin polymerization and actin cytoskeletal rearrangement. *Journal of Immunology*, 174, 2602-2611.
- HUGUES, S., FETLER, L., BONIFAZ, L., HELFT, J., AMBLARD, F. & AMIGORENA, S. 2004. Distinct T cell dynamics in lymph nodes during the induction of tolerance and immunity. *Nature Immunology*, 5, 1235-1242.
- HUMBLET-BARON, S., SATHER, B., ANOVER, S., BECKER-HERMAN, S., KASPROWICZ, D. J., KHIM, S., NGUYEN, T., HUDKINS-LOYA, K., ALPERS, C. E., ZIEGLER, S. F., OCHS, H., TORGERSON, T., CAMPBELL, D. J. & RAWLINGS, D. J. 2007. Wiskott-Aldrich syndrome protein is required for regulatory T cell homeostasis. *The Journal of clinical investigation*, 117, 407-18.
- HUMPHRIES, J. D., BYRON, A. & HUMPHRIES, M. J. 2006. Integrin ligands at a glance. *Journal of Cell Science*, 119, 3901-3903.

- HUPPA, J. B., AXMANN, M., MORTELMAIER, M. A., LILLEMEIER, B. F., NEWELL, E. W., BRAMESHUBER, M., KLEIN, L. O., SCHUTZ, G. J. & DAVIS, M. M. 2010. TCR-peptide-MHC interactions in situ show accelerated kinetics and increased affinity. *Nature*, 463, 963-7.
- HUPPA, J. B., GLEIMER, M., SUMEN, C. & DAVIS, M. M. 2003. Continuous T cell receptor signaling required for synapse maintenance and full effector potential. *Nature immunology*, 4, 749-55.
- HUSE, M. 2009. The T-cell-receptor signaling network. *Journal of Cell Science*, 122, 1269-1273.
- HUSE, M. 2011. Lymphocyte polarity, the immunological synapse and the scope of biological analogy. *Bioarchitecture*, 1, 180-185.
- HUSE, M. 2012. Microtubule-organizing center polarity and the immunological synapse: protein kinase C and beyond. *Front Immunol*, 3, 235.
- HUSE, M., KLEIN, L. O., GIRVIN, A. T., FARAJ, J. M., LI, Q. J., KUHNS, M. S. & DAVIS, M. M. 2007. Spatial and temporal dynamics of T cell receptor signaling with a photoactivatable agonist. *Immunity*, 27, 76-88.
- HUSE, M., LILLEMEIER, B. F., KUHNS, M. S., CHEN, D. S. & DAVIS, M. M. 2006. T cells use two directionally distinct pathways for cytokine secretion. *Nature Immunology*, 7, 247-255.
- HUTLOFF, A., DITTRICH, A. M., BEIER, K. C., ELJASCHEWITSCH, B., KRAFT, R., ANAGNOSTOPOULOS, I. & KROCZEK, R. A. 1999. ICOS is an inducible T-cell co-stimulator structurally and functionally related to CD28. *Nature*, 397, 263-266.
- ICHETOVKIN, I., HAN, J. H., PANG, K. M., KNECHT, D. A. & CONDEELIS, J. S. 2000. Actin filaments are severed by both native and recombinant Dictyostelium cofilin but to different extents. *Cell Motility and the Cytoskeleton*, 45, 293-306.
- ILANI, T., VASILIVER-SHAMIS, G., VARDHANA, S., BRETSCHER, A. & DUSTIN, M. L. 2009. T cell antigen receptor signaling and immunological synapse stability require myosin IIA. *Nature immunology*, 10, 531-9.
- IMAI, K., MORIO, T., ZHU, Y., JIN, Y. Z., ITOH, S., KAJIWARA, M., YATA, J., MIZUTANI, S., OCHS, H. D. & NONOYAMA, S. 2004. Clinical course of patients with WASP gene mutations. *Blood*, 103, 456-464.
- IMAMURA, H., TANAKA, K., HIHARA, T., UMIKAWA, M., KAMEI, T., TAKAHASHI, K., SASAKI, T. & TAKAI, Y. 1997. Bni1p and Bnr1p: Downstream targets of the Rho family small G-proteins which interact with profilin and regulate actin cytoskeleton in *Saccharomyces cerevisiae*. *Embo Journal*, 16, 2745-2755.
- INABA, K., INABA, M., ROMANI, N., AYA, H., DEGUCHI, M., IKEHARA, S., MURAMATSU, S. & STEINMAN, R. M. 1992. Generation of Large Numbers of Dendritic Cells from Mouse Bone-Marrow Cultures Supplemented with Granulocyte Macrophage Colony-Stimulating Factor. *Journal of Experimental Medicine*, 176, 1693-1702.
- ISAAC, B. M., ISHIHARA, D., NUSBLAT, L. M., GEVREY, J.-C., DOVAS, A., CONDEELIS, J. & COX, D. 2010. N-WASP has the ability to compensate for the loss of WASP in

- macrophage podosome formation and chemotaxis. *Experimental Cell Research*, 316, 3406-3416.
- ITANO, A. A., MCSORLEY, S. J., REINHARDT, R. L., EHST, B. D., INGULLI, E., RUDENSKY, A. Y. & JENKINS, M. K. 2003. Distinct dendritic cell populations sequentially present antigen to CD4 T cells and stimulate different aspects of cell-mediated immunity. *Immunity*, 19, 47-57.
- JENKINS, M. K., BURRELL, E. & ASHWELL, J. D. 1990. Antigen Presentation by Resting B-Cells - Effectiveness at Inducing T-Cell Proliferation Is Determined by Costimulatory Signals, Not T-Cell Receptor Occupancy. *Journal of Immunology*, 144, 1585-1590.
- JENKINS, M. K. & JOHNSON, J. G. 1993. Molecules Involved in T-Cell Costimulation. *Current Opinion in Immunology*, 5, 361-367.
- JENKINS, M. K., MUELLER, D., SCHWARTZ, R. H., CARDING, S., BOTTOMLEY, K., STADECKER, M. J., URDAHL, K. B. & NORTON, S. D. 1991. Induction and Maintenance of Anergy in Mature T-Cells. *Mechanisms of Lymphocyte Activation and Immune Regulation Iij*, 292, 167-176.
- JO, J. H., KWON, M. S., CHOI, H. O., OH, H. M., KIM, H. J. & JUN, C. D. 2010. Recycling and LFA-1-dependent trafficking of ICAM-1 to the immunological synapse. *J Cell Biochem*, 111, 1125-37.
- JONES, G. E., ZICHA, D., DUNN, G. A., BLUNDELL, M. & THRASHER, A. 2002. Restoration of podosomes and chemotaxis in Wiskott-Aldrich syndrome macrophages following induced expression of WASp. *International Journal of Biochemistry & Cell Biology*, 34, 806-815.
- JURDIC, P., SALTEL, F., CHABADEL, A. & DESTAING, O. 2006. Podosome and sealing zone: Specificity of the osteoclast model. *European Journal of Cell Biology*, 85, 195-202.
- KAIZUKA, Y., DOUGLASS, A. D., VARMA, R., DUSTIN, M. L. & VALE, R. D. 2007. Mechanisms for segregating T cell receptor and adhesion molecules during immunological synapse formation in Jurkat T cells. *Proceedings of the National Academy of Sciences of the United States of America*, 104, 20296-301.
- KANEHISA, J., YAMANAKA, T., DOI, S., TURKSEN, K., HEERSCHKE, J. N. M., AUBIN, J. E. & TAKEUCHI, H. 1990. A Band of F-Actin Containing Podosomes Is Involved in Bone-Resorption by Osteoclasts. *Bone*, 11, 287-293.
- KAPLAN, M. H., SCHINDLER, U., SMILEY, S. T. & GRUSBY, M. J. 1996. Stat6 is required for mediating responses to IL-4 and for development of Th2 cells. *Immunity*, 4, 313-9.
- KAPSENBERG, M. L. 2003. Dendritic-cell control of pathogen-driven T-cell polarization. *Nature Reviews Immunology*, 3, 984-993.
- KASZA, K. E., BROEDERSZ, C. P., KOENDERINK, G. H., LIN, Y. C., MESSNER, W., MILLMAN, E. A., NAKAMURA, F., STOSSEL, T. P., MACKINTOSH, F. C. & WEITZ, D. A. 2010. Actin Filament Length Tunes Elasticity of Flexibly Cross-Linked Actin Networks. *Biophysical Journal*, 99, 1091-1100.

- KEARNEY, E. R., PAPE, K. A., LOH, D. Y. & JENKINS, M. K. 1994. Visualization of Peptide-Specific T-Cell Immunity and Peripheral Tolerance Induction in-Vivo. *Immunity*, 1, 327-339.
- KELLY, A. E., KRANITZ, H., DOTSCHE, V. & MULLINS, R. D. 2006. Actin binding to the central domain of WASP/Scar proteins plays a critical role in the activation of the arp2/3 complex. *Journal of Biological Chemistry*, 281, 10589-10597.
- KEREN, K., YAM, P. T., KINKHABWALA, A., MOGILNER, A. & THERIOT, J. A. 2009. Intracellular fluid flow in rapidly moving cells. *Nature Cell Biology*, 11, 1219-U137.
- KHAYYAMIAN, S., HUTLOFF, A., BUCHNER, K., GRAFE, M., HENN, V., KROCZEK, R. A. & MAGES, H. W. 2002. ICOS-ligand, expressed on human endothelial cells, costimulates Th1 and Th2 cytokine secretion by memory CD4(+) T cells. *Proceedings of the National Academy of Sciences of the United States of America*, 99, 6198-6203.
- KHURANA, S. & GEORGE, S. P. 2011. The role of actin bundling proteins in the assembly of filopodia in epithelial cells. *Cell Adhesion & Migration*, 5, 409-420.
- KILE, B. T., PANOPOULOS, A. D., STIRZAKER, R. A., HACKING, D. F., TAHTAMOUNI, L. H., WILLSON, T. A., MIELKE, L. A., HENLEY, K. J., ZHANG, J. G., WICKS, I. P., STEVENSON, W. S., NURDEN, P., WATOWICH, S. S. & JUSTICE, M. J. 2007. Mutations in the cofilin partner Aip1/Wdr1 cause autoinflammatory disease and macrothrombocytopenia. *Blood*, 110, 2371-2380.
- KIM, A. S., KAKALIS, L. T., ABDUL-MANAN, N., LIU, G. A. & ROSEN, M. K. 2000. Autoinhibition and activation mechanisms of the Wiskott-Aldrich syndrome protein. *Nature*, 404, 151-8.
- KINASHI, T. 2005. Intracellular signalling controlling integrin activation in lymphocytes. *Nature Reviews Immunology*, 5, 546-559.
- KLOS DEHRING, D. A., CLARKE, F., RICART, B. G., HUANG, Y., GOMEZ, T. S., WILLIAMSON, E. K., HAMMER, D. A., BILLADEAU, D. D., ARGON, Y. & BURKHARDT, J. K. 2011. Hematopoietic lineage cell-specific protein 1 functions in concert with the wiskott-Aldrich syndrome protein to promote podosome array organization and chemotaxis in dendritic cells. *J Immunol*, 186, 4805-18.
- KOBIELAK, A., PASOLLI, H. A. & FUCHS, E. 2004. Mammalian formin-1 participates in adherens junctions and polymerization of linear actin cables. *Nature Cell Biology*, 6, 21-U2.
- KOLLURI, R., TOLIAS, K. F., CARPENTER, C. L., ROSEN, F. S. & KIRCHHAUSEN, T. 1996. Direct interaction of the Wiskott-Aldrich syndrome protein with the GTPase Cdc42. *Proceedings of the National Academy of Sciences of the United States of America*, 93, 5615-5618.
- KONZOK, A., WEBER, I., SIMMETH, E., HACKER, U., MANIAK, M. & MULLER-TAUBENBERGER, A. 1999. DAip1, a Dictyostelium homologue of the yeast actin-interacting protein 1, is involved in endocytosis, cytokinesis, and motility. *Journal of Cell Biology*, 146, 453-464.

- KORETZKY, G. A., ABTAHIAN, F. & SILVERMAN, M. A. 2006. SLP76 and SLP65: complex regulation of signalling in lymphocytes and beyond. *Nature Reviews Immunology*, 6, 67-78.
- KORN, T., BETTELLI, E., GAO, W., AWASTHI, A., JAGER, A., STROM, T. B., OUKKA, M. & KUCHROO, V. K. 2007. IL-21 initiates an alternative pathway to induce proinflammatory T(H)17 cells. *Nature*, 448, 484-7.
- KOSAKA, S., TAMAUCHI, H., TERASHIMA, M., MARUYAMA, H., HABU, S. & KITASATO, H. 2011. IL-10 controls Th2-type cytokine production and eosinophil infiltration in a mouse model of allergic airway inflammation. *Immunobiology*, 216, 811-820.
- KOVAR, D. R., HARRIS, E. S., MAHAFFY, R., HIGGS, H. N. & POLLARD, T. D. 2006. Control of the assembly of ATP- and ADP-actin by formins and profilin. *Cell*, 124, 423-435.
- KOYA, R. C., FUJITA, H., SHIMIZU, S., OHTSU, M., TAKIMOTO, M., TSUJIMOTO, Y. & KUZUMAKI, N. 2000. Gelsolin inhibits apoptosis by blocking mitochondrial membrane potential loss and cytochrome c release. *Journal of Biological Chemistry*, 275, 15343-15349.
- KOZMA, R., AHMED, S., BEST, A. & LIM, L. 1995. The Ras-Related Protein Cdc42hs and Bradykinin Promote Formation of Peripheral Actin Microspikes and Filopodia in Swiss 3t3 Fibroblasts. *Molecular and Cellular Biology*, 15, 1942-1952.
- KRAWCZYK, C., OLIVEIRA-DOS-SANTOS, A., SASAKI, T., GRIFFITHS, E., OHASHI, P. S., SNAPPER, S., ALT, F. & PENNINGER, J. M. 2002. Vav1 controls integrin clustering and MHC/peptide-specific cell adhesion to antigen-presenting cells. *Immunity*, 16, 331-343.
- KREISHMAN-DETRICK, M., GOLEY, E. D., BURDINE, L., DENISON, C., EGILE, C., LI, R., MURALI, N., KODADEK, T. J., WELCH, M. D. & ROSEN, M. K. 2005. NMR analyses of the activation of the Arp2/3 complex by neuronal Wiskott-Aldrich syndrome protein. *Biochemistry*, 44, 15247-15256.
- KRUMMEL, M. F. & ALLISON, J. P. 1996. CTLA-4 engagement inhibits IL-2 accumulation and cell cycle progression upon activation of resting T cells. *Journal of Experimental Medicine*, 183, 2533-2540.
- KRUMMEL, M. F., SJAASTAD, M. D., WULFING, C. & DAVIS, M. M. 2000. Differential clustering of CD4 and CD3 zeta during T cell recognition. *Science*, 289, 1349-1352.
- KUHNE, M. R., LIN, J., YABLONSKI, D., MOLLENAUER, M. N., EHRLICH, L. I. R., HUPPA, J., DAVIS, M. M. & WEISS, A. 2003. Linker for activation of T cells, zeta-associated protein-70, and Src homology 2 domain-containing leukocyte protein-76 are required for TCR-induced microtubule-organizing center polarization. *Journal of Immunology*, 171, 860-866.
- KUPFER, A., MOSMANN, T. R. & KUPFER, H. 1991. Polarized expression of cytokines in cell conjugates of helper T cells and splenic B cells. *Proceedings of the National Academy of Sciences of the United States of America*, 88, 775-9.
- KUPFER, A., SINGER, S. J., JANEWAY, C. A. & SWAIN, S. L. 1987. Co-clustering of Cd4 (L3t4) Molecule with the T-Cell Receptor Is Induced by Specific Direct

- Interaction of Helper T-Cells and Antigen-Presenting Cells. *Proceedings of the National Academy of Sciences of the United States of America*, 84, 5888-5892.
- LAKKAKORPI, P., TUUKKANEN, J., HENTUNEN, T., JARVELIN, K. & VAANANEN, K. 1989. Organization of Osteoclast Microfilaments during the Attachment to Bone Surface Invitro. *Journal of Bone and Mineral Research*, 4, 817-825.
- LAMBE, T., CRAWFORD, G., JOHNSON, A. L., CROCKFORD, T. L., BOURIEZ-JONES, T., SMYTH, A. M., PHAM, T. H., ZHANG, Q., FREEMAN, A. F., CYSTER, J. G., SU, H. C. & CORNALL, R. J. 2011. DOCK8 is essential for T-cell survival and the maintenance of CD8+ T-cell memory. *Eur J Immunol*, 41, 3423-35.
- LAOUIINI, D., ALENIUS, H., BRYCE, P., OETTGEN, H., TSITSIKOV, E. & GEHA, R. S. 2003. IL-10 is critical for Th2 responses in a murine model of allergic dermatitis. *Journal of Clinical Investigation*, 112, 1058-1066.
- LARGHI, P., WILLIAMSON, D. J., CARPIER, J. M., DOGNIAUX, S., CHEMIN, K., BOHINEUST, A., DANGLLOT, L., GAUS, K., GALLI, T. & HIVROZ, C. 2013. VAMP7 controls T cell activation by regulating the recruitment and phosphorylation of vesicular Lat at TCR-activation sites. *Nature Immunology*, 14, 723-+.
- LASSERRE, R., CHARRIN, S., CUCHE, C., DANCKAERT, A., THOULOZE, M. I., DE CHAUMONT, F., DUONG, T., PERRAULT, N., VARIN-BLANK, N., OLIVO-MARIN, J. C., ETIENNE-MANNEVILLE, S., ARPIN, M., DI BARTOLO, V. & ALCOVER, A. 2010. Ezrin tunes T-cell activation by controlling Dlg1 and microtubule positioning at the immunological synapse. *Embo Journal*, 29, 2301-2314.
- LE FLOC'H, A., TANAKA, Y., BANTILAN, N. S., VOISINNE, G., ALTAN-BONNET, G., FUKUI, Y. & HUSE, M. 2013. Annular PIP3 accumulation controls actin architecture and modulates cytotoxicity at the immunological synapse. *Journal of Experimental Medicine*, 210, 2721-2737.
- LEE, K. H., DINNER, A. R., TU, C., CAMPI, G., RAYCHAUDHURI, S., VARMA, R., SIMS, T. N., BURACK, W. R., WU, H., KANAGAWA, O., MARKIEWICZ, M., ALLEN, P. M., DUSTIN, M. L., CHAKRABORTY, A. K. & SHAW, A. S. 2003a. The immunological synapse balances T cell receptor signaling and degradation. *Science*, 302, 1218-1222.
- LEE, K. H., DINNER, A. R., TU, C., CAMPI, G., RAYCHAUDHURI, S., VARMA, R., SIMS, T. N., BURACK, W. R., WU, H., WANG, J., KANAGAWA, O., MARKIEWICZ, M., ALLEN, P. M., DUSTIN, M. L., CHAKRABORTY, A. K. & SHAW, A. S. 2003b. The immunological synapse balances T cell receptor signaling and degradation. *Science*, 302, 1218-22.
- LEE, K. H., HOLDORF, A. D., DUSTIN, M. L., CHAN, A. C., ALLEN, P. M. & SHAW, A. S. 2002. T cell receptor signaling precedes immunological synapse formation. *Science*, 295, 1539-42.
- LENARDO, M. J. 1991. Interleukin-2 Programs Mouse Alpha-Beta-Lymphocytes-T for Apoptosis. *Nature*, 353, 858-861.
- LEUPIN, O., ZARU, R., LAROCHE, T., MULLER, S. & VALITUTTI, S. 2000. Exclusion of CD45 from the T-cell receptor signaling area in antigen-stimulated T lymphocytes. *Current Biology*, 10, 277-280.

- LEVERRIER, Y., LORENZI, R., BLUNDELL, M. P., BRICKELL, P., KINNON, C., RIDLEY, A. J. & THRASHER, A. J. 2001. Cutting edge: the Wiskott-Aldrich syndrome protein is required for efficient phagocytosis of apoptotic cells. *J Immunol*, 166, 4831-4.
- LEWKOWICZ, E., HERIT, F., LE CLAINCHE, C., BOURDONCLE, P., PEREZ, F. & NIEDERGANG, F. 2008. The microtubule-binding protein CLIP-170 coordinates mDia1 and actin reorganization during CR3-mediated phagocytosis. *Journal of Cell Biology*, 183, 1287-1298.
- LI, F. & HIGGS, H. N. 2005. Dissecting requirements for auto-inhibition of actin nucleation by the formin, mDia1. *Journal of Biological Chemistry*, 280, 6986-6992.
- LI, S. J., CHANG, S. R., QI, X. X., RICHARDSON, J. A. & OLSON, E. N. 2006. Requirement of a myocardin-related transcription factor for development of mammary myoepithelial cells. *Molecular and Cellular Biology*, 26, 5797-5808.
- LIGHVANI, A. A., FRUCHT, D. M., JANKOVIC, D., YAMANE, H., ALIBERTI, J., HISSONG, B. D., NGUYEN, B. V., GADINA, M., SHER, A., PAUL, W. E. & O'SHEA, J. J. 2001. T-bet is rapidly induced by interferon-gamma in lymphoid and myeloid cells. *Proceedings of the National Academy of Sciences of the United States of America*, 98, 15137-42.
- LILLEMEIER, B. F., MORTELMAIER, M. A., FORSTNER, M. B., HUPPA, J. B., GROVES, J. T. & DAVIS, M. M. 2010. TCR and Lat are expressed on separate protein islands on T cell membranes and concatenate during activation. *Nature Immunology*, 11, 90-U106.
- LIN, J., MILLER, M. J. & SHAW, A. S. 2005. The c-SMAC: sorting it all out (or in). *The Journal of cell biology*, 170, 177-82.
- LINDER, S. 2007. The matrix corroded: podosomes and invadopodia in extracellular matrix degradation. *Trends in Cell Biology*, 17, 107-117.
- LINDER, S. & AEPFELBACHER, M. 2003. Podosomes: adhesion hot-spots of invasive cells. *Trends in Cell Biology*, 13, 376-385.
- LINDER, S., HUFNER, K., WINTERGERST, U. & AEPFELBACHER, M. 2000. Microtubule-dependent formation of podosomal adhesion structures in primary human macrophages. *Journal of Cell Science*, 113, 4165-4176.
- LINDER, S. & KOPP, P. 2005. Podosomes at a glance. *Journal of Cell Science*, 118, 2079-2082.
- LINDER, S., NELSON, D., WEISS, M. & AEPFELBACHER, M. 1999. Wiskott-Aldrich syndrome protein regulates podosomes in primary human macrophages. *Proceedings of the National Academy of Sciences of the United States of America*, 96, 9648-9653.
- LINDQUIST, R. L., SHAKHAR, G., DUDZIAK, D., WARDEMAN, H., EISENREICH, T., DUSTIN, M. L. & NUSSENZWEIG, M. C. 2004. Visualizing dendritic cell networks in vivo. *Nature Immunology*, 5, 1243-1250.
- LINSLEY, P. S., BRADY, W., GROSMARE, L., ARUFFO, A., DAMLE, N. K. & LEDBETTER, J. A. 1991. Binding of the B-Cell Activation Antigen B7 to Cd28 Costimulates T-Cell

- Proliferation and Interleukin-2 Messenger-Rna Accumulation. *Journal of Experimental Medicine*, 173, 721-730.
- LINSLEY, P. S., GREENE, J. L., TAN, P., BRADSHAW, J., LEDBETTER, J. A., ANASETTI, C. & DAMLE, N. K. 1992. Coexpression and Functional Cooperation of Ctl α -4 and Cd28 on Activated Lymphocytes-T. *Journal of Experimental Medicine*, 176, 1595-1604.
- LIU, B. Y., CHEN, W., EVAVOLD, B. D. & ZHU, C. 2014. Accumulation of Dynamic Catch Bonds between TCR and Agonist Peptide-MHC Triggers T Cell Signaling. *Cell*, 157.
- LIU, D., BRYCESON, Y. T., MECKEL, T., VASILIVER-SHAMIS, G., DUSTIN, M. L. & LONG, E. O. 2009. Integrin-dependent organization and bidirectional vesicular traffic at cytotoxic immune synapses. *Immunity*, 31, 99-109.
- LIU, Y. & JANEWAY, C. A. 1991. Microbial Induction of Costimulatory Activity for Cd4 T-Cell Growth. *International Immunology*, 3, 323-332.
- LOCKSLEY, R. M., KILLEEN, N. & LENARDO, M. J. 2001. The TNF and TNF receptor superfamilies: Integrating mammalian biology. *Cell*, 104, 487-501.
- LOOI, C. Y., SASAHARA, Y., WATANABE, Y., SATOH, M., HAKOZAKI, I., UCHIYAMA, M., WONG, W. F., DU, W., UCHIYAMA, T., KUMAKI, S., TSUCHIYA, S. & KURE, S. 2014. The open conformation of WASP regulates its nuclear localization and gene transcription in myeloid cells. *Int Immunol*.
- LORENZI, R., BRICKELL, P. M., KATZ, D. R., KINNON, C. & THRASHER, A. J. 2000. Wiskott-Aldrich syndrome protein is necessary for efficient IgG-mediated phagocytosis. *Blood*, 95, 2943-2946.
- LOWIN-KROPF, B., SHAPIRO, V. S. & WEISS, A. 1998. Cytoskeletal polarization of T cells is regulated by an immunoreceptor tyrosine-based activation motif-dependent mechanism. *Journal of Cell Biology*, 140, 861-871.
- LU, J., MENG, W. Y., POY, F., MAITI, S., GOODE, B. L. & ECK, M. J. 2007. Structure of the FH2 domain of Daam1: Implications for formin regulation of actin assembly. *Journal of Molecular Biology*, 369, 1258-1269.
- LUB, M., VANKOOYK, Y., VANVLIET, S. J. & FIGDOR, C. G. 1997. Dual role of the actin cytoskeleton in regulating cell adhesion mediated by the integrin lymphocyte function-associated molecule-1. *Molecular Biology of the Cell*, 8, 341-351.
- LUDFORD-MENTING, M. J., OLIARO, J., SACIRBEGOVIC, F., CHEAH, E. T. Y., PEDERSEN, N., THOMAS, S. J., PASAM, A., IAZZOLINO, R., DOW, L. E., WATERHOUSE, N. J., MURPHY, A., ELLIS, S., SMYTH, M. J., KERSHAW, M. H., DARCY, P. K., HUMBERT, P. O. & RUSSELL, S. M. 2005. A network of PDZ-containing proteins regulates T cell polarity and morphology during migration and immunological synapse formation. *Immunity*, 22, 737-748.
- MA, Z. G., MORRIS, S. W., VALENTINE, V., LI, M., HERBRICK, J. A., CUI, X. L., BOUMAN, D., LI, Y., MEHTA, P. K., NIZETIC, D., KANEKO, Y., CHAN, G. C. F., CHAN, L. C., SQUIRE, J., SCHERER, S. W. & HITZLER, J. K. 2001. Fusion of two novel genes, RBM15 and MKL1, in the t(1;22)(p13;q13) of acute megakaryoblastic leukemia. *Nature Genetics*, 28, 220-221.

- MABUCHI, I. 1983. An Actin-Depolymerizing Protein (Depactin) from Starfish Oocytes - Properties and Interaction with Actin. *Journal of Cell Biology*, 97, 1612-1621.
- MACATONIA, S. E., KNIGHT, S. C., EDWARDS, A. J., GRIFFITHS, S. & FRYER, P. 1987. Localization of Antigen on Lymph-Node Dendritic Cells after Exposure to the Contact Sensitizer Fluorescein Isothiocyanate - Functional and Morphological-Studies. *Journal of Experimental Medicine*, 166, 1654-1667.
- MACE, E. M., MONKLEY, S. J., CRITCHLEY, D. R. & TAKEI, F. 2009. A Dual Role for Talin in NK Cell Cytotoxicity: Activation of LFA-1-Mediated Cell Adhesion and Polarization of NK Cells. *Journal of Immunology*, 182, 948-956.
- MACE, E. M., ZHANG, J. Y., SIMINOVITCH, K. A. & TAKEI, F. 2010. Elucidation of the integrin LFA-1-mediated signaling pathway of actin polarization in natural killer cells. *Blood*, 116, 1272-1279.
- MACHESKY, L. M. & INSALL, R. H. 1998. Scar1 and the related Wiskott-Aldrich syndrome protein, WASP, regulate the actin cytoskeleton through the Arp2/3 complex. *Current Biology*, 8, 1347-1356.
- MACHESKY, L. M., MULLINS, R. D., HIGGS, H. N., KAISER, D. A., BLANCHOIN, L., MAY, R. C., HALL, M. E. & POLLARD, T. D. 1999. Scar, a WASp-related protein, activates nucleation of actin filaments by the Arp2/3 complex. *Proceedings of the National Academy of Sciences of the United States of America*, 96, 3739-3744.
- MACIVER, S. K. & HUSSEY, P. J. 2002. The ADF/cofilin family: actin-remodeling proteins. *Genome Biology*, 3.
- MACPHERSON, L., MONYPENNY, J., BLUNDELL, M. P., CORY, G. O., TOME-GARCIA, J., THRASHER, A. J., JONES, G. E. & CALLE, Y. 2012. Tyrosine phosphorylation of WASP promotes calpain-mediated podosome disassembly. *Haematologica-the Hematology Journal*, 97, 687-691.
- MALDONADO, R. A., IRVINE, D. J., SCHREIBER, R. & GLIMCHER, L. H. 2004. A role for the immunological synapse in lineage commitment of CD4 lymphocytes. *Nature*, 431, 527-32.
- MANZ, M. G., TRAVER, D., AKASHI, K., MERAD, M., MIYAMOTO, T., ENGLEMAN, E. G. & WEISSMAN, I. L. 2001. Dendritic cell development from common myeloid progenitors. *Hematopoietic Stem Cells 2000 Basic and Clinical Sciences*, 938, 167-174.
- MARCHAND, J. B., KAISER, D. A., POLLARD, T. D. & HIGGS, H. N. 2001. Interaction of WASP/Scar proteins with actin and vertebrate Arp2/3 complex. *Nature Cell Biology*, 3, 76-82.
- MARCHISIO, P. C., CIRILLO, D., TETI, A., ZAMBONINZALLONE, A. & TARONE, G. 1987. Rous-Sarcoma Virus-Transformed Fibroblasts and Cells of Monocytic Origin Display a Peculiar Dot-Like Organization of Cytoskeletal Proteins Involved in Microfilament Membrane Interactions. *Experimental Cell Research*, 169, 202-214.
- MARKIEWICZ, M. A., CARAYANNOPOULOS, L. N., NAIDENKO, O. V., MATSUI, K., BURACK, W. R., WISE, E. L., FREMONT, D. H., ALLEN, P. M., YOKOYAMA, W. M., COLONNA, M. & SHAW, A. S. 2005. Costimulation through NKG2D enhances

- murine CD8(+) CTL function: Similarities and differences between NKG2D and CD28 costimulation. *Journal of Immunology*, 175, 2825-2833.
- MASEDUNSKAS, A., SRAMKOVA, M., PARENTE, L., SALES, K. U., AMORNPHIMOLTHAM, P., BUGGE, T. H. & WEIGERT, R. 2011. Role for the actomyosin complex in regulated exocytosis revealed by intravital microscopy. *Proceedings of the National Academy of Sciences of the United States of America*, 108, 13552-13557.
- MASSAAD, M. J., RAMESH, N. & GEHA, R. S. 2013. Wiskott-Aldrich syndrome: a comprehensive review. *Year in Immunology*, 1285, 26-43.
- MAYYA, V. & DUSTIN, M. L. 2010. Actin Cytoskeleton and the Dynamics of Immunological Synapse. *Actin-Based Motility: Cellular, Molecular and Physical Aspects*, 103-124.
- MCGOUGH, A., POPE, B., CHIU, W. & WEEDS, A. 1997. Cofilin changes the twist of F-actin: Implications for actin filament dynamics and cellular function. *Journal of Cell Biology*, 138, 771-781.
- MCLELLAN, A. D., SORG, R. V., WILLIAMS, L. A. & HART, D. N. J. 1996. Human dendritic cells activate T lymphocytes via a CD40:CD40 ligand-dependent pathway. *European Journal of Immunology*, 26, 1204-1210.
- MEJILLANO, M. R., KOJIMA, S., APPLEWHITE, D. A., GERTLER, F. B., SVITKINA, T. M. & BORISY, G. G. 2004. Lamellipodial versus filopodial mode of the actin nanomachinery: Pivotal role of the filament barbed end. *Cell*, 118, 363-373.
- MELLER, N., MERLOT, S. & GUDA, C. 2005. CZH proteins: a new family of Rho-GEFs. *J Cell Sci*, 118, 4937-46.
- MELLMAN, I. & STEINMAN, R. M. 2001. Dendritic cells: specialized and regulated antigen processing machines. *Cell*, 106, 255-8.
- MEMPEL, T. R., HENRICKSON, S. E. & VON ANDRIAN, U. H. 2004. T-cell priming by dendritic cells in lymph nodes occurs in three distinct phases. *Nature*, 427, 154-9.
- MEMPEL, T. R., PITTET, M. J., KHAZAIE, K., WENINGER, W., WEISSLEDER, R., VON BOEHMER, H. & VON ANDRIAN, U. H. 2006. Regulatory T cells reversibly suppress cytotoxic T cell function independent of effector differentiation. *Immunity*, 25, 129-141.
- MENDOZA-NARANJO, A., BOUMA, G., PEREDA, C., RAMIREZ, M., WEBB, K. F., TITTARELLI, A., LOPEZ, M. N., KALERGIS, A. M., THRASHER, A. J., BECKER, D. L. & SALAZAR-ONFRAY, F. 2011. Functional gap junctions accumulate at the immunological synapse and contribute to T cell activation. *Journal of immunology*, 187, 3121-32.
- MERCHER, T., BUSSON-LE CONIAT, M., MONNI, R., MAUCHAUFFE, M., KHAC, F. N., GRESSIN, L., MUGNERET, F., LEBLANC, T., DASTUGUE, N., BERGER, R. & BERNARD, O. A. 2001. Involvement of a human gene related to the *Drosophila* spen gene in the recurrent t(1;22) translocation of acute megakaryocytic leukemia. *Proceedings of the National Academy of Sciences of the United States of America*, 98, 5776-5779.

- MERINO, E., ABEYWEERA, T. P., FIRTH, M. A., ZAWISLAK, C. L., BASU, R., LIU, X., SUN, J. C. & HUSE, M. 2012. Protein Kinase C-theta Clustering at Immunological Synapses Amplifies Effector Responses in NK Cells. *Journal of Immunology*, 189, 4859-4869.
- METZLER, W. J., BAJORATH, J., FENDERSON, W., SHAW, S. Y., CONSTANTINE, K. L., NAEMURA, J., LEYTZE, G., PEACH, R. J., LAVOIE, T. B., MUELLER, L. & LINSLEY, P. S. 1997. Solution structure of human CTLA-4 and delineation of a CD80/CD86 binding site conserved in CD28. *Nature Structural Biology*, 4, 527-531.
- MEYER-BAHLBURG, A., BECKER-HERMAN, S., HUMBLET-BARON, S., KHIM, S., WEBER, M., BOUMA, G., THRASHER, A. J., BATISTA, F. D. & RAWLINGS, D. J. 2008. Wiskott-Aldrich syndrome protein deficiency in B cells results in impaired peripheral homeostasis. *Blood*, 112, 4158-69.
- MIKI, H. & TAKENAWA, T. 1998. Direct binding of the verprolin-homology domain in N-WASP to actin is essential for cytoskeletal reorganization. *Biochemical and Biophysical Research Communications*, 243, 73-78.
- MILLARD, T. H., SHARP, S. J. & MACHESKY, L. M. 2004. Signalling to actin assembly via the WASP (Wiskott-Aldrich syndrome protein)-family proteins and the Arp2/3 complex. *Biochemical Journal*, 380, 1-17.
- MILLER, M. J., HEJAZI, A. S., WEI, S. H., CAHALAN, M. D. & PARKER, I. 2004a. T cell repertoire scanning is promoted by dynamic dendritic cell behavior and random T cell motility in the lymph node. *Proceedings of the National Academy of Sciences of the United States of America*, 101, 998-1003.
- MILLER, M. J., SAFRINA, O., PARKER, I. & CAHALAN, M. D. 2004b. Imaging the single cell dynamics of CD4(+) T cell activation by dendritic cells in lymph nodes. *Journal of Experimental Medicine*, 200, 847-856.
- MILLER, M. J., WEI, S. H., CAHALAN, M. D. & PARKER, I. 2003. Autonomous T cell trafficking examined in vivo with intravital two-photon microscopy. *Proceedings of the National Academy of Sciences of the United States of America*, 100, 2604-2609.
- MILLER, M. J., WEI, S. H., PARKER, I. & CAHALAN, M. D. 2002. Two-photon imaging of lymphocyte motility and antigen response in intact lymph node. *Science*, 296, 1869-1873.
- MILNER, J. D., SANDLER, N. G. & DOUEK, D. C. 2010. Th17 cells, Job's syndrome and HIV: opportunities for bacterial and fungal infections. *Curr Opin HIV AIDS*, 5, 179-83.
- MINEGISHI, Y., SAITO, M., NAGASAWA, M., TAKADA, H., HARA, T., TSUCHIYA, S., AGEMATSU, K., YAMADA, M., KAWAMURA, N., ARIGA, T., TSUGE, I. & KARASUYAMA, H. 2009. Molecular explanation for the contradiction between systemic Th17 defect and localized bacterial infection in hyper-IgE syndrome. *J Exp Med*, 206, 1291-301.
- MIOSSEC, P., KORN, T. & KUCHROO, V. K. 2009. Mechanisms of Disease: Interleukin-17 and Type 17 Helper T Cells. *New England Journal of Medicine*, 361, 888-898.

- MIRALLES, F., POSERN, G., ZAROMYTIDOU, A. I. & TREISMAN, R. 2003. Actin dynamics control SRF activity by regulation of its coactivator MAL. *Cell*, 113, 329-342.
- MIYAMOTO, Y. & YAMAUCHI, J. 2010. Cellular signaling of Dock family proteins in neural function. *Cell Signal*, 22, 175-82.
- MIYATAKE, S., NAKASEKO, C., UMEMORI, H., YAMAMOTO, T. & SAITO, T. 1998. Src family tyrosine kinases associate with and phosphorylate CTLA-4 (CD152). *Biochemical and Biophysical Research Communications*, 249, 444-448.
- MIZESKO, M. C., BANERJEE, P. P., MONACO-SHAWVER, L., MACE, E. M., BERNAL, W. E., SAWALLE-BELOHRADSKY, J., BELOHRADSKY, B. H., HEINZ, V., FREEMAN, A. F., SULLIVAN, K. E., HOLLAND, S. M., TORGERSON, T. R., AL-HERZ, W., CHOU, J., HANSON, I. C., ALBERT, M. H., GEHA, R. S., RENNER, E. D. & ORANGE, J. S. 2013. Defective actin accumulation impairs human natural killer cell function in patients with dedicator of cytokinesis 8 deficiency. *J Allergy Clin Immunol*, 131, 840-8.
- MODIANO, P., SALLOUM, E., GILLET-TERVER, M. N., BARBAUD, A., GEORGES, J. C., THOUVENOT, D., SCHMUTZ, J. L. & WEBER, M. 1995. Acyclovir-resistant chronic cutaneous herpes simplex in Wiskott-Aldrich syndrome. *Br J Dermatol*, 133, 475-8.
- MONICA GORDON-ALONSO, E. V., FRANCISCO SANCHEZ-MADRID 2010. Actin dynamics at the immunological synapse. *Cell Health and Cytoskeleton*.
- MONKS, C. R., FREIBERG, B. A., KUPFER, H., SCIAKY, N. & KUPFER, A. 1998. Three-dimensional segregation of supramolecular activation clusters in T cells. *Nature*, 395, 82-6.
- MONKS, C. R. F., KUPFER, H., TAMIR, I., BARLOW, A. & KUPFER, A. 1997. Selective modulation of protein kinase C-theta during T-cell activation. *Nature*, 385, 83-86.
- MONYPENNY, J., CHOU, H. C., BANON-RODRIGUEZ, I., THRASHER, A. J., ANTON, I. M., JONES, G. E. & CALLE, Y. 2011. Role of WASP in cell polarity and podosome dynamics of myeloid cells. *Eur J Cell Biol*, 90, 198-204.
- MOORE, K. W., MALEFYT, R. D., COFFMAN, R. L. & O'GARRA, A. 2001. Interleukin-10 and the interleukin-10 receptor. *Annual Review of Immunology*, 19, 683-765.
- MORALES-TIRADO, V., JOHANNSON, S., HANSON, E., HOWELL, A., ZHANG, J. Y., SIMINOVITCH, K. A. & FOWELL, D. J. 2004. Cutting edge: Selective requirement for the Wiskott-Aldrich syndrome protein in cytokine, but not chemokine, secretion by CD4(+) T cells. *Journal of Immunology*, 173, 726-730.
- MOREAU, H. D., LEMAITRE, F., TERRIAC, E., AZAR, G., PIEL, M., LENNON-DUMENIL, A. M. & BOUSSO, P. 2012. Dynamic In Situ Cytometry Uncovers T Cell Receptor Signaling during Immunological Synapses and Kinapses In Vivo. *Immunity*, 37, 351-363.
- MORLEY, S. C. 2012. The actin-bundling protein L-plastin: a critical regulator of immune cell function. *Int J Cell Biol*, 2012, 935173.
- MOSELEY, J. B., SAGOT, I., MANNING, A. L., XU, Y. W., ECK, J., PELLMAN, D. & GOODE, B. L. 2004. A conserved mechanism for Bni1- and mDia1-induced actin assembly

- and dual regulation of Bni1 by Bud6 and profilin. *Molecular Biology of the Cell*, 15, 896-907.
- MOSMANN, T. R., CHERWINSKI, H., BOND, M. W., GIEDLIN, M. A. & COFFMAN, R. L. 2005. Pillars article: Two types of murine helper T cell clone. I. Definition according to profiles of lymphokine activities and secreted proteins. *Journal of Immunology*, 175, 5-14.
- MOSMANN, T. R. & COFFMAN, R. L. 1989. Th1-Cell and Th2-Cell - Different Patterns of Lymphokine Secretion Lead to Different Functional-Properties. *Annual Review of Immunology*, 7, 145-173.
- MOSSMAN, K. D., CAMPI, G., GROVES, J. T. & DUSTIN, M. L. 2005. Altered TCR signaling from geometrically repatterned immunological synapses. *Science*, 310, 1191-3.
- MOULDING, D. A., BLUNDELL, M. P., SPILLER, D. G., WHITE, M. R. H., CORY, G. O., CALLE, Y., KEMPSKI, H., SINCLAIR, J., ANCLIFF, P. J., KINNON, C., JONES, G. E. & THRASHER, A. J. 2007. Unregulated actin polymerization by WASp causes defects of mitosis and cytokinesis in X-linked neutropenia. *Journal of Experimental Medicine*, 204, 2213-2224.
- MOULDING, D. A., RECORD, J., MALINOVA, D. & THRASHER, A. J. 2013. Actin cytoskeletal defects in immunodeficiency. *Immunological Reviews*, 256, 282-299.
- MULLINS, R. D., HEUSER, J. A. & POLLARD, T. D. 1998. The interaction of Arp2/3 complex with actin: nucleation, high affinity pointed end capping, and formation of branching networks of filaments. *Proceedings of the National Academy of Sciences of the United States of America*, 95, 6181-6.
- MURPHY, K. M. & REINER, S. L. 2002. The lineage decisions of helper T cells. *Nature reviews. Immunology*, 2, 933-44.
- MUSTELIN, T., WILLIAMS, S., TAILOR, P., COUTURE, C., ZENNER, G., BURN, P., ASHWELL, J. D. & ALTMAN, A. 1995. Regulation of the P70(Zap) Tyrosine Protein-Kinase in T-Cells by the Cd45 Phosphotyrosine Phosphatase. *European Journal of Immunology*, 25, 942-946.
- NABAVI, N., FREEMAN, G. J., GAULT, A., GODFREY, D., NADLER, L. M. & GLIMCHER, L. H. 1992. Signaling through the Mhc Class-II Cytoplasmic Domain Is Required for Antigen Presentation and Induces B7 Expression. *Nature*, 360, 266-268.
- NAKAMURA, F., STOSSEL, T. P. & HARTWIG, J. H. 2011. The filamins Organizers of cell structure and function. *Cell Adhesion & Migration*, 5, 160-169.
- NAUMANEN, P., LAPPALAINEN, P. & HOTULAINEN, P. 2008. Mechanisms of actin stress fibre assembly. *Journal of Microscopy-Oxford*, 231, 446-454.
- NEGULESCU, P. A., KRASIEVA, T. B., KHAN, A., KERSCHBAUM, H. H. & CAHALAN, M. D. 1996. Polarity of T cell shape, motility, and sensitivity to antigen. *Immunity*, 4, 421-430.
- NELSON, W. J. 2003. Adaptation of core mechanisms to generate cell polarity. *Nature*, 422, 766-774.
- NGUYEN, D. D., MAILLARD, M. H., COTTA-DE-ALMEIDA, V., MIZOGUCH, E., KLEIN, C., FUSS, I., NAGLER, C., MIZOGUCH, A., BHAN, A. K. & SNAPPER, S. B. 2007.

- Lymphocyte-dependent and Th2 cytokine-associated colitis in mice deficient in Wiskott-Aldrich syndrome protein. *Gastroenterology*, 133, 1188-1197.
- NGUYEN, K., SYLVAIN, N. R. & BUNNELL, S. C. 2008. T cell costimulation via the integrin VLA-4 inhibits the actin-dependent centralization of signaling microclusters containing the adaptor SLP-76. *Immunity*, 28, 810-821.
- NIGHTINGALE, T. D., WHITE, I. J., DOYLE, E. L., TURMAINE, M., HARRISON-LAVOIE, K. J., WEBB, K. F., CRAMER, L. P. & CUTLER, D. F. 2011. Actomyosin II contractility expels von Willebrand factor from Weibel-Palade bodies during exocytosis. *J Cell Biol*, 194, 613-29.
- NIKOLOV, N. P., SHIMIZU, M., CLELAND, S., BAILEY, D., AOKI, J., STROM, T., SCHWARTZBERG, P. L., CANDOTTI, F. & SIEGEL, R. M. 2010. Systemic autoimmunity and defective Fas ligand secretion in the absence of the Wiskott-Aldrich syndrome protein. *Blood*, 116, 740-747.
- NISHIKIMI, A., FUKUHARA, H., SU, W. J., HONGU, T., TAKASUGA, S., MIHARA, H., CAO, Q. H., SANEMATSU, F., KANAI, M., HASEGAWA, H., TANAKA, Y., SHIBASAKI, M., KANAHO, Y., SASAKI, T., FROHMAN, M. A. & FUKUI, Y. 2009. Sequential Regulation of DOCK2 Dynamics by Two Phospholipids During Neutrophil Chemotaxis. *Science*, 324, 384-387.
- NOBES, C. & HALL, A. 1994. Regulation and function of the Rho subfamily of small GTPases. *Curr Opin Genet Dev*, 4, 77-81.
- NOBES, C. D. & HALL, A. 1995. Rho, Rac, and Cdc42 Gtpases Regulate the Assembly of Multimolecular Focal Complexes Associated with Actin Stress Fibers, Lamellipodia, and Filopodia. *Cell*, 81, 53-62.
- NOLZ, J. C., MEDEIROS, R. B., MITCHELL, J. S., ZHU, P., FREEDMAN, B. D., SHIMIZU, Y. & BILLADEAU, D. D. 2007. WAVE2 regulates high-affinity integrin binding by recruiting vinculin and talin to the immunological synapse. *Molecular and Cellular Biology*, 27, 5986-6000.
- NOLZ, J. C., NACUSI, L. P., SEGOVIS, C. M., MEDEIROS, R. B., MITCHELL, J. S., SHIMIZU, Y. & BILLADEAU, D. D. 2008. The WAVE2 complex regulates T cell receptor signaling to integrins via Abl- and CrkL-C3G-mediated activation of Rap1. *Journal of Cell Biology*, 182, 1231-1244.
- NORTON, S. D., ZUCKERMAN, L., URDAHL, K. B., SHEFNER, R., MILLER, J. & JENKINS, M. K. 1992. The Cd28 Ligand, B7, Enhances Il-2 Production by Providing a Costimulatory Signal to T-Cells. *Journal of Immunology*, 149, 1556-1561.
- NOTARANGELO, L. D., NOTARANGELO, L. D. & OCHS, H. D. 2005. WASP and the phenotypic range associated with deficiency. *Current Opinion in Allergy and Clinical Immunology*, 5, 485-490.
- O'KEEFFE, M., HOCHREIN, H., VREMEC, D., CAMINSCHI, I., MILLER, J. L., ANDERS, E. M., WU, L., LAHOUD, H., HENRI, S., SCOTT, B., HERTZOG, P., TATARCZUCH, L. & SHORTMAN, K. 2002. Mouse plasmacytoid cells: Long-lived cells, heterogeneous in surface phenotype and function, that differentiate into CD8(+) dendritic cells only after microbial stimulus. *Journal of Experimental Medicine*, 196, 1307-1319.

- OCHS, H. D. & THRASHER, A. J. 2006. The Wiskott-Aldrich syndrome. *Journal of Allergy and Clinical Immunology*, 117, 725-738.
- ODDOS, S., DUNSBY, C., PURBHOO, M. A., CHAUVEAU, A., OWEN, D. M., NEIL, M. A., DAVIS, D. M. & FRENCH, P. M. 2008. High-speed high-resolution imaging of intercellular immune synapses using optical tweezers. *Biophys J*, 95, L66-8.
- OKADA, K., BLANCHOIN, L., ABE, H., CHEN, H., POLLARD, T. D. & BAMBURG, J. R. 2002. Xenopus actin-interacting protein 1 (XAip1) enhances cofilin fragmentation of filaments by capping filament ends. *Journal of Biological Chemistry*, 277, 43011-43016.
- OKADA, K., OBINATA, T. & ABE, H. 1999. XAIP1: a Xenopus homologue of yeast actin interacting protein 1 (AIP1), which induces disassembly of actin filaments cooperatively with ADF cofilin family proteins. *Journal of Cell Science*, 112, 1553-1565.
- OKADA, T., MILLER, M. J., PARKER, I., KRUMMEL, M. F., NEIGHBORS, M., HARTLEY, S. B., O'GARRA, A., CAHALAN, M. D. & CYSTER, J. G. 2005. Antigen-engaged B cells undergo chemotaxis toward the T zone and form motile conjugates with helper T cells. *Plos Biology*, 3, 1047-1061.
- OLIARO, J., VAN HAM, V., SACIRBEGOVIC, F., PASAM, A., BOMZON, Z., PHAM, K., LUDFORD-MENTING, M. J., WATERHOUSE, N. J., BOTS, M., HAWKINS, E. D., WATT, S. V., CLUSE, L. A., CLARKE, C. J. P., IZON, D. J., CHANG, J. T., THOMPSON, N., GU, M., JOHNSTONE, R. W., SMYTH, M. J., HUMBERT, P. O., REINER, S. L. & RUSSELL, S. M. 2010. Asymmetric Cell Division of T Cells upon Antigen Presentation Uses Multiple Conserved Mechanisms. *Journal of Immunology*, 185, 367-375.
- OLIVIER, A., JEANSON-LEH, L., BOUMA, G., COMPAGNO, D., BLONDEAU, J., SEYE, K., CHARRIER, S., BURNS, S., THRASHER, A. J., DANOS, O., VAINCHENKER, W. & GALY, A. 2006. A partial down-regulation of WASP is sufficient to inhibit podosome formation in dendritic cells. *Molecular therapy : the journal of the American Society of Gene Therapy*, 13, 729-37.
- ONO, S. 2003. Regulation of actin filament dynamics by actin depolymerizing factor/cofilin and actin-interacting protein 1: new blades for twisted filaments. *Biochemistry*, 42, 13363-70.
- ORANGE, J. S. 2008. Formation and function of the lytic NK-cell immunological synapse. *Nat Rev Immunol*, 8, 713-25.
- ORANGE, J. S., HARRIS, K. E., ANDZELM, M. M., VALTER, M. M., GEHA, R. S. & STROMINGER, J. L. 2003. The mature activating natural killer cell immunologic synapse is formed in distinct stages. *Proceedings of the National Academy of Sciences of the United States of America*, 100, 14151-14156.
- ORANGE, J. S., RAMESH, N., REMOLD-O'DONNELL, E., SASAHARA, Y., KOOPMAN, L., BYRNE, M., BONILLA, F. A., ROSEN, F. S., GEHA, R. S. & STROMINGER, J. L. 2002. Wiskott-Aldrich syndrome protein is required for NK cell cytotoxicity and colocalizes with actin to NK cell-activating immunologic synapses. *Proceedings*

- of the National Academy of Sciences of the United States of America, 99, 11351-11356.
- ORANGE, J. S., ROY-GHANTA, S., MACE, E. M., MARU, S., RAK, G. D., SANBORN, K. B., FASTH, A., SALTZMAN, R., PAISLEY, A., MONACO-SHAWVER, L., BANERJEE, P. P. & PANDEY, R. 2011. IL-2 induces a WAVE2-dependent pathway for actin reorganization that enables WASp-independent human NK cell function. *J Clin Invest*, 121, 1535-48.
- ORY, S., MUNARI-SILEM, Y., FORT, P. & JURDIC, P. 2000. Rho and Rac exert antagonistic functions on spreading of macrophage-derived multinucleated cells and are not required for actin fiber formation. *Journal of Cell Science*, 113, 1177-1188.
- OTOMO, T., TOMCHICK, D. R., OTOMO, C., PANCHAL, S. C., MACHIUS, M. & ROSEN, M. K. 2005. Structural basis of actin filament nucleation and processive capping by a formin homology 2 domain. *Nature*, 433, 488-494.
- OTTERBEIN, L. R., GRACEFFA, P. & DOMINGUEZ, R. 2001. The crystal structure of uncomplexed actin in the ADP state. *Science*, 293, 708-711.
- PADRICK, S. B., CHENG, H. C., ISMAIL, A. M., PANCHAL, S. C., DOOLITTLE, L. K., KIM, S., SKEHAN, B. M., UMETANI, J., BRAUTIGAM, C. A., LEONG, J. M. & ROSEN, M. K. 2008. Hierarchical regulation of WASP/WAVE proteins. *Molecular cell*, 32, 426-38.
- PADRICK, S. B., DOOLITTLE, L. K., BRAUTIGAM, C. A., KING, D. S. & ROSEN, M. K. 2011. Arp2/3 complex is bound and activated by two WASP proteins. *Proceedings of the National Academy of Sciences of the United States of America*, 108, E472-9.
- PALAZZO, A. F., COOK, T. A., ALBERTS, A. S. & GUNDERSEN, G. G. 2001. mDia mediates Rho-regulated formation and orientation of stable microtubules. *Nature Cell Biology*, 3, 723-729.
- PAPE, K. A., KHORUTS, A., MONDINO, A. & JENKINS, M. K. 1997. Inflammatory cytokines enhance the in vivo clonal expansion and differentiation of antigen-activated CD4(+) T cells. *Journal of Immunology*, 159, 591-598.
- PARK, H., LI, Z. X., YANG, X. O., CHANG, S. H., NURIEVA, R., WANG, Y. H., WANG, Y., HOOD, L., ZHU, Z., TIAN, Q. & DONG, C. 2005. A distinct lineage of CD4 T cells regulates tissue inflammation by producing interleukin 17. *Nature Immunology*, 6, 1133-1141.
- PARSONS, J. T. 1996. Integrin-mediated signalling: Regulation by protein tyrosine kinases and small GTP-binding proteins. *Current Opinion in Cell Biology*, 8, 146-152.
- PAUKER, M. H., HASSAN, N., NOY, E., REICHER, B. & BARDA-SAAD, M. 2012. Studying the Dynamics of SLP-76, Nck, and Vav1 Multimolecular Complex Formation in Live Human Cells with Triple-Color FRET. *Science signaling*, 5, rs3.
- PAUL, A. & POLLARD, T. 2008. The role of the FH1 domain and profilin in formin-mediated actin-filament elongation and nucleation. *Current Biology*, 18, 9-19.
- PEACH, R. J., BAJORATH, J., NAEMURA, J., LEYTZE, G., GREENE, J., ARUFFO, A. & LINSLEY, P. S. 1995. Both Extracellular Immunoglobulin-Like Domains of Cd80

- Contain Residues Critical for Binding T-Cell Surface-Receptors Ctl α -4 and Cd28. *Journal of Biological Chemistry*, 270, 21181-21187.
- PELLEGRIN, S. & MELLOR, H. 2007. Actin stress fibres. *Journal of Cell Science*, 120, 3491-3499.
- PEREZ, O. D., MITCHELL, D., JAGER, G. C., SOUTH, S., MURRIEL, C., MCBRIDE, J., HERZENBERG, L. A., KINOSHITA, S. & NOLAN, G. P. 2003. Leukocyte functional antigen 1 lowers T cell activation thresholds and signaling through cytohesin-1 and Jun-activating binding protein 1. *Nature Immunology*, 4, 1083-1092.
- PHILIPSEN, L., ENGELS, T., SCHILLING, K., GURBIEL, S., FISCHER, K. D., TEDFORD, K., SCHRAVEN, B., GUNZER, M. & REICHARDT, P. 2013. Multimolecular analysis of stable immunological synapses reveals sustained recruitment and sequential assembly of signaling clusters. *Mol Cell Proteomics*, 12, 2551-67.
- POLLARD, T. D. 2007. Regulation of actin filament assembly by Arp2/3 complex and formins. *Annual Review of Biophysics and Biomolecular Structure*, 36, 451-477.
- POLLARD, T. D., BLANCHOIN, L. & MULLINS, R. D. 2000. Molecular mechanisms controlling actin filament dynamics in nonmuscle cells. *Annual Review of Biophysics and Biomolecular Structure*, 29, 545-576.
- POLLARD, T. D. & BORISY, G. G. 2003. Cellular motility driven by assembly and disassembly of actin filaments. *Cell*, 112, 453-465.
- POLLARD, T. D. & COOPER, J. A. 2009. Actin, a Central Player in Cell Shape and Movement. *Science*, 326, 1208-1212.
- POO, W. J., CONRAD, L. & JANEWAY, C. A., JR. 1988. Receptor-directed focusing of lymphokine release by helper T cells. *Nature*, 332, 378-80.
- PORTER, J. C., BRACKE, M., SMITH, A., DAVIES, D. & HOGG, N. 2002. Signaling through integrin LFA-1 leads to filamentous actin polymerization and remodeling, resulting in enhanced T cell adhesion. *Journal of Immunology*, 168, 6330-6335.
- POSERN, G., SOTIROPOULOS, A. & TREISMAN, R. 2002. Mutant actins demonstrate a role for unpolymerized actin in control of transcription by serum response factor. *Molecular Biology of the Cell*, 13, 4167-4178.
- PULECIO, J., PETROVIC, J., PRETE, F., CHIARUTTINI, G., LENNON-DUMENIL, A. M., DESDOUETS, C., GASMAN, S., BURRONE, O. R. & BENVENUTI, F. 2010. Cdc42-mediated MTOC polarization in dendritic cells controls targeted delivery of cytokines at the immune synapse. *J Exp Med*, 207, 2719-32.
- PULECIO, J., TAGLIANI, E., SCHOLER, A., PRETE, F., FETLER, L., BURRONE, O. R. & BENVENUTI, F. 2008. Expression of Wiskott-Aldrich syndrome protein in dendritic cells regulates synapse formation and activation of naive CD8⁺ T cells. *J Immunol*, 181, 1135-42.
- PURBHOO, M. A., LIU, H. B., ODDOS, S., OWEN, D. M., NEIL, M. A. A., PAGEON, S. V., FRENCH, P. M. W., RUDD, C. E. & DAVIS, D. M. 2010. Dynamics of Subsynaptic Vesicles and Surface Microclusters at the Immunological Synapse. *Science Signaling*, 3.

- PURVIS, H. A., STOOP, J. N., MANN, J., WOODS, S., KOZIEN, A. E., HAMBLETON, S., ROBINSON, J. H., ISAACS, J. D., ANDERSON, A. E. & HILKENS, C. M. U. 2010. Low-strength T-cell activation promotes Th17 responses. *Blood*, 116, 4829-4837.
- QI, S. Y., GROVES, J. T. & CHAKRABORTY, A. K. 2001. Synaptic pattern formation during cellular recognition. *Proceedings of the National Academy of Sciences of the United States of America*, 98, 6548-6553.
- QUANN, E. J., LIU, X., ALTAN-BONNET, G. & HUSE, M. 2011. A cascade of protein kinase C isozymes promotes cytoskeletal polarization in T cells. *Nature Immunology*, 12, 647-U205.
- QUANN, E. J., MERINO, E., FURUTA, T. & HUSE, M. 2009. Localized diacylglycerol drives the polarization of the microtubule-organizing center in T cells. *Nature immunology*, 10, 627-35.
- RAK, G. D., MACE, E. M., BANERJEE, P. P., SVITKINA, T. & ORANGE, J. S. 2011. Natural Killer Cell Lytic Granule Secretion Occurs through a Pervasive Actin Network at the Immune Synapse. *Plos Biology*, 9.
- RANDALL, K. L., CHAN, S. S., MA, C. S., FUNG, I., MEI, Y., YABAS, M., TAN, A., ARKWRIGHT, P. D., AL SUWAIRI, W., LUGO REYES, S. O., YAMAZAKI-NAKASHIMADA, M. A., GARCIA-CRUZ MDE, L., SMART, J. M., PICARD, C., OKADA, S., JOUANGUY, E., CASANOVA, J. L., LAMBE, T., CORNALL, R. J., RUSSELL, S., OLIARO, J., TANGYE, S. G., BERTRAM, E. M. & GOODNOW, C. C. 2011. DOCK8 deficiency impairs CD8 T cell survival and function in humans and mice. *J Exp Med*, 208, 2305-20.
- RANDALL, K. L., LAMBE, T., JOHNSON, A. L., TREANOR, B., KUCHARSKA, E., DOMASCHENZ, H., WHITTLE, B., TZE, L. E., ENDERS, A., CROCKFORD, T. L., BOURIEZ-JONES, T., ALSTON, D., CYSTER, J. G., LENARDO, M. J., MACKAY, F., DEENICK, E. K., TANGYE, S. G., CHAN, T. D., CAMIDGE, T., BRINK, R., VINUESA, C. G., BATISTA, F. D., CORNALL, R. J. & GOODNOW, C. C. 2009. Dock8 mutations cripple B cell immunological synapses, germinal centers and long-lived antibody production. *Nat Immunol*, 10, 1283-91.
- REDONDO-MUNOZ, J., ESCOBAR-DIAZ, E., SAMANIEGO, R., TEROL, M. J., GARCIA-MARCO, J. A. & GARCIA-PARDO, A. 2006. MMP-9 in B-cell chronic lymphocytic leukemia is up-regulated by alpha 4 beta 1 integrin or CXCR4 engagement via distinct signaling pathways, localizes to podosomes, and is involved in cell invasion and migration. *Blood*, 108, 3143-3151.
- REICHER, B. & BARDA-SAAD, M. 2010. Multiple pathways leading from the T-cell antigen receptor to the actin cytoskeleton network. *FEBS Lett*, 584, 4858-64.
- REISLER, E. 1993. Actin molecular structure and function. *Current Opinion in Cell Biology*, 5, 41-47.
- RIDLEY, A. J. 2006. Rho GTPases and actin dynamics in membrane protrusions and vesicle trafficking. *Trends in Cell Biology*, 16, 522-529.
- RIDLEY, A. J. & HALL, A. 1992. The Small Gtp-Binding Protein Rho Regulates the Assembly of Focal Adhesions and Actin Stress Fibers in Response to Growth-Factors. *Cell*, 70, 389-399.

- RIDLEY, A. J., PATERSON, H. F., JOHNSTON, C. L., DIEKMANN, D. & HALL, A. 1992. The Small Gtp-Binding Protein Rac Regulates Growth-Factor Induced Membrane Ruffling. *Cell*, 70, 401-410.
- RIEDL, J., CREVENNA, A. H., KESSENBROCK, K., YU, J. H., NEUKIRCHEN, D., BISTA, M., BRADKE, F., JENNE, D., HOLAK, T. A., WERB, Z., SIXT, M. & WEDLICH-SOLDNER, R. 2008. Lifeact: a versatile marker to visualize F-actin. *Nature Methods*, 5, 605-607.
- RIVELINE, D., ZAMIR, E., BALABAN, N. Q., SCHWARZ, U. S., ISHIZAKI, T., NARUMIYA, S., KAM, Z., GEIGER, B. & BERSHADSKY, A. D. 2001. Focal contacts as mechanosensors: Externally applied local mechanical force induces growth of focal contacts by an mDia1-dependent and ROCK-independent mechanism. *Journal of Cell Biology*, 153, 1175-1185.
- RIVEROLEZCANO, O. M., MARCILLA, A., SAMESHIMA, J. H. & ROBBINS, K. C. 1995. Wiskott-Aldrich Syndrome Protein Physically Associates with Nck through Src Homology-3 Domains. *Molecular and Cellular Biology*, 15, 5725-5731.
- ROAKE, J. A., RAO, A. S., MORRIS, P. J., LARSEN, C. P., HANKINS, D. F. & AUSTYN, J. M. 1995. Dendritic Cell Loss from Nonlymphoid Tissues after Systemic Administration of Lipopolysaccharide, Tumor-Necrosis-Factor, and Interleukin-1. *Journal of Experimental Medicine*, 181, 2237-2247.
- RODAL, A. A., TETREAU, J. W., LAPPALAINEN, P., DRUBIN, D. G. & AMBERG, D. C. 1999. Aip1p interacts with cofilin to disassemble actin filaments. *Journal of Cell Biology*, 145, 1251-1264.
- RODRIGUEZ-FERNANDEZ, J. L., RIOL-BLANCO, L. & DELGADO-MARTIN, C. 2010. What Is the Function of the Dendritic Cell Side of the Immunological Synapse? *Science Signaling*, 3.
- RODRIGUEZ-PALMERO, M., HARA, T., THUMBS, A. & HUNIG, T. 1999. Triggering of T cell proliferation through CD28 induces GATA-3 and promotes T helper type 2 differentiation in vitro and in vivo. *European journal of immunology*, 29, 3914-24.
- ROHATGI, R., HO, H. Y. H. & KIRSCHNER, M. W. 2000. Mechanism of N-WASP activation by CDC42 and phosphatidylinositol 4,5-bisphosphate. *Journal of Cell Biology*, 150, 1299-1309.
- ROHATGI, R., MA, L., MIKI, H., LOPEZ, M., KIRCHHAUSEN, T., TAKENAWA, T. & KIRSCHNER, M. W. 1999. The interaction between N-WASP and the Arp2/3 complex links Cdc42-dependent signals to actin assembly. *Cell*, 97, 221-231.
- ROMERO, S., LE CLAINCHE, C., DIDRY, D., EGILE, C., PANTALONI, D. & CARLIER, M. F. 2004. Formin is a processive motor that requires profilin to accelerate actin assembly and associated ATP hydrolysis. *Cell*, 119, 419-429.
- ROSENBLATT, J., PELUSO, P. & MITCHISON, T. J. 1995. The Bulk of Unpolymerized Actin in Xenopus Egg Extracts Is Atp-Bound. *Molecular Biology of the Cell*, 6, 227-236.
- ROTHLEIN, R., DUSTIN, M. L., MARLIN, S. D. & SPRINGER, T. A. 1986. A Human Intercellular-Adhesion Molecule (Icam-1) Distinct from Lfa-1. *Journal of Immunology*, 137, 1270-1274.

- ROUILLER, I., XU, X. P., AMANN, K. J., EGILE, C., NICKELL, S., NICASTRO, D., LI, R., POLLARD, T. D., VOLKMANN, N. & HANEIN, D. 2008. The structural basis of actin filament branching by the Arp2/3 complex. *Journal of Cell Biology*, 180, 887-895.
- RUDD, C. E. & SCHNEIDER, H. 2003. Unifying concepts in CD28, ICOS and CTLA4 co-receptor signalling. *Nature Reviews Immunology*, 3, 544-556.
- RUDENSKY, A. Y., RATH, S., PRESTONHURLBURT, P., MURPHY, D. B. & JANEWAY, C. A. 1991. On the Complexity of Self. *Nature*, 353, 660-662.
- RUUSALA, A. & ASPENSTROM, P. 2004. Isolation and characterisation of DOCK8, a member of the DOCK180-related regulators of cell morphology. *FEBS Lett*, 572, 159-66.
- SABATOS, C. A., DOH, J., CHAKRAVARTI, S., FRIEDMAN, R. S., PANDURANGI, P. G., TOOLEY, A. J. & KRUMMEL, M. F. 2008. A synaptic basis for paracrine interleukin-2 signaling during homotypic T cell interaction. *Immunity*, 29, 238-248.
- SAFAEI, S., FAZLOLLAHI, M. R., HOUSHMAND, M., HAMIDIEH, A. A., BEMANIAN, M. H., ALAVI, S., MOUSAVI, F., POURPAK, Z. & MOIN, M. 2012. Detection of Six Novel Mutations in WASP Gene in Fifteen Iranian Wiskott-Aldrich Patients. *Iranian Journal of Allergy Asthma and Immunology*, 11, 345-348.
- SAGOT, I., RODAL, A. A., MOSELEY, J., GOODE, B. L. & PELLMAN, D. 2002. An actin nucleation mechanism mediated by Bni1 and profilin. *Nature Cell Biology*, 4, 626-631.
- SAIJO, M., SUZUTANI, T., MURONO, K., HIRANO, Y. & ITOH, K. 1998. Recurrent aciclovir-resistant herpes simplex in a child with Wiskott-Aldrich syndrome. *Br J Dermatol*, 139, 311-4.
- SAKUMA, C., SATO, M., TAKENOUCI, T., CHIBA, J. & KITANI, H. 2012. Critical Roles of the WASP N-Terminal Domain and Btk in LPS-Induced Inflammatory Response in Macrophages. *PloS one*, 7, e30351.
- SAKURADA, S., OKAMOTO, H., TAKUWA, N., SUGIMOTO, N. & TAKUWA, Y. 2001. Rho activation in excitatory agonist-stimulated vascular smooth muscle. *American Journal of Physiology-Cell Physiology*, 281, C571-C578.
- SALAZAR-FONTANA, L. I., BARR, V., SAMELSON, L. E. & BIERER, B. E. 2003. CD28 engagement promotes actin polymerization through the activation of the small Rho GTPase Cdc42 in human T cells. *Journal of immunology*, 171, 2225-32.
- SALLUSTO, F. & LANZAVECCHIA, A. 1994. Efficient Presentation of Soluble-Antigen by Cultured Human Dendritic Cells Is Maintained by Granulocyte-Macrophage Colony-Stimulating Factor Plus Interleukin-4 and down-Regulated by Tumor-Necrosis-Factor-Alpha. *Journal of Experimental Medicine*, 179, 1109-1118.
- SALOMON, B. & BLUESTONE, J. A. 1998. LFA-1 interaction with ICAM-1 and ICAM-2 regulates Th2 cytokine production. *Journal of immunology*, 161, 5138-42.
- SASAHARA, Y., RACHID, R., BYRNE, M. J., DE LA FUENTE, M. A., ABRAHAM, R. T., RAMESH, N. & GEHA, R. S. 2002. Mechanism of recruitment of WASP to the

- immunological synapse and of its activation following TCR ligation. *Mol Cell*, 10, 1269-81.
- SCHAMEL, W. W. A., ARECHAGA, I., RISUENO, R. M., VAN SANTEN, H. M., CABEZAS, P., RISCO, C., VALPUESTA, J. M. & ALARCON, B. 2005. Coexistence of multivalent and monovalent TCRs explains high sensitivity and wide range of response. *Journal of Experimental Medicine*, 202, 493-503.
- SCHIRENBECK, A., BRETSCHEIDER, T., ARASADA, R., SCHLEICHER, M. & FAIX, J. 2005. The Diaphanous-related formin dDia2 is required for the formation and maintenance of filopodia. *Nature Cell Biology*, 7, 619-U24.
- SCHMIDT-WEBER, C. B., ALEXANDER, S. I., HENAULT, L. E., JAMES, L. & LICHTMAN, A. H. 1999. IL-4 enhances IL-10 gene expression in murine Th2 cells in the absence of TCR engagement. *Journal of Immunology*, 162, 238-244.
- SCHMIDT, A. & HALL, A. 2002. Guanine nucleotide exchange factors for Rho GTPases: turning on the switch. *Genes & Development*, 16, 1587-1609.
- SCHURMAN, S. H. & CANDOTTI, F. 2003. Autoimmunity in Wiskott-Aldrich syndrome. *Current Opinion in Rheumatology*, 15, 446-453.
- SCHWARTZ, R. H. 1992. Costimulation of Lymphocytes-T - the Role of Cd28, Ctla-4, and B7/Bb1 in Interleukin-2 Production and Immunotherapy. *Cell*, 71, 1065-1068.
- SCHWARTZ, R. H., MUELLER, D. L., JENKINS, M. K. & QUILL, H. 1989. T-Cell Clonal Anergy. *Cold Spring Harbor Symposia on Quantitative Biology*, 54, 605-610.
- SCOTT, P. 1993. IL-12 - Initiation Cytokine for Cell-Mediated-Immunity. *Science*, 260, 496-497.
- SEAVITT, J. R., WHITE, L. S., MURPHY, K. M., LOH, D. Y., PERLMUTTER, R. M. & THOMAS, M. L. 1999. Expression of the p56(lck) Y505F mutation in CD45-deficient mice rescues thymocyte development. *Molecular and Cellular Biology*, 19, 4200-4208.
- SEDER, R. A., PAUL, W. E., DAVIS, M. M. & FAZEKAS DE ST GROTH, B. 1992. The Presence of Interleukin-4 during Invitro Priming Determines the Lymphokine-Producing Potential of Cd4+ T-Cells from T-Cell Receptor Transgenic Mice. *Journal of Experimental Medicine*, 176, 1091-1098.
- SEDWICK, C. E., MORGAN, M. M., JUSINO, L., CANNON, J. L., MILLER, J. & BURKHARDT, J. K. 1999. TCR, LFA-1, and CD28 play unique and complementary roles in signaling T cell cytoskeletal reorganization. *Journal of Immunology*, 162, 1367-1375.
- SELVARAJ, A. & PRYWES, R. 2003. Megakaryoblastic leukemia-1/2, a transcriptional co-activator of serum response factor, is required for skeletal myogenic differentiation. *Journal of Biological Chemistry*, 278, 41977-41987.
- SERBINA, N. V., SALAZAR-MATHER, T. P., BIRON, C. A., KUZIEL, W. A. & PAMER, E. G. 2003. TN/iNOS-producing dendritic cells mediate innate immune defense against bacterial infection. *Immunity*, 19, 59-70.
- SETH, A., OTOMO, C. & ROSEN, M. K. 2006. Autoinhibition regulates cellular localization and actin assembly activity of the diaphanous-related formins FRL alpha and mDia1. *Journal of Cell Biology*, 174, 701-713.

- SHAHINIAN, A., PFEFFER, K., LEE, K. P., KUNDIG, T. M., KISHIHARA, K., WAKEHAM, A., KAWAI, K., OHASHI, P. S., THOMPSON, C. B. & MAK, T. W. 1993. Differential T-Cell Costimulatory Requirements in Cd28-Deficient Mice. *Science*, 261, 609-612.
- SHAKHAR, G., LINDQUIST, R. L., SKOKOS, D., DUDZIAK, D., HUANG, J. H., NUSSENZWEIG, M. C. & DUSTIN, M. L. 2005. Stable T cell-dendritic cell interactions precede the development of both tolerance and immunity in vivo. *Nature Immunology*, 6, 707-714.
- SHAW, A. S. & DUSTIN, M. L. 1997. Making the T cell receptor go the distance: a topological view of T cell activation. *Immunity*, 6, 361-9.
- SHIMADA, A., NYITRAI, M., VETTER, I. R., KUHLMANN, D., BUGYI, B., NARUMIYA, S., GEEVES, M. A. & WITTINGHOFER, A. 2004. The core FH2 domain of diaphanous-related formins is an elongated actin binding protein that inhibits polymerization. *Molecular Cell*, 13, 511-522.
- SHIMODA, K., VANDEURSEN, J., SANGSTER, M. Y., SARAWAR, S. R., CARSON, R. T., TRIPP, R. A., CHU, C., QUELLE, F. W., NOSAKA, T., VIGNALI, D. A. A., DOHERTY, P. C., GROSVELD, G., PAUL, W. E. & IHLE, J. N. 1996. Lack of IL-4-induced Th2 response and IgE class switching in mice with disrupted Stat6 gene. *Nature*, 380, 630-633.
- SHORTMAN, K. & NAIK, S. H. 2007. Steady-state and inflammatory dendritic-cell development. *Nature Reviews Immunology*, 7, 19-30.
- SIMS, T. N. & DUSTIN, M. L. 2002. The immunological synapse: integrins take the stage. *Immunological Reviews*, 186, 100-117.
- SIMS, T. N., SOOS, T. J., XENIAS, H. S., DUBIN-THALER, B., HOFMAN, J. M., WAITE, J. C., CAMERON, T. O., THOMAS, V. K., VARMA, R., WIGGINS, C. H., SHEETZ, M. P., LITTMAN, D. R. & DUSTIN, M. L. 2007. Opposing effects of PKCtheta and WASp on symmetry breaking and relocation of the immunological synapse. *Cell*, 129, 773-85.
- SKOKOS, D., SHAKHAR, G., VARMA, R., WAITE, J. C., CAMERON, T. O., LINDQUIST, R. L., SCHWICKERT, T., NUSSENZWEIG, M. C. & DUSTIN, M. L. 2007. Peptide-MHC potency governs dynamic interactions between T cells and dendritic cells in lymph nodes. *Nature Immunology*, 8, 835-844.
- SMALL, J. V., STRADAL, T., VIGNAL, E. & ROTTNER, K. 2002. The lamellipodium: where motility begins. *Trends in Cell Biology*, 12, 112-120.
- SMITH-GARVIN, J. E., KORETZKY, G. A. & JORDAN, M. S. 2009. T Cell Activation. *Annual Review of Immunology*, 27, 591-619.
- SMITH, A., CARRASCO, Y. R., STANLEY, P., KIEFFER, N., BATISTA, F. D. & HOGG, N. 2005. A talin-dependent LFA-1 focal zone is formed by rapidly migrating T lymphocytes. *Journal of Cell Biology*, 170, 141-151.
- SMITH, B. A., DAUGHERTY-CLARKE, K., GOODE, B. L. & GELLES, J. 2013a. Pathway of actin filament branch formation by Arp2/3 complex revealed by single-molecule imaging. *Proceedings of the National Academy of Sciences of the United States of America*, 110, 1285-1290.

- SMITH, B. A., PADRICK, S. B., DOOLITTLE, L. K., DAUGHERTY-CLARKE, K., CORREA, I. R., XU, M. Q., GOODE, B. L., ROSEN, M. K. & GELLES, J. 2013b. Three-color single molecule imaging shows WASP detachment from Arp2/3 complex triggers actin filament branch formation. *Elife*, 2.
- SMITS, H. H., DE JONG, E. C., SCHUITEMAKER, J. H., GEIJTENBEEK, T. B., VAN KOOYK, Y., KAPSENBERG, M. L. & WIERENGA, E. A. 2002. Intercellular adhesion molecule-1/LFA-1 ligation favors human Th1 development. *Journal of immunology*, 168, 1710-6.
- SMOLIGOVETS, A. A., SMITH, A. W., WU, H. J., PETIT, R. S. & GROVES, J. T. 2012. Characterization of dynamic actin associations with T-cell receptor microclusters in primary T cells. *Journal of Cell Science*, 125, 735-742.
- SNAPPER, S. B., MEELU, P., NGUYEN, D., STOCKTON, B. M., BOZZA, P., ALT, F. W., ROSEN, F. S., VON ANDRIAN, U. H. & KLEIN, C. 2005. WASP deficiency leads to global defects of directed leukocyte migration in vitro and in vivo. *Journal of Leukocyte Biology*, 77, 993-998.
- SNAPPER, S. B., ROSEN, F. S., MIZOGUCHI, E., COHEN, P., KHAN, W., LIU, C. H., HAGEMANN, T. L., KWAN, S. P., FERRINI, R., DAVIDSON, L., BHAN, A. K. & ALT, F. W. 1998. Wiskott-Aldrich syndrome protein-deficient mice reveal a role for WASP in T but not B cell activation. *Immunity*, 9, 81-91.
- SOARES, H., HENRIQUES, R., SACHSE, M., VENTIMIGLIA, L., ALONSO, M. A., ZIMMER, C., THOULOZE, M. I. & ALCOVER, A. 2013. Regulated vesicle fusion generates signaling nanoterritories that control T cell activation at the immunological synapse. *Journal of Experimental Medicine*, 210, 2415-2433.
- SOMERSALO, K., ANIKEEVA, N., SIMS, T. N., THOMAS, V. K., STRONG, R. K., SPIES, T., LEBEDEVA, T., SYKULEV, Y. & DUSTIN, M. L. 2004. Cytotoxic T lymphocytes form an antigen-independent ring junction. *Journal of Clinical Investigation*, 113, 49-57.
- SOTIROPOULOS, A., GINEITIS, D., COPELAND, J. & TREISMAN, R. 1999. Signal-regulated activation of serum response factor is mediated by changes in actin dynamics. *Cell*, 98, 159-169.
- STICKEL, S. K. & WANG, Y. L. 1987. Alpha-Actinin Containing Aggregates in Transformed-Cells Are Highly Dynamic Structures. *Journal of Cell Biology*, 104, 1521-1526.
- STINCHCOMBE, J. C., BOSSI, G., BOOTH, S. & GRIFFITHS, G. M. 2001. The immunological synapse of CTL contains a secretory domain and membrane bridges. *Immunity*, 15, 751-761.
- STINCHCOMBE, J. C., MAJOROVITS, E., BOSSI, G., FULLER, S. & GRIFFITHS, G. M. 2006. Centrosome polarization delivers secretory granules to the immunological synapse. *Nature*, 443, 462-465.
- STINCHCOMBE, J. C., SALIO, M., CERUNDOLO, V., PENDE, D., ARICO, M. & GRIFFITHS, G. M. 2011. Centriole polarisation to the immunological synapse directs secretion from cytolytic cells of both the innate and adaptive immune systems. *BMC biology*, 9, 45.

- STOLL, S., DELON, J., BROTZ, T. M. & GERMAIN, R. N. 2002. Dynamic imaging of T cell-dendritic cell interactions in lymph nodes. *Science*, 296, 1873-1876.
- STOWERS, L., YELON, D., BERG, L. J. & CHANT, J. 1995. Regulation of the Polarization of T-Cells toward Antigen-Presenting Cells by Ras-Related Gtpase Cdc42. *Proceedings of the National Academy of Sciences of the United States of America*, 92, 5027-5031.
- STRADAL, T. E. B. & SCITA, G. 2006. Protein complexes regulating Arp2/3-mediated actin assembly. *Current Opinion in Cell Biology*, 18, 4-10.
- SU, H. C. 2010. Deducator of cytokinesis 8 (DOCK8) deficiency. *Curr Opin Allergy Clin Immunol*, 10, 515-20.
- SU, H. C., JING, H. & ZHANG, Q. 2011. DOCK8 deficiency. *Ann N Y Acad Sci*, 1246, 26-33.
- SUN, H. Q., YAMAMOTO, M., MEJILLANO, M. & YIN, H. L. 1999. Gelsolin, a multifunctional actin regulatory protein. *Journal of Biological Chemistry*, 274, 33179-33182.
- SUN, Y., BOYD, K., XU, W., MA, J., JACKSON, C. W., FU, A., SHILLINGFORD, J. M., ROBINSON, G. W., HENNIGHAUSEN, L., HITZLER, J. K., MA, Z. G. & MORRIS, S. W. 2006. Acute myeloid leukemia-associated Mkl1 (Mrtf-a) is a key regulator of mammary gland function. *Molecular and Cellular Biology*, 26, 5809-5826.
- SUN, Z. M., ARENDT, C. W., ELLMEIER, W., SCHAEFFER, E. M., SUNSHINE, M. J., GANDHI, L., ANNES, J., PETRZILKA, D., KUPFER, A., SCHWARTZBERG, P. L. & LITTMAN, D. R. 2000. PKC-theta is required for TCR-induced NF-kappa B activation in mature but not immature T lymphocytes. *Nature*, 404, 402-407.
- SYMONS, M., DERRY, J. M. J., KARLAK, B., JIANG, S., LEMAHIEU, V., MCCORMICK, F., FRANCKE, U. & ABO, A. 1996. Wiskott-Aldrich syndrome protein, a novel effector for the GTPase CDC42Hs, is implicated in actin polymerization. *Cell*, 84, 723-734.
- SZABO, S. J., KIM, S. T., COSTA, G. L., ZHANG, X. K., FATHMAN, C. G. & GLIMCHER, L. H. 2000. A novel transcription factor, T-bet, directs Th1 lineage commitment. *Cell*, 100, 655-669.
- TADOKORO, C. E., SHAKHAR, G., SHEN, S. Q., DING, Y., LINO, A. C., MARAVER, A., LAFAILLE, J. J. & DUSTIN, M. L. 2006. Regulatory T cells inhibit stable contacts between CD4(+) T cells and dendritic cells in vivo. *Journal of Experimental Medicine*, 203, 505-511.
- TAKEDA, K., TANAKA, T., SHI, W., MATSUMOTO, M., MINAMI, M., KASHIWAMURA, S., NAKANISHI, K., YOSHIDA, N., KISHIMOTO, T. & AKIRA, S. 1996. Essential role of Stat6 in IL-4 signalling. *Nature*, 380, 627-630.
- TAO, X., CONSTANT, S., JORRITSMA, P. & BOTTOMLY, K. 1997a. Strength of ICR signal determines the costimulatory requirements for Th1 and Th2 CD4(+) T cell differentiation. *Journal of Immunology*, 159, 5956-5963.
- TAO, X., GRANT, C., CONSTANT, S. & BOTTOMLY, K. 1997b. Induction of IL-4-producing CD4+ T cells by antigenic peptides altered for TCR binding. *Journal of immunology*, 158, 4237-44.

- TAYLOR, M. D., SADHUKHAN, S., KOTTANGADA, P., RAMGOPAL, A., SARKAR, K., D'SILVA, S., SELVAKUMAR, A., CANDOTTI, F. & VYAS, Y. M. 2010. Nuclear role of WASp in the pathogenesis of dysregulated TH1 immunity in human Wiskott-Aldrich syndrome. *Sci Transl Med*, 2, 37ra44.
- TERNBLAY, J. N., BERTELLI, E., ARQUES, J. L., REGOLI, M. & NICOLETTI, C. 2007. Production of IL-12 by Peyer patch-dendritic cells is critical for the resistance to food allergy. *Journal of Allergy and Clinical Immunology*, 120, 659-665.
- THOMAS, M. L. 1999. The regulation of antigen-receptor signaling by protein tyrosine phosphatases: a hole in the story. *Current Opinion in Immunology*, 11, 270-276.
- THOMAS, M. L. & BROWN, E. J. 1999. Positive and negative regulation of Src-family membrane kinases by CD45. *Immunology Today*, 20, 406-411.
- THRASHER, A. J. 2002. WASp in immune-system organization and function. *Nature Reviews Immunology*, 2, 635-646.
- THRASHER, A. J. & BURNS, S. O. 2010. WASP: a key immunological multitasker. *Nat Rev Immunol*, 10, 182-92.
- THUMMLER, K., LEIPE, J., RAMMING, A., SCHULZE-KOOPS, H. & SKAPENKO, A. 2010. Immune regulation by peripheral suppressor T cells induced upon homotypic T cell/T cell interactions. *Journal of Leukocyte Biology*, 88, 1041-1050.
- TIVOL, E. A., BORRIELLO, F., SCHWEITZER, A. N., LYNCH, W. P., BLUESTONE, J. A. & SHARPE, A. H. 1995. Loss of Ctl4-4 Leads to Massive Lymphoproliferation and Fatal Multiorgan Tissue Destruction, Revealing a Critical Negative Regulatory Role of Ctl4-4. *Immunity*, 3, 541-547.
- TOLAR, P., HANNA, J., KRUEGER, P. D. & PIERCE, S. K. 2009. The Constant Region of the Membrane Immunoglobulin Mediates B Cell-Receptor Clustering and Signaling in Response to Membrane Antigens. *Immunity*, 30, 44-55.
- TOMINAGA, T., SAHAI, E., CHARDIN, P., MCCORMICK, F., COURTNEIDGE, S. A. & ALBERTS, A. S. 2000. Diaphanous-related formins bridge Rho GTPase and Src tyrosine kinase signaling. *Molecular Cell*, 5, 13-25.
- TORRES, E. & ROSEN, M. K. 2003. Contingent phosphorylation/dephosphorylation provides a mechanism of molecular memory in WASP. *Molecular cell*, 11, 1215-27.
- TRAVER, D., AKASHI, K., MANZ, M., MERAD, M., MIYAMOTO, T., ENGLEMAN, E. G. & WEISSMAN, I. L. 2000. Development of CD8 alpha-positive dendritic cells from a common myeloid progenitor. *Science*, 290, 2152-2154.
- TSENG, S. Y., LIU, M. L. & DUSTIN, M. L. 2005. CD80 cytoplasmic domain controls localization of CD28, CTLA-4, and protein kinase C theta in the immunological synapse. *Journal of Immunology*, 175, 7829-7836.
- TSENG, S. Y., WAITE, J. C., LIU, M. L., VARDHANA, S. & DUSTIN, M. L. 2008. T cell-dendritic cell immunological synapses contain TCR-dependent CD28-CD80 clusters that recruit protein kinase C theta. *Journal of Immunology*, 181, 4852-4863.

- TSUBOI, S. & MEERLOO, J. 2007. Wiskott-Aldrich syndrome protein is a key regulator of the phagocytic cup formation in macrophages. *Journal of Biological Chemistry*, 282, 34194-34203.
- TSUN, A., QURESHI, I., STINCHCOMBE, J. C., JENKINS, M. R., DE LA ROCHE, M., KLECZKOWSKA, J., ZAMOYSKA, R. & GRIFFITHS, G. M. 2011. Centrosome docking at the immunological synapse is controlled by Lck signaling. *Journal of Cell Biology*, 192, 663-674.
- UEDA, H., MORPHEW, M. K., MCINTOSH, J. R. & DAVIS, M. M. 2011. CD4+ T-cell synapses involve multiple distinct stages. *Proceedings of the National Academy of Sciences of the United States of America*, 108, 17099-104.
- VAANANEN, H. K., ZHAO, H., MULARI, M. & HALLEEN, J. M. 2000. The cell biology of osteoclast function. *Journal of Cell Science*, 113, 377-381.
- VALITUTTI, S., MULLER, S., SALIO, M. & LANZAVECCHIA, A. 1997. Degradation of T cell receptor (TCR)-CD3- ζ complexes after antigenic stimulation. *Journal of Experimental Medicine*, 185, 1859-1864.
- VALLOTTON, P., GUPTON, S. L., WATERMAN-STORER, C. M. & DANUSER, G. 2004. Simultaneous mapping of filamentous actin flow and turnover in migrating cells by quantitative fluorescent speckle microscopy. *Proceedings of the National Academy of Sciences of the United States of America*, 101, 9660-9665.
- VAN TROYS, M., HUYCK, L., LEYMAN, S., DHAESE, S., VANDEKERKHOVE, J. & ARNPE, C. 2008. Ins and outs of ADF/cofilin activity and regulation. *European Journal of Cell Biology*, 87, 649-667.
- VANDERMERWE, P. A., BODIAN, D. L., DAENKE, S., LINSLEY, P. & DAVIS, S. J. 1997. CD80 (B7-1) binds both CD28 and CTLA-4 with a low affinity and very fast kinetics. *Journal of Experimental Medicine*, 185, 393-403.
- VANSEVENTER, G. A., SHIMIZU, Y., HORGAN, K. J. & SHAW, S. 1990. The Lfa-1 Ligand Icam-1 Provides an Important Costimulatory Signal for T-Cell Receptor-Mediated Activation of Resting T-Cells. *Journal of Immunology*, 144, 4579-4586.
- VARDHANA, S., CHOUDHURI, K., VARMA, R. & DUSTIN, M. L. 2010. Essential Role of Ubiquitin and TSG101 Protein in Formation and Function of the Central Supramolecular Activation Cluster. *Immunity*, 32, 531-540.
- VARMA, R., CAMPI, G., YOKOSUKA, T., SAITO, T. & DUSTIN, M. L. 2006. T cell receptor-proximal signals are sustained in peripheral microclusters and terminated in the central supramolecular activation cluster. *Immunity*, 25, 117-27.
- VAVYLONIS, D., YANG, Q. B. & O'SHAUGHNESSY, B. 2005. Actin polymerization kinetics, cap structure, and fluctuations. *Proceedings of the National Academy of Sciences of the United States of America*, 102, 8543-8548.
- VELDHOEN, M., HOCKING, R. J., ATKINS, C. J., LOCKSLEY, R. M. & STOCKINGER, B. 2006. TGF β in the context of an inflammatory cytokine milieu supports de novo differentiation of IL-17-producing T cells. *Immunity*, 24, 179-89.
- VICENTE-MANZANARES, M., MA, X. F., ADELSTEIN, R. S. & HORWITZ, A. R. 2009. Non-muscle myosin II takes centre stage in cell adhesion and migration. *Nature Reviews Molecular Cell Biology*, 10, 778-790.

- VIGNALI, D. A. A., COLLISON, L. W. & WORKMAN, C. J. 2008. How regulatory T cells work. *Nature Reviews Immunology*, 8, 523-532.
- VIOLA, A., SCHROEDER, S., SAKAKIBARA, Y. & LANZAVECCHIA, A. 1999. T lymphocyte costimulation mediated by reorganization of membrane microdomains. *Science*, 283, 680-682.
- VOLKMAN, B. F., PREHODA, K. E., SCOTT, J. A., PETERSON, F. C. & LIM, W. A. 2002. Structure of the N-WASP EVH1 domain-WIP complex: insight into the molecular basis of Wiskott-Aldrich Syndrome. *Cell*, 111, 565-76.
- VOLKMANN, N., AMANN, K. J., STOILOVA-MCPHIE, S., EGILE, C., WINTER, D. C., HAZELWOOD, L., HEUSER, J. E., LI, R., POLLARD, T. D. & HANEIN, D. 2001. Structure of Arp2/3 complex in its activated state and in actin filament branch junctions. *Science*, 293, 2456-2459.
- WABNITZ, G. H., LOHNEIS, P., KIRCHGESSNER, H., JAHRAUS, B., GOTTWALD, S., KONSTANDIN, M., KLEMKE, M. & SAMSTAG, Y. 2010. Sustained LFA-1 cluster formation in the immune synapse requires the combined activities of L-plastin and calmodulin. *Eur J Immunol*, 40, 2437-49.
- WALSENG, E., BAKKE, O. & ROCHE, P. A. 2008. Major histocompatibility complex class II-peptide complexes internalize using a clathrin- and dynamin-independent endocytosis pathway. *Journal of Biological Chemistry*, 283, 14717-14727.
- WALTON, J. 1979. Lead Aspartate, an En-Bloc Contrast Stain Particularly Useful for Ultrastructural Enzymology. *Journal of Histochemistry & Cytochemistry*, 27, 1337-1342.
- WANG, C., MORLEY, S. C., DONERMEYER, D., PENG, I., LEE, W. P., DEVOSS, J., DANILENKO, D. M., LIN, Z. H., ZHANG, J. A., ZHOU, J., ALLEN, P. M. & BROWN, E. J. 2010. Actin-Bundling Protein L-Plastin Regulates T Cell Activation. *Journal of Immunology*, 185, 7487-7497.
- WANG, D. Z., LI, S. J., HOCKEMEYER, D., SUTHERLAND, L., WANG, Z. G., SCHRATT, G., RICHARDSON, J. A., NORDHEIM, A. & OLSON, E. N. 2002. Potentiation of serum response factor activity by a family of myocardin-related transcription factors. *Proceedings of the National Academy of Sciences of the United States of America*, 99, 14855-14860.
- WANG, Y. N. & JOHNSON, P. 2005. Expression of CD45 lacking the catalytic protein tyrosine phosphatase domain modulates Lck phosphorylation and T cell activation. *Journal of Biological Chemistry*, 280, 14318-14324.
- WASSERMAN, S. 1998. FH proteins as cytoskeletal organizers. *Trends in Cell Biology*, 8, 111-115.
- WATANABE, N., MADAULE, P., REID, T., ISHIZAKI, T., WATANABE, G., KAKIZUKA, A., SAITO, Y., NAKAO, K., JOCKUSCH, B. M. & NARUMIYA, S. 1997. p140mDia, a mammalian homolog of *Drosophila* diaphanous, is a target protein for Rho small GTPase and is a ligand for profilin. *Embo Journal*, 16, 3044-3056.
- WATERHOUSE, P., PENNINGER, J. M., TIMMS, E., WAKEHAM, A., SHAHINIAN, A., LEE, K. P., THOMPSON, C. B., GRIESSER, H. & MAK, T. W. 1995. Lymphoproliferative Disorders with Early Lethality in Mice Deficient in Ctl α -4. *Science*, 270, 985-988.

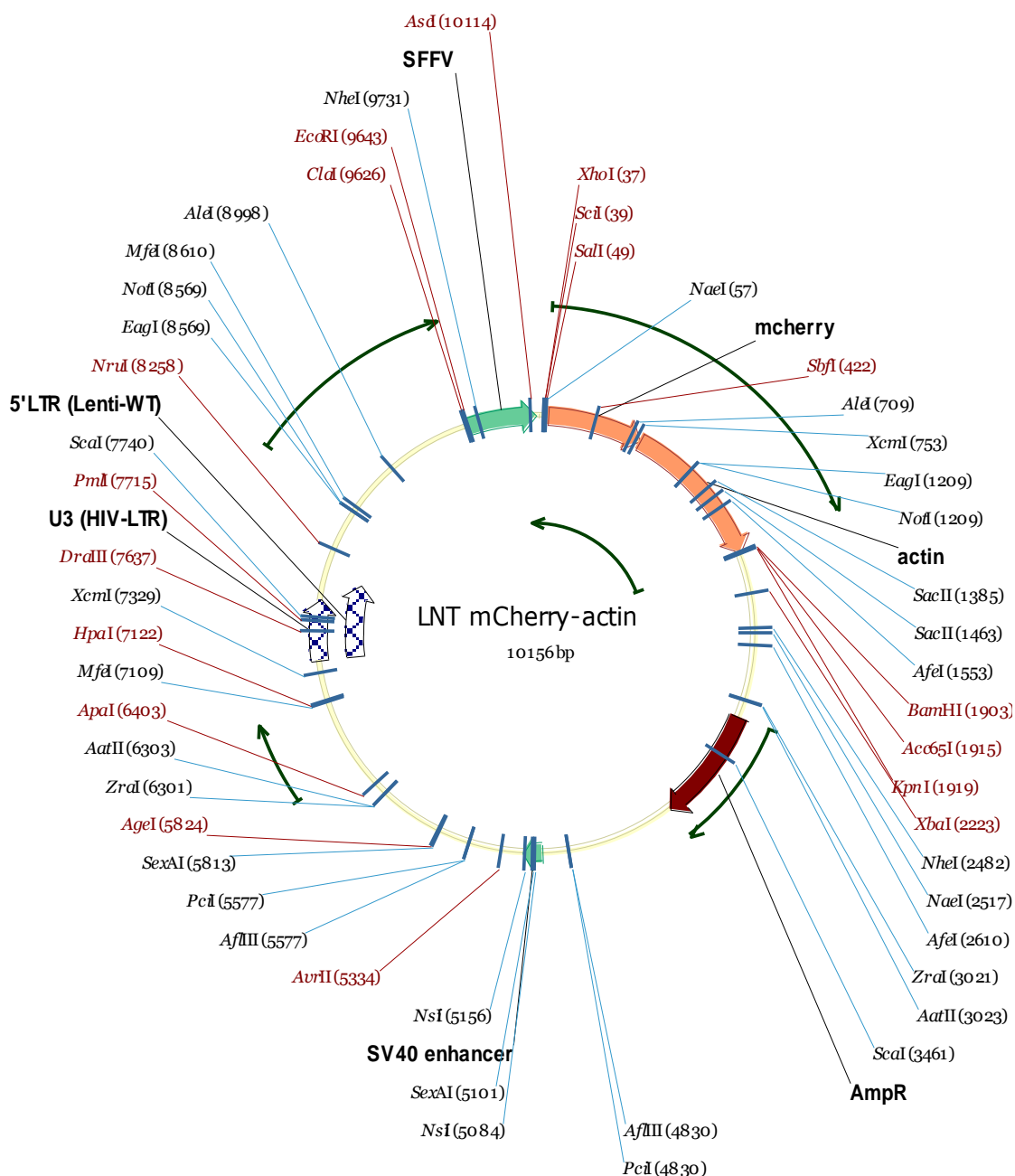
- WAY, M. & WEEDS, A. 1988. Nucleotide-Sequence of Pig Plasma Gelsolin - Comparison of Protein-Sequence with Human Gelsolin and Other Actin-Severing Proteins Shows Strong Homologies and Evidence for Large Internal Repeats. *Journal of Molecular Biology*, 203, 1127-1133.
- WEAVER, C. T., HAWRYLOWICZ, C. M. & UNANUE, E. R. 1988. T-Helper Cell Subsets Require the Expression of Distinct Costimulatory Signals by Antigen-Presenting Cells. *Proceedings of the National Academy of Sciences of the United States of America*, 85, 8181-8185.
- WEBER, K. S. C., WEBER, C., OSTERMANN, G., DIERKS, H., NAGEL, W. & KOLANUS, W. 2001. Cytohesin-1 is a dynamic regulator of distinct LFA-1 functions in leukocyte arrest and transmigration triggered by chemokines. *Current Biology*, 11, 1969-1974.
- WEI, L., LAURENCE, A., ELIAS, K. M. & O'SHEA, J. J. 2007a. IL-21 is produced by Th17 cells and drives IL-17 production in a STAT3-dependent manner. *Journal of Biological Chemistry*, 282, 34605-34610.
- WEI, S. H., SAFRINA, O., YU, Y., GARROD, K. R., CAHALAN, M. D. & PARKER, I. 2007b. Ca²⁺ signals in CD4(+) T cells during early contacts with antigen-bearing dendritic cells in lymph node. *Journal of Immunology*, 179, 1586-1594.
- WEITZ-SCHMIDT, G., WELZENBACH, K., BRINKMANN, V., KAMATA, T., KALLEN, J., BRUNS, C., COTTENS, S., TAKADA, Y. & HOMMEL, U. 2001. Statins selectively inhibit leukocyte function antigen-1 by binding to a novel regulatory integrin site. *Nature Medicine*, 7, 687-692.
- WELCH, M. D., IWAMATSU, A. & MITCHISON, T. J. 1997. Actin polymerization is induced by Arp2/3 protein complex at the surface of *Listeria monocytogenes*. *Nature*, 385, 265-269.
- WEN, Y., ENG, C. H., SCHMORANZER, J., CABRERA-POCH, N., MORRIS, E. J. S., CHEN, M., WALLAR, B. J., ALBERTS, A. S. & GUNDERSEN, G. G. 2004. EB1 and APC bind to mDia to stabilize microtubules downstream of Rho and promote cell migration. *Nature Cell Biology*, 6, 820-U1.
- WEST, M. A., PRESCOTT, A. R., ESKELINEN, E. L., RIDLEY, A. J. & WATTS, C. 2000. Rac is required for constitutive macropinocytosis by dendritic cells but does not control its downregulation. *Current Biology*, 10, 839-848.
- WESTERBERG, L., LARSSON, M., HARDY, S. J., FERNANDEZ, C., THRASHER, A. J. & SEVERINSON, E. 2005. Wiskott-Aldrich syndrome protein deficiency leads to reduced B-cell adhesion, migration, and homing, and a delayed humoral immune response. *Blood*, 105, 1144-1152.
- WESTERBERG, L., WALLIN, R. P., GREICIUS, G., LJUNGGREN, H. G. & SEVERINSON, E. 2003. Efficient antigen presentation of soluble, but not particulate, antigen in the absence of Wiskott-Aldrich syndrome protein. *Immunology*, 109, 384-91.
- WESTERBERG, L. S., DE LA FUENTE, M. A., WERMELING, F., OCHS, H. D., KARLSSON, M. C. I., SNAPPER, S. B. & NOTARANGELO, L. D. 2008. WASP confers selective advantage for specific hematopoietic cell populations and serves a unique role in marginal zone B-cell homeostasis and function. *Blood*, 112, 4139-4147.

- WILLIAMS, G. S., COLLINSON, L. M., BRZOSTEK, J., EISSMANN, P., ALMEIDA, C. R., MCCANN, F. E., BURSHTYN, D. & DAVIS, D. M. 2007. Membranous structures transfer cell surface proteins across NK cell immune synapses. *Traffic*, 8, 1190-204.
- WILLIAMSON, D. J., OWEN, D. M., ROSSY, J., MAGENAU, A., WEHRMANN, M., GOODING, J. J. & GAUS, K. 2011. Pre-existing clusters of the adaptor Lat do not participate in early T cell signaling events. *Nature Immunology*, 12, 655-U214.
- WINQUIST, R. J., DESAI, S., FOGAL, S., HAYNES, N. A., NABOZNY, G. H., REILLY, P. L., SOUZA, D. & PANZENBECK, M. 2001. The role of leukocyte function-associated antigen-1 in animal models of inflammation. *European Journal of Pharmacology*, 429, 297-302.
- WORTH, A. J. J., METELO, J., BOUMA, G., MOULDING, D., FRITZSCHE, M., VERNAY, B., CHARRAS, G., CORY, G. O. C., THRASHER, A. J. & BURNS, S. O. 2013. Disease-associated missense mutations in the EVH1 domain disrupt intrinsic WASp function causing dysregulated actin dynamics and impaired dendritic cell migration. *Blood*, 121, 72-84.
- WU, L. & LIU, Y. J. 2007. Development of dendritic-cell lineages. *Immunity*, 26, 741-750.
- WULFING, C. & DAVIS, M. M. 1998. A receptor/cytoskeletal movement triggered by costimulation during T cell activation. *Science*, 282, 2266-9.
- WULFING, C., SUMEN, C., SJAASTAD, M. D., WU, L. C., DUSTIN, M. L. & DAVIS, M. M. 2002. Costimulation and endogenous MHC ligands contribute to T cell recognition. *Nature Immunology*, 3, 42-47.
- WYNN, T. A. 2003. IL-13 effector functions. *Annual Review of Immunology*, 21, 425-456.
- XIE, J. M., TATO, C. M. & DAVIS, M. M. 2013. How the immune system talks to itself: the varied role of synapses. *Immunological Reviews*, 251, 65-79.
- XU, X. P., ROUILLER, I., SLAUGHTER, B. D., EGILE, C., KIM, E., UNRUH, J. R., FAN, X. X., POLLARD, T. D., LI, R., HANEIN, D. & VOLKMANN, N. 2012. Three-dimensional reconstructions of Arp2/3 complex with bound nucleation promoting factors. *Embo Journal*, 31, 236-247.
- XU, Y. W., MOSELEY, J. B., SAGOT, I., POY, F., PELLMAN, D., GOODE, B. L. & ECK, M. J. 2004. Crystal structures of a formin homology-2 domain reveal a tethered dimer architecture. *Cell*, 116, 711-723.
- YANG, C., CZECH, L., GERBOTH, S., KOJIMA, S. I., SCITA, G. & SVITKINA, T. 2007. Novel roles of formin mDia2 in lamellipodia and filopodia formation in motile cells. *Plos Biology*, 5, 2624-2645.
- YANG, Y. P. & WILSON, J. M. 1996. CD40 ligand-dependent T cell activation: Requirement of B7-CD28 signaling through CD40. *Science*, 273, 1862-1864.
- YI, J., WU, X. F. S., CRITES, T. & HAMMER, J. A. 2012. Actin retrograde flow and actomyosin II arc contraction drive receptor cluster dynamics at the immunological synapse in Jurkat T cells. *Molecular Biology of the Cell*, 23, 834-852.

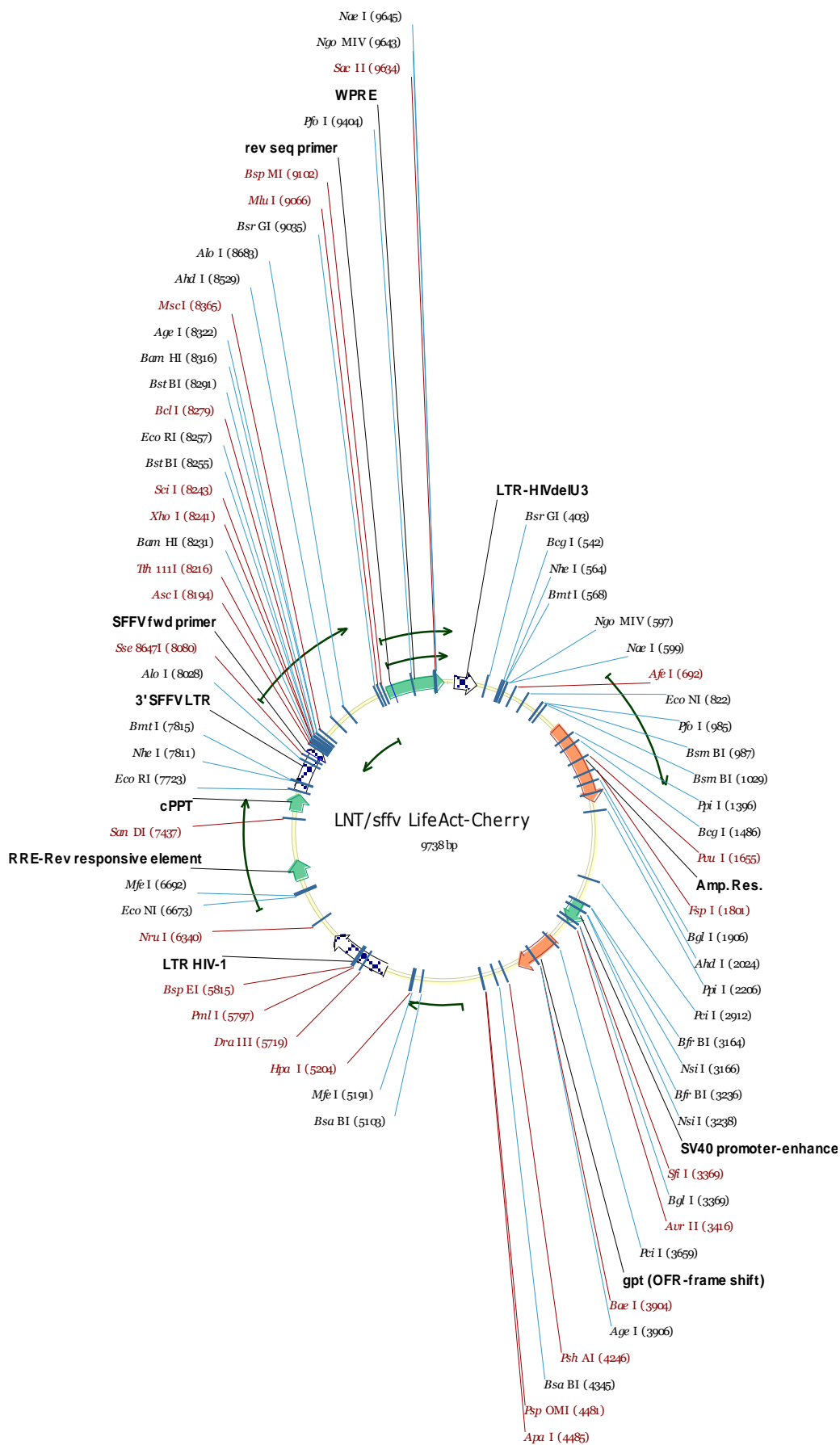
- YI, J. S., WU, X. F., CHUNG, A. H., CHEN, J. K., KAPOOR, T. M. & HAMMER, J. A. 2013. Centrosome repositioning in T cells is biphasic and driven by microtubule end-on capture-shrinkage. *Journal of Cell Biology*, 202, 779-792.
- YOKOSUKA, T., SAKATA-SOGAWA, K., KOBAYASHI, W., HIROSHIMA, M., HASHIMOTO-TANE, A., TOKUNAGA, M., DUSTIN, M. L. & SAITO, T. 2005. Newly generated T cell receptor microclusters initiate and sustain T cell activation by recruitment of Zap70 and SLP-76. *Nature immunology*, 6, 1253-62.
- YU, C. H., WU, H. J., KAIZUKA, Y., VALE, R. D. & GROVES, J. T. 2010. Altered actin centripetal retrograde flow in physically restricted immunological synapses. *PloS one*, 5, e11878.
- YU, Y., FAY, N. C., SMOLIGOVETS, A. A., WU, H. J. & GROVES, J. T. 2012. Myosin IIA Modulates T Cell Receptor Transport and CasL Phosphorylation during Early Immunological Synapse Formation. *Plos One*, 7.
- ZHANG, J., SHEHABELDIN, A., DA CRUZ, L. A., BUTLER, J., SOMANI, A. K., MCGAVIN, M., KOZIERADZKI, I., DOS SANTOS, A. O., NAGY, A., GRINSTEIN, S., PENNINGER, J. M. & SIMINOVITCH, K. A. 1999. Antigen receptor-induced activation and cytoskeletal rearrangement are impaired in Wiskott-Aldrich syndrome protein-deficient lymphocytes. *J Exp Med*, 190, 1329-42.
- ZHANG, L. J., LUO, J., WAN, P., WU, J., LASKI, F. & CHEN, J. O. 2011. Regulation of cofilin phosphorylation and asymmetry in collective cell migration during morphogenesis. *Development*, 138, 455-464.
- ZHANG, Q., DAVIS, J. C., DOVE, C. G. & SU, H. C. 2010. Genetic, clinical, and laboratory markers for DOCK8 immunodeficiency syndrome. *Dis Markers*, 29, 131-9.
- ZHANG, Q., DAVIS, J. C., LAMBORN, I. T., FREEMAN, A. F., JING, H., FAVREAU, A. J., MATTHEWS, H. F., DAVIS, J., TURNER, M. L., UZEL, G., HOLLAND, S. M. & SU, H. C. 2009. Combined immunodeficiency associated with DOCK8 mutations. *N Engl J Med*, 361, 2046-55.
- ZHANG, Y. B. & WANG, H. Y. 2012. Integrin signalling and function in immune cells. *Immunology*, 135, 268-275.
- ZHU, J. & PAUL, W. E. 2010. Peripheral CD4+ T-cell differentiation regulated by networks of cytokines and transcription factors. *Immunological reviews*, 238, 247-62.
- ZHU, J. H., LUO, B. H., XIAO, T., ZHANG, C. Z., NISHIDA, N. & SPRINGER, T. A. 2008. Structure of a Complete Integrin Ectodomain in a Physiologic Resting State and Activation and Deactivation by Applied Forces. *Molecular Cell*, 32, 849-861.
- ZHU, Q. L., ZHANG, M., BLAESE, R. M., DERRY, J. M. J., JUNKER, A., FRANCKE, U., CHEN, S. H. & OCHS, H. D. 1995. The Wiskott-Aldrich Syndrome and X-Linked Congenital Thrombocytopenia Are Caused by Mutations of the Same Gene. *Blood*, 86, 3797-3804.
- ZIEGLER, S. F., RAMSDELL, F. & ALDERSON, M. R. 1994. The activation antigen CD69. *Stem cells*, 12, 456-65.
- ZYSS, D., EBRAHIMI, H. & GERGELY, F. 2011. Casein kinase I delta controls centrosome positioning during T cell activation. *Journal of Cell Biology*, 195, 781-797.

Appendix

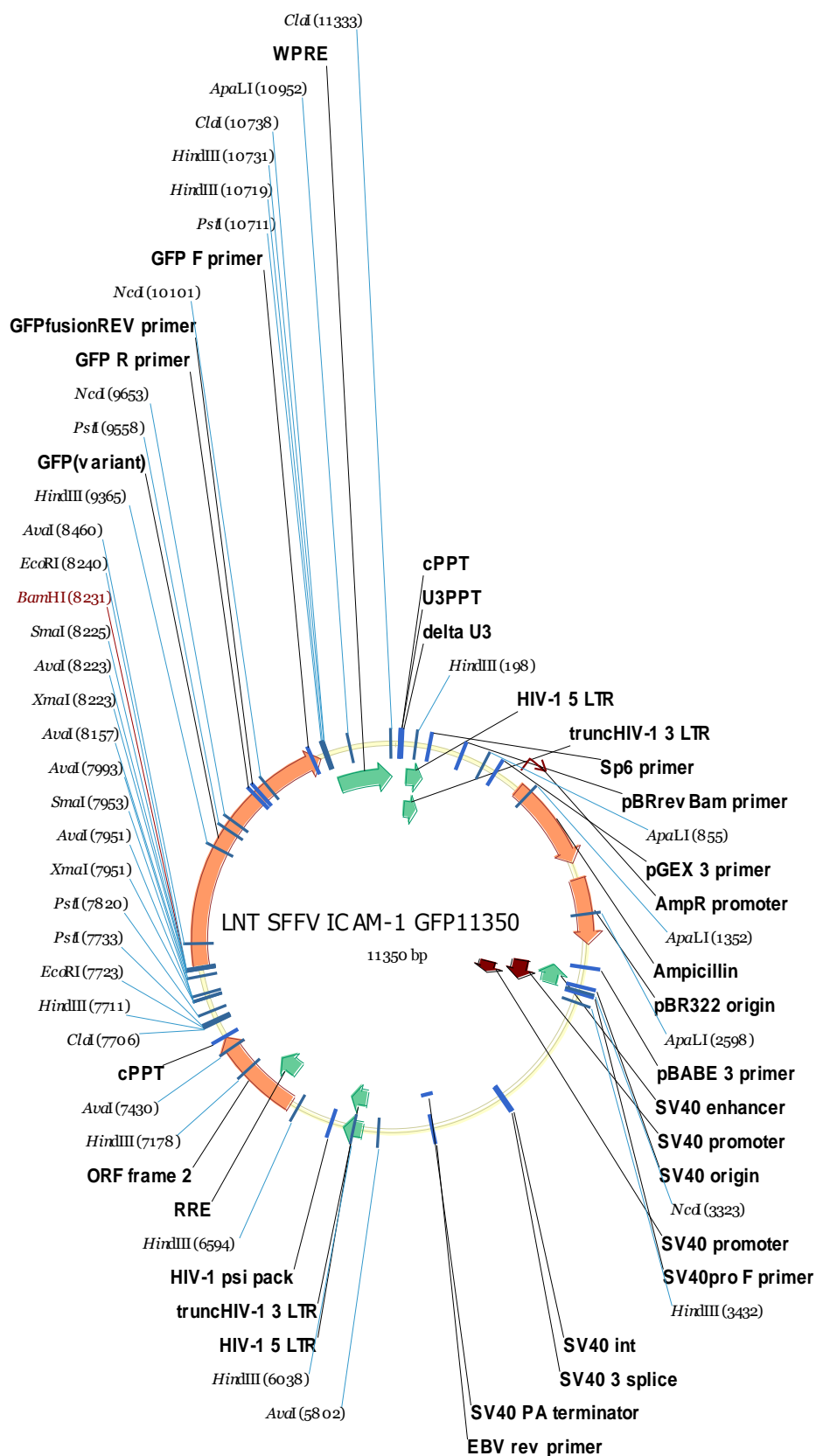
1. Constructs LNT_mCherry-Actin



LNT_LifeAct-mCherry



LNT_ICAM-1-EGFP



2. Anti-MHCII + Anti-ICAM-I (0.25µg/ml) bilayer

